**UNIVERSITY OF NAPLES "FEDERICO II"**

**DEPARTMENT OF AGRICULTURAL SCIENCES**

Ph.D. IN SUSTAINABLE AGRICULTURAL AND FORESTRY SYSTEMS AND FOOD SECURITY

XXXIV CYCLE

# Metabolomics for the selection of beneficial microorganisms and/or their functional metabolites for agricultural uses

Candidate: Alessia Staropoli

Coordinator: Prof. Albino Maggio

Tutor: Francesco Vinale

Academic Years 2018/2021

# INDEX

# Introduction

Since the end of Second World War, agriculture has undergone a significant intensification with the introduction of chemical pesticides[1]. Organochlorine insecticides were introduced in the 1940s and globally spread, due to the easy manufacture and application, thus starting a revolution in pest control[2]. Since then, several chemical pesticides and fertilizer have been commercialized and overexploited by farmers to increase crops yield and to manage plant pathogens in the way of preventing infections. However, the immoderate use of chemical products contributed to the development of resistance of pathogen populations[3,4], to environment contamination[5], such as pollution of water, atmosphere and soil[6], and to human diseases rise[7–9]. Increasing public awareness of all the risks connected to the use of chemicals, has moved the focus from intensive agricultural practices (crop yield) to the application of sustainable agriculture, using eco-friendly biological agents complemented with physical and cultural methods[5,10,11].

## Sustainable agriculture

In 1987, the United Nations Brundtland Commission defined sustainable development as "*meeting the needs of the present without compromising the ability of future generations to meet their own needs*"[12]. Sustainable agriculture is one of the achievements which sustainable development refers to, and it is defined as "*the management and conservation of the natural resource base, and the orientation of technological change in such a manner as to ensure the attainment of continued satisfaction of human needs for present and future generations. Sustainable agriculture conserves land, water, and plant and animal genetic resources, and is environmentally non-degrading, technically appropriate, economically viable and socially acceptable*"[13]. Sustainable agriculture comprises different sectors (crops, livestock, forestry, fisheries, and aquaculture) that have been individually improved, leading in many cases to a competition for space and resources (natural and economic). A holistic approach of sustainability should look forward to create synergies between sectors in order to reduce or even eliminate trade-offs[14]. Integrated Farming Systems (IFS) fit in this context since it considers a whole farm approach for both crops and livestock to produce benefits through their mutual interactions[15]. For instance, livestock produces manure that can be used to improve crop productivity and sustainability (by reducing the application of mineral fertilizer), while crops provide grasslands and feeds and it also contribute to sequestrate greenhouse gases emitted by livestock[16].

*Integrated Crop Management*

IFS incorporates Integrated Crop Management (ICM) whose focus is on crops only, and it is defined by Rowe and Powelson (2008)[17] as "*the application of a totally*

*integrated set of production practices that results in a quality crop produced in a manner that optimizes economic return and minimizes environmental impacts and undesirable social effects*". The implementation of ICM requires effective strategies that include biological, cultural and physical control, and host plant resistance. The integration of all these practices is strongly encouraged because it has been demonstrated to have synergistic effects in enhancing crops growth and yield[18] as well as soil fertility[19]. The addition of organic amendments (biochar, manure, vermicompost) can support nutrient recycling, microbial decomposition and other soil processes[20,21]. Augmenting crops' quality and yield also means to protect plants from weeds, pests and pathogens (i.e., insects, nematodes, bacteria and fungi) and other abiotic stresses (drought, salinity, low or high temperatures) in a sustainable way.

*Integrated Pest Management*

Integrated Pest Management (IPM) is focused on crop protection from diseases caused by pests. This model for crop protection has been ideated in the 1960s as a consequence of the raising awareness of the harmful effects of pesticides on the environment[22], considering the innovations and the integration of biological and chemical control[23]. The actual definition of IPM provided by the Food and Agriculture Organization (FAO) is as follows: "I*ntegrated Pest Management (IPM) means the careful consideration of all available pest control techniques and subsequent integration of appropriate measures that discourage the development of pest populations and keep pesticides and other interventions to levels that are economically justified and reduce or minimize risks to human health and the environment. IPM emphasizes the growth of a healthy crop with the least possible disruption to agro-ecosystems and encourages natural pest control mechanisms*"[24]. The primary aim of IPM is to minimize pesticides use by adopting preventive and/or suppressive measures for harmful organisms, which can include physical, genetic or biological techniques (crop rotation, seedbed sanitation, use of resistant cultivars) and by monitoring pest levels with in-field observations or with warning systems where available. According to Higley and Pedigo (1996)[25], plants are able to tolerate a certain level of injury without reaching the economic injury level (EIL), defined as the lowest pest density that can cause economic damage to plants[25]. In order to avoid economic losses, pest management starts at an appropriate time before pest population has reached the EIL; this time is defined as economic threshold (ET)[26]. Whereas the pest population has reached the ET, one or more pest management inputs can be used. IPM strongly recommends the choice of sustainable biological, physical and other non-chemical methods. Chemical pesticides can be applied only when their use is economically justified, and there are no other alternatives. In such case, the product must be as more specific as possible to the target and the least harmful to non-target organisms (including humans) and to the environment.

FAO's guidelines and definition of IPM have been approved in the EU and its application has been made mandatory for all professional farmers since 2014, as stated in the Directive 2009/128/EC of the European Parliament and of the Council[27]. The Directive, again, encourages the use of ecological alternatives to pesticides, unless it is strictly

necessary and the use of all methods available is regulated by eight general principles [28]. Attention is also given to aerial spraying, which is prohibited except for special cases reported in paragraph 2 of Art.9 (pp. 77-78), and to the training of professional and non-professional users on the use of pesticides and on the equipment used for application (Art. 5, pp-75-76 and Annex I, p. 82) [27].

The Regulation concerning plant protection products has also been published in 2009, in order to set rules for the authorization of plant protection products in commercial form and for their placing on the market, use and control within the Community[29] (EC1107/209). This Regulation intends to reduce the risks to both human and animal health and to the environment, giving dispositions supported by the precautionary principle. This concept should be applied especially when there is scientific uncertainty about the risks of a product that is supposed to be authorized in the territory. Any product (in the form in which it is supplied to the user), consisting of or containing active substances, safeners, synergists, co-formulants and adjuvants, is subjected to a protocol before its approval. Microorganisms, having general or specific action to plants or against harmful organisms, are also considered as active substances.

Bioproducts are microbial based pesticides or fertilizers (also called biopesticides and biofertilizers, respectively) that can increase crop productivity by enhancing plant nutrition and that can protect crops from pathogens and pests[30]. These products are formulated with beneficial microorganisms and/or their metabolites which offer advantages and are not harmful for the environment and other living species[6].

## Beneficial microorganisms

Microorganisms are an integral component of the Earth's living system since they are natural inhabitants of the soil and a vital and important part of the rhizosphere[31]. The narrow zone of soil surrounding plant roots is called rhizosphere, which has a biotic component of various microbes. The rhizosphere is enriched with several nutrients and root exudates constituted by amino acids, carbohydrates, organic acid and secondary metabolites[32]. These support the growth of microbial groups that perform several functions. Specifically, beneficial microorganisms exert positive effects on plant development, such as nutrient cycling or protection from biotic (pathogens and pests) and abiotic (salinity, heat, drought) stress[33]. Beneficial microbes can include bacteria, fungi, viruses, and can be divided into two main groups: biological control agents (BCAs) which protect plants by controlling pathogens and pests, and plant growth promoting microorganisms (PGPMs) which enhance plant growth and health[34]. These two groups often intersect due to multiple functions exploited by the same microorganism for both plant nutrition and protection[30]. In fact, increasing plant health can in turn reduce risk infection, as well as protecting plants from pathogens can indirectly promote plant growth.

### Biocontrol agents

Stenberg et al in 2021 defined biological control as *the exploitation of living agents (including viruses) to combat pestilential organisms directly or indirectly, for human good. Biological control always involves three separate players: a biocontrol agent, a pest and a human stakeholder benefitting from the pest control service provided by the biocontrol agent*[35].

BCAs can protect plants against pests and pathogens directly or indirectly using several mechanisms of action. Direct protection involves antibiosis and parasitism, while indirect mechanisms include competition and induction of systemic resistance[36]. All these mechanisms will be explained in detail, also providing examples of known microorganisms commonly used as biocontrol agents.

*Antibiosis*

One of the most studied direct activity against pathogens is antibiotic production. Antimicrobial metabolites are natural products derived from secondary metabolism, belonging to several classes of compounds and characterized by a low-molecular weight. These molecules are toxic or are able to inhibit to other microorganisms[36,37]. They are produced and released to the environment at low concentration. Most of known antibiotics are produced by actinomycetes (8700), followed by fungi (4900) and other bacteria (2900)[38].

Broad-spectrum antimicrobial metabolites have been reported produced by several bacterial genera such as *Agrobacterium*, *Arthrobacter, Azotobacter, Bacillus*, *Burkholderia*, *Pseudomonas*, *Rhizobium, Serratia*, *Stenotrophomonas*, *Streptomyces*[36,39,40]. *Bacillus* and *Pseudomonas* species have been investigated for the production of lipopeptide bio-surfactants, such as iturin, surfactin, and fengycin [41,42]. Melo et al in 2016 and Liu et al in 2019 reported that bioactive lipopeptides made by *B. subtilis* can necrotize epithelial cells causing death of target insect[43,44]. Many antibiotic metabolites produced by Pseudomonads, such as 2,4-diacetylphloroglucinol (DAPG), pyrrolnitrin and phenazine, have been studied[45]. DAPG can damage membrane and inhibit zoospores formation of *Pythium* sp[46]. Most fungal antagonists are of the genera *Aspergillus*, *Beauveria*, *Metarhizium*, *Penicillium* and *Trichoderma* that can produce antimicrobial compounds. Bassiacridin and beauvericin produced by *Beauveria* and destruxins produced by *Metarhizium* are active against entomopathogens[47,48]. For *Trichoderma*, 6-pentyl-α-pyrone (6-PP), harzianic acid, gliovirin, gliotoxin, viridin and many more compounds with antimicrobial activity have been characterized[49,50]. Genomic information reveals that these bacteria and fungi have the potential to produce many other secondary metabolites with possible antimicrobial activity which are yet to characterize.

*Parasitism*

Parasitism is the direct competitive interaction between two organisms in which one (parasite) obtains nutrients from the other (host)[36]. Biotrophic parasites gain nutrients from the host cells without killing the host, so the two organisms interact in a stable and balanced way[51]. A necrotrophic parasite invades its host and gets nutrients after killing host's cells. Direct mechanisms of parasitism are related to the secretion of cell wall degrading enzymes (CWDEs) (i.e., chitinases, β-glucanases, proteases, cellulases,

catalases), combined in some cases with excretion of secondary metabolites[11]. These lytic enzymes disrupt the structural stability and integrity of pathogen's cell walls and pest's tissues leading to the disorganization of the cytoplasm[52].

Parasitism has been reported for bacterial genera such as *Bacillus*, *Pseudomonas*, *Serratia*, *Streptomyces*[33,43,53-57]. Several studies reported the chitinolytic actions of *Serratia marcescens* against pathogenic fungi such as *Fusarium oxysporum* and *Rhizoctonia solani*[33]. *S. marcescens* inhibits fungal growth by curling, rupture, or partial swelling of hyphae[53]. *Streptomyces* and *Paenibacillus* strains produce cellulase and β-1,3-glucanase that degrade cell walls of pathogenic fungi, such as *Sclerotinia sclerotiorum* and *F. oxysporum*[54]. Moreover, *B. cereus* and *B. cepacia* secrete different enzymes, including amylase, β-1,3-glucanase, cellulase and protease able to break the cell walls of several soil-borne pathogenic microbes[55]. *B. thuringiensis*, the primary entomopathogenic bacterium, produces intracellular inclusions, comprised of endotoxins, that destroy insect cell structures by modifying transmembrane potential and so inducing osmotic cell lysis[43,56]. *Bdellovibrio bacteriovirus* is a unique predatory bacterium with the ability to invade and derive nutrients from the cytoplasm of other Gram-negative bacteria[57]. The most studied mycoparasites belong to the genus *Trichoderma*[58–62]. For instance, *T. asperellum*, *T. virens*, *T. atroviride*, and *T. harzianum* are well-known to release CWDEs, often in combination with antibiotic secondary metabolites, against common soil-borne pathogens such as *Fusarium*, *Aspergillus* or *Rhizoctonia* amongst others[63–65].

*Competition*

Ecological competition occurs when two or more organisms battle to obtain nutrients or resources in general (light, water or space)[35]. Many biocontrol agents can aggressively colonize soils and consequently hinder pathogens establishment by competing with them. This indirect mode of action is extremely effective in controlling necrotrophic pathogens due to their dependency on exogenous nutrients during significant parts of their life cycle[66,67]. Competition for carbon source and for amino acid, considered as nitrogen source, plays a key role in antagonistic interactions[68]. Besides carbohydrates and nitrogen sources, another limiting factor for microbial growth is the low iron availability in a soluble form. Iron is essential for microbes growth but, although abundant in soil, it is not frequently accessible because the oxidized form ($Fe^{3+}$) reacts to produce insoluble oxides ($Fe(OH)_3$) which cannot be readily used by microorganisms[69–71]. In iron-limiting conditions, several biocontrol agents can produce iron-chelating compounds called siderophores. Siderophores are low-molecular weight (<1 kDa) molecules with high affinity for ferric iron[72]. Siderophores-producing strains can exert biological control through competition for iron inhibiting pathogens growth[73]. Siderophores can be grouped in major classes (e.g., catecholate, carboxylate, phenolates, hydroxamates, pyoverdines) depending on ligand type, iron-directing functional group, and structural feature[74]. Several siderophores producing bacteria, such as *Azotobacter*, *Bacillus*, *Bradyrhizobium*, *Streptomyces*, *Serratia*, *Rhizobium* and *Pseudomonas*, have been investigated[75]. Strains of *P. fluorescens* and *P. aeruginosa* produce pyoverdine and pyochelin form of siderophores with high affinity for $Fe^{3+}$ [72]. Iron competition is also the mode of action of several fungal antagonists able

to release siderophores, such as *Penicillum*, *Aspergillus*, *Fusarium, Ustilago, Trichoderma*. Most fungal siderophores belong the hydroxamate class (e.g. ferrichromes, coprogens, triacetylfusarinines)[72]. *T. harzianum* strain M10 produces harzianic acid (HA), a tetramic acid derivatives which exerts its siderophore action due to its chemical structure. This exo-metabolite is able to bind $Fe^{3+}$and other heavy and non-heavy metals[49].

*Induction of systemic resistance*

Plants have a broad variety of physical and chemical mechanisms as constitutive defense against pathogens. Additionally, plants can often show intrinsic defenses as response to various agents, including beneficial microorganisms. This physiological state of improved defensive ability is called induced systemic resistance (ISR)[76]. Ethylene and jasmonate signaling is involved in triggering ISR as these hormones play a significant role in enhancing the defense response of plants against a wide variety of phytopathogens[77]. Consequently, plants' cell walls are strengthened, metabolic responses are altered and more in general plants' physiology is modified[78]. Species of *Pseudomonas* and *Bacillus* demonstrated to induce systemic resistance in several different hosts[79,80]. Several strains of *Trichoderma* can stimulate plants defense mechanisms by secreting specific elicitors, such as volatile organic compounds, peptaibols or polyketides[81–83], that are recognized by plant cell receptors, increasing the microbe-associated molecular patterns (MAMPs)-triggered immunity (MTI) [84].

**Plant growth promoting microorganisms**

Microorganisms can positively influence crops by stimulating plants growth, enhancing their nutrient uptake and/or use efficiency, making plants less susceptible to abiotic (but also biotic) stress and by improving crop quality traits[85,86]. Plant growth promoting microorganisms (PGPMs) exert positive effect through numerous ways which can be divided into a group of direct mechanisms, including nutrient solubilization (i.e. P, Fe), nitrogen fixing, phytohormones production, and a group of indirect mechanisms, including IRS (described in the previous paragraph) and induction or resistance against abiotic stress.

*Phosphate solubilization*

Phosphorus (P) is the one of the most important plant macronutrients, together with potassium (K), and it is essential for all major physiological and biochemical processes for the plant (cell division, photosynthesis, energy transfer, respiration, biosynthesis of macromolecules)[87]. Phosphorous is also important for root system development, stem strength and length, crop production and quality[88]. Although most soils are rich in both inorganic (calcium phosphates in alkaline soils or iron/aluminum phosphates in acidic soils) and organic forms (inositol and sugar phosphates) of phosphorous, only a slight fraction (0.1%) is available for plants, in the form of orthophosphates ($HPO_4^{2-}$ and $H_2PO_4^-$)[89–91].

Bacteria, fungi and actinomycetes are involved in the phosphate solubilizing process since they are an integral component of the natural P-cycle[92]. The phosphate-solubilizing microorganisms (PSMs) transform insoluble phosphates in the soluble form through different mechanisms as release of organic acids, chelation, and ion exchange reactions[93]. Several organic acids, such as acetate, citrate, lactate, ketogluconate, gluconate, succinate, malate, oxalate, can chelate cations of the phosphate salt, thereby converting phosphorous in a soluble form. Moreover, the production of organic acids also lowers the pH of the soil increasing the solubility of phosphates in alkaline soils[94]. Bacterial strains of the genera *Pseudomonas*, *Bacillus*, *Rhizobium*, and *Enterobacter*, along with *Penicillium* and *Aspergillus* fungi, have been reported to solubilize P through proton excretion and organic acids production[95–97].

The solubilization of organic phosphorous to soluble form is defined as P-mineralization. This process involves the release of phosphatases, enzymes involved in the hydrolysis of phosphor-ester and phosphor-anhydride bonds of organic phosphate compounds, thereby releasing inorganic phosphorus that will be immobilized by plants. Bacteria from the genera *Bacillus*, *Burkholderia*, *Pseudomonas*, and *Streptomyces* exhibit phosphatase activity and improve the growth of various crops, while *Aspergillus*, *Penicillium*, and two *Trichoderma* strains are reported as phosphatase-producing fungi[98–101].

*Iron uptake*

Iron (Fe) is one of the major micronutrients required for growth and development of plants. It has a role as cofactor for several enzymes, it is involved in photosynthesis, synthesis and protection of DNA, and in regulation of respiration[102]. Although iron is one of the most abundant elements on Earth, its availability in soils is low due to the oxidation to the ferric ($Fe^{3+}$) ion, which forms insoluble products.

Plants can cope with this condition by producing phyto-siderophores able to chelate iron and thus making it available for the uptake[103,104]. Furthermore, beneficial microbes can mediate this process through the release of siderophores in soil that bound iron from ferric oxides, phosphates or citrates[105]. The Fe-siderophore complex is recognized by specific receptors on cell membrane of plant roots and then taken up[106,107]. As mentioned above, several beneficial microbes can release chelating agents for ferric ion as a way to compete with pathogens. These beneficial agents can also mobilize iron to plants and improve growth and productivity of plants, beside protecting them from pathogens.

*Nitrogen fixation*

Nitrogen ($N_2$) is an essential element for proper growth, development and productivity of plants, since it plays a role in several structural, biochemical and physiological processes[108]. Although representing the 80% of the atmosphere, gaseous nitrogen cannot be used by plants as they can only take soil-available nitrogen as ammonia or nitrate through root system. Ammonium is directly incorporated and used to synthetize amino acids, whereas nitrate has to be converted to ammonium[109].

It is possible to convert inert nitrogen into organic compounds containing N, through a process called fixation which is biologically exploited by specific bacteria (biological nitrogen fixation, BNF). These bacteria are ubiquitous and can be divided into two

groups: symbiotic and non-symbiotic bacteria. *Rhizobium* genus belongs to the former group[110], while *Azotobacter*, *Azospirillum*, *Enterobacter*, *Pseudomonas,* amongst others, belong to the free-living diazotrophic bacteria[111]. BNF is carried out by a series of enzymatically complex reactions, involving dinitrogenase reductases (iron protein that provides reducing power electrons) and dinitrogenases (a protein with metallic cofactor that uses the electrons to reduce nitrogen to ammonia)[112,113].

*Phytohormone production*

Phytohormones are molecules derived from plant biosynthetic pathways, that perform their functions either locally or via transport to other sites within the plant tissues. Phytohormones act at low concentrations to mediate growth, development, nutrient provision, particularly under biotic or abiotic stress[114]. Plant hormones include abscisic acid (ABA), gibberellins (GA), brassinosteroids (BSs), jasmonic acid (JA), cytokinins (CKs), ethylene (ET) and indole acetic acid (IAA) that is part of auxins group[115]. Indole acetic acid, cytokinins and gibberellins are well-characterized hormones also produced by numerous bacteria and fungi[116,117].

Microbial-produced IAA affects root length and increases surface area for improved uptake of nutrients and water. IAA can be synthetized following different pathways, such as via indole-3- pyruvic acid and indole-3-acetic aldehyde, via tryptamine and indole-3-acetic aldehyde and via indole-3-acetamide[118,119]. *Bacillus*, *Pseudomonas* and *Streptomyces*, along with endophytic fungi are examples of plant growth promoting microbes able to release indole acetic acid[120–122].

Cytokinins are critical in various physiological and developmental processes including apical dominance, seed germination, nodule formation, root elongation, vascular development, and plant-pathogen-interactions[123]. The production of cytokinins comes from ATP/ADP/AMP or from the tRNA degradation pathway biosynthesis[124]. Bacteria, such as *Bacillus*, *Agrobacterium*, *Pseudomonas*, and *Klebsiella* and several fungal species, whether saprophytic or symbiotic, are known to synthetize cytokinins in the rhizosphere thus leading to stimulation of plant growth or helping plants to cope with biotic and abiotic stress[124–126].

Gibberellins are terpenoid involved in diverse stages of plant growth as: i) germination, ii) cell division, iii) stem elongation, iv) internode expansion, v) flowering[127]. Like auxins and cytokinin, beneficial microbes are also able to bio synthetize gibberellins [128]. Among bacteria, the characterization of gibberellins was first reported in *Rhizobium meliloti*, while for fungi it was reported in *Gibberella fujikuroi*[129,130]. Since then, several fungal and bacterial genera, including *Bacillus*, *Pseudomonas* and *Trichoderma* have been reported as gibberellins producers[131–133].

*Tolerance to abiotic stress*

Crops require different conditions to reach optimal growth and yield and if these conditions are not satisfied, plants react with specific stressful stimulus[134,135]. Salinity, drought, temperature or metal contamination are the most common abiotic factors that plants have to face. Various studies reported that PGPMs can positively affect plants also by improving their tolerance to these stress[136–144].

High soil salinity is one of the most significant environmental stresses that results in decreased crop productivity and quality. Salinity negatively affects roots biomass, ionic balance, water and nutrients uptake, photosynthesis[136]. Salt is transported and accumulated within the roots, thus inducing inhibition of cell division, and causing ionic imbalance. Moreover, high levels of salt lower soil water potential resulting in cellular dehydration. A decreased uptake on nutrients implicates a minor uptake on magnesium, thus hindering photosynthesis[145]. Microbes can mitigate the effects of salt stress in plants by producing phytohormones, siderophores, antioxidants and osmolytes, by fixing nitrogen into the soil and also by accumulating salt in their cytoplasm, which balances the osmotic condition of cells[146]. The role of several rhizosphere microbes belonging to the genera *Pseudomonas*, *Azotobacter*, *Bacillus*, *Trichoderma*, *Phoma*, *Penicillium*, *Piriformospora*, and *Fusarium* in mitigation of multiple kinds of abiotic stresses has been reported[147–157].

Water deficiency is a serious concern worldwide, that derives from either scarcity of water sources or from heavy contamination with pollutants. Drought stress negatively affects physiological status of plants, including the photosynthetic capability due to a lower content of chlorophyll[158]. Persistent water stress decreases leaf water potential and stomatal opening, reduces leaf size, suppresses root growth, and delays plant growth and productivity[159]. Furthermore, peroxidation may be induced by reactive oxygen species (ROS) produced during drought stress, leading to negative impact on antioxidant metabolism[160]. Plants have different mechanisms to minimize use of water resources and manage their growth in case they face adverse conditions[161]. Nonetheless, a variety of microorganisms can effectively help plants surviving to water-deficit conditions. Tolerance mechanisms, such as formation of thick cell wall, secretions of exopolysaccharides or osmolytes, entering a dormant phase[137]. Several bacterial and fungal strains are reported to release phytohormones and other molecules like proline, trehalose and glycine betaine, that help during this stressing condition[137]. Strains of *Pseudomonas* and *Bacillus* produce proline, sugars and free amino acids helping plants to improve growth and water content[162]. Abscisic acid is the principal hormone responsible for survival of in water deficit conditions and its production can be triggered by application of PGPMs like *Azospirillum*[163]. Several *Trichoderma* strains are well-knows producers of phytohormones, including gibberellins, abscisic acid, indole acetic acid and ethylene which are involved in plant development and protection from biotic and abiotic stress. *Trichoderma*-based treatments have been reported to promote growth under water stress condition[116]. Finally, co-inoculation of *Azotobacter chroococcum* and *Trichoderma harzianum* increased growth and protected plants during water and nitrogen deficiency[164].

Both high and low temperatures significantly reduce plant yield and productivity, since temperature affects the fluidity of the cell membrane, reduces the water content, and hinders enzyme activity and cell division[136]. Adverse climate influences plants at different levels reducing seed germination, photosynthesis, respiration and membrane permeability[160]. Plants have developed different mechanisms based on heat/cold shock proteins and antioxidative enzymes, which expression is enhanced in stress situations, together with an alteration of phytohormones levels[165]. Moreover, several beneficial

microorganisms are also involved: rhizobacteria and arbuscular mycorrhizal fungi can effectively protect plants by inducing the expression of enzymes and secondary metabolites related to heat and cold temperature stress[166–169].

Pollutants have become a worldwide environmental issue in the last century. Different pollutants, including heavy metals, chlorinated organic compounds and polycyclic aromatic hydrocarbons, are found in water, soil, and air, and have attracted public attention due to the increasing concern for the security of agricultural products. Heavy metals (mercury, lead, arsenic, cadmium) can contaminate the soil agro-ecosystem either through natural weathering of metal-rich parent material or through anthropogenic activities[170]. Several bioremediation methods have been developed and application of microbes has been demonstrated to be an effective method to reduce metal concentration in soil[171]. Mechanisms such as chelation, detoxification of absorbed metal through enzymatic activities, reducing the uptake of heavy metal and sequestering them in the exopolysaccharide layer are adopted by the microorganisms to decrease the toxicity of heavy metals[172,173]. Other pollution-causing agents are polymers, solvents, oils, biocides, chlorinated organic compounds and polycyclic aromatic hydrocarbons (PHA) [174]. It has been reported the ability of microbes to degrade most of these contaminants by transformation into less or completely nontoxic residues[175, 176].

## Secondary metabolites produced by beneficial microbes

The production of bioactive secondary metabolites (SMs) is an important factor for the beneficial effects of selected microbial strains. These are heterogeneous natural compounds, belonging to diverse chemical classes with low molecular weight (typically <3kDa)[177]. Secondary metabolism is associated to the shift from biomass production to metabolite biosynthesis to offer a benefit for the producer. Environmental stimuli can trigger the production of a specific natural compound or a group of them that can serve as weapons against competitors for nutrients and space, as agents of symbiosis with plants or other organisms, as sexual hormones or as differentiation effectors[178]. SMs biosynthesis starts from a limited number of precursors of primary metabolites (i.e., amino acids, acetyl-CoA) that follow specialized pathways and conduct to different natural compounds[179]. In the following paragraphs some of the most important classes of compounds are briefly described.

*Non-ribosomal peptides*

Non-ribosomal peptides (NRPs) are synthesized by large multimodule enzymes named non-ribosomal peptide synthetases (NRPSs). Each module contains several domains for the recognition, activation, binding of a module-specific amino acid and peptide bond formation between the growing chain and the next amino acid. The last module also contains a domain that allows the release of the peptide. The biosynthesis proceeds through a thiotemplate mechanism, in which an amino acid is first recognized and

activated by adenylation with ATP, then is bonded, by thioesterification with 4'-phosphopantetheine, to the carrier domain that transports the substrate to the condensation domain to form the peptide bond between adjacent monomer units. Product release, either as linear or cyclic peptide, is catalyzed by a thioesterase domain at the C-terminal. The multitude of monomers, both proteinogenic and non-proteinogenic amino acids, together with possible modifications of the substrate during the synthesis by other catalytic domains (i.e., epimerization domain and cyclization domain) contribute to the overall complexity of NRPs[180,181]. An example of NRPs are peptaibols produced by *Trichoderma* species, which are characterized by the presence of α-aminoisobutyric acid residues, a C-terminal hydroxylated amino acid, and a N-terminal alkylated amino acid[182]. Siderophores, another important class of NRPs, are iron-chelating compounds produced by microorganisms that play an important role in microbe-plant and microbe-pathogen interaction. Well-studied siderophores are pyoverdines from *Pseudomonas*, desferrioxamine from *Streptomyces* and coprogens from *Trichoderma*[183,184].

*Polyketides*

Polyketides (PKs) are the most abundant and structurally diverse microbial secondary metabolites. PKs are synthesized by highly complex polyketide synthase (PKS), which are a family of multidomain enzymes. The biosynthesis of these natural compounds is another example of thiotemplate process and is related to fatty acids mechanism. The process allows for a greater complexity and variability of the products due to the optional event of ketone reduction occurring during PKs synthesis[185]. The mechanism involves an acyl carrier protein that binds the growing acyl chain, acyl transferases that select the elongation units (usually short chain carboxylic acids) and upload them to the carrier protein, and a ketosynthase that catalyzes the bond formation between the assembled chain and the new unit. At the C-terminal there is a thioesterase responsible for product release. Other domains such as ketoreductase, dehydratase and enoyl reductase are optional for reductive modifications at the end of the main process. The most common fungal PKSs belong to type I characterized by only one module that repeatedly carry out reactions to elongate the acyl chain. Bacteria have both non-iterative type I PKSs, containing individual modules with domains for each elongation step and iterative type II PKSs. Aflatoxins, tetracyclines, erythromycin are among the most famous microbial polyketides[183,186].

*PK-NRP hybrids*

Many metabolites with remarkable biological activities contain a polyketide backbone combined to an amino acid. Several fungal and bacterial genomic analyses showed evidence of PKS-NRPS hybrid clusters having elements from both classes of enzymes due to structural and catalytic similarities[187].

Important examples of bacterial hybrid molecules include yersiniabactin, a siderophore and virulence factor produced by *Yersinia pestis*, rhizoxin, first isolated from the fungal endosymbiont *Burkholderia rhizoxinica* and then from *Pseudomonas fluorescens*[188–191]. Fungal PKS-NRPS hybrid synthetases are involved in the biosynthesis of several secondary metabolites, including the yellow pigment tenellin produced by *Beauveria bassiana* (an important entomopathogenic fungus) and harzianic acid, a siderophore tetramic acid

derivative produced by *T. harzianum*, that showed a concentration-dependent growth promoting and antibiotic activity and a good affinity with iron[49,192,193].

*Terpenes*

Terpenes are one of the largest classes of natural products, comprising several agriculturally important bioactive secondary metabolites. They can be linear or cyclic, unsaturated, differently derivatized and have common biosynthetic precursors: isopentenyl diphosphate (IPP) and dimethylallyl diphosphate (DMAPP). The repetitive addition of precursors and the involvement of different enzymes lead to the formation of structurally diverse terpenes, classified according to the number of IPP units contained in the backbone: hemiterpenes ($C_5$), monoterpenes ($C_{10}$), sesquiterpenes ($C_{15}$), diterpenes ($C_{20}$), sesterterpenes ($C_{25}$), triterpenes ($C_{30}$), and tetraterpenes ($C_{40}$)[194]. Trichotecenes, carotenoids, aristolochenes are examples of fungal terpenes, while geosmin, emitted by *Streptomyces* spp., is an example of bacterial terpene. Finally, gibberellins are terpenes widespread among fungi, bacteria and plants[182,183,195–197]. Some important microbial metabolites, belonging to the groups of natural products mentioned above, are reported in **Figure** 1.

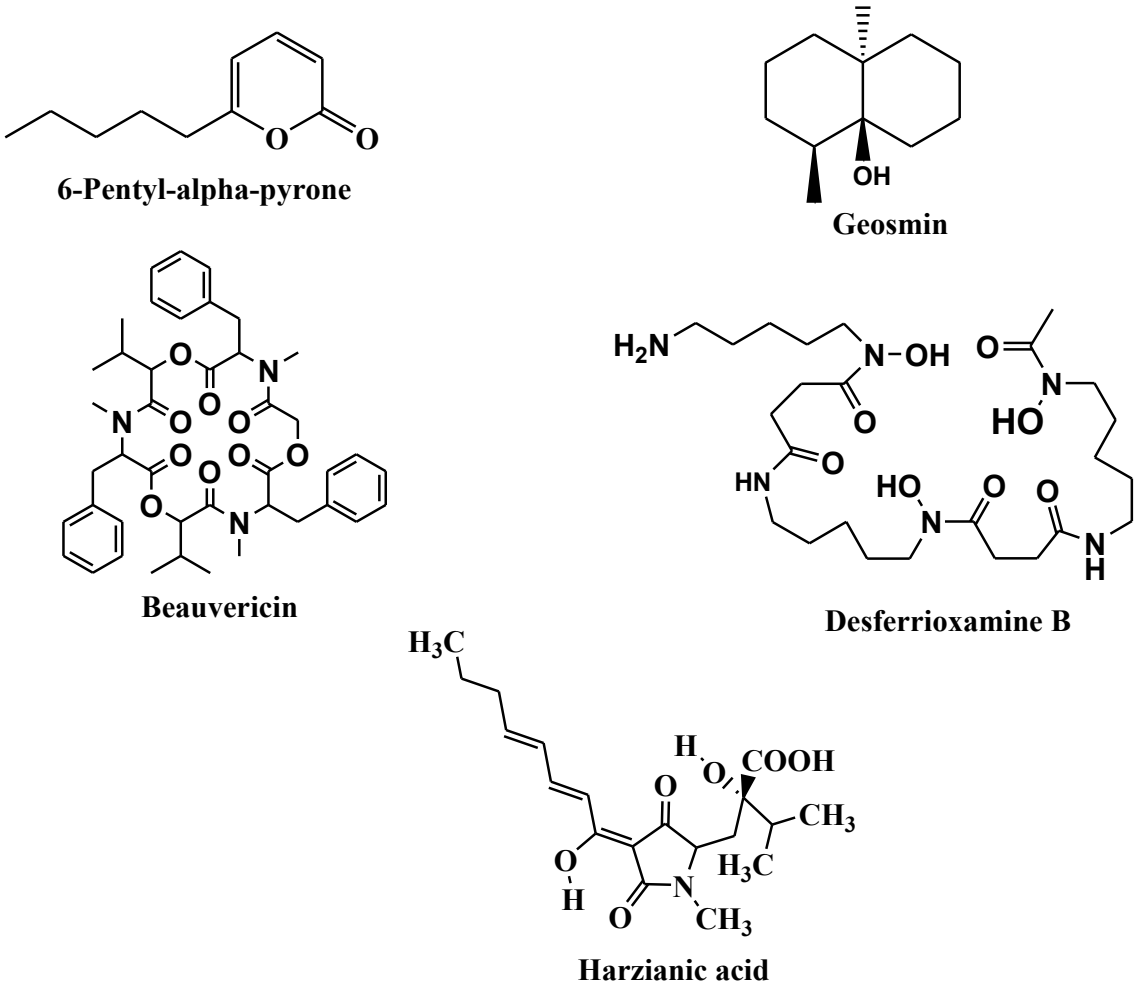


**Figure** 1**:** Chemical structures of important bioactive secondary metabolites produced by *Trichoderma* (6-pentyl-alpha-pyrone, harzianic acid); *Streptomyces* (geosmin, desferrioxamine B); and *Beauveria* (beauvericin).

## Aim of the research

The global market for plant bioproducts continues to evolve due to the change in legislations and regulations, to the conversion from conventional farming system to ICM and IPM and to the increasing population awareness about pollution and other environmental issues[196,197].

Most of the novel eco-sustainable approaches employed for plant protection and growth promotion involve the use of single-strain inoculants, while a growing body of evidence demonstrates the great potential of beneficial association of microorganisms and natural bioactive products[198–200]. Synthetic microbial consortia (bacteria-bacteria, fungi-fungi or bacteria-fungi), co-application of two or more different microorganisms, or of microbes and natural products could activate synergistic beneficial effects or establish innovative microbial communities when the application of a single inoculant fails[197,201–204].

Selected microbial strains play a pivotal role as primary source of secondary metabolites for drug discovery and application in both medical and agricultural fields[205,206]. The research process traditionally focuses on the extraction and purification of single bioactive compounds from fermentation broth and/or mycelium in standard laboratory conditions. However, the number of new metabolites is getting lower due to the re-isolation of known molecules. Extensive whole-genome sequencing of several microorganisms has revealed a great number of genes, encoding biosynthetic enzymes, that are not expressed under standard laboratory conditions[207–210]. In order to fully exploit the potential of these genes, different strategies have been developed such as genome mining, microbial metagenomics, heterologous expression and variation of culture conditions[207,211–213]. The latter strategy is considered the simplest and most effective tool to identify novel natural products and it is called "one strain many compounds" (OSMAC) strategy[214]. It is well known that different stimuli can trigger the activation or up-regulation of biosynthetic pathways that lead to the production of specific secondary metabolites. It is possible to artificially mimic changes in the environment by variation of culture conditions, such as medium composition, pH, temperature and oxygen concentration[215–218]. Co-cultivation with other strain(s) also fits into the OSMAC strategy; it has been demonstrated that the interaction between microorganisms (competitive, antagonistic or compatible) or with the plants (i.e. plant tissues) leads to the characterization of new molecules, not detected in standard single strain cultures[219–221].

In this context, 'omics studies can help to understand the mechanisms of these interactions and can guide the selection of active principles (microbes and/or bioactive metabolites) for new bio-formulates.

With the aim of discovering new formulations for agricultural uses based on microbials and/or bioactive metabolites, a metabolomic approach has been used to investigate the compatibility of different beneficial strains (i.e., *Trichoderma, Streptomyces*,

*Azotobacter*). Therefore the selected combinations have been tested on different crops of agricultural importance (parsley, basil, olive drupes), in order to evaluate the effect of these combinations on yield, growth, pathogens biocontrol and nutritional value. Moreover, the metals chelating properties of harzianic acid (a known *Trichoderma* bioactive compound) have been evaluated in order to discover new possible applications in soil remediation and/or as biostimulant. Metabolomics demonstrated to be a versatile tool to evaluate treatment performances and chelating effects.

Below, there is a summary of the papers published, reporting results obtained by using different metabolomic approaches.

- Improvement of Nutraceutical Value of Parsley Leaves (*Petroselinum crispum*) upon Field Applications of Beneficial Microorganisms;
- Bioformulations with Beneficial Microbial Consortia, a Bioactive Compound and Plant Biopolymers Modulate Sweet Basil Productivity, Photosynthetic Activity and Metabolites;
- Effect of Selected *Trichoderma* Strains and Metabolites on Olive Drupes;
- Bivalent Metal-Chelating Properties of Harzianic Acid Produced by *Trichoderma pleuroticola* Associated to the Gastropod *Melarhaphe neritoides*;
- Coordination Properties of the Fungal Metabolite Harzianic Acid toward Toxic Heavy Metals.

horticulturae

MDPI

*Article*

# Improvement of Nutraceutical Value of Parsley Leaves (*Petroselinum crispum*) upon Field Applications of Beneficial Microorganisms

**Alessia Staropoli [1,2,*], Anastasia Vassetti [1], Maria Michela Salvatore [3], Anna Andolfi [3,4], Maria Isabella Prigigallo [5], Giovanni Bubici [5], Marina Scagliola [6], Pasquale Salerno [6] and Francesco Vinale [2,4,7]**

1 Department of Agricultural Sciences, University of Naples Federico II, 80055 Portici, Italy; an.vassetti@libero.it
2 Institute for Sustainable Plant Protection, National Research Council, 80055 Portici, Italy; frvinale@unina.it
3 Department of Chemical Sciences, University of Naples Federico II, 80126 Naples, Italy; mariamichela.salvatore@unina.it (M.M.S.); andolfi@unina.it (A.A.)
4 BAT Center—Interuniversity Center for Studies on Bioinspired Agro-Environmental Technology, University of Naples Federico II, 80055 Portici, Italy
5 Institute for Sustainable Plant Protection, National Research Council, 70126 Bari, Italy; mariaisabella.prigigallo@ipsp.cnr.it (M.I.P.); giovanni.bubici@ipsp.cnr.it (G.B.)
6 Spagro srl, 76121 Barletta, Italy; marina_89@alice.it (M.S.); info@spagro.it (P.S.)
7 Department of Veterinary Medicine and Animal Productions, University of Naples Federico II, 80137 Naples, Italy
* Correspondence: alessia.staropoli@unina.it

**Abstract:** Parsley (*Petroselinum crispum*) is an important aromatic herb that has gained importance in food and cosmetic industry, and it is used as medicinal plant due to the presence of compounds with biological activity. Several studies have demonstrated antioxidant, antimicrobial or cancer chemopreventive activity of different parts of parsley plants. We showed that the nutritional value of parsley leaves can be improved by treatments with beneficial microorganisms on the field crop. *Streptomyces fulvissimus* strain AtB-42 and *Trichoderma harzianum* strain T22 were applied, as singly or in combination (microbial consortium), at transplanting and two weeks later. After harvesting, plants were subjected to metabolomic analysis by LC and GC-MS. Spectrometric analysis resulted in the identification of seven polar metabolites. Results showed a significant difference in relative abundance of these metabolites among treatments. The AtB-42 application, alone or in combination with T22, induced the accumulation of petroselinic acid, while T22, alone or in combination, induced the accumulation of xanthotoxol/bergaptol and its derivative xanthotoxin/bergapten. The microbial consortium increased the accumulation of capsanthone compared to single treatments. No statistically relevant differences were found for the volatile fraction. It can be concluded that *S. fulvissimus* and *T. harzianum* significantly induced metabolic profile change of parsley and the accumulation of metabolites with nutraceutical value.

**Keywords:** microbe-assisted crop production; *Streptomyces*; *Trichoderma;* metabolomics; LC-MS

## 1. Introduction

Parsley (*Petroselinum crispum* (Mill.) Fuss; family *Apiaceae*) is an aromatic herb which has gained popularity for the food and cosmetic industries due to its antioxidant compounds [1]. The presence of a broad range of active compounds detected in this

plant allows the application of parsley as medicinal plant with various proven pharmacological properties including antioxidant, hepatoprotective and neuroprotective [2–4]. Parsley leaf, stem and roots are rich in minerals and bioactive metabolites such as vitamins (vitamin C being the most abundant), essential oils, pigments, polyphenols and fatty acids [5,6]. Liberal et al. (2020) [7] analyzed the phenolic profile and bioactivity of hydroethanolic extracts from parsley leaf samples from 25 cultivars finding that the leaves of all the varieties of *P. crispum* tested were a good source of natural products that confer health benefits. Characterization of these extracts showed the presence of apigenin and kaempferol as the most abundant phenolic compounds, with antioxidant and antimicrobial activity against bacteria and fungi.

Many studies have been conducted in order to evaluate the effect of production factors on yield and on phytochemicals content of different crops [8,9]. Among these, the application of beneficial microorganisms plays an important role in the modern agriculture due to their ability to control phytopathogenic agents through multiple mechanisms, such as antibiosis, mycoparasitism and competition for nutrients and space [10,11]. Biological control involves the use of beneficial organisms, selected strains and/or their metabolites, which can produce positive effects on plants by promoting their growth, increasing resistance levels and promoting the assimilation of nutrients. In the recent years, many microorganisms have been used as Biological Control Agents (BCAs) including strains belonging to bacterial genera and species such as *Agrobacterium*, *Pseudomonas*, *Streptomyces* and *Bacillus*; and fungal genera and species such as *Gliocladium*, *Trichoderma*, *Ampelomyces*, *Candida* and *Coniothyrium* [12]. Streptomycetes are Gram-positive filamentous bacteria in the *Streptomycetaceae* family, widely distributed in soils and rhizospheres. Streptomycetes are one of the major microbial sources of antibiotic molecules used in pharmaceutical and agricultural sector. They produce a wide variety of bioactive secondary metabolites, such as antifungal, antiviral, antitumor, anti-hypertensive and immunosuppressant molecules [13,14]. Moreover, Streptomycetes have an exceptionally large number of hydrolytic enzymes enabling them to interact with other organisms in the environment. All these biological features suggest that Streptomycetes are excellent biological control agents [15–18]. Selected *Trichoderma* species are used as biocontrol agents and bio-stimulants due to their ability to protect plants, compete with pathogens and produce several biologically active compounds including cell wall degrading enzymes and secondary metabolites [19]. The ability of *T. harzianum* strain T22 and *T. atroviride* strain P1 to improve growth was investigated in several experiments on lettuce, tomato and pepper plants under field conditions [16]. It was also tested on parsley plants demonstrating an increase in total fresh and dry mass and root system, superior to the controls when applied on soil under greenhouse conditions [20].

The present study aimed to evaluate the effects of beneficial microorganisms on the metabolic profile of parsley. *Streptomyces fulvissimus* (strain AtB-42) and *T. harzianum* (strain T22) have been selected for the present study due to their well-known characteristic as bio-stimulants and biological control agents [15–21]. In order to investigate the chemical profile of parsley plants (*P. crispum* var. *neapolitanum*) and to detect their changes after treatments, a metabolomic approach based on mass spectrometry was used.

## 2. Materials and Methods

### *2.1. Field Trial*

The trial was established in an open field located at 41°13′22.0″ N, 16°20′00.2″ E, Andria, Apulia, Italy. In January, 30-day old parsley seedlings were transplanted in single rows at 10 cm distance on the row and 20 cm between rows. The trial consisted of four treatments: control (C), *T. harzianum* strain T22 (T), *S. fulvissimus* strain AtB-42 (S) and a combination of the two microorganisms (S + T). The treatments were carried out at transplanting by dipping roots for 15 min in conidia/spore suspensions ($1 \times 10^7$ conidia

or spores per milliliter) and one month later by soil drenching 25 mL per plant of conidia/spore suspensions ($1 \times 10^7$ conidia or spores per milliliter).

Starting from a glycerol stock collection tube (Corning® cryogenic vials, Merck KGaA, Darmstadt, Germany), AtB-42 inoculum was prepared in 1 L bottles with 300 mL potato dextrose broth (PDB, Condalab, Madrid, Spain), incubated at 25 °C and 200 rpm for 7 days. Then, the culture was centrifuged at 8000× *g* for 10 min to remove the supernatant and resuspend the pellet in sterile distilled water. Spore concentration was estimated by using a Thoma chamber. *S. fulvissimus* strain AtB-42 was previously selected from a consortium of ca. 300 rhizosphere-competent isolates [15]. *Trichoderma harzianum* strain T22 was purchased from Koppert (Trianum WG, Koppert Biological Systems, Piracicaba, SP, Brazil). Inoculum of *T. harzianum* strain T22 was prepared by suspending the commercial product in water to achieve the desired conidia concentration (final concentration for treatments: $10^7$ spore $mL^{-1}$).

A randomized complete block design with three blocks was adopted. Blocks were separated by untreated plants (extra plants) to avoid any contamination during the applications of microorganisms. Thirty plants per treatment in each block were used for a total of 360 plants in the entire trial.

Plants were cultivated according to the agronomic practices commonly used in the farm. At the end of crop cycle (three months), plant height and shoot fresh weight were measured on 10 plants per treatment. Twenty plants (five biological replicates per treatment) were stored at −80 °C until the metabolomics analysis was completed. Biometric index data were analyzed by one-way ANOVA using Minitab statistical software (Minitab, LLC, State College, PA, USA). Significant differences among treatments were estimated according to Tukey's test with a 0.05 significance level.

### *2.2. Metabolite Extraction*

Lyophilized powder obtained from leaves was subjected to extraction in organic solvents. In particular, 100 mg of powder for each biological replicate was suspended in 2 mL of methanol (MeOH; LC-MS purity) and vortexed for 30 s. Samples were then centrifuged for 10 min at 14,000 rpm at 4 °C. Each supernatant was diluted 1:10 in MeOH and injected into the LC-MS qTOF (liquid chromatography-mass spectrometry-quadrupole-time of flight) system. All reagents used were purchased from Sigma-Aldrich (St. Louis, MO, USA) unless otherwise stated.

### *2.3. Isolation of Volatile Fraction*

Leaf samples (50 g) stored at −80 °C were hydrodistilled with 600 mL of distilled water in Clevenger apparatus for 2 h according to the European Pharmacopoeia [22]. The water containing dissolved oils was extracted three times with dichloromethane (50 mL), and the extracts were collected and dried over anhydrous sodium sulphate. The samples were stored in sealed glass vials at −20 °C before the analysis. The extraction was carried out by triplicate.

### *2.4. LC-MS Analysis*

Analyses were conducted on an Agilent HP 1260 Infinity Series liquid chromatograph coupled to a Q-TOF mass spectrometer and equipped with a DAD system (Agilent Technologies, Santa Clara, CA, USA). A Zorbax Extend C-18 column (4.6 × 50 mm, 3.5 µm, Agilent Technologies) was used for chromatographic separation, held at a constant temperature of 37 °C. The analyses were performed at a 0.6 mL $min^{-1}$ flow rate, using a linear gradient system composed of 0.1% (v/v) formic acid in water (eluent A) and 0.1% (v/v) formic acid in acetonitrile (eluent B). The gradient program was as follows: from 5% to 70% eluent B in 4 min, isocratic at 70% of eluent B from 4 to 5 min; from 70% to 80% of eluent B from 5 to 8 min and from 80% to 100% eluent B from 8 to 10 min; and,

finally, lowering to starting conditions (5% eluent B) from 10 to 15 min. After returning to the initial conditions, equilibration was achieved after 1 min. The injection volume was 10 µL. UV spectra were collected by DAD every 0.4 s from 190 to 750 nm, with a resolution of 2 nm. The MS system was equipped with a Dual Electrospray Ionization (ESI) source and operated both in positive and negative mode. The capillary was maintained at 2000 V, fragmentor voltage at 180 V, cone 1 (skimmer 1) at 45 V and Oct RFV at 750 V. Gas flow rate was set at 11 L $min^{-1}$, at 350 °C, and the nebulizer was set at 45 psig. Mass spectra were recorded within the *m/z* range 100–1700 as centroid spectra, with three scans per second. In order to perform real time mass-lock correction, a solution consisted of purine ($C_5H_4N_4$, *m/z* 121.050873, 10 µmol $L^{-1}$), and hexakis (1H,1H,3H-tetrafluoropentoxy)-phosphazene ($C_{18}H_{18}O_6N_3P_3F_{24}$, *m/z* 922.009798, 2 µmol $L^{-1}$) was constantly infused by an Isocratic pump (1260 Infinity Series, Agilent Technologies) with a flow rate of 0.06 mL $min^{-1}$. All MS and HPLC parameters were set with Agilent MassHunter Data Acquisition Software, rev. B.05.01.

### *2.5. GC-MS Analysis*

The analyses of the essential oils were performed by using an Agilent 6850 GC (Agilent Technologies) coupled to an Agilent 5973 Inert MS. The amount of 2 µL of each sample was injected in splitless mode into an HP-5MS capillary column (5% phenyl methyl poly siloxane stationary phase). The injection temperature was 250 °C, and the temperature ramp raised the column temperature from 70 °C to 280 °C: 70 °C for 1 min; 10 °C·$min^{-1}$ until reaching 170 °C; and 30 °C·min-1 until reaching 280 °C. Subsequently, it was held at 280 °C for 5 min. Helium was used as a carrier gas at a flow rate of 1 mL $min^{-1}$. The solvent delay was set to 4 min. Measurements were performed under electron impact (EI) ionization (70 eV) in full scan mode (*m/z* 29–550) at a frequency of 3.9 Hz. The EI ion source and quadrupole mass filter temperatures were kept, respectively, at 200 °C and 250 °C.

The identification of compounds was based on comparison of their mass spectra with those recorded in the NIST 14 mass spectral library (https://www.nist.gov/srd/nist-standard-reference-database-1a, accessed on 09/07/2021). Furthermore, the identification was supported by Kovats retention index (RI) calculated for each analyte by the Kovats equation, using the standard *n*-alkane mixture in the range C7-C40 (Sigma-Aldrich, Saint Louis, MO, USA).

### *2.6. Statistical Analysis of Metabolomics Data*

Statistical analysis was carried out by using Mass Profile Professional software, version 13.1.1 (Agilent Technologies). Raw data of leaf extracts were grouped by the treatment applied in the field (i.e., single strains or microbial consortium), and these groups were subjected to one-way ANOVA ($p$-value < 0.05) and to fold change ≥ 2.0. Thus, the results obtained were subjected to principal components analysis (PCA) and hierarchical clustering in order to compare metabolic profiles of plants and to detect differences induced by different treatments. Statistically relevant compounds were identified using a plant database, FooDB Version 1.0 (www.foodb.ca, accessed on 10/03/2021; freely available), and by comparison with data available in the literature. Among the detected molecules, only those with a mass error below 10 ppm and a sufficient score were reported.

## 3. Results

### *3.1. Plant Growth*

Beneficial microbial treatments positively affected the growth and development of parsley. At the end of crop cycle (3 months), plant height increased in plants treated with

single cultures (T22 or AtB42) compared to the control, and the fresh weight increased in all treatments compared to the control (Figure 1).

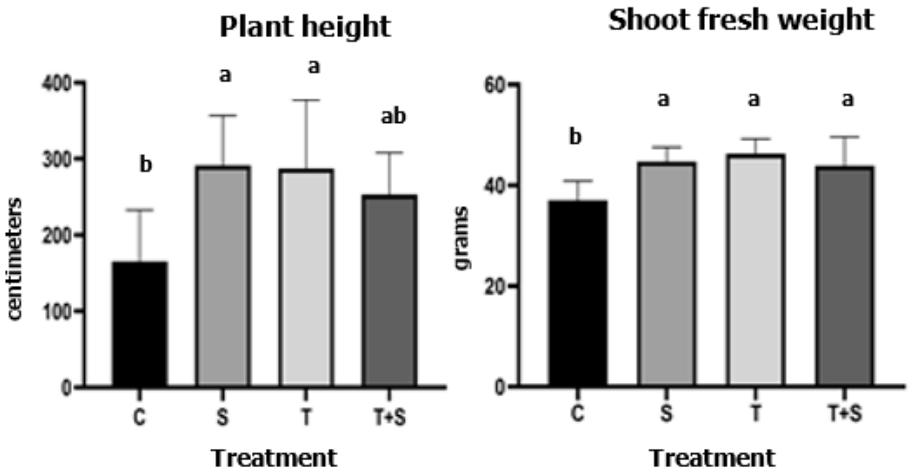


**Figure 1.** Variation of plant height (**left**) and shoot fresh weight (**right**) of parsley plants treated with *Streptomyces fulvissimus* AtB-42 (S), *Trichoderma harzianum* T22 (T), microbial consortium (S + T) and control group (C). Treatments with the same letter are not significantly different according to Tukey's test ($p$-value < 0.05). Error bars represent standard deviation.

### *3.2. Metabolomic Analysis*

An extraction protocol, starting from lyophilized leaf powder, was carried out. The extracts were subjected to LC-MS analysis. The resulting total ion chromatograms (TIC) and mass spectra were analyzed, and putatively identified compounds were obtained by comparison with data reported in literature and a freely available electronic food database (FooDB). Figure 2 shows the chromatogram of the extract of T22-treated plants (recorded in positive mode). Putatively identified metabolites are reported in Table 1, while Figures S1 and S2 show the comparisons between the recorded chromatograms for the different conditions in positive and negative mode, respectively.

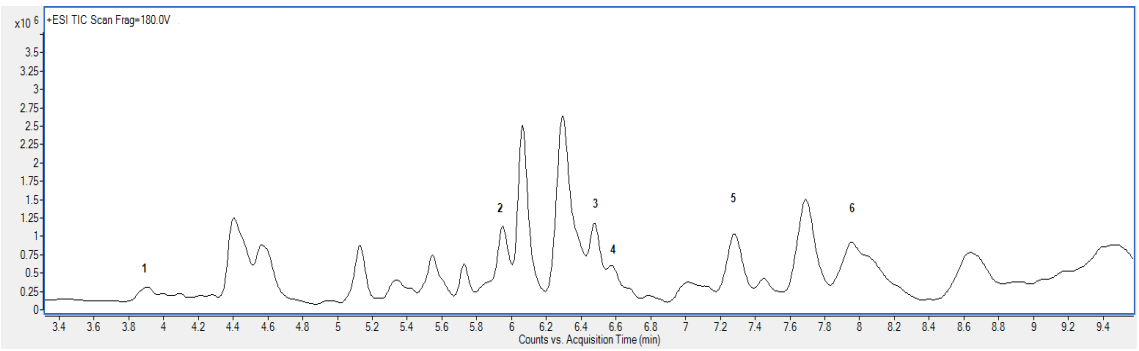


**Figure 2.** Magnified total ion chromatogram of the extract of T22-treated plants recorded in positive mode. Putatively identified metabolites and the corresponding peak numbers in the figure are reported in Table 1.

**Table 1.** Putatively identified metabolites in parsley extract obtained by LC-MS analysis. Data include peak number as reported in Figure 2, retention time, experimental and theoretical mono-isotopic mass and molecular formula.

| N. | Compound | RT (min) | Experimental Mass (Da) | Theoretical Mass (Da) | Molecular Formula |
|---|---|---|---|---|---|
| 1 | Isorhamnetin 3,7-di-*O*-beta-glucopyranoside | 3.848667 | 640.1663 | 640.1639 | $C_{28}H_{32}O_{17}$ |

| | | | | | |
|---|---|---|---|---|---|
| 2 | Xanthotoxin/Bergapten * | 6.000033 | 216.0427 | 216.0422 | $C_{12}H_8O_4$ |
| 3 | Capsanthone | 6.425001 | 582.4098 | 582.4072 | $C_{40}H_{54}O_3$ |
| 4 | Petroselinic acid | 6.530999 | 282.257 | 282.2558 | $C_{18}H_{34}O_2$ |
| 5 | Bergaptol/Xanthotoxol * | 7.286808 | 202.0272 | 202.0266 | $C_{11}H_6O_4$ |
| 6 | Piperochromanoic acid | 7.955463 | 356.198 | 356.1988 | $C_{22}H_{28}O_4$ |
| - | Quinic acid ** | 0.9503336 | 192.0642 | 192.0633 | $C_7H_{12}O_6$ |

* Stereoisomers for which it was not possible to make a distinction in the chromatogram. ** Putatively identified molecule from LC-MS analysis performed in negative mode.

Data obtained by LC-MS analysis, i.e., molecular weights, retention times and intensity values, were analyzed statistically. Results were then subjected to Principal Component Analysis (Figure 3) and depicted as hierarchical cluster (Figures S3 and S4). The two graphs indicate that there is a difference in metabolic profiles depending on the treatment applied on parsley plants. A distinct separation among samples differently treated is evident in principal components (PC1–PC2) of the variance in the LC-MS dataset, particularly for data obtained in negative mode.

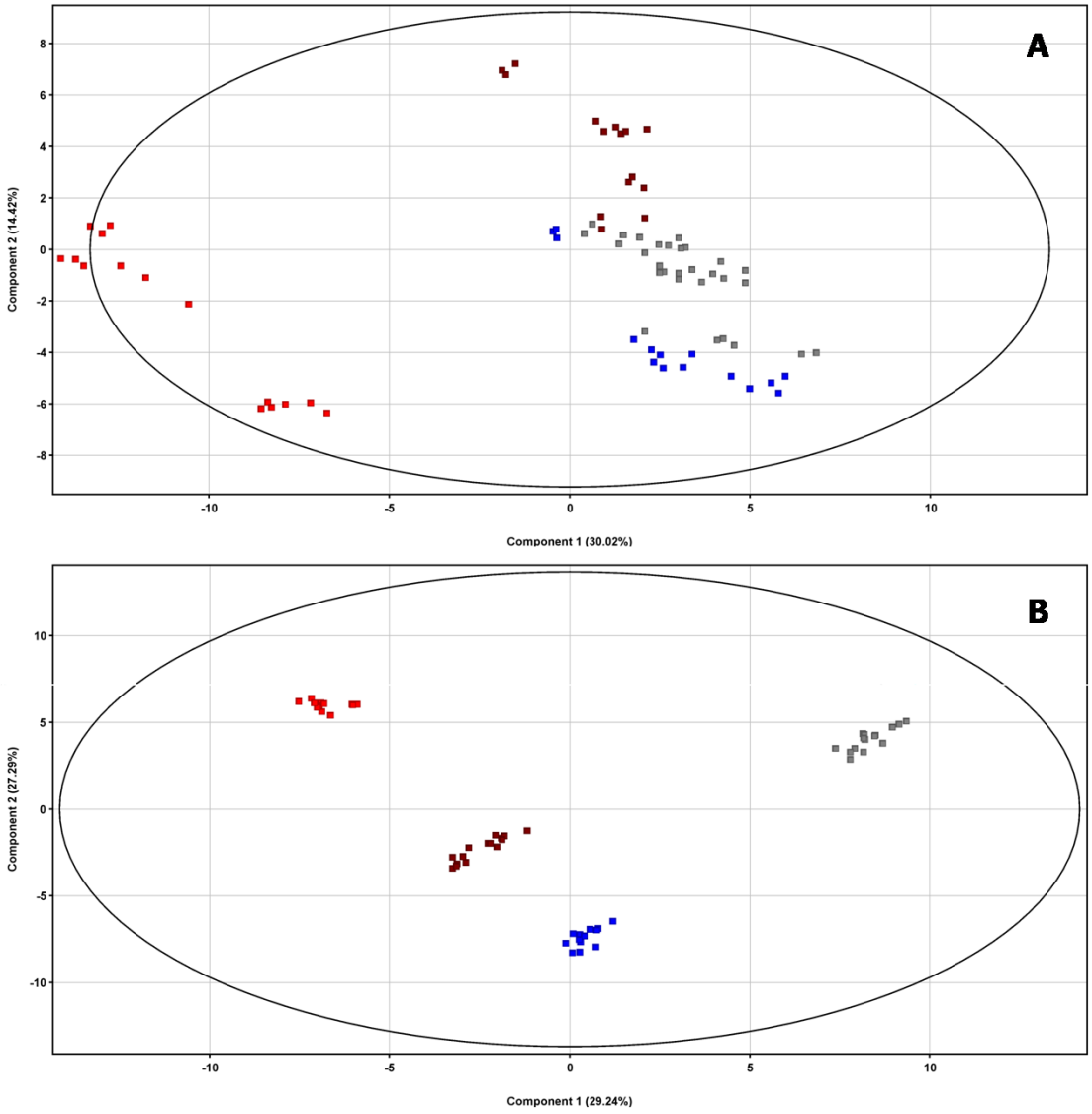


**Figure 3.** Principal components analysis (PCA) score plots of the LC-MS data acquired for positive (**A**) and negative (**B**) mode. Each group of replicates subjected to different treatments is depicted with a different color: control group (C) is red; *Streptomyces* group (S) is blue; *Trichoderma* group (T) is grey; microbial consortium (S + T) is brown.

Metabolomic analysis highlighted several differentially accumulated metabolites (Tables S1 and S2) for which their abundance is dependent on the treatment applied, and it is related to the function performed in plant. Among those metabolites, six were identified in positive mode analysis and one in negative mode and reported in Table 2 together with regulation against control group and single cultures.

**Table 2.** Putatively identified metabolites that are differentially accumulated in plants treated with *Streptomyces* (S), *Trichoderma* (T) or a mix of those two (S + T) compared to control group (C) plants and the microbial consortium (S + T) compared to *Streptomyces* (S) and *Trichoderma* (T) single culture.

| Compound | Regulation | | | | |
|---|---|---|---|---|---|
| | S vs. C | T vs. C | S + T vs. C | S + T vs. S | S + T vs. T |
| Xanthotoxin/Bergapten * | ↓ | ↑ | ↓ | ↓ | ↓ |
| Piperochromanoic acid | ↑ | ↑ | ↓ | ↓ | ↓ |
| Xanthotoxol/Bergaptol * | ↓ | ↓ | ↓ | ↑ | ↓ |
| Isorhamnetin 3,7-di-O-beta-glucopyranoside | ↓ | ↓ | ↓ | ↓ | ↓ |
| Petroselinic acid | ↑ | ↓ | ↓ | ↓ | ↑ |
| Capsanthone | ↓ | ↓ | ↓ | ↑ | ↑ |
| Quinic acid | ↑ | ↑ | ↑ | ↑ | ↑ |

* Stereoisomers for which it was not possible to make a distinction in the chromatogram. ↑ Upregulated against C, S or T group. ↓ Downregulated against C, S or T group.

With the aim to reveal potential differences in volatile compounds produced by *P. crispum* treated with different beneficial microorganisms, GC-MS analyses of the hydrodistilled oils of leaves were conducted. Many investigators have studied the chemical composition of the volatile fraction of parsley, and it has been found to be variable [23–26]. The essential oils of samples were essentially constituted by apiol, α-pinene, 1,3,8-p-mentha-triene, myristicin, β-phellandrene and myrcene. Apiol is the main constituent in the examined parsley cultivars. The results of our investigation show no significant effect of treatments on the volatile fraction of the parsley leaves.

All the structures of the molecules putatively identified by LC and/or GC-MS analyses are reported in Figure 4.

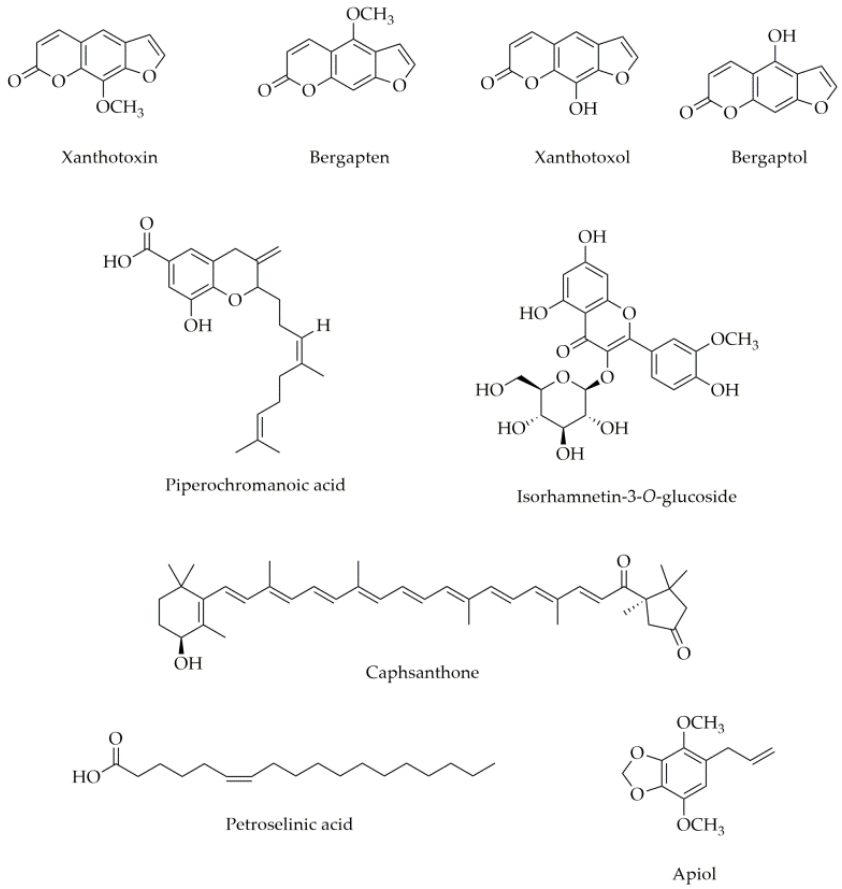


**Figure 4.** Structures of the molecules putatively identified from LC-MS and GC-MS analysis. Apiol is the metabolite identified from GC-MS analysis, and it is the most abundant compound in parsley volatile fraction.

## 4. Discussion

In the present study we investigated the effects of *S. fulvissimus* strain AtB-42, *T. harzianum* strain T22 and their mixture on a parsley crop in the field, together with the alteration of the plant metabolic profile after treatments. T22 and AtB42 were selected because they are well-known BCAs and bioactive metabolite-producers. Our data (Figure 1) show that single inoculants (T22 or AtB-42) affected the growth by increasing plant height after two treatments, while the microbial consortium (T22 + AtB-42) positively affected the shoot fresh weight. These data are consistent with other studies which have shown the effect of different fungal and bacterial strains on different crops [20,27–30].

Previous research has documented the biological activity (antioxidant, hepatoprotective, antimicrobial) of several classes of phytochemicals that can be found in different parts of parsley, such as flavonoids, coumarins or lipids [31–35]. However, to our knowledge, this is the first study to investigate the change in parsley metabolome induced by treatments with biocontrol agents. It is evident from Table 2 that the application of different treatments based on beneficial microbes affected the metabolic profile of parsley both in terms of different molecules detected and in terms of relative abundance. Among the differentially accumulated molecules, we putatively identified xanthotoxin/bergapten, piperochromanoic acid, xanthotoxol/bergaptol, isorhamnetin 3,7-di-*O*-beta-glucopyranoside, petroselinic acid, capsanthone and quinic acid. These metabolites belong to different classes of natural products and are the main active components already isolated and detected in parsley [5].

Coumarin and its derivatives (bergapten, isopimpinellin and xanthotoxin, etc.) are a class of compounds widely distributed in *Apiaceae* family, which is one of the most

prominent food sources of coumarins. These molecules are reported to have curative, preventive or nutritive value and also showed antimicrobial activity [36]. Pathogen-infected plants of several species demonstrated an increased level in coumarin derivatives [37]. Cultured parsley cells treated with fungal elicitors increased the production of furanocoumarins xanthotoxol and bergaptol, and it was also demonstrated that xanthotoxin and bergapten were the most abundant coumarin derivatives accumulated in the culture fluid of elicitor-treated parsley cells [38]. Our findings show that bergaptol/xanthotoxol was less abundant in treated plants compared to control. Furthermore, from the comparison of plants treated with AtB-42 + T22 consortium (S + T) and plants treated with AtB-42 (S) alone, bergaptol/xanthotoxol was more abundant in the first group. A similar trend applies to their product xanthoxin/bergapten that resulted in less abundance in treated plants than in control, except for plants treated with T22 (T) in which a greater accumulation of this compound was evident. We may suppose that the application of beneficial microorganisms such as *Trichoderma* and *Streptomyces* explicated an effect as biocontrol agents preventing any pathogen infection and inducing a minor production of coumarins and their derivatives.

The compound isorhamnetin 3,7-di-*O*-beta-glucopyranoside belongs to flavonoids, which are a class of compounds dominant in parsley. Flavonoids are plant natural products with a wide range of activity: They contribute to plant color, have roles in plant growth and development and exhibit a wide range of biological properties including antimicrobial, insecticidal and estrogenic activities [39]. Flavonoids extracted from parsley leaves demonstrated antioxidant, hepato-protective and antidiabetic properties in vivo [5]. As reported in Table 2, this compound is always downregulated in treated plants compared to the control. However, plants treated with *Streptomyces* (S) or *Trichoderma* (T) alone showed a greater accumulation of isorhamnetin 3,7-di-*O*-beta-glucopyranoside compared to plants treated with both microorganisms (S + T).

Petroselinic acid is a fatty acid that was isolated for the first time from *P. crispum* seeds oil in 1909 and is present as a major component in parsley seeds. Petroselinic acid is an important oleochemical active principle for food, cosmetic, chemical and pharmaceutical industry due to its interesting properties such as anti-aging and anti-inflammatory. A considerable amount of antimicrobial activity against several bacteria, yeast and mold species was observed [40,41]. In the present study, we detected a greater accumulation of this compound in plants treated with *Streptomyces* (S) against control and in plants treated with microbial consortium (S + T) vs. *Trichoderma* (T) treated plants. Yeganehpoor et al. in 2017 [42] estimated the effects of different conditions, including bio-fertilizer-based treatments, on chemical profile of coriander. A higher level of petroselinic acid was detected in plants treated with bio-fertilizer and in plants subjected to water stress.

Piperochromanoic acid belongs to a class of compounds known as prenol lipids. Prenol lipids (PR) are synthesized from the 5-carbon precursors isopentenyl diphosphate and dimethylallyl diphosphate. The simple isoprenoids (linear alcohols, diphosphates and so on) are formed by the successive addition of C5 units and are classified according to the number of these terpene units. This class includes the carotenoids, which are precursors of vitamin A and possess antioxidant effects [43].

Lipids are one of the most important biomolecules found in all plant tissues: they are a major component of bio-membranes and platform for lipid signaling. Abiotic stress such as water deficiency and high temperature triggers lipid-dependent signaling cascades, which control the expression of specific gene clusters and activate plant adaptation processes [44]. The application of single inoculants of *Trichoderma* (T) and *Streptomyces* (S) enhanced the production of piperochromanoic acid compared to the control.

Capsanthone is a member of the chemical class of xanthophylls, which are carotenoids containing an oxygenated carotene backbone. Carotenoids are pigments found in photosynthetic bacteria, some species of archaea and fungi, plants and animals. These

compounds also act as photo-protectors, antioxidants, color attractants and precursors of plant hormones. [45]. The abundance of capsanthone is increased in plants treated with the mix (S + T) compared to plants treated with single culture of *Streptomyces* (S) and *Trichoderma* (T).

Quinic acid is a dominant acid in green coffee beans and is also a product of the degradation of chlorogenic acids, which are one of the most abundant polyphenols present in green coffee beans and certain fruits and vegetables. Chlorogenic acids have been shown to contribute to the antioxidant, anti-inflammatory, antipyretic and antineoplastic properties of green coffee bean extracts [46]. A recent study demonstrated that methanol extract of *P. crispum* has an important level of quinic acid. Furthermore, this extract showed antioxidant activity, anti-adhesion and anti-proliferative proprieties against human glioblastoma cells [47]. Quinic acid detected through LC-MS analysis was upregulated in treated plants. This result is in agreement with previous studies that evaluated the effects of single specie or microbial consortia on pea plants [48] and of a combination of *T. harzianum* and compost on maize leaves [49].

The results of our investigation show no significant effect of treatments on the volatile fraction of parsley leaves. Dini et al. and Gębarowska et al. reported changes in the volatolome of olive tree and coriander after treatments with *T. harzianum* strain T22 [8,50]. Moreover, Coppola et al. demostrated that T22 enhanced tomato defense responses against aphids by inducing a higher production of volatile organic compounds (VOCs) [51].

In this investigation, the experimental design, based on interaction of parsley and beneficial microbes in field conditions, has been used as model to improve sustainable agricultural products. *S. fulvissimus* strain AtB-42 and *T. harzianum* strain T22, when either applied as single inoculants or in consortium, produce significant changes in the chemical profile of parsley leaves. The enhanced production of metabolites with antioxidant, anti-inflammatory or also anti-aging activity improve the commercial value of parsley.

Some compounds, such as isorhamnetin 3,7-di-*O*-beta-glucopyranoside, piperochromanoic acid and capsanthone, have been detected for the first time in parsley, and their abundance in plant tissue is still unknown. Further research is needed to gain deeper understanding of the biosynthetic pathway that results in the production of these molecules.

**Supplementary Materials:** The following are available online at https://www.mdpi.com/article/ 10.3390/horticulturae7090281/s1, Figure S1: Magnified total ion chromatogram of parsley extracts recorded in positive mode. From the top to the bottom: C is control group; S is *Streptomyces* group; S + T is the microbial consortium *Streptomyces* + *Trichoderma*; T is *Trichoderma* group, Figure S2: Total ion chromatogram of parsley extracts recorded in negative mode. From the top to the bottom: C is control group; S is *Streptomyces* group; S + T is the microbial consortium *Streptomyces* + *Trichoderma*; T is *Trichoderma* group, Figure S3: Hierarchical clustering heatmap of statistically different metabolites in control (C) group; microbial consortium of *Streptomyces* and *Trichoderma* (S + T) group; *Streptomyces* (S) group and *Trichoderma* (T) group. This result is obtained starting from LC-MS data recorded in positive mode and subjected to statistical analysis (one-way ANOVA $p < 0.05$ and fold change > 2.0), Figure S4: Hierarchical clustering heatmap of statistically different metabolites in control (C) group; microbial consortium of *Streptomyces* and *Trichoderma* (S + T) group; *Streptomyces* (S) group and *Trichoderma* (T) group. This result is obtained starting from LC-MS data recorded in negative mode and subjected to statistical analysis (one-way ANOVA $p < 0.05$ and fold change > 2.0), Table S1: Metabolites obtained from LC-MS data (positive mode) that are differentially accumulated in plants treated with *Streptomyces* (S), *Trichoderma* (T) or a mix of those two (S + T) compared to control group (C) plants and the microbial consortium (S + T) compared to *Streptomyces* (S) and *Trichoderma* (T) single

culture, Table S2: Metabolites obtained from LC-MS data (negative mode) that are differentially accumulated in plants treated with *Streptomyces* (S), *Trichoderma* (T) or a mix of those two (S + T) compared to control group (C) plants and the microbial consortium (S + T) compared to *Streptomyces* (S) and *Trichoderma* (T) single culture.

**Author Contributions:** Conceptualization, F.V. and G.B.; field trials and *Streptomyces* preparation: M.I.P., G.B., P.S., M.S. and P.S.; LC-MS analysis, A.S., F.V. and A.V.; GC-MS analysis, A.A. and M.M.S.; data curation, A.S., A.V., M.M.S. and A.A.; writing—original draft preparation, A.S. and A.V.; writing—review and editing, A.S., A.A., G.B., M.S and F.V. All authors have read and agreed to the published version of the manuscript.

**Funding:** This work was supported by PROTECTION Project (MISE CRESO grant number Protection no. F/050421/01-03/X32).

**Data Availability Statement:** The data presented in this study are available on request from the corresponding author.

**Conflicts of Interest:** The authors declare no conflicts of interest.

## References

1. Mahmood, S.; Hussain, S.; Malik, F. Critique of medicinal conspicuousness of Parsley (*Petroselinum crispum*): A culinary herb of Mediterranean region. *Pak. J. Pharm. Sci*. **2014**, *27*,193-202.
2. Farzaei, M.H.; Abbasabadi, Z.; Ardekani, M.R.S.; Rahimi, R.; Farzaei, F. Parsley: A review of ethnopharmacology, phytochemistry and biological activities. *J. Tradit. Chin. Med.* **2013**, *33*, 815–826.
3. Dini, I. Chapter 14—Spices and Herbs as Therapeutic Foods. In *Handbook of Food Bioengineering, Food Quality: Balancing Health and Disease*; Holban, A.M., Mihai Grumezescu, A., Eds.; Academic Press: Cambridge, MA, USA, 2018; pp. 433–469.
4. Dini, I.; Laneri, S. Nutricosmetics: A brief overview. *Phytother. Res*. **2019**, *33*, 3054–3063.
5. Dobricev, N.; Zabkur, J.; Voca, S.; Pliestic, S.; Galic, A.; Delic, A.; Fabek Uher, S. Bioactive compounds content and nutritional potential of different parsley parts (*Petroselinum crispum* Mill.). *J. Cent. Eur. Agric*. **2019**, *20*, 900–910.
6. Agyare, C.; Appiah, T.; Boakye, Y.D.; Apenteng, J.A. *Petroselinum crispum*: A review. In *Medicinal Spices and Vegetables from Africa, Therapeutic Potential Against Metabolic, Inflammatory, Infectious and Systemic Diseases*, 1st ed.; Kuete, V., Ed.; Academic Press: Cambridge, MA, USA, 2017; pp. 527–547.
7. Liberal, A.; Fernandes, A.; Polyzos, N.; Petropoulos, S.A.; Dias, M.I.; Pinela, J.; Petrović, J.; Soković, M.; Ferreira, I.C.F.R.; Barros, L. Bioactive properties and phenolic compound profiles of turnip-rooted, plain-leafed and curly-leafed parsley cultivars. *Molecules*. **2020**, *25*, 5606.
8. Dini, I.; Marra, R.; Cavallo, P.; Pironti, A.; Sepe, I.; Troisi, J.; Scala, G.; Lombari, P.; Vinale, F. *Trichoderma* Strains and Metabolites selectively increase the production of volatile organic compounds (VOCs) in Olive trees. *Metabolites* **2021**, *11*, 213.
9. Dini, I.; Graziani, G.; Gaspari, A.; Fedele, F.L.; Sicari, A.; Vinale, F.; Cavallo, P.; Lorito, M.; Ritieni, A. New strategies in the cultivation of Olive trees and repercussions on the nutritional value of the Extra Virgin Olive oil. *Molecules* **2020**, *25*, 2345.
10. Vejan, P.; Abdullah, R.; Khadiran, T.; Ismail, S.; Nasrulhaq Boyce, A. Role of plant growth promoting rhizobacteria in agricultural sustainability—A review. *Molecules.* **2016**, *21*, 573.
11. Vinale, F.; Sivasithamparam, K.; Ghisalberti, E.L.; Marra, R.; Woo, S.L.; Lorito, M. *Trichoderma*–plant–pathogen interactions. *Soil Biol. Biochem*. **2008**, *40*, 1–10.
12. Bubici, G. *Streptomyces* spp. as biocontrol agents against *Fusarium* species. *CAB Rev*. **2018**, *13*, 50.

13. Sivalingam, P.; Hong, K.; Pote, J.; Prabakar, K. Extreme environment *Streptomyces*: Potential sources for new antibacterial and anticancer drug leads? *Int. J. Microbiol.* **2019**, *2019*, 20.
14. Manteca, Á.; Yagüe, P. *Streptomyces* Differentiation in liquid cultures as a trigger of secondary metabolism. *Antibiotics* **2018**, *7*, 41.
15. Bubici, G.; Marsico, A.D.; D'Amico, M.; Amenduni, M.; Cirulli, M. Evaluation of *Streptomyces* spp. for the biological control of corky root of tomato and *Verticillium* wilt of eggplant. *Appl. Soil Ecol.* **2013**, *72*, 128–134.
16. Vinale, F.; Sivasithamparam, K. Beneficial effects of *Trichoderma* secondary metabolites on crops. *Phytother. Res.* **2020**, *34*, 2835–2842.
17. Ebrahimi-Zarandi, M.; Bonjar, G.H.S.; Riseh, R.S.; El-Shetehy, M.; Saadoun, I.; Barka, E.A. Exploring two *Streptomyces* species to control *Rhizoctonia solani* in tomato. *Agronomy* **2021**, *11*, 1384.
18. Bonaldi, M.; Chen, X.; Kunova, A.; Pizzatti, C.; Saracchi, M.; Cortesi, P. Colonization of lettuce rhizosphere and roots by tagged *Streptomyces. Front. Microbiol.* **2015**, *6*, 25.
19. Dini, I.; Graziani, G.; Fedele, F.L.; Sicari, A.; Vinale, F.; Castaldo, L.; Ritieni, A. Effects of *Trichoderma* biostimulation on the phenolic profile of Extra-Virgin Olive oil and Olive oil by-products. *Antioxidants* **2020**, *9*, 284.
20. Barroso, F.M.; Pereira Costa Muniz, P.H.; Milan, M.D.; Silva dos Santos, W.; Cássia de Faria Ferreira, N.; Rodriguez, F.; Carvalho, D.D.C. Growth promotion of Parsley (*Petroselinum crispum* L.) using commercial strains of *Trichoderma* spp. *J. Agric. Sci.* **2019**, *11*, 493–499.
21. Saraylou, M.; Nadian Ghomsheh, H.; Enayatizamir, N.; Rangzan, N.; St. Clair Senn, S. Some plant growth promoting traits of *Streptomyces* species isolated from various crop rhizospheres with high root colonization ability of spinach (*Spinacia oleracea* L.). *Appl. Ecol. Environ. Sci.* **2021**, *19*, 3069–3081.
22. European Pharmacopoeia Commission. *European Pharmacopoeia*; Maisonneuve: Sainte-Ruffine, France, 1975; pp. 68–80.
23. Gruszecki, R. The effect of growth stage on essential oil composition of 'Hamburg' parsley. *Acta Hort*. **2007**, *826*, 391–396.
24. Lamarti, A.; Badoc, A.; Bouriquet, R. A chemotaxonomic evaluation of *Petroselinum crispum* (Mill.) AW Hill (parsley) marketed in France. *J. Essent. Oil Res.* **1991**, *3*, 425–433.
25. Snoussi, M.; Dehmani, A.; Noumi, E.; Flamini, G.; Papetti, A. Chemical composition and antibiofilm activity of *Petroselinum crispum* and *Ocimum basilicum* essential oils against *Vibrio* spp. strains. *Microb. Pathog*. **2016**, *90*, 13–21.
26. Petropoulos, S.A.; Daferera, D.; Akoumianakis, C.A.; Passam, H.C.; Polissiou, M.G. (2004). The effect of sowing date and growth stage on the essential oil composition of three types of parsley (*Petroselinum crispum*). *J. Sci. Food Agric.* **2004**, *84*, 1606–1610.
27. John, R.P.; Tyagi, R.D.; Prevost, D.; Brar, S.K.; Pouleur, S.; Surampalli, R.Y. Mycoparasitic *Trichoderma viride* as a biocontrol agent against *Fusarium oxysporum* f. sp. *Spadzuki* and *Pythium arrhenomanes* as a growth promoter of soybean. *Crop. Prot.* **2010**, *29*, 1452–1459.
28. Doni, F.; Anizan, I.; Che Radziah, C.M.Z.; Salman, A.H.; Rodzihan, M.H.; Wan Mohtar, W.Y. Enhancement of rice seed germination and vigour by *Trichoderma* spp. *Res. J. App. Sci. Eng. Technol.* **2014**, *7*, 4547–4552.
29. Pascale, A.; Vinale, F.; Manganiello, G.; Nigro, M.; Lanzuise, S.; Ruocco, M.; Marra, R.; Lombardi, N.; Woo, S.L.; Lorito, M. *Trichoderma* and its secondary metabolites improve yield and quality of grapes. *Crop. Prot.* **2017**, *92*, 176–181.
30. Suárez-Moreno, Z.R.; Vinchira-Villarraga, D.M.; Vergara-Morales, D.I.; Castellanos, L.; Ramos, F.A.; Guarnaccia, C.; Degrassi, G.; Venturi, V.; Moreno-Sarmiento,

N. Plant-growth promotion and biocontrol properties of three *Streptomyces* spp. isolates to control bacterial rice pathogens. *Front. Microbiol.* **2019**, *10*, 290.
31. Novak, A.F.; Clark, G.C.; Dupuy, H.P. Antimicrobial activity of some ricinoleic acid derivatives. *J. Am. Oil Chem. Soc*. **1960**, *38*, 321–324.
32. Abdellatief, S.A.; Galal, A.A.A.; Farouk, S.M.; Abdel-Daim, M.M. Ameliorative effect of parsley oil on cisplatin-induced hepato-cardiotoxicity: A biochemical, histopathological, and immunochemical study. *Biomed. Pharmacother.* **2017**, *86*, 482–491.
33. El-Sayed, M.M.; Metwally, N.H.; Ibrahim, I.A.; Abdel-Hady, H.; Abdel-Wahab, B.S.A. Antioxidant activity, total phenolic and flavonoid contents of *Petroselinum crispum* Mill. *J. Appl. Life Sci*. **2018**, *19*, 1–7.
34. Caboni, P.; Saba, M.; Oplos, C.; Aissani, N.; Maxia, A.; Menkissoglu-Spiroudi, U.; Casu, L.; Ntalli, N. Nematicidal activity of furanocoumarins from parsley against *Meloidogyne* spp. *Pest.Magan. Sci.* **2015**, *71*, 1099–1105.
35. de Menezes Epifanio, N.M.; Cavalcanti, L.R.I.; dos Santos, K.F.; Duarte, P.S.C.; Kachlicki, P.; Ozarowski, M.; Riger, C.J.; de Almeida Chaves, D.S. Chemical characterization and in vivo antioxidant activity of parsley (*Petroselinum crispum*) aqueous extract. *Food Funct.* **2020**, *11*, 5346–5356.
36. Matos, M.J.; Santana, L.; Uriarte, E.; Abreu, O.A.; Molina, E.; Yordi, E.G. Coumarins—An important class of phytochemicals. In *Phytochemicals—Isolation, Characterization and Role in Human Health*, 1st ed.; Venket Rao, A.V.A., Rao, L.G., Eds.; IntechOpen: London, UK, 2015.
37. Murray, R.D.H.; Mendez, J.; Brown, S.A. *The Natural Coumarins. Occurance, Chemistry and Biochemistry*, 1st ed.; John Wiley & Sons Ltd.: New York, NY, USA, 1982.
38. Hauffe, K.D.; Hahlbrock, K.; Scheel, D. Elicitor-stimulated furanocoumarin biosynthesis in cultured parsley cells: S-adenosyl-L-methionine: bergaptoI and S-adenosyl-L-methionine: Xanthotoxol O-methyltransferases. *Z. Naturforsch C*. **1986**, *41*, 228–239.
39. Harborne, J.B. Flavonol O-glycosides. In *The Handbook of Natural Flavonoids*, 1st ed.; Harborne, J.B., Baxter, H., Eds.; John Wiley & Sons Ltd.: New York, NY, USA, 1999; Volume 1, pp. 297–548.
40. Uitterhaegen, E.; Sampaio, K.A.; Delbeke, E.I.P.; De Greyt, W.; Cerny, M.; Evon, P.; Merah, O.; Talou, T.; Stevens, C.V. Characterization of French coriander oil as source of petroselinic acid. *Molecules*. **2016**, *21*, 1202.
41. Placek, L.L. Review on petroselinic acid and its derivatives. *J Am Oil Chem Soc*. **1963**, *40*, 319–329.
42. Yeganehpoor, F.; Zehtab-Salmasi, S.; Ghassemi-Golezani, K.; Shafagh-Kolvanagh, J.; Dastborhan, S. The effect of water stress, salicylic acid and bio-fertilizer on quality of leaf and seed essential oil, and oil components of coriander. *Net J Agric Sci.* **2017**, *5*, 38–47.
43. Donato, P.; Dugo, P.; Mondello, L. *Chapter 8: Separation of Lipids.* In *Liquid Cromathography*, 2nd ed.; Elsevier, Amsterdam, Netherlands; 2017.
44. Hou, Q.; Ufer, G.; Bartels, D. Lipid signaling in plant responses to abiotic stress. *Plant Cell Environ.* **2016**, *39*, 1029–1048.
45. Maoka, T. Carotenoids as natural functional pigments. *J. Nat. Med.* **2020**, *74*, 1–16.
46. Narita, Y.; Inouye, K. Chlorogenic acids from coffee. In *Coffee in Health and Disease Prevention*, 1st ed.; Preedy, V.R., Ed.; Elsevier Science & Technology: Amsterdam, The Netherlands, 2014; Volume 1, pp. 189–197.
47. Aissani, N.; Albouchi, F.; Sebai, H. Anticancer Effect in human glioblastoma and antioxidant activity *of Petroselinum crispum L*. methanol extract. *Nutr. Cancer.* **2020**, *29*, 1–9.

48. Jain, A.; Singh, A.; Chaudhary, A.; Singh, S.; Singh, H.B. Modulation of nutritional and antioxidant potential of seeds and pericarp of pea pods treated with microbial consortium. *Food Res. Int.* **2014**, *64*, 275–282.
49. Vinci, G.; Cozzolino, V.; Mazzei, P.; Monda, H.; Spaccini, R.; Piccolo, A. An alternative to mineral phosphorus fertilizers: The combined effects of *Trichoderma harzianum* and compost on *Zea mays*, as revealed by $^{1}$H NMR and GC-MS metabolomics. *PLoS ONE*. **2018**, *13*, e0209664.
50. Gębarowska, E.; Pytlarz-Kozicka, M.; Nöfer, J.; Łyczko, J.; Adamski, M.; Szumny, A. The effect of *Trichoderma* pp. on the composition of volatile secondary metabolites and biometric parameters of coriander (*Coriandrum sativum* L.). *J. Food Qual.* **2019**, *2019*, 5687032.
51. Coppola, M.; Cascone, P.; Chiusano, M.L.; Colantuono, C.; Lorito, M.; Pennacchio, F.; Rao, R.; Woo, S.L.; Guerrieri, E.; Digilio, M.C. *Trichoderma harzianum* enhances tomato indirect defense against aphids. *Insect Sci.* **2017**, *24*, 1025–1033.

*Article*

# Supplementary materials: Improvement of Nutraceutical Value of Parsley Leaves (*Petroselinum crispum)* upon Field Applications of Beneficial Microorganisms

**Alessia Staropoli[1,2*], Anastasia Vassetti[1], Maria Michela Salvatore[3], Anna Andolfi[3,4], Maria Isabella Prigigallo[5], Giovanni Bubici[5], Marina Scagliola[6], Pasquale Salerno[6] and Francesco Vinale[2,4,7]**

**TableS1.** Metabolites obtained from LC-MS data (positive mode), that are differentially accumulated in plants treated with *Streptomyces* (S), *Trichoderma* (T) or a mix of those two (S+T) compared to control group (C) plants and the microbial consortium (S+T) compared to *Streptomyces* (S), *Trichoderma* (T) single culture.

| Compound | Mass (Da) | Ln (Fold Change) | | | | |
|---|---|---|---|---|---|---|
| | | S vs. C | T vs. C | S+T vs. C | S+T vs S | S+T vs T |
| Styrene | 104.0627 | 21,233128 | 21,28731 | -0,074560165 | -21,307688 | -21,36187 |
| $C_{11}H_{23}O$ | 185.1782 | -20,871048 | -10,715798 | -20,77758 | 0,09346771 | -10,061782 |
| Bergaptol/ Xanthotoxol* | 202.0272 | 20,277876 | 19,712917 | 20,48061 | 0,20273292 | 0,76769114 |
| Xanthotoxin/Bergapthen* | 216.0427 | 20,23557 | 20,004814 | 20,39623 | 0,1606602 | 0,3914169 |
| Rotundine B | 233.1789 | 20,003548 | 20,18695 | 20,114727 | 0,11117959 | -0,0722242 |
| $C_{10}H_{19}NO_7$ | 265.1172 | -3,6536846 | 0,057913303 | -3,7408605 | -0,087175846 | -3,7987738 |
| $C_{16}H_{35}NO_2$ | 273.2676 | 20,174923 | 20,127983 | 20,177908 | 0,002984881 | 0,04992515 |
| Petroselinic acid | 282.257 | 0,6994004 | 0,8276119 | -1,1479632 | -1,8473636 | -1,9755751 |
| $C_{20}H_{35}NO_2$ | 321.2681 | -4,3183737 | -0,006582439 | -1,0713919 | 3,2469816 | -1,0648096 |
| Hyperjovinol B | 332.198 | -19,221182 | -0,99390304 | -0,743564 | 18,477617 | 0,25033903 |
| $C_{22}H_{43}NO$ | 337.3358 | 19,672241 | 19,617838 | 19,652145 | -0,020095706 | 0,034308046 |
| Piperochromanoic acid | 356.198 | 18,248592 | 18,527262 | -0,074560165 | -18,323153 | -18,601822 |
| $C_{17}H_{39}N_4O_3S$ | 379.274 | 19,704937 | 19,600945 | 19,81222 | 0,10728264 | 0,2112735 |
| $C_{19}H_{25}N_5O_6$ | 419.1808 | 18,70136 | 18,571812 | 18,785557 | 0,08419633 | 0,21374518 |
| $C_{25}H_{34}N_4O_2$ | 422.2688 | -1,0106063 | -0,5555207 | -0,5077439 | 0,50286233 | 0,04777682 |
| $C_{23}H_{35}N_5O_3$ | 429.2746 | -0,821465 | -1,3801929 | -1,2259859 | -0,40452087 | 0,15420699 |
| $C_{26}H_{49}N_2O_3$ | 437.3739 | -3,9967847 | -0,4573155 | -0,22560757 | 3,771177 | 0,23170793 |
| $C_{24}H_{42}O_7$ | 442.2926 | 19,269941 | 19,148727 | 19,439392 | 0,16945037 | 0,29066512 |
| $C_{25}H_{49}N_5O_2$ | 451.3895 | 18,932167 | 19,004044 | 18,864655 | -0,06751266 | -0,13938913 |
| $C_{27}H_{41}N_2O_4$ | 457.306 | -2,0492868 | 2,9139493 | -2,982212 | -0,9329252 | -5,896161 |
| $C_{25}H_{32}N_7O_2$ | 462.2614 | -0,16802788 | 17,894062 | -0,074560165 | 0,09346771 | -17,968622 |
| $C_{25}H_{49}N_5O_3$ | 467.3844 | -0,06121111 | 5,6531143 | 2,6398673 | 2,7010784 | -3,013247 |
| 495.3346 | 495.3346 | 0,34400874 | -0,8140577 | -0,6760938 | -1,0201025 | 0,13796389 |
| $C_{27}H_{53}N_5O_3$ | 495.4159 | -1,4102228 | -1,3853886 | -1,4837484 | -0,07352567 | -0,09835982 |
| $C_{28}H_{49}N_9$ | 511.411 | -1,1269317 | -0,7952111 | -1,2407053 | -0,113773584 | -0,44549417 |
| $C_{30}H_{57}N_2O_5$ | 525.4262 | -14,094639 | 3,4324927 | -2,1690602 | 11,925578 | -5,601553 |
| $C_{31}H_{59}N_2O_5$ | 539.4424 | 14,300248 | 12,014479 | 16,880615 | 2,5803668 | 4,8661366 |
| $C_{23}H_{28}N_{10}O_6$ | 540.2202 | -0,16802788 | 16,675978 | 14,77404 | 14,942068 | -1,9019375 |
| $C_{30}H_{53}N_9O$ | 555.4371 | -0,16802788 | -0,30589485 | 20,052979 | 20,221006 | 20,358873 |
| Capsanthone | 582.4098 | -0,16802788 | -0,30589485 | 18,509792 | 18,67782 | 18,815687 |
| $C_{33}H_{63}N_2O_7$ | 599.4639 | -0,16802788 | -0,30589485 | 18,49334 | 18,661367 | 18,799234 |
| $C_{33}H_{59}N_9O_2$ | 613.4796 | 17,773788 | -0,30589485 | 17,48442 | -0,28936672 | 17,790316 |
| $C_{33}H_{51}N_2O_9$ | 619.3597 | -18,611687 | -18,749554 | -4,055524 | 14,556163 | 14,69403 |

| | | | | | | |
|---|---|---|---|---|---|---|
| $C_{37}H_{48}N_4O_5$ | 628.3615 | -17,749094 | -17,886961 | -0,40953028 | 17,339563 | 17,47743 |
| Isorhamnetin 3,7-di-O-beta-glucopyranoside | 640.1663 | -0,47018123 | -17,639072 | -0,5747576 | -0,10457635 | 17,064314 |
| $C_{32}H_{28}NO_{14}$ | 650.1525 | 9,430138 | -0,30589485 | 2,0435104 | -7,386627 | 2,3494053 |

***** Stereoisomers for which it was not possible to make a distinction in the chromatogram.

**TableS2.** Metabolites obtained from LC-MS data (negative mode), that are differentially accumulated in plants treated with *Streptomyces* (S), *Trichoderma* (T) or a mix of those two (S+T) compared to control group (C) plants and the microbial consortium (S+T) compared to *Streptomyces* (S), *Trichoderma* (T) single culture.

| **Compound** | **Mass (Da)** | **Ln (Fold Change)** | | | | |
|---|---|---|---|---|---|---|
| | | S vs. C | T vs. C | S+T vs. C | S+T vs S | S+T vs T |
| Quinic acid | 192.0642 | 19.887115 | 20.968676 | 20.24096 | 0.35384262 | -0.72771645 |
| (Z,Z,Z)-Octadeca-9,12,15-trienoic acid | 278.2252 | -0.08422239 | -19.020306 | -19.298847 | -19.214624 | -0.27854156 |
| Nordihydrocapsiate | 294.1834 | 18.09749 | 0.2026043 | -0.07593727 | -18.173428 | -0.27854156 |
| Colneleic acid | 294.2201 | 19.09545 | 0.2026043 | 18.635998 | -0.45945194 | 18.433393 |
| Sucrose | 342.1182 | -21.005697 | -20.720173 | -0.5616127 | 20.444084 | 20.15856 |
| $C_{26}H_{20}NO_2$ | 378.1503 | 0.082920074 | 18.693682 | -0.07593727 | 0.006982803 | -18.769619 |
| $C_{12}H_{18}N_3O_{11}$ | 380.0935 | 3.77224 | 6.3687778 | 6.334033 | 2.561793 | -0.03474465 |
| $C_{11}H_{12}N_{10}O_6$ | 380.0954 | 13.355883 | -2.281044 | -3.8360806 | -17.191963 | -1.5550365 |
| $C_{12}H_{18}N_7O_8$ | 388.1225 | -2.89076 | 0.17742908 | -0.07747638 | 2.8132834 | -0.25490546 |
| $C_{12}H_{34}N_8O_{10}$ | 450.2387 | 0.082920074 | 18.759348 | -0.07593727 | 0.006982803 | -18.835285 |
| Cilistol a | 456.2852 | 0.066390194 | -19.038605 | -19.317146 | -19.383537 | -0.27854156 |
| $C_{23}H_{40}O_9$ | 460.2677 | 18.33072 | 0.2026043 | 18.438322 | 0.107599616 | 18.235718 |
| $C_{23}H_{46}O_9$ | 466.3147 | 19.192417 | 0.2026043 | -0.07593727 | -19.268354 | -0.27854156 |
| $C_{28}H_{34}N_3O_4$ | 476.254 | -6.595832 | -6.3103075 | 12.653781 | 19.249613 | 18.964088 |
| $C_{28}H_{36}N_3O_4$ | 478.2696 | 18.70491 | 18.73321 | -0.07593727 | -18.780848 | -18.809147 |
| $C_{19}H_{28}N_{16}$ | 480.2688 | 0.082920074 | 19.755817 | -0.07593727 | 0.006982803 | -19.831755 |
| $C_{25}H_{42}O_9$ | 486.2836 | 0.082920074 | 0.2026043 | -0.07593727 | 0.006982803 | -0.27854156 |
| $C_{26}H_{40}N_4O_5$ | 488.2988 | 18.616465 | 18.807993 | 18.677116 | 0.06065011 | -0.13087809 |
| $C_{18}H_{43}N_5O_{10}$ | 489.3026 | 18.68542 | 0.2026043 | 19.84922 | 1.1638017 | 19.646616 |
| $C_{26}H_{39}N_8O_4$ | 527.3091 | 2.832656 | 4.009903 | 3.584489 | 0.7518332 | -0.42541403 |
| $C_{19}H_{34}O_{17}$ | 534.1816 | -19.257658 | -18.972134 | -19.250675 | 0.006982803 | -0.27854156 |
| $C_{25}H_{36}N_{10}O_5$ | 556.2872 | -0.75310814 | 0.20781177 | -0.25587013 | 0.49723804 | -0.4636819 |
| 565.152 | 565.152 | 0.082920074 | 19.403019 | 19.307016 | 19.389936 | -0.09600169 |
| $C_{32}H_{40}N_7O_4$ | 586.3147 | 0.08443248 | 0.45108438 | 0.009214163 | -0.07521832 | -0.4418702 |
| 606.1595 | 606.1595 | 18.048233 | 18.294506 | 17.79564 | -0.25259352 | -0.4988656 |
| $C_{24}H_{17}N_{15}O_7$ | 627.1443 | -18.992393 | 0.46386808 | 0.08813183 | 19.080526 | -0.37573624 |
| $C_{30}H_{18}N_{10}O_7$ | 630.1358 | -18.92042 | 0.53584146 | -18.913437 | 0.006982803 | -19.44928 |
| Kaempferol 3-(6"-acetylgalactoside)-7-rhamnoside | 636.1695 | 0.082920074 | 17.88488 | -0.07593727 | 0.006982803 | -17.960817 |
| $C_{30}H_{30}O_{18}$ | 678.1471 | -6.8933015 | -1.3959728 | -1.2626923 | 5.6306095 | 0.13328058 |
| $C_{31}H_{28}N_4O_{14}$ | 680.1591 | -0.16431296 | -18.937742 | -0.00396993 | 0.16034304 | 18.933771 |
| $C_{29}H_{30}N_3O_{18}$ | 708.152 | -18.679964 | -18.39444 | -18.672981 | 0.006982803 | -0.27854156 |

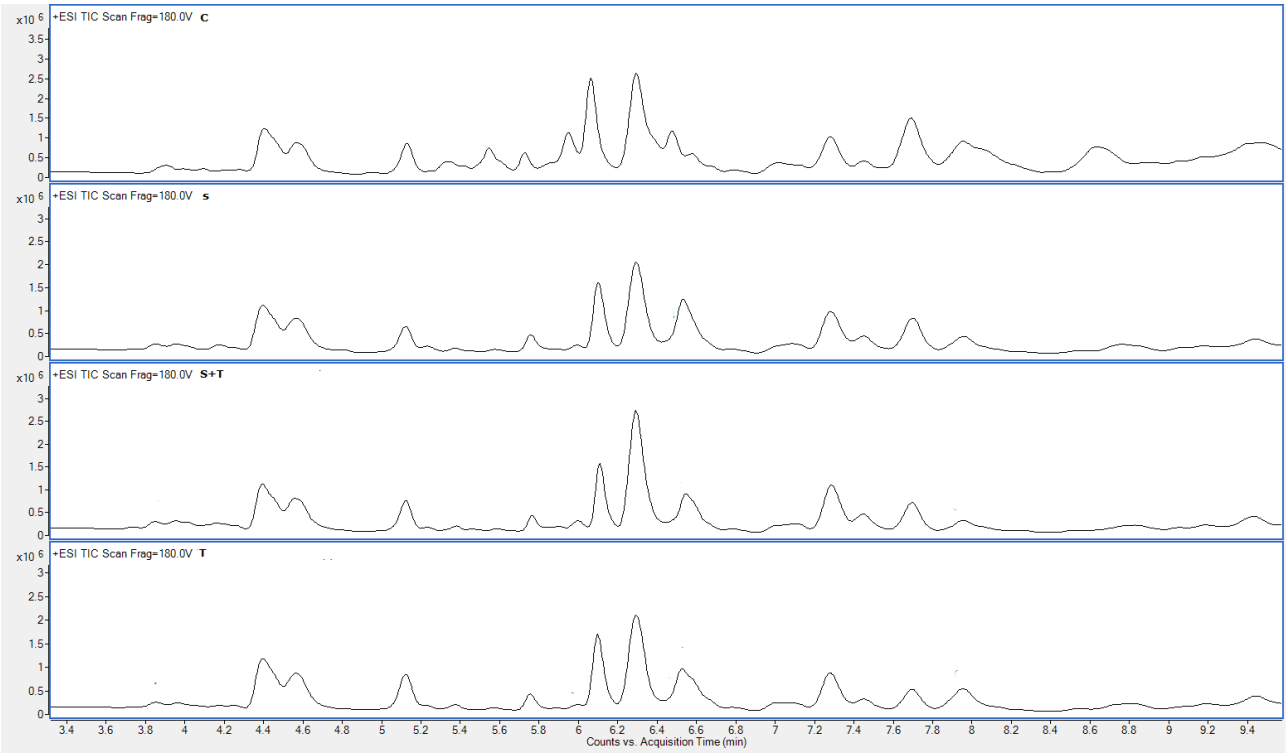


**FigureS1.** Magnified total ion chromatogram of parsley extracts recorded in positive mode. From the top to the bottom: C is control group; S is *Streptomyces* group; S+T is the microbial consortium *Streptomyces* + *Trichoderma*; T is *Trichoderma* group.

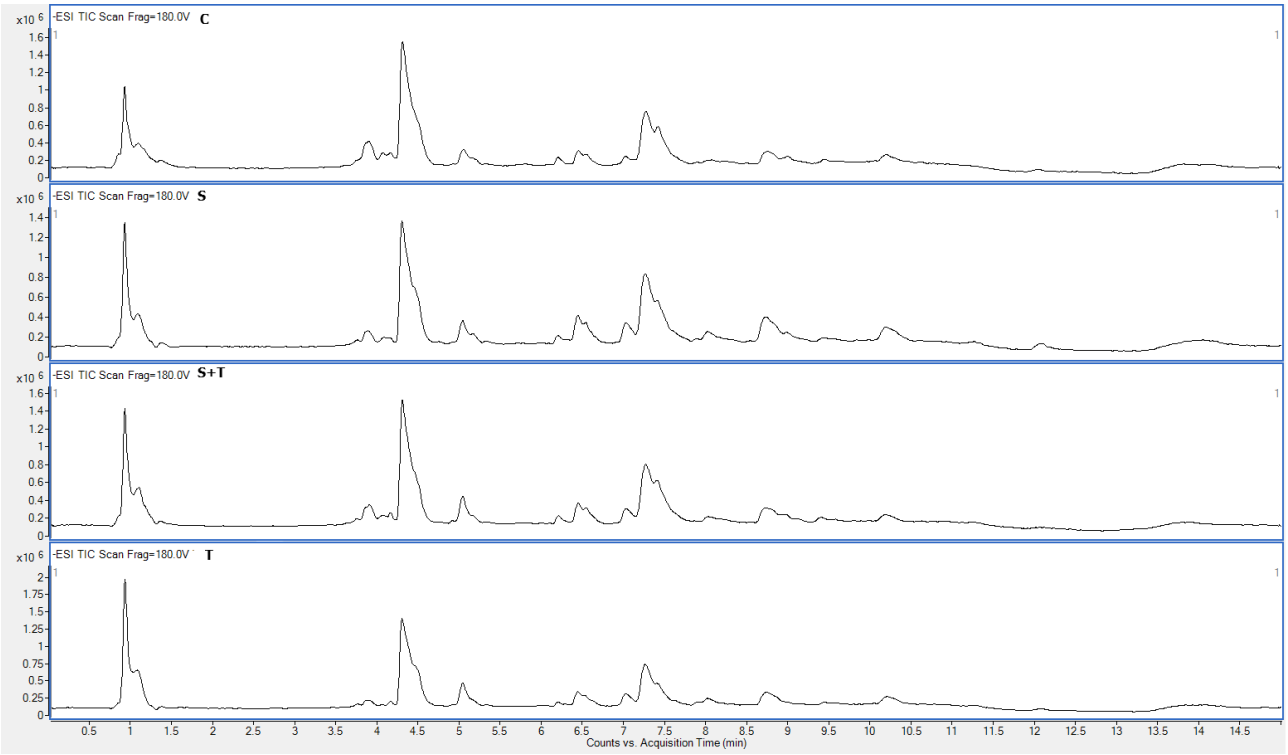


**FigureS2.** Total ion chromatogram of parsley extracts recorded in negative mode. From the top to the bottom: C is control group; S is *Streptomyces* group; S+T is the microbial consortium *Streptomyces* + *Trichoderma*; T is *Trichoderma* group.

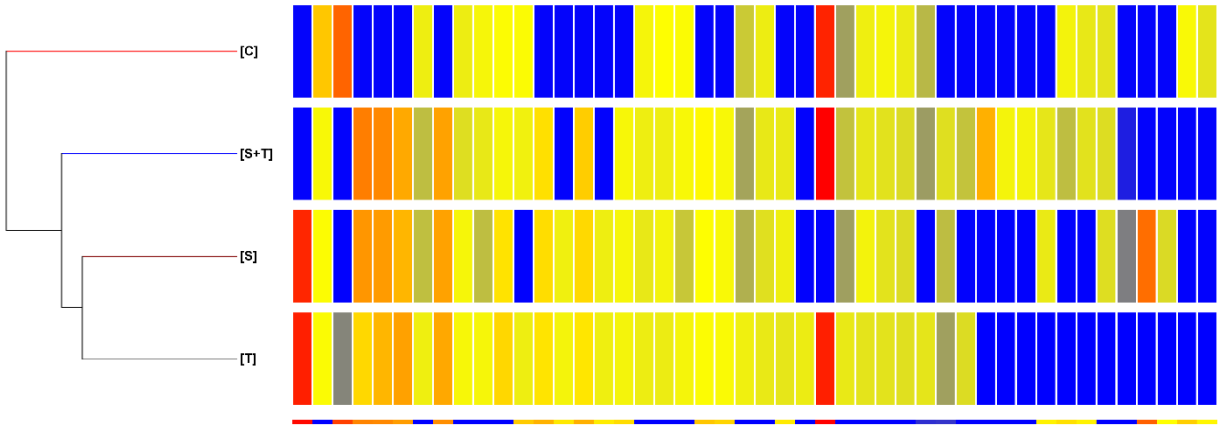


**FigureS3.** Hierarchical clustering heatmap of statistically different metabolites in control (C) group; microbial consortium of *Streptomyces* and *Trichoderma* (S+T) group; *Streptomyces* (S) group and *Trichoderma* (T) group. This result is obtained starting from LC-MS data recorded in positive mode and subjected to statistical analysis (one-way ANOVA $p < 0.05$ and fold change >2.0).

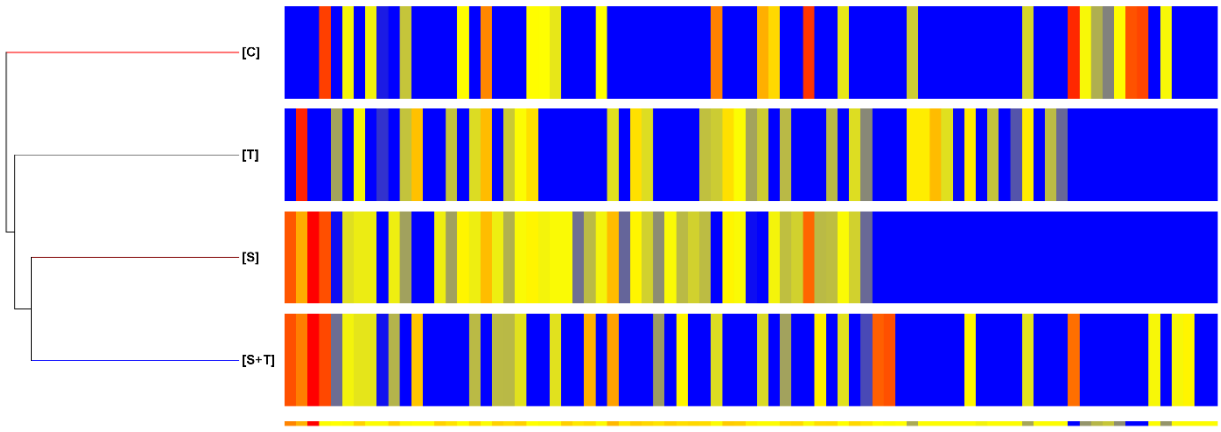


**FigureS4.** Hierarchical clustering heatmap of statistically different metabolites in control (C) group; microbial consortium of *Streptomyces* and *Trichoderma* (S+T) group; *Streptomyces* (S) group and *Trichoderma* (T) group. This result is obtained starting from LC-MS data recorded in negative mode and subjected to statistical analysis (one-way ANOVA $p < 0.05$ and fold change >2.0).

pathogens

MDPI

*Article*

# Bioformulations with Beneficial Microbial Consortia, a Bioactive Compound and Plant Biopolymers Modulate Sweet Basil Productivity, Photosynthetic Activity and Metabolites

**Ernesto Comite [1,†], Christophe El-Nakhel [1,†], Youssef Rouphael [1], Valeria Ventorino [1,2], Olimpia Pepe [1,2], Assunta Borzacchiello [3], Francesco Vinale [4,5], Daniela Rigano [6], Alessia Staropoli [1,5], Matteo Lorito[1] and Sheridan L. Woo [2,5,6,*]**

[1] Department of Agricultural Sciences, University of Naples Federico II, 80055 Portici, Italy; ernesto.comite@unina.it (E.C.); christophe.elnakhel@unina.it (C.E.-N.); youssef.rouphael@unina.it (Y.R.); valeria.ventorino@unina.it (V.V.); olipepe@unina.it (O.P.); alessia.staropoli@unina.it (A.S.); lorito@unina.it (M.L.)
[2] Task Force on Microbiome Studies, University of Naples Federico II, 80055 Portici, Italy
[3] National Research Council, Institute for Composite Polymers and Biomaterials, 80125 Napoli, Italy; assunta.borzacchiello@cnr.it (A.B.)
[4] Department of Veterinary Medicine and Animal Production, University of Naples Federico II, 80137 Naples, Italy; frvinale@unina.it (F.V.)
[5] Institute for Sustainable Plant Protection, National Research Council, 80055 Portici, Italy
[6] Department of Pharmacy, University of Naples Federico II, 80131 Naples, Italy; drigano@unina.it (D.R.)
* Correspondence: woo@unina.it (S.L.W.)
† Authors had equal contribution (co-first authors)

**Abstract:** Increasing attention is being given to the development of innovative formulations to substitute the use of synthetic chemicals to improve agricultural production and resource use efficiency. Alternatives can include biological products containing beneficial microorganisms and bioactive metabolites able to inhibit plant pathogens, induce systemic resistance and promote plant growth. The efficacy of such bioformulations can be increased by the addition of polymers as adjuvants or carriers. *Trichoderma afroharzianum* T22, *Azotobacter chroococcum* 76A and 6-pentyl-α-pyrone (6PP; a *Trichoderma* secondary metabolite) were administrated singularly or in a consortium, with or without a carboxymethyl cellulose-based biopolymer (BP) and tested on sweet basil (*Ocimum basilicum* L.) grown in a protected greenhouse. The effect of the treatments on basil yield, photosynthetic activity and secondary metabolites production was assessed. Photosynthetic efficiency was augmented by the applications of the bioformulations. The applications to the rhizosphere with BP + 6PP and BP + T22 + 76A increased the total fresh weight of basil by 26.3% and 23.6%, respectively. Untargeted LC-MS qTOF analysis demonstrated that the plant metabolome was significantly modified by the treatments. Quantification of the profiles for the major phenolic acids indicated that the treatment with the T22 + 76A consortium increased rosmarinic acid content by 110%. The use of innovative bioformulations containing microbes, their metabolites and a biopolymer was found to modulate the cultivation of fresh basil by improving yield and quality, thus providing the opportunity to develop farming systems with minimal impact on the environmental footprint from the agricultural production process.

**Keywords:** 6-pentyl-α-pyrone; rosmarinic acid; *Ocimum basilicum* L.; *Trichoderma*; *Azotobacter*

## 1. Introduction

Basil (*Ocimum basilicum* L.*)* is a member of the Lamiaceae family, which represents one of the most widely used medicinal and aromatic plants throughout the world

[1,2]. There are many basil varieties, but the most commonly known cultivar is the sweet basil or Genovese basil, an important ingredient in the Mediterranean diet where it is used as a fresh leafy herb condiment or garnish, and is the major constituent in the "genovese" pesto sauce [3,4]. Members of the Lamiaceae, including basil, mint and salvia, are known to produce compounds such as phenolic acids and essential oils that provide the typical aromas attributed to the given plant species. Basil is known to contain antioxidant compounds [3,4] that can provide health benefits to consumers by protecting cells from damage evoked by oxidative stress and free radicals, accountable for numerous degenerative diseases [5,6]. Specifically, among the many secondary metabolites identified in basil, the essential oils are recognized as being effective in reducing antioxidant and antimicrobial stress [7], and the phenolic acids are known to have preventive protective effects on human well-being [5,6,8,9].

Phenolic compounds are secondary metabolites ubiquitous in plants that play an important role in chemical plant defense to pathogen-pest attack [10]. The presence of phenolic compounds in food or herbal products may be beneficial to human health upon regular consumption since they may serve as functional food ingredients improving nutritional or nutraceutical properties and/or contributing to reduce some age-related diseases due to their antioxidant properties [10]. Among the numerous phenolic compounds present in basil, three phenolic acids are of particular interest due to their known applications in the field of human health: (i) *p*-coumaric acid and its conjugates are known for their antioxidant, anti-inflammatory, antitumor and anti-ulcer activities, playing an important role in mitigating arteriosclerosis, UV-induced eye damage, gout and diabetes [11]; (ii) caffeic acid has an inhibitory effect on the proliferation of tumor cells [12] and shows antioxidant activity both in vitro and in vivo [13]; (iii) rosmarinic acid, which is present in most plants of the Lamiaceae family [14], has antioxidant and pharmacological activities, as well as the ability to reduce allergies and pollinosis [15], plus it has demonstrated antimicrobial and insect-repellent capacities [16]. The accumulation and biosynthesis of phenolic compounds in basil have been noted to depend upon the plant genotype and physiology, plus the environmental factors, such as climate, cultivation technique and phenological phase of harvest [17]. In particular, the nutritional status of the crop farmed in a given agricultural system will have a direct impact on plant growth, subsequent metabolism and the produced phytochemical complex [4].

In recent years, there has been a growing interest among consumers and the scientific community in the search for innovative and eco-sustainable strategies to increase agricultural production, to meet food needs and reduce environmental impact. Among the possible solutions there is the use of plant biostimulants, agricultural products that include beneficial microorganisms (such as arbuscular mycorrhiza fungi and *Trichoderma* spp.) and natural substances (humic acids, seaweed and plant extracts, protein hydrolysate and silicon) able to stimulate plant vigor, growth and yield, even in sub-optimal conditions. These exemplify a valid alternative to chemical products that do not threaten biodiversity, able to reduce harmful effects to human health and the environment by decreasing the use of synthetic fertilizers and toxic pesticides [18–21]. The beneficial microorganisms that can be used as biostimulants include fungi such as *Trichoderma* spp. and bacteria belonging to *Azotobacter,* which can also be functionally complementary in a consortium acting as plant biostimulants [22]. Soil plant growth-promoting rhizobacteria (PGPR), such as the nitrogen-fixer *Azotobacter,* are important for their ability to produce regulatory and growth promoter compounds such as phytohormones, vitamins and antifungal metabolites, and to be involved in nutrient processes such as nitrogen cycling, phosphate solubilization [23], mobilization of iron [24] and the biodegradation of many commonly used pesticides, as demonstrated by *Azotobacter chroococcum* [25]. Other microorganisms with PGPR-similar effects include selected *Trichoderma* strains, capable of establishing diverse beneficial interactions with the plant, including biological control of pathogens, plant growth promotion (PGP) effects and induction of resistance [26–28]. *Trichoderma*

spp. and other endophytic fungi have become more prominent on the agricultural scene in recent decades, owing to their beneficial effects and positive yield properties noted on crops [26,29]. Potentially new biological compounds to consider are secondary metabolites or bioactive substances from various microbial and plant sources that also have biostimulant or protective effects to the plant. *Trichoderma* spp. produce over 250 metabolic products, including secondary metabolites, peptides, proteins and cell-wall-degrading enzymes [22] with biological activity. For example, the 6 pentyl-α-pyrone (6PP), which produces the coconut aroma typical to some *Trichoderma* species, has demonstrated efficacy in the containment of known phytopathogenic fungi [30,31] and plant growth stimulation effects [32,33].

Consortia of beneficial microbes and bioactive compounds can be combined with natural and inorganic products such as algae, polymers and products of animal origin for more efficient and dependable agricultural formulations. Another innovative aspect, which responds to the current need for eco-sustainable products, comprises the use of macromolecules of natural origins, such as biopolymers. These substances can function as "carriers" of microbes (such as *Azotobacter* and *Trichoderma*) and/or PGP substances. The positive effects can be related to the in-situ delivery and activity [34,35], as well as to the stabilization of microbial/natural compound formulations. Biopolymers can be formulated from biocompatible and biodegradable products, such as carbohydrate polymers, which have a great ability to absorb water and contain a large amount of nutrients and compounds of agricultural interest within their structure [36]. These polymers already find numerous useful applications in human health, including use as carriers in the delivery of some vaccines [37], anticancer drugs [38], antivirals [39] and therapeutic proteins and peptides [40]. Although, different studies investigated the role of some *Trichoderma* and PGPR strains in relation to their biostimulant action in horticulture [41,42], the combinatorial actions of beneficial microbial consortia and vegetal biopolymers have received very limited attention. Thus, exploiting the multiple properties of these beneficial microorganisms, in combination with a plant-based biopolymer, may represent promising strategies that target the formulation of more efficient biostimulant products.

Accordingly, the overall objective of this work was to evaluate bioformulations containing beneficial microorganisms, *Trichoderma afroharzianum* T22 (a fungus) and *Azotobacter chroococcum* 76A (a bacterium), the *Trichoderma* produced metabolite 6PP, applied singly or in consortia, with or without a biopolymer of plant origin in the cultivation of sweet basil, to determine effects on the plant (i) growth parameters, (ii) physiology, (iii) modulation of targeted and untargeted metabolites, and subsequently (iv) to identify the best bioformulation to enhance the desirable basil characteristics. The obtained results could be of major importance, contributing lines of research for developing new biological formulations for applications in agriculture, specifically to improve sweet basil production.

## 2. Results

### *2.1. Growth and Yield Parameters*

The effects of the ten biological treatments on sweet basil were evaluated by measuring biometric parameters: leaf number per plant, harvested leaf yield fresh weight (FW), total aboveground plant biomass (leaves + stem) FW and dry weight (DW), root DW and percentage of total dry matter (DM) (Table 1). Water control (CTRL) plants registered the highest leaf number per plant, with BP + 6PP plants being similar, and the BP-treated plants had the lowest number of leaves. The paired applications of BP + 76A, BP + 6PP and T22 + 76A were similar among themselves, as were the single treatments with T22, 76A or 6PP. However, the highest leaf yield was noted in the plants treated with the combination of BP + T22 + 76A and the lowest with T22 + 76A. The total plant FW and DW were most positively influenced by the combinations of BP + 6PP or BP + T22 + 76A applied to the basil plants. The 6PP, BP + 6PP and BP + T22 + 76A treatments increased

by 22.2% and 23.5% total FW and total DW on average, respectively, compared to CTRL treatment. Inoculation with 76A produced the greatest root DW, 52% higher than CTRL, whereas no significant differences were noted among the other formulations. It can also be mentioned that no disease symptoms were observed on the basil plants during cultivation in the field.

### *2.2. SPAD Index, Colorimetric Components*

Both the SPAD index and the leaf colorimetric parameters of the basil plants were measured (Table 2). The bioformulations BP, T22, 76A, BP + T22, BP +76A and T22 + 76A significantly increased the SPAD index of treated plants on average by 6.4%, in comparison to the control. As for the leaf colorimetric indices, none of the bioformulations had a significant impact on the brightness (L*), or b* indices. However, for the color parameter a*, BP + T22, 6PP and 76A applications showed significant differences in regard to the control (Table 2).

### *2.3. Physiological Parameters*

Among the physiological parameters measured, only the net $CO_2$ assimilation rate ($A_{CO2}$) and the maximum quantum use efficiency of the photosystem II (Fv/Fm) demonstrated significant changes ($p < 0.001$) due to the bioformulation applications (Table 3). Stomatal resistance ($r_s$) and transpiration rate E were not influenced by the different treatments. However, the $CO_2$ net assimilation rate with the applications of BP, T22, 76A, BP + 76A and T22 + 76A bioformulations exhibited an increase of 11.8%, 11.8%, 16.0%, 9.3% and 11.3 %, respectively, compared to CTRL**.** Among these latter bioformulations, except for T22 + 76A, all treatments had comparable Fv/Fm values that were higher than those recorded by CTRL. Furthermore, three of these treatments, with the single components, demonstrated Fv/Fm values higher than those recorded in the CTRL.

**Table 1.** Effect on the biometric parameters of basil plants treated with the different bioformulations containing the biopolymer (BP), *Trichoderma afroharzianum* (T22), *Azotobacter chroococcum* (76A), or the secondary metabolite (6PP), plus a water control (CTRL), used individually or in combination.

| Treatment | Leaf Number (no. plant$^{-1}$) | Leaf Yield FW (g plant$^{-1}$) | Aboveground Biomass FW (g plant$^{-1}$) | Aboveground Biomass DW (g plant$^{-1}$) | Root DW (g plant$^{-1}$) | DM (%) |
|---|---|---|---|---|---|---|
| CTRL | 290.6 a | 93.85 bcd | 153.0 cd | 17.48 c | 4.44 d | 11.42 |
| BP | 208.7 f | 92.81 bcd | 166.8 bc | 18.58 bc | 4.79 cd | 11.14 |
| T22 | 236.6 cde | 86.52 cd | 151.2 cd | 17.54 c | 4.99 bcd | 11.59 |
| 76A | 219.8 ef | 94.15 bc | 159.7 bc | 18.87 bc | 6.75 a | 11.80 |
| 6PP | 226.1 def | 90.83 bcd | 178.3 ab | 20.95 ab | 5.24 bcd | 11.76 |
| BP + T22 | 227.4 def | 86.64 cd | 148.2 cd | 16.54 c | 5.81 b | 11.18 |
| BP + 76A | 255.7 bc | 87.06 cd | 153.0 cd | 17.71 c | 5.59 bc | 11.61 |
| BP + 6PP | 272.8 ab | 106.26 ab | 193.2 a | 21.56 a | 4.72 cd | 11.16 |
| T22 + 76A | 265.2 b | 77.41 d | 130.8 d | 16.19 c | 5.17 bcd | 12.39 |
| BP + T22 + 76A | 241.5 cd | 109.62 a | 189.1 a | 22.19 a | 5.67 bc | 11.73 |
| Significance | *** | ** | *** | *** | *** | ns |

Different letters within each column indicate significant differences according to Duncan's multiple-range test ($p$= 0.05).
ns, **, *** non-significant or significant at $p \leq 0.01$ and 0.001, respectively.

**Table 2.** Effect of the different bioformulations with the biopolymer (BP), *Trichoderma afroharzianum* (T22), *Azotobacter chroococcum* (76A), the secondary metabolite (6PP) and water (CTRL), used individually or in combination, on SPAD index and leaf colorimetric indices (L*, a* [–a* = green)], b* [(+b* = yellow]) of basil plants.

| Treatment | SPAD Index | L* | a* | b* |
|---|---|---|---|---|
| CTRL | 33.95 d | 41.69 | −6.80 c | 14.65 |
| BP | 36.17 ab | 41.10 | −6.30 abc | 13.38 |
| T22 | 36.97 a | 41.17 | −6.46 bc | 14.05 |
| 76A | 35.78 ab | 41.75 | −6.22 ab | 13.47 |
| 6PP | 34.26 cd | 41.24 | −6.20 ab | 12.96 |
| BP + T22 | 35.30 bc | 41.09 | −5.87 a | 12.45 |
| BP + 76A | 36.19 ab | 42.03 | −6.37 abc | 13.14 |
| BP + 6PP | 33.80 d | 41.78 | −6.52 bc | 14.48 |
| T22 + 76A | 36.28 ab | 41.78 | −6.27 abc | 13.08 |
| BP + T22 + 76A | 35.09 bcd | 40.05 | −6.61 bc | 13.87 |
| Significance | *** | ns | * | ns |

Different letters within each column indicate significant differences according to Duncan's multiple-range test ($p$ = 0.05).
ns, *, *** non-significant or significant at $p \leq 0.05$ and 0.001, respectively.

**Table 3.** Effect on the physiological parameters of basil plants: rate of $CO_2$ net assimilation ($A_{CO2}$), stomatal resistance ($r_s$), transpiration rate (E) and photosystem II efficiency (Fv/Fm) of the different formulations with the biopolymer (BP), *Trichoderma afroharzianum* (T22), *Azotobacter chroococcum* (76A), or the secondary metabolite (6PP), and a water control (CTRL), used individually or in combination.

| Treatment | $A_{CO2}$ ($\mu$mol $CO_2$ $m^{-2}$ $s^{-1}$) | $r_s$ ($m^2$ $s^1$ $mol^{-1}$) | E (mol $H_2O$ $m^{-2}$ $s^{-1}$) | Fv/Fm |
|---|---|---|---|---|
| CTRL | 15.75 d | 3.85 | 4.62 | 0.81 bc |
| BP | 17.61 ab | 4.69 | 4.27 | 0.82 a |
| T22 | 17.62 ab | 4.90 | 4.48 | 0.83 a |
| 76A | 18.28 a | 4.05 | 4.46 | 0.82 a |
| 6PP | 16.55 cd | 4.77 | 4.24 | 0.82 ab |
| BP + T22 | 16.43 cd | 3.84 | 4.80 | 0.81 bc |
| BP + 76A | 17.22 bc | 4.43 | 4.52 | 0.81 bc |
| BP + 6PP | 16.48 cd | 5.18 | 4.41 | 0.79 d |
| T22 + 76A | 17.54 ab | 4.36 | 4.86 | 0.80 c |
| BP + T22 + 76A | 16.55 cd | 4.59 | 4.49 | 0.81 c |
| Significance | *** | ns | ns | *** |

Different letters within each column indicate significant differences according to Duncan's multiple-range test ($p$ = 0.05).
ns, *** non-significant or significant at $p \leq 0.001$, respectively.

### *2.4. Untargeted Metabolomic Analysis and Compounds Differentially Expressed in the Organic Extracts*

Untargeted LC-MS qTOF analysis of plant extracts indicated that the metabolomic profiles were significantly modified after the application of the bioformulates. In particular, multivariate analysis revealed the separation coupled to the chemical composition of the untargeted compounds of the treated basil, as clearly demonstrated in the Principal Component Analysis (PCA; Figure 1) and the hierarchical clustering (Figure 2). The untargeted LC-MS qTOF analysis of the basil leaf extracts allowed for the identification of 99 compounds that were differential in respect to the CTRL. Among these compounds, eighteen compounds were putatively identified by comparison to a database containing a collection of known characterized secondary metabolites (in house database). In particular, among the different phenolic compounds and flavonoids, it was noted the presence of three hydroxycinnamic acids, ferulic acid, *p*-coumaric acid, caffeic acid, as well as the caffeic acid ester rosmarinic acid (Table 4).

**Table 4.** Metabolites putatively identified in leaf extracts of basil plants treated with different bioformulations in the field. For each compound, mass, retention time (RT), chemical empirical formula and similarity score are reported.

| Compound | Mass | RT | Chemical Empirical Formula | Similarity Score |
|---|---|---|---|---|
| Isocitric acid | 192.0279 | 0.976 | $C_6H_8O_7$ | 83.63 |
| Caffeic acid | 180.0418 | 2.362 | $C_9H_8O_4$ | 87.15 |
| 4-hydroxybenzoic acid | 138.0319 | 2.853 | $C_7H_6O_3$ | 85.75 |
| Luteolin-3-*O*-glucuronide | 448.1219 | 3.888 | $C_{21}H_{18}O_{12}$ | 98.66 |
| Ferulic acid | 194.0577 | 4.159 | $C_{10}H_{10}O_4$ | 86.95 |
| Lupinisoflavone E | 438.1652 | 4.182 | $C_{25}H_{26}O_7$ | 67.85 |
| Phenylacetic acid | 136.0518 | 4.336 | $C_8H_8O_2$ | 86.73 |
| Tricetin 3'-methyl ether 7-glucuronide | 492.0885 | 4.439 | $C_{22}H_{20}O_{13}$ | 87.54 |
| Medioresinol | 388.1731 | 4.463 | $C_{21}H_{24}O_7$ | 97.86 |
| Foliasalacioside A2 | 434.2136 | 4.644 | $C_{19}H_{32}O_8$ | 93.11 |
| Apigenin-7-*O*-glucoside | 432.1993 | 4.714 | $C_{21}H_{20}O_{10}$ | 83.72 |
| 7-hydroxycoumarin | 162.0316 | 5.006 | $C_9H_6O_3$ | 86.6 |
| Rosmarinic acid | 360.0843 | 5.015 | $C_{18}H_{16}O_8$ | 99.32 |
| Quercetin-5,3'-dimethyl ether-3-glucoside | 492.1269 | 5.026 | $C_{23}H_{24}O_{12}$ | 49.67 |
| *p*-coumaric acid | 164.0837 | 5.148 | $C_9H_8O_3$ | 87.36 |
| Cirsimaritin | 314.079 | 5.613 | $C_{17}H_{14}O_6$ | 99.65 |
| Rotundic acid | 488.3499 | 6.571 | $C_{30}H_{48}O_5$ | 96.79 |
| Colneleic acid | 294.2194 | 6.961 | $C_{18}H_{30}O_3$ | 98.47 |

The PCA analysis (Figure 1) of all compounds indicated that the principal components (PCs) accounted for 33.86% of the total variance, PC1 20.06% and PC2 13.80%. As previously noted in the heatmap (Figure 2), the multivariate analysis clearly demonstrates the separation of treatment T22 + 76A from the other bioformulations in the ordination, positioned to the far left of PC1, whereas the other treatments grouped together in the center. The distribution along PC2 indicated a group of compounds determined by the presence of BP alone in the bioformulations, which were positioned in the upper quadrants of the graph, whereas, there were the groupings of the combinations, BP + 6PP and BP + 76A positioned at the bottom of the ordination. The hierarchical clustering analysis (Figure 2) highlighted a clear separation of the metabolic profile of the plants treated with T22 + 76A from the other treatments. The rest of the nine treatments grouped together were then separated into two groups, in which one cluster contained all T22 treatments, as well as the application of BP alone and the BP + T22 + 76A combination, whereas the second cluster contained 6PP, 76A and CTRL singly, plus the combinations with the biopolymer.

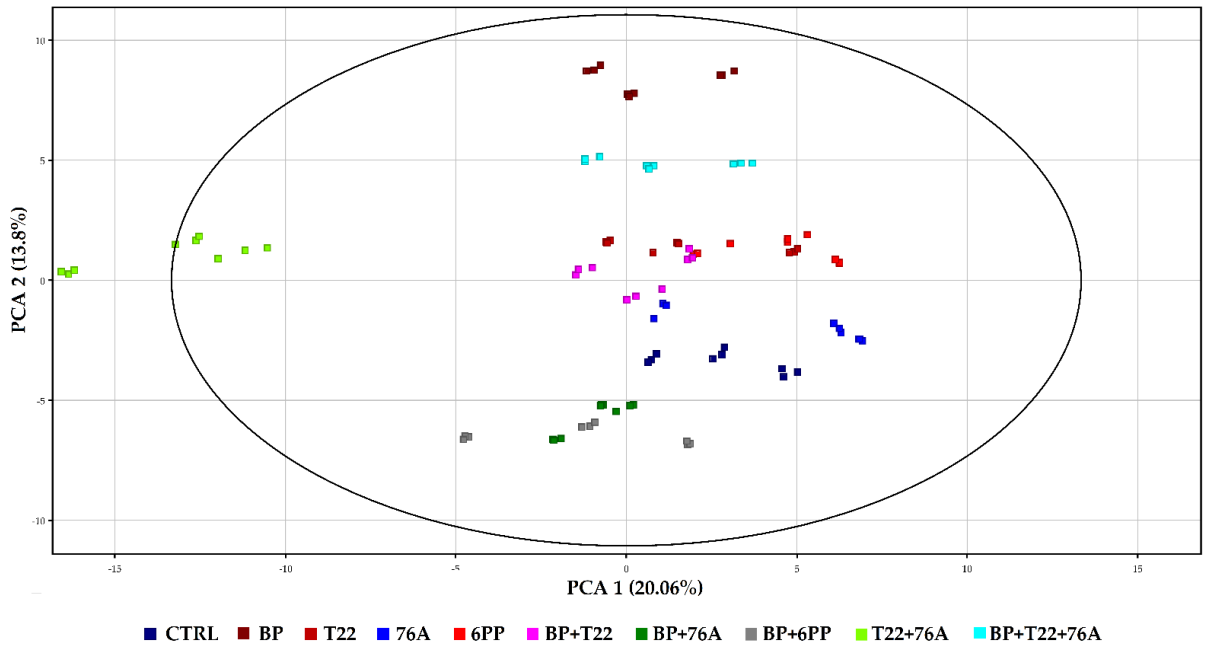


**Figure 1.** Analysis of the principal components (PCA) of the compounds identified in the leaf extracts of basil plants treated with the single components (BP, T22, 76A, 6PP, and CTRL) and with the relative combinations (BP + T22 + 76A, BP + 6PP, T22 + 76A, BP + 76A). The eigenvalues are represented with a total value of 33.86%, divided into PCA1 (20.06%) and PCA2 (13.8%).

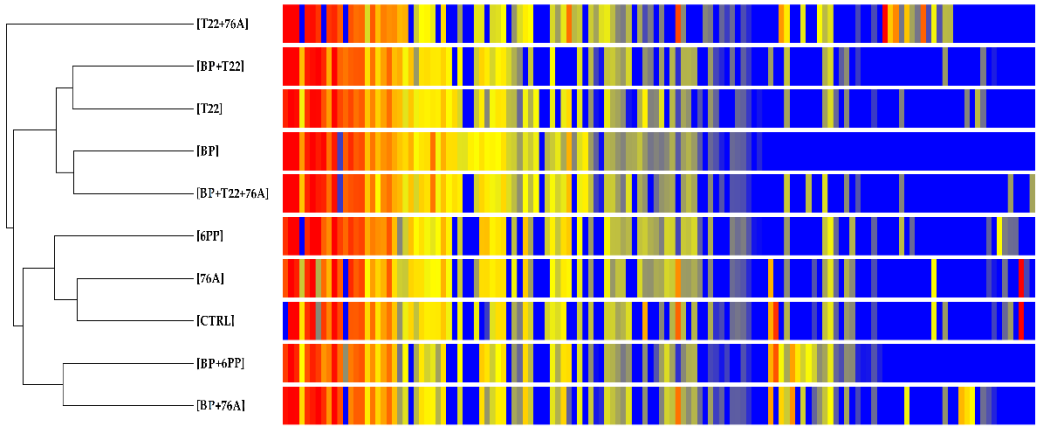


**Figure 2.** Abundance of the compounds in basil, treated with the bioformulations, as determined by LC-MS analysis and characterized in the heatmap. Plants were treated with bioformulations containing the single components (BP, T22, 76A, 6PP), the relative combinations (BP + T22 + 76A, BP + 6PP, T22 + 76A, BP + 76A, BP + T22), and a water (CTRL). The abundance of each compound is associated with a color scale ranging from blue (less abundant) to red (more abundant).

### *2.5. Targeted Metabolomic Analysis: Quantification of p-Coumaric, Caffeic and Rosmarinic Acids*

The most typical and important phenolic metabolites in the basil extracts, *p*-coumaric, caffeic and rosmarinic acids, were quantified to commercial standards as a reference. In particular, the highest concentrations of *p*-coumaric acid were found in basil treated with 76A (4.49 mg/g DW), followed by BP + 76A and BP + 6PP; the lowest levels were noted in BP and T22 + 76A treatments (Figure 3A). The quantity of caffeic acid demonstrated that after treatments with BP + T22 + 76A, BP + 6PP and T22 + 76A, the values were similar to that of CTRL. For all other treatments, it can be noted that values were lower than CTRL, particularly for 6PP and 76A singular treatments, which registered the

lowest values of caffeic acid, 0.19 and 0.18 mg/g DW, respectively (Figure 3B). For rosmarinic acid, the T22 + 76A treatment produced the highest concentration (1.17 mg/g DW) that was two-times higher than that of CTRL (0.56 mg/g DW). The lowest accumulation of rosmarinic acid was observed with the single treatments of 76A and 6PP, below the level of the CTRL (Figure 3C).

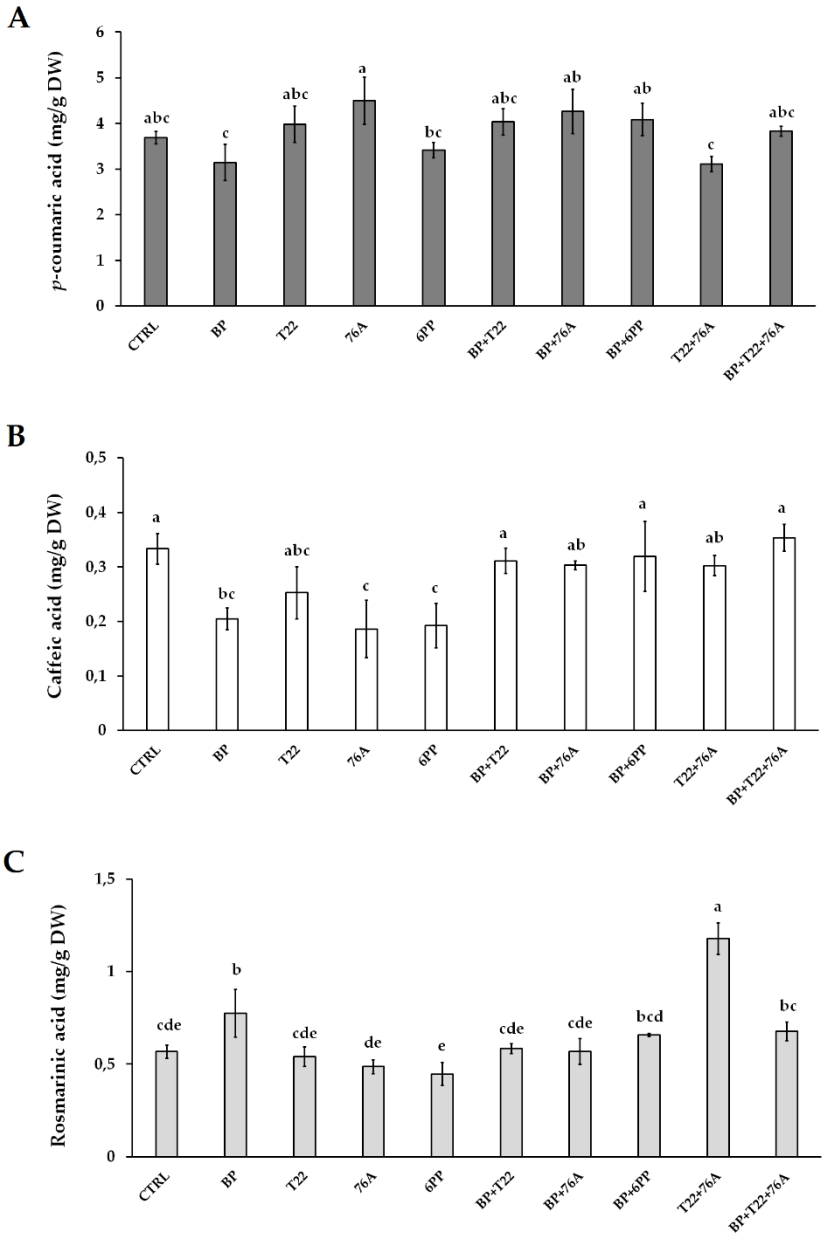


**Figure 3.** Concentration (mg/g DW) of *p*-coumaric acid (**A**), caffeic acid (**B**) and rosmarinic acid (**C**) in the leaf extracts of basil plants treated with the single components (BP, T22, 76A, 6PP), the relative combinations (BP + T22 + 76A, BP + 6PP, T22 + 76A, BP + 76A, BP + T22) and a water control (CTRL). Values are significant at $p \leq 0.001$, and values followed by different letters are significantly different according to Duncan's test at $p \leq 0.05$.

## 3. Discussion

Designing and formulating new microbial-based agricultural products, with biocontrol or biostimulant activity, is of particular interest for improving plant parameters such as growth promotion and yield, resistance to pathogens and pests, and the production of useful phytocompounds. This potential can be influenced by the individual

microorganisms present in the bioformulations, and in some cases enhanced by the combined action of beneficial microbial consortia (i.e., containing endophytic fungi and/or PGPR), with their bioactive metabolites, and other natural components. In this study, the application of two beneficial microorganisms, *Trichoderma afroharzianum* T22, a fungal biocontrol agent, and *Azotobacter chroococcum* 76A, a nitrogen-fixing bacteria, a fungal secondary metabolite (6 pentyl-α-pyrone) and bio-based polymer were tested to determine the effects of the stand-alone or combined application on sweet basil. These microorganisms were able to colonize the soil rhizosphere, and in the plant–microbe interactions established, many physical and biochemical activities were stimulated that could increase plant/root system development as noted in other studies [26,33,41,42]. Furthermore, findings from other investigations were confirmed, indicating that this effect could be improved with the addition of macromolecules of natural origins, such as vegetal-based biopolymers [34,36,43]. In fact, the current work demonstrated that the microbial consortium with the BP induced a significant increase in yield fresh weight, total biomass and total dry weight when compared to the single microbial consortium and control treatments. The increased total fresh, dry biomass, and root dry weights observed in the present study were similarly noted by Sabra et al. [44] on basil treated with a combination of the beneficial fungi *Rhizophagus irregularis* and *Serendipita indica* in comparison to CTRL treatment. The growth-promoting action exerted by *Trichoderma*, causing a direct stimulation of root development, has been attributed to the release into the rhizo-soil of small peptides, auxins, volatiles and other active signaling compounds [26,27,31,41] or by the indirect manner through which the fungus influences the solubilization of soil minerals [26,45] to increase macro- and micronutrient availability, transport and/or plant absorption [29,33,41]. Many of these studies obtained similar results when plants (i.e., corn) were treated with the same *Trichoderma* beneficial fungus combined with a conventional fertilizer [26,41]. Moreover, Shirzadi et al. [46] obtained better agronomic traits in basil (plant height, shoot fresh weight and dry weight) when treatments included combinations of mycorrhizal fungi with *Azotobacter* that were associated to the secretion of molecules by the bacteria that affected plant growth, including vitamin B, nicotinic acid, gibberellin, cytokine, etc., other than its capacity for biological nitrogen fixation. In addition, basil plants inoculated with *Azotobacter* alone showed an increase in dry weight, as supported in a study by Roshanpour et al. [47].

Recently, Silletti et al. [48] reported the potential complementation of *Azotobacter* and *Trichoderma* as a PGP consortium, whereby the combined biological activities in the mixture were able to increase the plant biostimulation effect over that of the single component treatments. This could also be due to the multiple positive associations that occur among various microorganisms [49–51], which may provide both greater efficacy in disease control as well as plant growth promotion when compared to products containing the single microbial agent [52]. The present investigation indicated that the *Trichoderma* secondary metabolite (6PP), known for its auxin-like properties that effected plant growth [30] of different horticultural crops [32,33,53], was able to generate an increased plant growth-promoting effect on sweet basil when combined with the BP that was greater than that of the metabolite applied singly. The addition of the biopolymer to the microbes and the metabolite formulations provided a positive plant effect, possibly by improving the product composition and the mode of delivery of the active ingredients to the plant [34,35]. In addition, the carboxymethyl cellulose (CMC) composition of the biopolymer could also have provided a potential source of nutrients both to the microbial consortia of the bioformulation, the beneficial microorganisms in the rhizosphere, as well as to the plant itself, thus providing an overall improvement of plant fitness in these growth conditions [34,36,43,54]. The positive effect of the BP application alone was noted to improve the photosynthetic efficiency (Fv/Fm) of the basil in the current work, confirming the observations recently made by Carillo et al. [43], who observed that the single

biopolymer treatment enhanced the production of some phytocompounds, such as GABA and MEA, involved in the photorespiration processes of tomato fruits.

The use of microorganisms in agriculture can also influence the rate and assimilatory pigments of photosynthesis; recent studies demonstrated the importance of microorganisms in physiological processes of plants. For example, fungi of the *Trichoderma* genus improved the chlorophyll synthesis of romaine lettuce and wall rocket plants [54,55], whereas *Azotobacter chroococcum* 76A increased the physiological parameters on microtome tomato [56]. In this study, all microbial treatments, particularly *Trichoderma afroharzianum* T22, showed higher chlorophyll values than the CTRL. In addition, the treatment with *Azotobacter chroococcum* 76A indicated greater phytostimulation efficacy with higher significant values of sweet basil in root dry weight, rate of $CO_2$ net assimilation and photosynthetic efficiency that can be related to a better fitness of the plant. The colonization of roots by *Trichoderma* may enhance growth response due to the enhancement of carbohydrate metabolism, photosynthetic and respiratory rates [45], thus triggering the plants physiological processes that improve the photosynthesis rate and stomatal conductance [57]. Silletti et al. noted that the photosynthetic rate was similarly higher in wheat when treated with *Trichoderma* or with *Azotobacter* [48], whereas the bacteria was found to release phytohormones that could stimulate photosynthesis in basil [47]. The co-inoculation of *Piriformospora indica* and *Trichoderma virens* was found to produce an improvement of chlorophyll fluorescence parameters [58], whereas, in the present study, only the inoculation of T22 alone demonstrated an improvement in photosystem II efficiency in basil. In addition, Gonzalez-Rodriguez and co-workers [59] depicted an increase in the photosynthesis parameters, such as total chlorophyll and photosynthesis in pineapple in vitro plantlets treated with *Azotobacter chroococcum*.

On the global market, much attention is being given by consumers to purchase foods that have been cultivated in low-environmental-impact systems, i.e., organic farming, or with reduced chemical products (fertilizers and pesticides), and to select nutrient-dense products that have a higher health value and nutritional content. This perspective has fostered a growing interest in the development of research and cultivation practices focused on improving the properties of the plant compounds found in various food products in order to provide an essential human diet that contributes to the overall well-being of the consumer.

Basil has been widely used in traditional medicine [60,61] as a digestive stimulant [62] and is recognized for its antibacterial [63], antitumor [60] and anticonvulsant [64] properties. In particular, basil is rich in phenolic acids, which contribute to its strong antioxidant capacity [65–67], a property that exerts beneficial effects on human health—the vascular and nervous system [8]—reducing the effects associated with various degenerative diseases such as Alzheimer's [5], Parkinson's [6] and dementia [9]. These compounds are known to positively protect key biological constituents such as lipoproteins, membranes and DNA from oxidative processes [68]. Due to the importance of phenolic compounds for consumer health, their quantity indirectly attributes an extra value to the crops that improves the nutritional and functional properties of vegetables and herbs [69].

The evaluation of the phenolic components produced by the plant in response to the application of diverse bioformulations during cultivation in the field indicated that the metabolic profile of the different basil leaf extracts was highlighted by a differential abundance of biologically important metabolites, including p-coumaric acid, caffeic acid, and rosmarinic acid, known for their health properties [11–13,15,16]. In particular, this study shows that the treatment of basil plants with *Azotobacter chroococcum* 76A alone increased the production of p-coumaric acid, while the *Trichoderma afroharzianum* T22 + *Azotobacter chroococcum* 76A treatment induced a major production of rosmarinic acid. In general, the quantity of caffeic acid in the basil extracts was less affected by the biological treatments, and not clearly associated to specific treatments.

Other studies have demonstrated how the use of microorganisms can influence the essential oil and phenolic components on basil. For instance, the inoculum of AMF improved the concentration of rosmarinic acid, chicoric acid and caffeic acid on 4 basil cultivars [70], growth and aroma volatiles (e.g., linalool) on sweet basil in heavy-metal-contaminated soil [44], plus the use of different commercial microbial bio-based products increased the percentage of different metabolites (e.g., caffeic acid) on different basil cultivars [57]. Moreover, our results indicate that the simultaneous application of *Trichoderma afroharzianum* T22 with *Azotobacter chroococcum* 76A induced a better modulation of phenolics metabolism when compared to the single applications of *Trichoderma* and *Azotobacter*, especially for rosmarinic and caffeic acid, as is in line with findings by Sabra et al. [44] affirming that the dual application of beneficial fungi and its associated bacteria generated an enhancement of sweet basil nutraceutical value.

The application of the microbial, fungal bioactive compounds and biopolymer components in various bioformulations was found to differentially modify the agronomic characteristics and the metabolic profile of basil plants, in some cases increasing the quantity of the phenolic compounds, thus producing a qualitatively superior final product. In fact, phenolics strongly contribute to basil antioxidant capacity and biological properties [65–67], so through the increase of these components, well known for their many applications in the field of human health [11–13,15,16], the consumer can obtain a more valuable basil with enhancing health properties. However, ongoing studies will determine the effects of these biological formulations on Genovese basil and the other phytocompounds it produces, such as essential oils, that are important for the characteristics of aroma and the biocontrol of disease agents, that contribute to the unique qualities of this Mediterranean food and medicinal plant.

## 4. Materials and Methods

### *4.1. Application of Microbial Biostimulants*

The microbial biostimulant treatments involved the use of different microorganisms, their components and natural molecules. Nine biostimulant treatments were adopted: (i) *Trichoderma afroharzianum* strain T22 (ex-*Trichoderma harzianum* [71]) commercial formulation of Trianum-P (Koppert Biological Systems, Rotterdam, the Netherlands) implemented at a final concentration of $10^7$ spore $mL^{-1}$, (ii) *Azotobacter chroococcum* strain 76A ([72]; freeze-dried bacterial cells in a final concentration of $10^7$ CFU $mL^{-1}$), (iii) 6 pentyl-α-pyrone (6PP) concentration of $10^{-6}$ M (Sigma-Aldrich, Milan, Italy), (iv) biopolymer (BP; diluted in water) composed of carboxymethyl cellulose (CMC), a polyanion derived from cellulose used as a thickener, emulsifier and nutrient carrier in agriculture with the addition of Pluronic F-127 (PF-127), as reported in [43], (v) T22 ($10^6$ spores $mL^{-1}$) + 76A ($10^7$ CFU $mL^{-1}$), (vi) BP + T22 ($10^7$ spores $mL^{-1}$), (vii) BP + 76A ($10^7$ CFU $mL^{-1}$), (viii) BP + T22 ($10^6$ spores $mL^{-1}$) + 76A ($10^7$ CFU $mL^{-1}$) and (ix) BP + 6PP ($10^{-6}$ M); additionally, (x), a control treatment, only water, was administrated at the same volume as the other treatments. The liquid bioformulations with the microorganisms and the metabolite were prepared in water throughout the experiment. The treatments containing the biopolymer were always diluted with water in a 1:1 proportion (BP: water), which included the final concentration of the other components in the total final volume of the bioformulation.

### *4.2. Plant Material, Greenhouse Experimental Design and Treatments*

Sweet basil (*Ocimum basilicum* L. cv Genovese) was used in this experiment, carried out in a protected greenhouse of the BiPaF Section of the Department of Agriculture, University of Naples Federico II, Portici (NA, Italy). A randomized complete-block scheme with a total of 10 treatments was replicated three-times (total 300 plants). Commercial seedlings were transplanted to the field in June. The first application of the

biological treatments was carried out at the time of transplant using a root dip method [43,55]. After two weeks, the treatments were repeated by watering 25 mL of the bioformulation treatments to the base of each plant. Plants were observed weekly for any developing leaf or root disease symptoms.

### *4.3. Sampling and Yield Assessment*

In July 2019, 34 days after transplanting, the plants were cut above the first node. For each treatment, 5 plants were harvested per replicate, for a total of 15 plants per treatment, from which destructive biometric analyses were conducted to evaluate the marketable production. In particular, the number of leaves, yield fresh weight (FW of the leaves) and total biomass (leaves + stems) FW were measured immediately after harvest. Subsequently, a sub-sample of each plant fresh sample, plus the washed roots, were placed in a forced-air oven at 65 °C for approx. 72 h, to obtain a constant dry weight (DW) of the plant material, then total dry matter (DM%) was calculated as DW/FW × 100.

### *4.4. SPAD Index and Colorimetric Components*

SPAD index measurements were performed on young fully expanded basil leaves (between midrib and leaf margin) using a Chlorophyll Meter (Minolta SPAD-502, Osaka, Japan). A total of 30 measurements were acquired per replicate and reported to one mean value. Leaf colorimetry was determined by measuring the colorimetric indices (L*, a*, b*) of 10 young fully expanded leaves per replicate using a colorimeter Minolta Chroma meter, CM-2600d (Minolta Camera Co. Ltd., Osaka, Japan).

### *4.5. Determination of Leaf Gas Exchange and Photosystem II Efficiency*

Before harvest, a portable gas exchange analyzer (LCA-4; ADC BioScientific Ltd., Hoddesdon, UK) was used to determine the net assimilation rate of $CO_2$, the stomatal resistance and the transpiration rate of basil plants ($A_{CO2}$, $r_s$ and E, respectively). Three physiological measurements were determined per replicate. For the maximum quantum use efficiency of the Photosystem II (Fv/Fm), measurements were performed with a portable fluorometer (Plant Stress Kit, Opti-Sciences, Hudson, NH, USA), where four measurements per replicate were performed.

### *4.6. Preparation of Basil Leaves Extracts*

For the metabolomic analysis, fresh leaf samples were collected from each replicate, submerged in liquid nitrogen, then stored at −80 °C. The samples were freeze dried for 72 h, and the leaf tissue was pulverized using a mortar and pestle. A 200 mg aliquot of the lyophilized powdered material was suspended in 2 mL of an 80:20 methanol/$H_2O$ solution (solvent 99.9% for LC-MS). The sample was agitated for 1 min by vortexing, then centrifuged for 15 min at a speed of 5000 rpm at a temperature of 4 °C. The supernatant was filter sterilized (0.22 µm syringe filter) and stored in glass vials, at 4 °C until analysis.

### *4.7. LC-MS analysis—Targeted and Untargeted Metabolome*

Following the method described by Marra et al. [73], the spectrometric analysis of the plant extracts was performed by an LC-MS Q-TOF Agilent Technologies (Santa Clara, CA, USA), equipped with a 1260 Infinity series HPLC with DAD detector, and a mass spectrometer Q-TOF (model G6540) with Dual ESI source. The plant extracts were separated with a reverse-phase analytical Ascentis ® Express C18 column (2.7 µm, 50 mm x 3.0 mm id, Supelco ©, Bellefonte, PA, USA). The identification and quantification of the three phenolic acids *p*-coumaric, caffeic and rosmarinic were obtained by comparing the mass and the retention time (RT) to standard compounds (Sigma-Aldrich, St. Louis, USA). These standards were analyzed with the same LC-MS method and the

quantification was obtained by interpolating the averaged data with a previously constructed calibration curve.

### *4.8. Statistical Analysis*

Data were statistically analyzed (One-way Anova) with SPSS v. 21 (IBM Corp., Armonk, NY, USA). Bioformulations of beneficial microbial consortia and vegetal biopolymers effects on yield, growth parameters, SPAD index, leaf colorimetry, physiological analysis and phenolics profile were analyzed using Duncan's multiple range test performed at $p = 0.05$. Statistical analysis of basil extracts metabolic profile was carried out using Mass Profile Professional, version 13.1.1 (Agilent Technologies). One-way ANOVA ($p > 0.05$) with Tukey–HSD post hoc was implemented to evaluate the differential significance of samples. Eventually, a fold change > 2.0 was used. The results obtained were then subjected to principal component analysis (PCA) to depict the difference between the different biostimulant treatments. A grouping of the samples was then made based on the abundance of continuous variables (Hierarchical clustering) by combining the technical replicates. Statistically relevant compounds were identified using: an in-house database containing information on over 2000 secondary metabolites produced by plants; the library METLIN provided from Agilent, containing over 15,000 natural metabolites and di- and tri-peptides; information available from literature.

## 5. Conclusions

The implementation of bioformulations with the association of specially selected microorganisms, bioactive substances and biopolymer allowed us to define and present new bioformulations for use in agriculture. The outcome of the developed bioformulations consisted of improved parameters of Genovese basil, in terms of growth promotion, yield increase and the efficiency of photosystem II and photosynthesis in general. Furthermore, these treatments significantly modulate the plant metabolome and increase differentially the production of three beneficial phenolic compounds: *p*-coumaric acid, caffeic acid and rosmarinic acid. In summary, for the agronomic parameters evaluated, the highest fresh weight yields (marketable produce) were noted in the plants treated with the combinations of BP + T22 + 76A or BP + 6PP. Regarding the biochemical profiles of the phenolic plant compounds in basil, plants receiving the T22 + 76A treatment exhibited the greatest production of rosmarinic acid, whereas *Azotobacter chroococcum* 76A alone displayed the best increased production of *p*-coumaric acid. Therefore, the new formulations based on a consortium of *Trichoderma*, *Azotobacter*, 6 pentyl-α-pyrone and a plant biopolymer are presented as innovative products in improving the production of Genovese basil. The application of these bioformulations can have a dual positive effect, achieving both better eco-sustainable agriculture and the opportunity to obtain a final product with improved yield and bioactive secondary metabolites content.

**Author Contributions:** Conceptualization, S.L.W. and Y.R.; methodology, Y.R., O.P., A.B., F.V., D.R., S.L.W.; investigation, E.C. and C.E.-N., validation, E.C., and S.L.W.; formal analysis, C.E.-N., E.C., F.V., D.R., A.S. and Y.R.; data curation, C.E.-N., E.C. and A.S.; writing—original draft preparation, C.E.-N., Y.R., E.C. and S.L.W.; writing—review and editing, E.C., C. E-N., Y.R., V.V., O.P., A.B., F. V. , D.R., A.S., M.L. and S.L.W.; supervision, Y.R. and S.L.W.; project administration, F.V. and S.L.W.; funding acquisition, F.V., M.L. and S.L.W. All authors have read and agreed to the published version of the manuscript.

**Funding:** This research was funded by POR FESR CAMPANIA 2014/2020-O.S. 1.1 (grant number Bioagro 559); MISE CRESO (grant number Protection no. F/050421/01-03/X32); European Union Horizon 2020 Research and Innovation Program, ECOSTACK (grant agreement no. 773554).

**Acknowledgments:** The authors would like to thank Dr. Antonio Pannico for the photosynthesis measurements and statistical analysis, Dr. Alessandro Robertiello for the liquid fermentation of *Azotobacter chroococcum* 76A, Francesco Cristofano for the fluorescence measurements, Francesco Iannotta and Connie Gallo for greenhouse and laboratory activities, Anastasia Vassetti and Raffaele Loffredo for their assistance on LC-MS analysis, as well as Koppert Biological Systems, Rotterdam, the Netherlands, for providing the commercial formulation of the biofungicide Trianum P (T22).

**Conflicts of Interest:** The authors declare no conflict of interest.

## References

1. Rouphael, Y.; Giordano, M.; Pannico, A.; Di Stasio, E.; Raimondi, G.; El-Nakhel, C.; Di Mola, I.; Mori, M.; De Pascale, S. Nutritional quality of hydroponically grown basil in response to salinity and growing season. In *International Symposium on New Technologies for Environment Control, Energy-Saving and Crop Production in Greenhouse and Plant 2017*; Yang, Q., Li, T., Eds.; ISHS Acta Horticulturae: Beijing, China, 2018; Volume 1227, pp. 693–698, doi:10.17660/actahortic.2018.1227.88.
2. Corrado, G.; Lucini, L.; Miras-Moreno, B.; Chiaiese, P.; Colla, G.; De Pascale, S.; Rouphael, Y. Metabolic Insights into the Anion-Anion Antagonism in Sweet Basil: Effects of Different Nitrate/Chloride Ratios in the Nutrient Solution. *Int. J. Mol. Sci.* **2020**, *21*, 2482, doi:10.3390/ijms21072482.
3. Corrado, G.; Formisano, L.; De Micco, V.; Pannico, A.; Giordano, M.; El-Nakhel, C.; Chiaiese, P.; Sacchi, R.; Rouphael, Y. Understanding the Morpho-Anatomical, Physiological, and Functional Response of Sweet Basil to Isosmotic Nitrate to Chloride Ratios. *Biology* **2020**, *9*, 158, doi:10.3390/biology9070158.
4. Corrado, G.; Chiaiese, P.; Lucini, L.; Miras-Moreno, B.; Colla, G.; Rouphael, Y. Successive Harvests Affect Yield, Quality and Metabolic Profile of Sweet Basil (*Ocimum basilicum* L.). *Agron.* **2020**, *10*, 830, doi:10.3390/agronomy10060830.
5. Dai, Q.; Borenstein, A.R.; Wu, Y.; Jackson, J.C.; Larson, E.B. Fruit and Vegetable Juices and Alzheimer's Disease: The Kame Project. *Am. J. Med.* **2006**, *119*, 751–759, doi:10.1016/j.amjmed.2006.03.045.
6. Checkoway, H.; Powers, K.; Smith-Weller, T.; Franklin, G.M.; Longstreth, W.T.; Swanson, P.D. Parkinson's Disease Risks Associated with Cigarette Smoking, Alcohol Consumption, and Caffeine Intake. *Am. J. Epidemiol.* **2002**, *155*, 732–738, doi:10.1093/aje/155.8.732.
7. Hussain, A.I.; Anwar, F.; Sherazi, S.T.H.; Przybylski, R. Chemical composition, antioxidant and antimicrobial activities of basil (*Ocimum basilicum* L.) essential oils depends on seasonal variations. *Food Chem.* **2008**, *108*, 986–995, doi:10.1016/j.foodchem.2007.12.010.
8. Vauzour, D.; Rodriguez-Mateos, A.; Corona, G.; Oruna-Concha, M.J.; Spencer, J.P.E. Polyphenols and Human Health: Prevention of Disease and Mechanisms of Action. *Nutrients.* **2010**, *2*, 1106–1131, doi:10.3390/nu2111106.
9. Commenges, D.; Scotet, V.; Renaud, S.; Jacqmin-Gadda, H.; Barberger-Gateau, P.; Dartigues, J.-F. Intake of flavonoids and risk of dementia. *Eur. J. Epidemiol.* **2000**, *16*, 357–363, doi:10.1023/a:1007614613771.
10. Quideau, S.; Deffieux, D.; Douat-Casassus, C.; Pouysegu, L. ChemInform Abstract: Plant Polyphenols: Chemical Properties, Biological Activities, and Synthesis. *Angew. Chem. Int. Ed.* **2011**, *42*, 586–621, doi:10.1002/chin.201117261.
11. Pragasam, S.J.; Venkatesan, V.; Rasool, M. Immunomodulatory and Anti-inflammatory Effect of p-Coumaric Acid, a Common Dietary Polyphenol on Experimental Inflammation in Rats. *Inflammation* **2013**, *36*, 169–176, doi:10.1007/s10753-012-9532-8.

12. Rajendra Prasad, N.; Karthikeyan, A.; Karthikeyan, S.; Venkata Reddy, B. Inhibitory effect of caffeic acid on cancer cell proliferation by oxidative mechanism in human HT-1080 fibrosarcoma cell line. *Mol. Cell. Biochem.* **2011**, *349*, 11–19, doi:10.1007/s11010-010-0655-7.
13. Olthof, M.R.; Hollman, P.C.H.; Katan, M.B. Chlorogenic Acid and Caffeic Acid Are Absorbed in Humans. *J. Nutr.* **2001**, *131*, 66–71, doi:10.1093/jn/131.1.66.
14. Hakkim, F.L.; Shankar, C.G.; Girija, S. Chemical Composition and Antioxidant Property of Holy Basil (*Ocimum sanctum* L.) Leaves, Stems, and Inflorescence and Their in Vitro Callus Cultures. *J. Agric. Food Chem.* **2007**, *55*, 9109–9117, doi:10.1021/jf071509h.
15. Sanbongi, C.; Takano, H.; Osakabe, N.; Sasa, N.; Natsume, M.; Yanagisawa, R.; Inoue, K.-I.; Sadakane, K.; Ichinose, T.; Yoshikawa, T. Rosmarinic acid in perilla extract inhibits allergic inflammation induced by mite allergen, in a mouse model. *Clin. Exp. Allergy* **2004**, *34*, 971–977, doi:10.1111/j.1365-2222.2004.01979.x.
16. Bais, H.P.; Walker, T.S.; Schweizer, H.P.; Vivanco, J.M. Root specific elicitation and antimicrobial activity of rosmarinic acid in hairy root cultures of *Ocimum basilicum*. *Plant Physiol. Biochem.* **2002**, *40*, 983–995, doi:10.1016/s0981-9428(02)01460-2.
17. Kiferle, C.; Lucchesini, M.; Mensuali, A.; Maggini, R.; Raffaelli, A.; Pardossi, A. Rosmarinic acid content in basil plants grown in vitro and in hydroponics. *Centr. Eur. J. Biol.* **2011**, *6*, 946–957, doi:10.2478/s11535-011-0057-1.
18. Colla, G.; Rouphael, Y. Biostimulants in horticulture. *Sci. Hortic.* **2015**, *196*, 1–2, doi:10.1016/j.scienta.2015.10.044.
19. Chouyia, F.E.; Romano, I.; Fechtali, T.; Fagnano, M.; Fiorentino, N.; Visconti, D.; Idbella, M.; Ventorino, V.; Pepe, O. P-Solubilizing *Streptomyces roseocinereus* MS1B15 With Multiple Plant Growth-Promoting Traits Enhance Barley Development and Regulate Rhizosphere Microbial Population. *Front. Plant Sci.* **2020**, *11*, 1137, doi:10.3389/fpls.2020.01137.
20. Romano, I.; Ventorino, V.; Ambrosino, P.; Testa, A.; Chouyia, F.E.; Pepe, O. Development and Application of Low-Cost and Eco-Sustainable Bio-Stimulant Containing a New Plant Growth-Promoting Strain *Kosakonia pseudosacchari* TL13. *Front. Microbiol.* **2020**, *11*, 11, doi:10.3389/fmicb.2020.02044.
21. Vinale, F.; Sivasithamparam, K. Beneficial effects of *Trichoderma* secondary metabolites on crops. *Phytother. Res.* **2020**, *34*, 2835–2842, doi:10.1002/ptr.6728.
22. Woo, S.L.; Pepe, O. Microbial Consortia: Promising Probiotics as Plant Biostimulants for Sustainable Agriculture. *Front. Plant Sci.* **2018**, *9*, 1801, doi:10.3389/fpls.2018.01801.
23. Wani, S.A.; Chand, S.; Ali, T. Potential use of *Azotobacter chroococcum* in crop production: An overview. *Curr. Agric. Res.* **2013**, *1*, 35–38, doi:10.12944/CARJ.1.1.04.
24. Rizvi, A.; Khan, M.S. Heavy metal induced oxidative damage and root morphology alterations of maize (Zea mays L.) plants and stress mitigation by metal tolerant nitrogen fixing *Azotobacter chroococcum*. *Ecotoxicol. Environ. Saf.* **2018**, *157*, 9–20, doi:10.1016/j.ecoenv.2018.03.063.
25. Gurikar, C.; Naik, M.K.; Sreenivasa, M.Y. *Azotobacter*: PGPR Activities with Special Reference to Effect of Pesticides and Biodegradation. In *Microbial Inoculants in Sustainable Agricultural Productivity*; Singh, D., Singh, H., Prabha R, Eds.; Springer International Publishing: Cham, Switzerland, 2015; Volume 1, pp. 229–244, doi:10.1007/978-81-322-2647-5_13.
26. Harman, G.E.; Howell, C.R.; Viterbo, A.; Chet, I.; Lorito, M. *Trichoderma* species—opportunistic, avirulent plant symbionts. *Nat. Rev. Microbiol.* **2004**, *2*, 43–56, doi:10.1038/nrmicro797.
27. Shoresh, M.; Harman, G.E. The relationship between increased growth and resistance induced in plants by root colonizing microbes. *Plant Signal. Behav.* **2008**, *3*, 737–739, doi:10.4161/psb.3.9.6605.

28. Raaijmakers, J.M.; Paulitz, T.; Steinberg, C.; Alabouvette, C.; Moënne-Loccoz, Y. The rhizosphere: A playground and battlefield for soilborne pathogens and beneficial microorganisms. *Plant Soil* **2009**, *321*, 341–361, doi:10.1007/s11104-008-9568-6.
29. Lorito, M.; Woo, S. *Trichoderma*: A Multi-Purpose Tool for Integrated Pest Management. In *Principles of Plant-Microbe Interactions*; Lugtenberg, B., Ed.; Springer International Publishing: Cham, Switzerland, 2015; pp. 345–353, doi:10.1007/978-3-319-08575-3_36.
30. Vinale, F.; Sivasithamparam, K.; Ghisalberti, E.L.; Marra, R.; Woo, S.L.; Lorito, M. *Trichoderma*–plant–pathogen interactions. *Soil Biol. Biochem.* **2008**, *40*, 1–10, doi:10.1016/j.soilbio.2007.07.002.
31. Vinale, F.; Sivasithamparam, K.; Ghisalberti, E.L.; Woo, S.L.; Nigro, M.; Marra, R.; Lombardi, N.; Pascale, A.; Ruocco, M.; Lanzuise, S.; et al. *Trichoderma* Secondary Metabolites Active on Plants and Fungal Pathogens. *Open Mycol. J.* **2014**, *8*, 127–139, doi:10.2174/1874437001408010127.
32. Vinale, F.; Sivasithamparam, K.; Ghisalberti, E.L.; Ruocco, M.; Woo, S.L.; Lorito, M. *Trichoderma* Secondary Metabolites that Affect Plant Metabolism. *Nat. Prod. Commun.* **2012**, *7*, 1545–1550, doi:10.1177/1934578x1200701133.
33. Vinale, F.; Nigro, M.; Sivasithamparam, K.; Flematti, G.; Ghisalberti, E.L.; Ruocco, M.; Varlese, R.; Marra, R.; Lanzuise, S.; Eid, A.; et al. Harzianic acid: A novel siderophore from *Trichoderma harzianum*. *FEMS Microbiol. Lett.* **2013**, *347*, 123–129, doi:10.1111/1574-6968.12231.
34. Lucini, L.; Rouphael, Y.; Cardarelli, M.; Bonini, P.; Baffi, C.; Colla, G. A Vegetal Biopolymer-Based Biostimulant Promoted Root Growth in Melon While Triggering Brassinosteroids and Stress-Related Compounds. *Front. Plant Sci.* **2018**, *9*, 472, doi:10.3389/fpls.2018.00472.
35. Le Mire, G.; Nguyen, M.L.; Fassotte, B.; du Jardin, P.; Verheggen, F.; Delaplace, P.; Jijakli, M. Review: Implementing plant biostimulants and biocontrol strategies in the agroecological management of cultivated ecosystems. *Biotechnol. Agron. Soc. Environ*. **2016**, *20*, 299–313, doi:10.25518/1780-4507.12717.
36. Guilherme, M.R.; Aouada, F.A.; Fajardo, A.; Martins, A.F.; Paulino, A.; Davi, M.F.; Rubira, A.; Muniz, E. Superabsorbent hydrogels based on polysaccharides for application in agriculture as soil conditioner and nutrient carrier: A review. *Eur. Polym. J.* **2015**, *72*, 365–385, doi:10.1016/j.eurpolymj.2015.04.017.
37. Coeshott, C.M.; Smithson, S.L.; Verderber, E.; Samaniego, A.; Blonder, J.M.; Rosenthal, G.J.; Westerink, M.A.J. Pluronic®F127-based systemic vaccine delivery systems. *Vaccine* **2004**, *22*, 2396–2405, doi:10.1016/j.vaccine.2003.11.064.
38. Zhang, W.; Shi, Y.; Chen, Y.; Yu, S.; Hao, J.; Luo, J.; Sha, X.; Fang, X. Enhanced antitumor efficacy by Paclitaxel-loaded Pluronic P123/F127 mixed micelles against non-small cell lung cancer based on passive tumor targeting and modulation of drug resistance. *Eur. J. Pharm. Biopharm.* **2010**, *75*, 341–353, doi:10.1016/j.ejpb.2010.04.017.
39. Ensign, L.M.; Lai, S.K.; Wang, Y.-Y.; Yang, M.; Mert, O.; Hanes, J.; Cone, R. Pretreatment of Human Cervicovaginal Mucus with Pluronic F127 Enhances Nanoparticle Penetration without Compromising Mucus Barrier Properties to Herpes Simplex Virus. *Biomacromolecules* **2014**, *15*, 4403–4409, doi:10.1021/bm501419z.
40. Akash, M.S.H.; Rehman, K.; Chen, S. Pluronic F127-Based Thermosensitive Gels for Delivery of Therapeutic Proteins and Peptides. *Polym. Rev.* **2014**, *54*, 573–597, doi:10.1080/15583724.2014.927885.
41. López-Bucio, J.; Pelagio-Flores, R.; Herrera-Estrella, A. *Trichoderma* as biostimulant: Exploiting the multilevel properties of a plant beneficial fungus. *Sci. Hortic.* **2015**, *196*, 109–123, doi:10.1016/j.scienta.2015.08.043.
42. Ruzzi, M.; Aroca, R. Plant growth-promoting rhizobacteria act as biostimulants in horticulture. *Sci. Hortic.* **2015**, *196*, 124–134, doi:10.1016/j.scienta.2015.08.042.

43. Carillo, P.; Woo, S.L.; Comite, E.; El-Nakhel, C.; Rouphael, Y.; Fusco, G.M.; Borzacchiello, A.; Lanzuise, S.; Vinale, F. Application of *Trichoderma harzianum*, 6-Pentyl-α-pyrone and Plant Biopolymer Formulations Modulate Plant Metabolism and Fruit Quality of Plum Tomatoes. *MDPI Plants* **2020**, *9*, 771, doi:10.3390/plants9060771.
44. Sabra, M.; Aboulnasr, A.; Franken, P.; Perreca, E.; Wright, L.P.; Camehl, I. Beneficial Root Endophytic Fungi Increase Growth and Quality Parameters of Sweet Basil in Heavy Metal Contaminated Soil. *Front. Plant Sci.* **2018**, *9*, 1726, doi:10.3389/fpls.2018.01726.
45. Vinci, G.; Cozzolino, V.; Mazzei, P.; Monda, H.; Spaccini, R.; Piccolo, A. An alternative to mineral phosphorus fertilizers: The combined effects of *Trichoderma harzianum* and compost on *Zea mays*, as revealed by 1H NMR and GC-MS metabolomics. *PLoS ONE* **2018**, *13*, e0209664, doi:10.1371/journal.pone.0209664.
46. Shirzadi, F.; Ardakani, M.R.; Asadirahmani, H.; Asgari, A. Effects of mycorrhiza (*Glomus intraradices*) azotobacter (*Azotobacter chroococcum*) and vermicompost on yield and essential oil of basil (*Ocimum basilicum* L.) in organic agriculture. *Int. J. Biosc.* **2015**, *6*, 1–6, doi:10.12692/ijb/6.7.1-6.
47. Roshanpour, N.; Darzi, M.T.; Hadi, M.H.S. Effects of plant growth promoter bacteria on biomass and yield of basil (*Ocimum basilicum* L.). *Int. J. Adv. Biol. Biom. Res*. **2014**, *2*, 2077–2085.
48. Silletti, S.; Di Stasio, E.; Van Oosten, M.J.; Ventorino, V.; Pepe, O.; Napolitano, M.; Marra, R.; Woo, S.L.; Cirillo, V.; Maggio, A. Biostimulant Activity of *Azotobacter chroococcum* and *Trichoderma harzianum* in Durum Wheat under Water and Nitrogen Deficiency. *Agronomy* **2021**, *11*, 380, doi:10.3390/agronomy11020380.
49. Jetiyanon, K. Defensive-related enzyme response in plants treated with a mixture of *Bacillus* strains (IN937a and IN937b) against different pathogens. *Biol. Control.* **2007**, *42*, 178–185, doi:10.1016/j.biocontrol.2007.05.008.
50. Kannan, V.; Sureendar, R. Synergistic effect of beneficial rhizosphere microflora in biocontrol and plant growth promotion. *J. Basic Microbiol.* **2008**, *49*, 158–164, doi:10.1002/jobm.200800011.
51. Srivastava, R.; Khalid, A.; Singh, U.; Sharma, A. Evaluation of arbuscular mycorrhizal fungus, fluorescent *Pseudomonas* and *Trichoderma harzianum* formulation against *Fusarium oxysporum* f. sp. *lycopersici* for the management of tomato wilt. *Biol. Control.* **2010**, *53*, 24–31, doi:10.1016/j.biocontrol.2009.11.012.
52. Stockwell, V.O.; Johnson, K.B.; Sugar, D.; Loper, J.E. Mechanistically Compatible Mixtures of Bacterial Antagonists Improve Biological Control of Fire Blight of Pear. *Phytopathol* **2011**, *101*, 113–123, doi:10.1094/phyto-03-10-0098.
53. Pascale, A.; Vinale, F.; Manganiello, G.; Nigro, M.; Lanzuise, S.; Ruocco, M.; Marra, R.; Lombardi, N.; Woo, S.L.; Lorito, M. *Trichoderma* and its secondary metabolites improve yield and quality of grapes. *Crop. Prot.* **2017**, *92*, 176–181, doi:10.1016/j.cropro.2016.11.010.
54. Rouphael, Y.; Carillo, P.; Colla, G.; Fiorentino, N.; Sabatino, L.; El-Nakhel, C.; Giordano, M.; Pannico, A.; Cirillo, V.; Shabani, E.; et al. Appraisal of Combined Applications of *Trichoderma virens* and a Biopolymer-Based Biostimulant on Lettuce Agronomical, Physiological, and Qualitative Properties under Variable N Regimes. *Agron.* **2020**, *10*, 196, doi:10.3390/agronomy10020196.
55. Caruso, G.; El-Nakhel, C.; Rouphael, Y.; Comite, E.; Lombardi, N.; Cuciniello, A.; Woo, S.L. *Diplotaxis tenuifolia* (L.) DC. Yield and Quality as Influenced by Cropping Season, Protein Hydrolysates, and *Trichoderma* Applications. *MDPI Plants* **2020**, *9*, 697, doi:10.3390/plants9060697.
56. Van Oosten, M.J.; Di Stasio, E.; Cirillo, V.; Silletti, S.; Ventorino, V.; Pepe, O.; Raimondi, G.; Maggio, A. Root inoculation with *Azotobacter chroococcum* 76A enhances tomato plants adaptation to salt stress under low N conditions. *BMC Plant Biol.* **2018**, *18*, 205, doi:10.1186/s12870-018-1411-5.

57. Teliban, G.-C.; Burducea, M.; Zheljazkov, V.; Dincheva, I.; Badjakov, I.; Munteanu, N.; Mihalache, G.; Cojocaru, A.; Popa, L.-D.; Stoleru, V. The Effect of Myco-Biocontrol Based Formulates on Yield, Physiology and Secondary Products of Organically Grown Basil. *Agriculture* **2021**, *11*, 180, doi:10.3390/agriculture11020180.
58. Bahari Saravi, H.; Gholami, A.; Pirdashti, H.; Baradaran Firouzabadi, M.; Asghari, H. The effects of endophyte symbiosis and spermidine foliar application on chlorophyll fluorescence and photosynthetic pigments of stevia (*Stevia rebaudiana* Bertoni) medicinal plant under salinity conditions. *J. Plant Proc. Func.* **2019**, *8*, 47–64.
59. González-Rodríguez, R.M.; Serrato, R.; Molina, J.G.; Aragon, C.; Olalde, V.; E Pulido, L.; Dibut, B.; Lorenzo, J.C. Biochemical and physiological changes produced by *Azotobacter chroococcum* (INIFAT5 strain) on pineapple in vitro-plantlets during acclimatization. *Acta Physiol. Plant.* **2013**, *35*, 3483–3487, doi:10.1007/s11738-013-1373-z.
60. Holm, Y. Bioactivity of basil. In *Basil: The genus Ocimum*; Hiltunen, R., Holm, Y., Eds.; Harwood Academic Publishers: Amsterdam, The Netherlands, 1999; Volume 10, pp. 113–135.
61. Chanwitheesuk, A.; Teerawutgulrag, A.; Rakariyatham, N. Screening of antioxidant activity ad antioxidant compounds of some edible plants of Thailand. *Food Chem.* **2005**, *92*, 491–497, doi:10.1016/j.foodchem.2004.07.035.
62. Suppakul, P.; Miltz, J.; Sonneveld, K.; Bigger, S.W. Antimicrobial Properties of Basil and Its Possible Application in Food Packaging. *J. Agric. Food Chem.* **2003**, *51*, 3197–3207, doi:10.1021/jf021038t.
63. Carović-Stanko, K.; Orlic, S.; Politeo, O.; Strikić, F.; Kolak, I.; Milos, M.; Šatović, Z. Composition and antibacterial activities of essential oils of seven *Ocimum* taxa. *Food Chem.* **2010**, *119*, 196–201, doi:10.1016/j.foodchem.2009.06.010.
64. Freire, C.M.M.; Marques, M.; Costa, M. Effects of seasonal variation on the central nervous system activity of *Ocimum gratissimum* L. essential oil. *J. Ethnopharmacol.* **2006**, *105*, 161–166, doi:10.1016/j.jep.2005.10.013.
65. Shan, B.; Cai, Y.Z.; Sun, M.; Corke, H. Antioxidant capacity of 26 spice extracts and characterization of their phenolic constituents. *J. Agri. Food Chem.* **2005**, *53*, 7749–7759, doi:10.1021/jf051513y.
66. Surveswaran, S.; Cai, Y.-Z.; Corke, H.; Sun, M. Systematic evaluation of natural phenolic antioxidants from 133 Indian medicinal plants. *Food Chem.* **2007**, *102*, 938–953, doi:10.1016/j.foodchem.2006.06.033.
67. Lee, J.; Scagel, C.F. Chicoric acid found in basil (*Ocimum basilicum* L.) leaves. *Food Chem.* **2009**, *115*, 650–656, doi:10.1016/j.foodchem.2008.12.075.
68. Szeto, Y.T.S.; Kwok, T.C.; Benzie, I. Effects of a long-term vegetarian diet on biomarkers of antioxidant status and cardiovascular disease risk. *Nutrition* **2004**, *20*, 863–866, doi:10.1016/j.nut.2004.06.006.
69. Orsini, F.; Maggio, A.; Rouphael, Y.; De Pascale, S. "Physiological quality" of organically grown vegetable. *Sci. Hortic.* **2016**, *208*, 131–139, doi:10.1016/j.scienta.2016.01.033.
70. Scagel, C.F.; Lee, J. Phenolic Composition of Basil Plants Is Differentially Altered by Plant Nutrient Status and Inoculation with Mycorrhizal Fungi. *Hort. Sci.* **2012**, *47*, 660–671, doi:10.21273/hortsci.47.5.660.
71. Cai, F.; Druzhinina, I.S. In honor of John Bissett: Authoritative guidelines on molecular identification of *Trichoderma*. *Fungal Divers.* **2021**, *107*, 1–69, doi:10.1007/s13225-020-00464-4.
72. Viscardi, S.; Ventorino, V.; Duran, P.; Maggio, A.; De Pascale, S.; Mora, M.L.; Pepe, O. Assessment of plant growth promoting activities and abiotic stress tolerance of *Azotobacter chroococcum* strains for a potential use in sustainable agriculture. *J. soil Sci. Plant Nutr.* **2016**, *16*, 848–863, doi:10.4067/s0718-95162016005000060.

73. Marra, R.; Vinale, F.; Cesarano, G.; Lombardi, N.; D'Errico, G.; Crasto, A.; Mazzei, P.; Piccolo, A.; Incerti, G.; Woo, S.L.; et al. Biochars from olive mill waste have contrasting effects on plants, fungi and phytoparasitic nematodes. *PLoS ONE* **2018**, *13*, e0198728, doi:10.1371/journal.pone.0198728.

applied sciences

MDPI

*Article*

# Effect of Selected *Trichoderma* Strains and Metabolites on Olive Drupes

**Irene Dini [1,*], Marica Pascale [2], Alessia Staropoli [2,3], Roberta Marra [2] and Francesco Vinale [3,4,5,*]**

[1] Department of Pharmacy, University of Naples Federico II, Via Domenico Montesano 49, 80131 Napoli, Italy
[2] Department of Agricultural Sciences, University of Naples Federico II, 80055 Portici, Italy; marica.pascale@unina.it (M.P.); alessia.staropoli@unina.it (A.S.); robmarra@unina.it (R.M.)
[3] Institute for Sustainable Plant Protection, National Research Council, Portici, 80055 Portici, Italy
[4] Department of Veterinary Medicine and Animal Productions, University of Naples Federico II, 80138 Naples, Italy
[5] BAT Center—Interuniversity Center for Studies on Bioinspired Agro-Environmental Technology, University of Naples Federico II, 80055 Portici, Italy
* Correspondence: irdini@unina.it (I.D.); frvinale@unina.it (F.V.)

**Abstract:** Beneficial fungal strains of the genus *Trichoderm*a are used as biofungicides and plant growth promoters. *Trichoderma* strains promote the activation of plant defense mechanisms of action, including the production of phenolic metabolites. In this work, we analyzed the effects of selected *Trichoderma* strains (*T. asperellum* KV906, *T. virens* GV41, and *T. harzianum* strains TH1, M10, and T22) and their metabolites (harzianic acid and 6-pentyl-α-pyrone) on drupes of young olive trees (4 yr-old) cv. *Carolea.* This study used the untargeted analysis of drupe metabolome, carried out by LC–MS Q-TOF, to evaluate the phenolics profiles and target metabolomics approach to detect oleuropein and luteolin. The untargeted approach showed significant differences in the number and type of phenolic compounds in olive drupes after *Trichoderma* applications (by root dipping and drench soil irrigation method) compared to control. The levels of oleuropein (secoiridoid) and luteolin (flavonoid) varied according to the strain or metabolite applied, and in some cases, were less abundant in treated plants than in control. In general, flavonoids' levels were influenced more than secoiridoids' production. The dissimilar aptitudes of the biological treatments could depend on the selective competence to cooperate with the enzymes involved in producing the secondary metabolites to defend plants by environmental stresses. Our results suggest that using selected fungi of the genus *Trichoder*ma and their metabolites could contribute to selecting the nutraceutical properties of the olive drupe. The use of the metabolites would bring further advantages linked to the dosage in culture and storage.

**Keywords:** secondary metabolites; phenolic compounds; LC–MS Q-TOF; *Olea europaea*; *Trichoderma*; metabolomics

## 1. Introduction

Since ancient times olive trees (*Olea europaea* L.) have been cultivated throughout the Mediterranean area for their fruits and oil production. Each country has its local cultivars because the human selection and pedoclimatic conditions have resulted in genetic variations [1–4]. In Italy, many trees sprout spontaneously, and oil and table cultivars are grown mainly in Calabria, Apulia, Sicily, and Campania, where centuries-old trees and archaeological finds document their presence from old times [5]. Extravirgin olive oil (EVOO) is obtained from crushing the olive drupe and separating olive oil by pres-

ure, centrifugation, and percolation (selective filtration process) [6]. EVOO is present in all variants of the Mediterranean diet. The latter is a healthy diet adopted by the Italian and Greek population of the 1960s [7], reducing the risk of cardiovascular disease, cancer, type 2 diabetes, and cognitive disorders [8]. It is characterized by high consumption of vegetables, fruit, salads, bread, whole grains, legumes/beans, nuts, seeds, moderate use of wine, and EVOO as the primary source of fat [8]. The EVOO has protective effects on human health due to the high content of monounsaturated fatty acids (MUFAs) and secondary bioactive molecules, including phenolic compounds, tocopherols, phytosterols, and carotenoids [9]. The phenolic compounds in EVOO range from 50 to 800 mg/kg [10,11]. They consist of phenolic alcohols (e.g., tyrosol and hydroxytyrosol), phenolic acids (e.g., vanillic, caffeic, coumaric, protocatechuic, ferulic, and p-hydroxybenzoic,), flavones (e.g., apigenin, apigenin-7-O-glucoside, luteolin, luteolin-7-O-glucoside), lignans (e.g., pinoresinol and acetoxypinoresinol,), and secoiridoids (e.g., oleacein, oleuropein, oleocanthal, and p-HPEA-EA) [12] responsible for EVOO bitterness, pungency, fragrance, and antioxidative properties [13]. Fruit's maturation, cultivar varieties, pedoclimate condition [14], and the type of oil extraction processes affect the phenolic quality and concentration [15]. The oleuropein, tyrosol, and hydroxytyrosol (the main phenolic compounds in EVOO) [12] have antioxidant, anti-inflammatory, immunomodulatory, and neuroprotective activities [16]. The EVOO's polyphenols protect blood lipids against oxidative stress [17,18]. Therefore The EVOO's phenolics are used in supplements for the prevention of chronic degenerative diseases such as cardiovascular and cancer [19], in antiaging cosmetics [20,21], in the food industry as flavorings or preservers [22–24], and in functional foods preparations [25,26]. Olive plants make the phenolics in response to abiotic stress and pathogen attack [27–32]. Dini et al. in 2020 and 2021 investigated the effects of some *Trichoderma* strain applied to olive trees to evaluate a selective phenols production [33,34]. Nowadays, fungi belonging to the genus *Trichoderma* are commonly used in agriculture as biocontrol agents (they inhibit soils and air diseases) and plant growth promoters [35,36]. They also enhance the abiotic stress tolerance (e.g., salinity, drought), yields production, nutritional uptake, leaf area, root system growth, and activate protective mechanisms against oxidative injury [37,38]. Some *Trichoderma* strains produce secondary metabolites such as 6-pentyl-a-pyrone (volatile antibiotics), heptelidic acid, and peptaibols to help in metal transport, symbiosis, differentiation, and competition with another organism [39,40], and phenols against oxidative damage [41–43]. Phenols decrease cardiovascular pathologies, hypoglycemia, hypotension, and hypocholesterolemia and prevent angiogenesis, inflammation [44], and cancer [45].

In the present work, we report the effect of selected *Trichoderma* strains (e.g., *T. asperellum* KV906, *T. harzianum* strains TH1, M10, and T22; and *T. virens* GV41) and their metabolites (e.g., harzianic acid (HA), and 6-pentyl-α-pyrone –(6PP)) upon in vivo application, on weight and phenol metabolites of the olive drupes in consideration of the commodity and nutraceutical importance of their potential effects.

## 2. Materials and Methods

### *2.1. Microbial Strains*

Five *Trichoderma* strains (*T. asperellum* strain KV906, *T. harzianum* strains TH1, M10, and T22; and *T. virens* strain GV41) were used in this work. Strains were provided by Department of Agricultural Sciences of the University of Naples Federico II, after cultivation on previously described conditions [46].

A hemocytometer (Neubauer- improved, BRAND GMBH + CO KG, Wertheim, Germany) was used to establish the concentration of the spore suspensions.

### *2.2. Trichoderma Bioactive Metabolites*

6PP and HA were used in this work. The former was extracted from *T. atroviride* strain P1 [47] And the latter from *T. harzianum* strain M10 [48]. Metabolite solutions used for treatments were obtained by resuspending HA and 6PP in distilled water and ethyl acetate 0.01% (*v*/*v*) to facilitate the process. Once a clear solution was made, ethyl acetate was evaporated under nitrogen flow.

### *2.3. Plant Material*

4 yr-old olive trees (*Olea europaea* L cv. *Carole*a.) were used for experimental purposes. The plants were grown into plastic pots (50 cm diameter × 40 cm high) located in a field at the University of Naples Federico II-Department of Agricultural Sciences (Portici, Italy). Each pot contained one plant and 50 L of universal soil (granulated pumice, peat, and coconut fiber). Once a week, the plants were watered to field capacity. No nutrients were added.

### *2.4. Experimental Design*

Eight treatments were performed (including water control), using five *Trichoderma strains* and two metabolites. The field trial was performed in a randomized block design. *Trichoderma* metabolite solutions ($1 \times 10^{-6}$ M), or spore suspensions ($1 \times 10^{6}$ sp $mL^{-1}$) were inoculated through root system exposure at the time of transplant (10 min, 1 L $plant^{-t}$) by root dip, and every 30 days (400 mL $plant^{-1}$) by soil irrigation (six applications in total). Each treatment was performed on fifteen plants (5 plants in each replicate and 3 biological replicates per treatment). Drupes were collected and weighed with an electronic digital scale (Precisa Instruments AG, model XB220A, Dietikon, Switzerland). Finally, drupes samples were stored at −80 °C until extraction of metabolites.

### *2.5. Chemicals*

Solvents (methanol, water, formic acid, acetonitrile) were purchased from Sigma-Aldrich (Sigma-Aldrich, St. Louis, MO, USA). ESI–TOF tune mix was bought from Agilent Technologies (Agilent Technologies, Santa Clara, CA, USA).

### *2.6. Olive Metabolites Extraction*

Talhaoui et al., method [49], with some modifications, was used to extract the phenolic compounds. Briefly, drupes were freeze-dried and crushed. 200 mg of powder were extracted twice in an ultrasonic bath for 10 min (Model 6.5l200 H, Dakshin, India), using 5 mL of a solution of methanol/water (50/50, *v*/*v*) and then centrifuged (Hettich GmbH & Co., Tuttlingen, Germany) at 4000 rpm, 4 °C for 10 min. The supernatants were collected, dried in a speed-vac (Savant SpeedVac, Thermo Fisher Scientific, Waltham, MA, USA) and dissolved in 2 mL of a solution of methanol/water (50/50, *v*/*v*). Finally, the extracts thus obtained were filtered (Millipore 0.45 μm) and stored in the dark (at −80 °C) until use.

### *2.7. Phenolics' Isolation, Identification, and Quantification*

#### 2.7.1. Metabolites' Analysis

The analysis of metabolites was performed on an Agilent HP 1260 Infinity Series liquid chromatograph (Agilent Technologies, Santa Clara, CA, USA) equipped with a DAD system (Agilent Technologies, Santa Clara, CA, USA) and a Q-TOF mass spectrometer model G6540B (Agilent Technologies, Santa Clara, CA, USA).

#### Chromatographic Conditions

An InfinityLab Poroshell 120 EC-C18 column (2.1 mm × 100 mm, 2.7 μm) (Agilent Technologies, Santa Clara, CA, USA), at controlled temperature (25 °C) was used as stationary phase. Two eluents: phase A (0.1% (*v*/*v*) formic acid in water) and phase B

(0.1% (*v*/*v*) formic acid in acetonitrile) were employed as mobile phase. The gradient was set as follows: 0 min, 95% A; 4 min, 91% A; 7 min, 88% A; 8 min, 85% A; 9 min, 84% A; 14 min, 80% A; 15 min, 78% A; 18 min, 72% A; 19 min, 70% A; 20 min, 69% A; 21.50 min, 68% A; 23 min, 66% A; 24 min, 65% A; 25.5 min, 60% A; 27 min, 50% A; 30 min, 0% A; 35 min, 0% A; and 37 min, 95% A. Flow rate was 0.5 mL $min^{-w}$.

Spectroscopic and Spectrometric Conditions

The UV spectra were recorded every 0.4 s, with a resolution of 2 nm, from 190 to 750 nm by DAD (Agilent Technologies, Santa Clara, CA, USA).

The MS system was equipped with a dual ESI (electrospray ionization) source and operated in negative mode as reported by Tafuri et al. [50]. All the parameters were controlled by the Agilent MassHunter Data Acquisition Software, version B.05.01. Mass spectra were recorded in the mass range 100–1600 *m*/*z* (3 scans per second). Hexakis ($^{1}$H,$^{1}$H, $^{3}$H-tetrafluoropentoxy)-phosphazene ($C_{18}H_{18}O_6N_3P_3F_{24}$ at *m*/*z* 922.009798, 2 µmol $L^{-9}$) (Sigma-Aldrich, St. Louis, MO, USA)., and purine ($C_5H_4N_4$ at *m*/*z* 121.050873, 10 µmol $L^{-1}$) (Sigma-Aldrich, St. Louis, MO, USA). were injected in the source (0.060 mL $min^{-e}$) to perform the lock mass correction in real-time. The capillary was set at 4000 V, cone 1 (skimmer 1) at 45 V, fragmentor at 180 V. Gas temperature was 350 °C, and the nebulizer was at 45 psi. The injection volume was 5 µL. For each treatment, three biological samples were analyzed in triplicate.

Mass Profiler Professional (Agilent Technologies, MPP v 13.1.1, Santa Clara, CA, USA) was used for molecular feature normalization, alignment, compound identification, and statistical analysis. MPP normalization and alignment parameters were: minimum number of ions (2); abundance filter (>5000 counts); intercept (0.4 min), alignment RT window, and slope (0%); intercept (2 mDa), alignment mass window, and slope (20 ppm). Only masses occurring in two of three samples were accepted. Masses found in blank runs from filtered masses were used to remove background noise. The ion chromatogram (EIC) was extracted with ±20 ppm single ion expansion with MassHunter software v B.06.00 (Agilent Technologies, Santa Clara, CA, USA).

2.7.2. Phenolics' Identification

The phenolics were identified by Mass Hunter Qualitative Analysis Software version B.06.00 (Agilent Technologies, Santa Clara, CA, USA). Identification was achieved by comparison with in-house databases (comprising data from METLIN library) and with existing literature data. Empirical formulas, calculated by isotope model (common organic molecules, ppm limit = 10, limit charge state to a maximum of 2, and use $^{+}$H or $^{-}$H, or sodium and potassium adducts) were given for unidentified compounds. Experimental retention time, monoisotopic mass, and UV max of standards confirmed the identification.

2.7.3. Phenolics' Quantification

The quantification of phenolics was performed by using oleuropein and luteolin commercial standards purchased from Sigma-Aldrich (Sigma-Aldrich, St. Louis, MO, USA) dissolved in methanol: water (50:50, *v*/*v*) to make standard calibration curves (Table S1).

*2.8. Statistical Analysis*

Statistical analysis was performed by SPSS V24 statistic software (IBM Corporation, Armonk, NY, USA). One-way ANOVA analyzed the data of SPAD index. Significant differences among treatments were compared using Fisher's least significant difference (LSD) post hoc tests and S–N–K (Student–Newman–Keuls) (with 0.05 level of significance). The Student's t-test (with a 0.05 level of significance) determined significant differences.

## 3. Results

### *3.1. Effect of Treatments on the Olive Trees Drupe's Weight*

In the first year of production, the average weight of the drupes for each treatment was evaluated. All treatments, except *T. harzianum* M10 and *T. asperellum* KV906, positively affected the drupes' average weight compared to the control (Table 1).

**Table 1.** Effects of treatments with *Trichoderma* spp. strains T22, M10, GV41, TH1, KV906 or its metabolites 6-pentyl-α-pyrone (6PP) and harzianic acid (HA) on average weights of the drupes collected from the experimental field. The control (CTRL) was not treated with biostimulants.

| Treatment | Drupe's Average Weight (g) |
|---|---|
| GV41 | 8.10 [b] |
| M10 | 5.66 [a] |
| T22 | 7.61 [b] |
| TH1 | 6.63 [b] |
| KV906 | 5.90 [a] |
| 6PP | 6.12 [b] |
| HA | 9.40 [b] |
| CTRL | 5.85 [a] |

Different letters within each column indicate significant differences ($p < 0.05$).

### *3.2. Characterization of Olive Drupe Metabolome*

Thirteen phenolic compounds were identified based on total ion chromatogram (TIC), mass/UV–VIS, spectra, and literature data. Identification parameters (retention time, UV maximum absorption, experimental and calculated monoisotopic masses, molecular formula) are reported in Table 2.

**Table 2.** Phenolics' identification parameters.

| Compound | RT (min) | UV Max (nm) | Experimental Mass | Mass Theoretical | Formula |
|---|---|---|---|---|---|
| **Secoiridoids** | | | | | |
| Oleuropein aglycone | 10.90 | 235; 271 | 378.1569 | 378.13 | $C_{16}H_{26}O_{16}$ |
| Oleuropein isomer a | 19.10 | 240; 280 | 540.1840 | 540.18 | $C_{25}H_{32}O_{13}$ |
| Oleuropein isomer b | 20.10 | 235; 280 | 540.1848 | 540.184 | $C_{25}H_{32}O_{13}$ |
| 2″-Methoxyoleuropein | 15.81 | 236; 280 | 570.1942 | 570.19 | $C_{26}H_{34}O_{14}$ |
| Ligstroside | 20.52 | 230; 280 | 524.1900 | 524.19 | $C_{25}H_{32}O_{12}$ |
| **Flavonoids** | | | | | |
| Luteolin | 20.80 | 255; 286 | 286.0488 | 286.05 | $C_{15}H_{35}O_{14}$ |
| Luteolin rutinoside | 11.90 | 248; 267 | 594.1589 | 594.16 | $C_{27}H_{30}O_{15}$ |
| Luteolin di-glucoside | 12.25 | 248; 267; 335 | 610.1537 | 610.15 | $C_{27}H_{30}O_{16}$ |
| Rutin | 14.60 | 253 | 610.1539 | 610.15 | $C_{27}H_{30}O_{16}$ |
| **Simple phenols** | | | | | |
| Hydroxytyrosol-glucoside | 4.75 | 230; 280 | 316.1160 | 316.12 | $C_{14}H_{20}O_{8}$ |
| Verbascoside | 14.55 | 234; 329 | 624.2064 | 624.20 | $C_{29}H_{36}O_{15}$ |
| **Oleosides** | | | | | |
| Oleoside methyl ester | 6.33 | 235 | 404.1321 | 404.13 | $C_{17}H_{24}O_{11}$ |
| Secologanoside | 7.45 | 234 | 390.1151 | 390.12 | $C_{16}H_{22}O_{11}$ |

### *3.3. Untargeted Metabolomics Analyses of Phenolics in Olive Drupes*

Untargeted metabolomic analyses were carried out on the olives harvested from treated plants. There was a tendency for the number of down-regulated compounds to increase (Table 3). In general, a more significant number of compounds were observed whose abundance was lower when compared to the control. The metabolite 6PP and *Trichoderma* sp. strains GV41 and KV906 influenced the metabolic response in drupes more than control.

**Table 3**. Number of metabolites whose production is higher (UP) or lower (DOWN) compared to the control (CTRL) in the drupes obtained from treated plants (*Trichoderma* spp. strains T22, M10, GV41, TH1, KV906 or its metabolites 6-pentyl-α-pyrone (6PP) and harzianic acid (HA).

| Treatments | UP vs. CTRL | DOWN vs. CTRL |
|---|---|---|
| GV41 | 21 | 30 |
| M10 | 16 | 44 |
| T22 | 10 | 38 |
| TH1 | 16 | 35 |
| KV906 | 21 | 44 |
| HA | 12 | 36 |
| 6PP | 28 | 39 |

Replicate samples were grouped and subjected to variance analysis (one-way ANOVA, $p < 0.05$) and to fold change (FC > 2.0), comparing metabolite abundances in treatments vs. water-treated plants (CTRL). hierarchical cluster analysis, Statistical analysis revealed 88 metabolites differentially accumulated among treatments that are depicted as hierarchical cluster in Figure 1. The metabolic profiling revealed that drupes from olive plants treated with the *Trichoderma* sp**.** strain M10, KV906, T22, and metabolite HA were grouped separately. TH1 determined no differences in terms of phenolic's levels compared to the control.

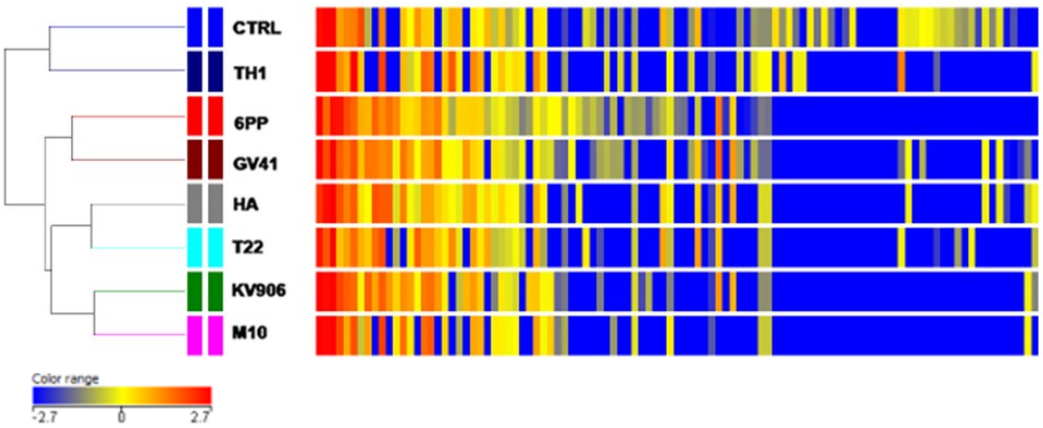


**Figure 1.** Hierarchical clustering heat map of differential metabolic profiles from olive drupe extracts. Samples are indicated by treatments with Trichoderma strains (TH1, GV41, T22, M10, and KV906) or secondary metabolites (HA and 6PP). Control was plants treated with water. Red color indicates higher phenolic abundance (>0), blue colors lower (<0), yellow a neutral change from the overall average abundance. Statistical significance was tested by one-way ANOVA ($p < 0.05$).

Successively, the variations in metabolite accumulation between increased (UP) or decreased (DOWN) compounds, as compared to the control, were analyzed for T22, M10 and HA.

Venn diagram showed that 30 down-regulated compounds were in common among all treatments, while 4 metabolites were exclusively in the metabolome of T22-treated samples and 4 in those exposed to M10. No compound was found to be specific for HA treatment Four metabolites were common to T22 and M10 treatments and 6 to M10 and HA. In contrast, no compounds were found to be common to T22 and HA treatments. Concerning the up-regulated compounds, 5 were common to all treatments, 8 exclusive of M10, 1 for HA, none for T22; 1 metabolite was common between treatments with T22 and M10, 2 between M10 and HA and 4 between HA and T22. (Figure 2).

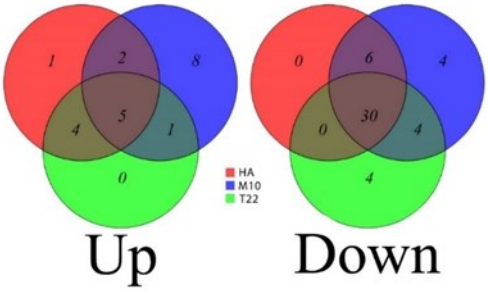


**Figure 2.** Venn diagrams of phenolic compounds whose abundance in the olive drupe metabolome is lower (**DOWN**) or higher (**UP**) compared to the control (CTRL). Samples treated with T22 are reported in green; with M10 in blu and with HA in red.

Untargeted metabolomic analysis revealed the presence of several differentially accumulated metabolites in treated or not-treated drupes. Among these, thirteen metabolites were putatively identified by comparison with an in-house database and standard compounds (Table 4).

**Table 4.** Metabolites identified in the drupe extracts of olive trees subjected to field applications of biological treatments. Samples are indicated by treatments with *Trichoderma* strains (TH1, GV41, T22, M10, and KV906) or secondary metabolites (HA and 6PP). Identifications were confirmed by comparing results with known compounds in an in-house database/standards and selecting matching (≥95%).

| Compound | Regulation Against Control Group (CTRL) | | | | | | |
|---|---|---|---|---|---|---|---|
| | **M10** | **KV906** | **GV41** | **TH1** | **T22** | **6PP** | **HA** |
| Oleuropein aglycon | ↑ | ↑ | ↑ | ↑ | ↑ | ↑ | ↑ |
| Oleuropein isomer a | ↓ | ↓ | ↓ | ↓ | ↓ | ↓ | ↓ |
| Oleuropein isomer b | ↓ | ↓ | ↓ | ↓ | ↓ | ↓ | ↓ |
| 2-Methoxyoleuropein | ↓ | ↓ | ↑ | ↑ | ↓ | ↓ | ↓ |
| Ligstroside | ↓ | ↓ | ↓ | ↓ | ↓ | ↓ | ↓ |
| Luteolin | ↑ | ↑ | ↑ | ↑ | ↓ | ↑ | ↑ |
| Luteolin rutinoside | ↑ | ↑ | ↑ | ↑ | ↑ | ↑ | ↑ |
| Luteolin di-glucoside | ↑ | ↑ | ↑ | ↑ | ↑ | ↑ | ↑ |
| Rutin | ↓ | ↓ | ↓ | ↓ | ↓ | ↑ | ↓ |
| Hydroxytyrosol glucoside | ↓ | ↓ | ↑ | ↑ | ↑ | ↓ | ↑ |
| Verbascoside | ↑ | ↑ | ↑ | ↑ | ↓ | ↑ | ↓ |
| Oleoside methyl ester | ↓ | ↓ | ↑ | ↑ | ↑ | ↓ | ↑ |
| Secologanoside | ↓ | ↓ | ↓ | ↑ | ↓ | ↓ | ↓ |

↑ Increased production of the metabolite in treated vs. control. ↓ Decreased production of the metabolite in treated vs. control.

### *3.4. Targeted Metabolomics Analyzes of Phenolics in Olive Drupes*

Oleuropein (secoiridoid) and luteolin (flavonoid) concentrations were considered to evaluate the phenolics' level trends. Oleuropein content increased in the drupes of plants treated with 6PP, GV41, and T22 (Figure 3).

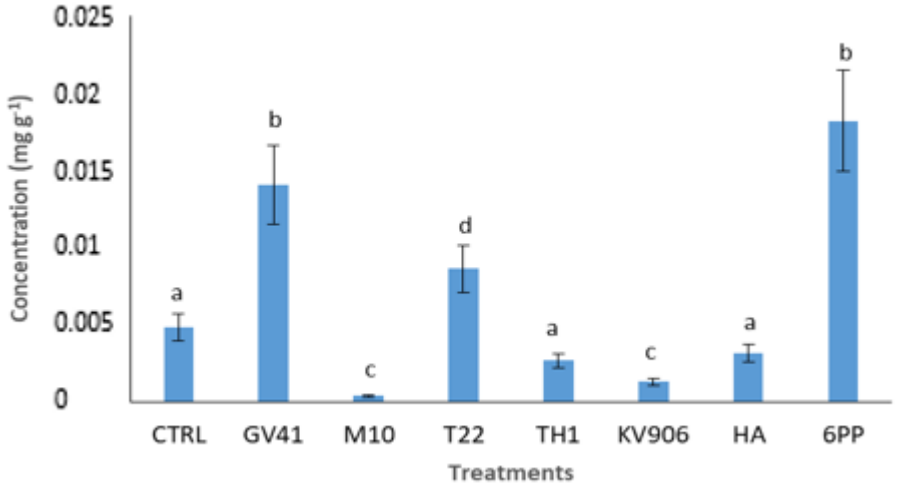


**Figure 3**. Oleuropein content in drupes. Samples are indicated by treatments with *Trichoderma* strains (TH1, GV41, T22, M10, and KV906) or secondary metabolites (HA and 6PP). Values are the means of three replicates ± SE. Different letters indicate significant differences ($p < 0.05$).

The secondary metabolite 6PP and the *Trichoderma* strains GV41, KV906, HA, and M10, increased the luteolin's level in drupes (Figure 4).

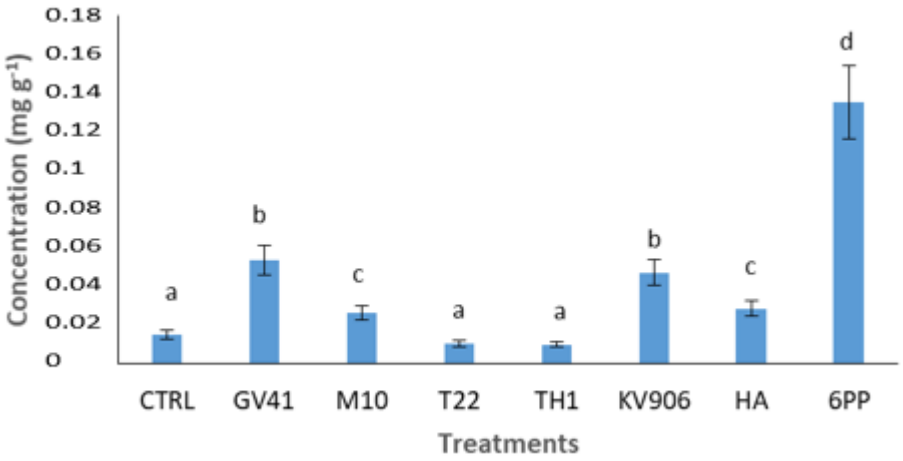


**Figure 4.** Luteolin content in drupes. Samples are indicated by treatments with *Trichoderma* strains (TH1, GV41, T22, M10, and KV906) or secondary metabolites (HA and 6PP). Values are the means of three replicates ± SE. Different letters indicate significant differences ($p < 0.05$).

## 4. Discussion

Today, it is considered a priority to limit pesticides against phytopathogenic agents or replace them with products of biological origin. The use of mycoparasitic fungi, particularly those belonging to the genus *Trichoderma*, has met considerable success [11]. The world market of biopharmaceuticals proposes over 50 bioformulates containing *Trichoderma* strains as active ingredients [51]. The considerable achievement of *Trichoderma* fungi in agriculture is due to their suppression of pathogenic species, both terricolous and foliar, among the most harmful, such as those belonging to the genera *Fusarium*, *Sclerotinia*, *Botrytis*, and *Pythium* [52]. Microbial inocula to promote plant development and/or control phytopathogenic agents is still not very widespread in tree crops. Few studies evaluated the effect of beneficial microorganisms on the fitness of the olive tree and provided helpful information for the use of bioformulates in the open field. The present work aims to evaluate the effects of the field applications of *Trichoderma* spp. strains and

some of their metabolites on young olive trees' drupes weight and nutraceutical content contained therein.

The olive is the most representative tree in Italy, with both historical and productive significance. There are three types of olives on the market: olive for oil production, olive for the table, and dual-use. Fruit size, oil content flesh, and weight/pit weight ratio determine the inclusion in the product classes. Olives for oil production have an average weight below 3, table-use have an average weight higher than 5, dual-use between 3 and 5 [53]. Extensive research has been conducted on multiple species to understand the mechanisms that control fruit size [54]. Environmental and genetic factors affect the fruits' growth potential [55]. In particular, the water's volume and the type of irrigation used for cultivation are noteworthy [56]. Water deficit makes high reactive oxygen species (ROS) (e.g., hydrogen peroxide, hydroxyl radical superoxide anion, and singlet oxygen) [57]. ROS can damage DNA, lipids, and protein, thereby affecting plants' metabolism [58]. Plants react to ROS, making enzymes with different biological activities (e.g., catalase, ascorbate peroxidase, superoxide dismutase, monodehydroascorbate reductase, dehydroascorbate reductase, guaiacol peroxidase, and glutathione reductase) [59] and primary or secondary metabolites (e.g., polyols, soluble sugars, alkaloids, free amino acids, and phenols) [60]. In this work, all treatments (excluding M10 and KV906) enhanced drupe weight, probably due to *Trichoderma* strains' ability to induce root growth, preserve nutritional uptake, and interfere with phenolics' productions [61]. The diverse response to bio-treatments was probably linked to the different abilities of each strain and metabolite to interact with the plant's secondary defense mechanisms [15]. The variation in phenolics (variety and levels) was tested using targeted and untargeted metabolomics to evaluate the interaction of *Trichoderma* spp. and metabolites with the plant defense mechanism. Targeted metabolomics uses analytical techniques and suitable multivariate statistical analysis (MSA) tools to evaluate some metabolites simultaneously [62]. The untargeted approach determines unknown and known metabolic changes basing on data-independent acquisition (DIA). DIA methods make complex fragmentation spectra. In downstream data analysis steps, fragment ions are matched with precursor ions based on mass and retention time [63].

In this study, an untargeted metabolomic approach was used to evaluate phenolic profiles for olive drupes. The analysis of chromatograms led to the putative identification of thirteen differentially accumulated compounds among all treatments. Oleuropein (the main secoiridoid) and luteolin (the main flavonoid) concentration increased in treated samples compared to control. Metabolomic profiles of olive drupes following the application of M10, KV906, T22, and metabolite HA were grouped separately. This result may indicate that the olive plants have a similar response when inoculated with *Trichoderma* fungi and treated with their metabolites [51]. However, the identified differential metabolites were not always common to all treatments (Figure 1). The targeted metabolomics method estimated the effects of each biological treatment on the phenolic' levels in the olive's drupes. Four more representative phenolic classes (flavonoids, secoiridoids, simple phenols, and oleosides) were considered. Following the treatments, an increase in the oleuropein's content and a decrease in the oleuropein's precursors (11-methyl ester and ligstroside) concentrations were determined, demonstrating the ability of *Trichoderma* and its metabolites to interact with the enzyme β-glucosidase [64] responsible for this biotransformation (Figure 5) [65].

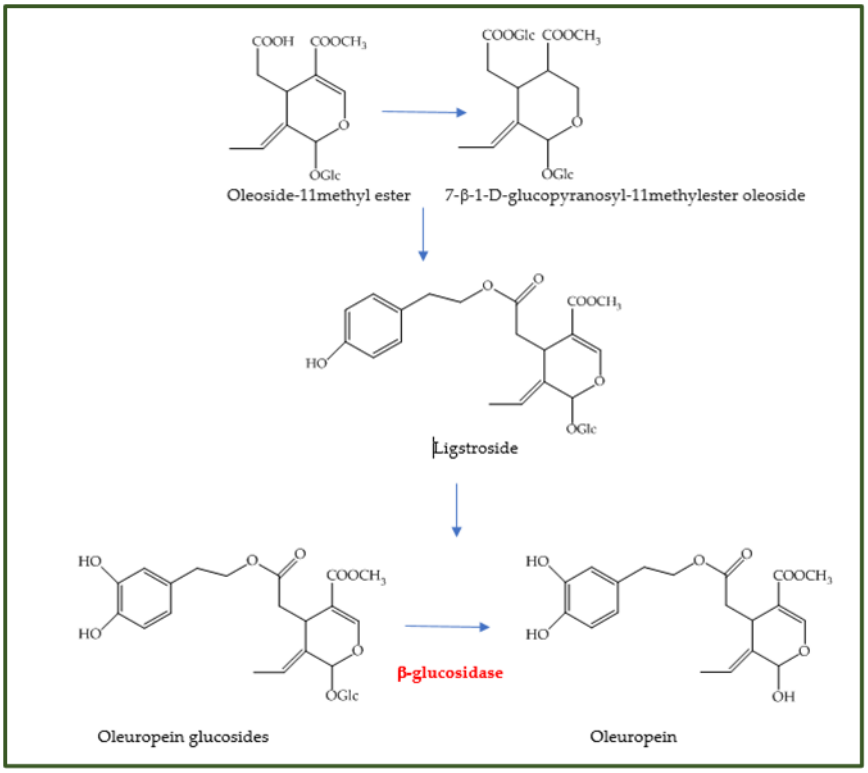


**Figure 5.** Oleuropein biosynthesis.

About flavonoids, an improvement of the flavone luteolin's level (except in olive drupes obtained from plants treated by T22) and a decrease in the flavonol rutin's concentration (except in olive drupes obtained from plants treated by 6PP) were observed in all tested samples (Table 4), indicating the ability of the treatments (except T22 and 6PP) to affect principally the flavone synthase activity rather than flavonol synthase (Figure 6).

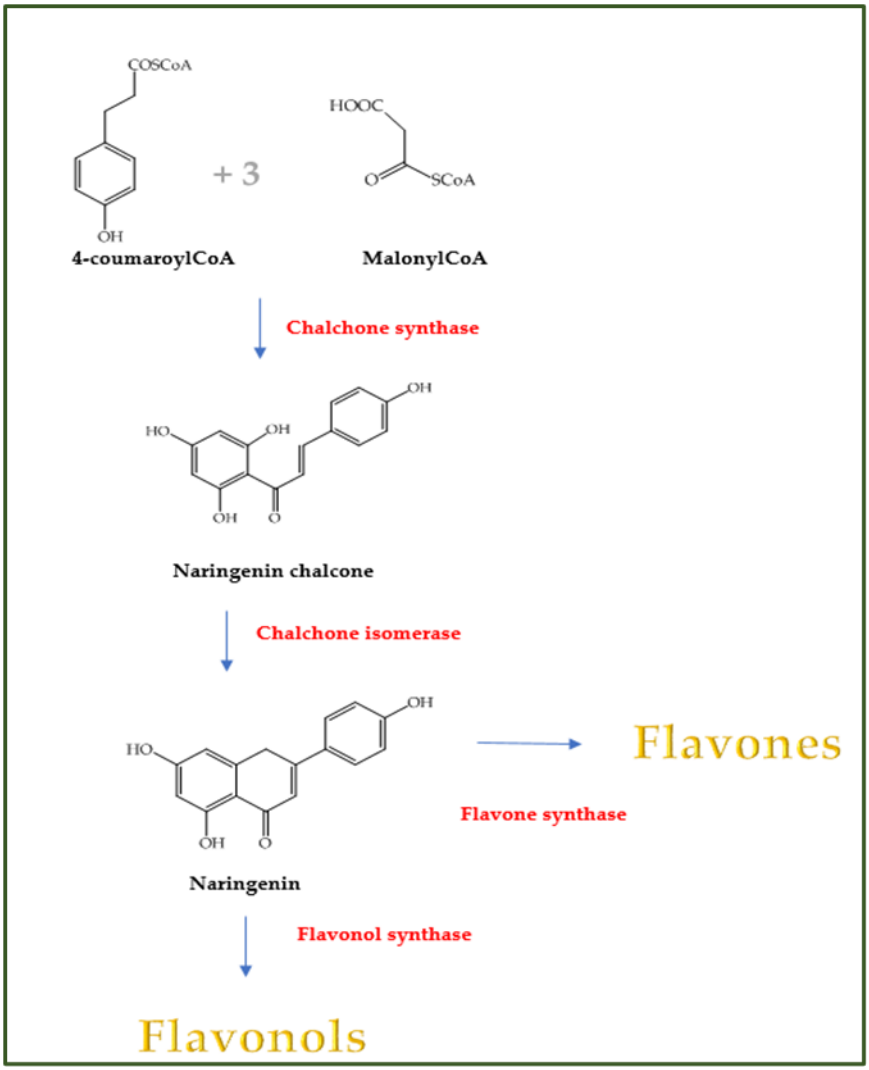


**Figure 6.** Flavonoid's biosynthesis [66].

Finally, the levels' variation of oleuropein and luteolin in olive drupes after the biotreatment was studied in detail. Oleuropein and luteolin were used as indicators of the secoiridoids and flavonoids variation, respectively. Oleuropein acts in *Olea europaea* as signaling molecule to protect the plant against UV-B radiation [67]. It has beneficial properties on human health, preventing cancer, cardiovascular diseases, inflammatory and oxidant damages [68]. Luteolin avoids oxidative and inflammatory processes with important implications for preventing neurodegenerative, cancer, and cardiovascular diseases and fortifying the immune system [69,70]. All *Trichoderma* spores and metabolites treatments affect the secoiridoid oleuropein and flavonoid luteolin levels (in some cases, they were less abundant in treated plants) and generally influenced the flavonoids more than secoiridoids production. The biological treatment (6PP, GV41, and T22) improved the oleuropein content, while the luteolin levels were higher after 6PP, GV41, M10, HA, and KV906 treatments confirming a different interaction capacity of the biotreatments with the enzymes involved in the two biosynthetic pathways.

## 5. Conclusions

*Trichoderma* strains and their bioactive metabolites used to cultivate the olive tree (*O. europaea* cv. Carolea) influence the weight of the drupes and the composition of phenolic compounds they contain, although in different ways depending on the strain or metabolite applied. All *Trichoderma* treatments influenced the production of flavonoids

more than secoiridoids. The biological treatments' different abilities could depend on their selective aptitude to interact with the enzymes involved in flavonoid and secoiridoid production. Our results show that using the *Trichoderma* fungi and their metabolites represents a suitable alternative to synthetic fungicide since they are biocontrol agents and influence other desirable characteristics such as the size and nutraceutical properties of the olives. Furthermore, they suggest that in the future, the use of metabolites is preferable to that living fungi as they give the same biological effects beneficial for cultivation and to guarantee the nutraceutical properties of olives, avoiding some of the limitations related to the application of living microbes (difficulty in dosing concentrations to be applied on the plant and storage complications).

**Supplementary Materials:** The following are available online at https://www.mdpi.com/article/10 .3390/app11188710/s1, Table S1. Analytical parameters used to perform the calibration curves.

**Author Contributions:** writing—original draft preparation, I.D. and F.V.; data curation, M.P. and A.S.; Formal analysis, A.S. and R.M.; Formal analysis and writing, F.V.; Investigation, A.S. and R.M.; project administration, F.V. All authors have read and agreed to the published version of the manuscript.

**Funding:** This work was supported by the following project: MIUR—PON [grant number Linfa 03PE_00026_1].

**Data Availability Statement:** Data is contained within the article or supplementary material.

**Conflicts of Interest:** The authors declare no conflict of interest.

## References

1. Vossen, P. Olive Oil: History, Production, and Characteristics of the World's Classic Oils. *HortScience* **2007**, *42*, 1093–1100.
2. Kaniewski, D.; Van Campo, E.; Boiy, T.; Terral, J.-F.; Khadari, B.; Besnard, G. Primary domestication and early uses of the emblematic olive tree: Palaeobotanical, historical and molecular evidence from the Middle East. *Biol. Rev. Camb. Philos. Soc.* **2012**, *87*, 885–899.
3. Besnard, G.; Baradat, P.; Bervillé, A. Genetic relationships in the olive (Olea europaea L.) reflect multilocal selection of cultivars. Theor. Appl. Genet. **2001**, 102, 251–258.
4. Angiolillo, A.; Reale, S.; Pilla, F.; Baldoni, L. Molecular Analysis of Olive Cultivars in the Molise Region of Italy. Genet. Resour. Crop Evol. **2006**, 53, 289–295.
5. Marra, F.P.; Caruso, T.; Costa, F.; Di Vaio, C.; Mafrica, R.; Marchese, A. Genetic relationships, structure and parentage simulation among the olive tree (Olea europaea L. subsp. europaea) cultivated in Southern Italy revealed by SSR markers. *Tree Genet. Genomes* **2013**, *9*, 961–973.
6. Kapellakis, I.E.; Tsagarakis, K.P.; Crowther, J.C. Olive oil history, production and by-product management. *Rev. Environ. Sci. Biotechnol*. **2008**, *7*, 1–26.
7. Mazzocchi, A.; Leone, L.; Agostoni, C.; Pali-Schöll, I. The Secrets of the Mediterranean Diet. Does [Only] Olive Oil Matter? *Nutrients* **2019**, *11*, 2941.
8. Schwingshackl, L.; Morze, J.; Hoffmann, G. Mediterranean diet and health status: Active ingredients and pharmacological mechanisms. *Br. J. Pharmacol*. **2019**.
9. Dini, I.; Laneri, S. Spices, Condiments, Extra Virgin Olive Oil and Aromas as Not Only Flavorings, but Precious Allies for Our Wellbeing. *Antioxidants* **2021**, *10*, 868.
10. Pedan, V.; Popp, M.; Rohn, S.; Nyfeler, M.; Bongartz, A. Characterization of Phenolic Compounds and Their Contribution to Sensory Properties of Olive Oil. *Molecules* **2019**, *24*, 2401.

11. Dini, I.; Seccia, S.; Senatore, A.; Coppola, D.; Morelli, E. Development and Validation of an Analytical Method for Total Polyphenols Quantification in Extra Virgin Olive Oils. *Food Anal. Methods* **2020**, *13,* 457–464.
12. Dini, I.; Graziani, G.; Fedele, F.L.; Sicari, A.; Vinale, F.; Castaldo, L.; Ritieni, A. Effects of *Trichoderma* Biostimulation on the Phenolic Profile of Extra-Virgin Olive Oil and Olive Oil By-Products. *Antioxidants* **2020**, *9*, 284.
13. Bendini, A.; Cerretani, L.; Carrasco-Pancorbo, A.; Gómez-Caravaca, A.M.; Segura-Carretero, A.; Fernández-Gutiérrez, A.; Lercker, G. Phenolic molecules in virgin olive oils: A survey of their sensory properties, health effects, antioxidant activity and analytical methods. An overview of the last decade. *Molecules* **2007**, *12*, 1679–1719.
14. Dini, I.; Graziani, G.; Fedele, F.L.; Sicari, A.; Vinale, F.; Castaldo, L.; Ritieni, A. An environmentally friendly practice used in olive cultivation capable of increasing commercial interest in waste products from oil processing. *Antioxidants* **2020**, *9*, 466.
15. Casas, R.; Estruch, R.; Sacanella, E. The Protective Effects of Extra Virgin Olive Oil on Immune-mediated Inflammatory Responses. *Endocr. Metab. Immune Disord. Drug Targets* **2018**, *18*, 23–35.
16. Santangelo, C.; Vari, R.; Scazzocchio, B.; De Sanctis, P.; Giovannini, C.; D'Archivio, M.; Masella, R. Anti-inflammatory Activity of Extra Virgin Olive Oil Polyphenols: Which Role in the Prevention and Treatment of Immune-Mediated Inflammatory Diseases? *Endocr. Metab. Immune Disord. Drug Targets* **2018**, *18,* 36–50.
17. EFSA Panel on Dietetic Products, Nutrition and Allergies (NDA). Scientific Opinion on the substantiation of a health claim related to polyphenols in olive and maintenance of normal blood HDL cholesterol concentrations (ID 1639, further assessment) pursuant to Article 13(1) of Regulation (EC) No 1924/2006. *EFSA J.* **2012**, *10*.
18. Tetens, I. *EFSA Panel on Dietetic Products, Nutrition and Allergies (NDA); Scientific Opinion on the Substantiation of a Health Claim Related to Glucosamine and Maintenance of Lycopene, Proanthocyanidins, Vitamin C, Vitamin E, Selenium and Beta-Carotene and Contribution to Normal Collagen Formation (ID 1669) and Protection of the Skin from UV-Induced Damage (ID 1669) Pursuant to Article 13(1) of Regulation (EC) No 1924/2006*; European Food Safety Authority (EFSA): Parma, Italy, 2011.
19. Stark, A.; Zecharia, M. Olive oil in the prevention of breast and colon carcinogenesis. In *Olives and Olive Oil in Health and Disease Prevention*; Academic Press: Cambridge, MA, USA, 2021; pp. 337–345.
20. Dini, I.; Laneri, S. The New Challenge of Green Cosmetics: Natural Food Ingredients for Cosmetic Formulations. *Molecules* 2021, *26*, 3921.
21. Dini, I.; Falanga, D.; Di Lorenzo, R.; Tito, A.; Carotenuto, G.; Zappelli, C.; Grumetto, L.; Sacchi, A.; Laneri, S.; Apone, F. An Extract from Ficus carica Cell Cultures Works as an Anti-Stress Ingredient for the Skin. *Antioxidants* **2021**, *10*, 515.
22. Dini, I. Spices and herbs as therapeutic foods. In Food Quality: Balancing Health and Disease; Holban, A.M., Grumezescu, A.M.,Eds.; Academic Press: New York, NY, USA; Elservier: London, UK, 2018; pp. 433–469.
23. Fanelli, F.; Cozzi, G.; Raiola, A.; Dini, I.; Mulè, G.; Logrieco, A.F.; Ritieni, A. Raisins and Currants as Conventional Nutraceuticals in Italian Market: Natural Occurrence of Ochratoxin A. *J. Food Sci.* **2017**, *82*, 2306–2312.
24. Dini, I.; Laneri, S. Nutricosmetics: A brief overview. *Phytother. Res*. **2019**, *33*, 3054–3063.
25. Cavallo, P.; Dini, I.; Sepe, I.; Galasso, G.; Fedele, F.L.; Sicari, A.; Bolletti Censi, S.; Gaspari, A.; Ritieni, A.; Lorito, M.; et al. An innovative olive pâté with nutraceutical properties. *Antioxidants* **2020**, *9*, 581.
26. Dini, I.; Izzo, L.; Graziani, G.; Ritieni, A. The Nutraceutical Properties of "Pizza Napoletana Marinara TSG" a Traditional Food Rich in Bioaccessible Antioxidants. *Antioxidants* **2021**, *10*, 495.

27. Rahioui, B.; Aissam, S.; Messaouri, H.; Moukhli, A.; Khadari, B.; Ei, M.C. Role of phenolic metabolism in the defense of the olive-tree against leaf-spot disease caused by *Spilocaea oleagina*. *Int. J. Agric. Biol.* **2013**, *15*, 273–278.
28. Rahioui, B.; El-Aabidine, A.Z.; Baissac, Y.; El-Boustani, E.; Khadari, B.; Jay Allemand, C.; El-Modafar, C. Phenolic compounds of olive-tree leaves and their relationship with the resistance to the leaf-spot disease caused by *Spilocaea oleagina*. *Am. Eurasian J. Agric. Environ. Sci.* **2009**, *5*, 204–214.
29. Markakis, E.A.; Tjamos, S.E.; Antoniou, P.P.; Roussos, P.A.; Paplomatas, E.J.; Tjamos, E.C. Phenolic responses of resistant and susceptible olive cultivars induced by defoliating and nondefoliating *Verticillium dahlia* pathotypes. *Plant Dis.* **2010**, *94*, 1156–1162.
30. Petridis, A.; Therios, I.; Samouris, G.; Tananaki, C. Salinity-induced changes in phenolic compounds in leaves and roots of four olive cultivars (*Olea europaea* L.) and their relationship to antioxidant activity. *Environ. Exp. Bot.* **2012**, *79*, 37–43.
31. Cetinkaya, H.; Koc, M.; Kulak, M. Monitoring of mineral and polyphenol content in olive leaves under drought conditions: Application chemometric techniques. *Ind. Crop. Prod.* **2016**, *88*, 78–84.
32. Mechria, B.; Tekayaa, M.; Hammamia, M.; Chehabb, H. Root verbascoside and oleuropein are potential indicators of drought resistance in olive trees (*Olea europaea* L.). *Plant Physiol. Biochem.* **2019**, *141*, 407–414.
33. Dini, I.; Graziani, G.; Gaspari, A.; Fedele, F.L.; Sicari, A.; Vinale, F.; Cavallo, P.; Lorito, M.; Ritieni, A. New strategies in the cultivation of olive trees and repercussions on the nutritional value of the extra virgin olive oil. *Molecules* **2020**, *25*, 2345.
34. Dini, I.; Marra, R.; Cavallo, P.; Pironti, A.; Sepe, I.; Troisi, J.; Scala, G.; Lombari, P.; Vinale, F. *Trichoderma* Strains and Metabolites Selectively Increase the Production of Volatile Organic Compounds (VOCs) in Olive Trees. *Metabolites* **2021**, *11*, 213.
35. Woo, S.L.; Ruocco, M.; Vinale, F.; Nigro, M.; Marra, R.; Lombardi, N.; Pascale, A.; Lanzuise, S.; Manganiello, G.; Lorito, M. *Trichoderma*-based products and their widespread use in agricolture. *Open Mycol. J.* **2014**, *8*, 71–126.
36. Lorito, M.; Woo, S.L.; Harman, G.E.; Monte, E. Translational research on *Trichoderma*: From 'omics to the field. *Annu. Rev. Phytopathol.* **2010**, *48*, 395–417.
37. Hermosa, R.; Viterbo, A.; Chet, I.; Monte, E. Plant-beneficial effects of *Trichoderma* and of its genes. *Microbiology* **2012**, *158*, 17–25.
38. Mona, S.A.; Hashem, A.; Abd Allah, E.F.; Alqarawi, A.A.; Soliman, D.W.K.; Wirth, S.; Egamberdieva, D. Increased resistance of drought by *Trichoderma harzianum* fungal treatment correlates with increased secondary metabolites and proline content. *J. Integr. Agric.* **2017**, *16*, 1751–1757.
39. Mukherjee, P.K.; Horwitz, B.A.; Kenerley, C.M. Secondary metabolism in *Trichoderma* - a genomic perspective *Microbiology* **2012**, *158*, 35-45.
40. Khan, R.A.A.; Najeeb, S.; Hussain, S.; Xie, B.; Li, Y. Bioactive Secondary Metabolites from *Trichoderma* spp. against Phytopathogenic Fungi. *Microorganisms* **2020**, *8*, 817.
41. Pascale, A.; Vinale, F.; Manganiello, G.; Nigro, M.; Lanzuise, S.; Ruocco, M.; Marra, R.; Lombardi, N.; Woo, S.L.; Lorito, M. *Trichoderma* and its secondary metabolites improve yield and quality of grapes. *Crop Prot.* **2017**, *92*, 176–181.
42. Mastouri, F.; Bjorkman, T.; Harman, G.E. *Trichoderma harzianum* enhances antioxidant defense of tomato seedlings and resistance to water deficit. *Mol. Plant Microbe Interact.* **2012**, *25*, 1264–1271.
43. Rouphael, Y.; Carillo, P.; Colla, G.; Fiorentino, N.; Sabatino, L.; El-Nakhel, C.; Giordano, M.; Pannico, A.; Cirillo, V.; Shabani, E.; et al. Appraisal of combined applications of *Trichoderma virens* and a biopolymer-based biostimulant on lettuce agronomical, physiological, and qualitative properties under variable regimes. *Agronomy* **2020**, *10*, 196.

44. Stoclet, J.C.; Chataigneau, T.; Ndiaye, M.; Oak, M.H.; El Bedoui, J.; Chataigneau, M.; Shini-Kerth, V.B. Vascular protection by dietary polyphenols. *Eur. J. Pharm.* **2004**, *500*, 299–313.
45. Ruzzolini, J.; Peppicelli, S.; Andreucci, E.; Bianchini, F.; Scardigli, A.; Romani, A.; La Marca, G.; Nediani, C.; Calorini, L. Oleuropein, the Main Polyphenol of *Olea europaea* Leaf Extract, Has an Anti-Cancer Effect on Human BRAF Melanoma Cells and Potentiates the Cytotoxicity of Current Chemotherapies. *Nutrients* **2018**, *10*, 1950.
46. Marra, R.; Lombardi, N.; d'Errico, G.; Troisi, J.; Scala, G.; Vinale, F.; Woo, S.L.; Bonanomi, G.; Lorito, M. Application of *Trichoderma* strains and metabolites enhances soybean productivity and nutrient content. *J. Agric. Food Chem.* **2019**, *67*, 1814–1822.
47. Vinale, F.; Nicoletti, R.; Lacatena, F.; Marra, R.; Sacco, A.; Lombardi, N.; d'Errico, G.; Digilio, M.C.; Lorito, M.; Woo, S.L. Secondary metabolites from the endophytic fungus *Talaromyces pinophilus*. *Nat. Prod. Res.* **2017**, *31*, 1778–1785.
48. Vinale, F.; Flematti, G.; Sivasithamparam, K.; Lorito, M.; Marra, R.; Skelton, B.W.; Ghisalberti, E.L. Harzianic acid, an antifungal and plant growth promoting metabolite from *Trichoderma harzianum*. *J. Nat. Prod.* **2009**, *72*, 2032–2035.
49. Talhaoui, N.; Gómez-Caravaca, A.M.; León, L.; de la Rosa, R.; Segura-Carretero, A.; Fernández-Gutiérrez, A. Determination of phenolic compounds of 'Sikitita' olive leaves by HPLC-DAD-TOF-MS. Comparison with its parents' Arbequina' and 'Picual' olive leaves. *LWT-Food Sci. Technol.* **2014**, *58*, 28–34.
50. Tafuri, S.; Cocchia, N.; Carotenuto, D.; Vassetti, A.; Staropoli, A.; Mastellone, V.; Peretti, V.; Ciotola, F.; Albarella, S.; Del Prete, C.; et al. Chemical Analysis of *Lepidium meyenii* (Maca) and Its Effects on Redox Status and on Reproductive Biology in Stallions. *Molecules* **2019**, *24*, 1981.
51. Marra, R.; Coppola, M.; Pironti, A.; Grasso, F.; Lombardi, N.; d'Errico, G.; Sicari, A.; Bolletti Censi, S.; Woo, S.L.; Rao, R.; Vinale, F. The Application of *Trichoderma* Strains or Metabolites Alters the Olive Leaf Metabolome and the Expression of Defense-Related Genes. *J. Fungi* **2020**, *6*, 369.
52. Patkowska, E.; Mielniczuk, E.; Jamiołkowska, A.; Skwaryło-Bednarz, B.; BłaŻewicz-Woźniak, M. The Influence of *Trichoderma* harzianum Rifai T-22 and Other Biostimulants on Rhizosphere Beneficial Microorganisms of Carrot. Agronomy **2020**, 10, 1637.
53. Giuffrè, A.M. Biometric evaluation of twelve olive cultivars under rainfed conditions in the region of Calabria, South Italy. Emir. J. Food Agric. **2017**, 29, 696.
54. Rosati, A.; Zipanćič, M.; Caporali, S.; Padula G. Fruit weight is related to ovary weight in olive (Olea europaea L.). *Sci. Hortic*. **2009**, *122*, 399-403.
55. Hannachi, H.; Breton, C.; Msallem, M.; El-Hadj, S. B.; El-Gazzah, M.; Bervillé,A. Differences between native and introduced olive cultivars as revealed by morphology of drupes, oil composition and SSR polymorphisms: A case study in Tunisia. *Sci. Hortic.* **2008**, *116*, 280-290.
56. Smirnoff, N. The role of active oxygen in the response of plants to water deficit and desiccation. *New Phytol.* **1993,** *125*, 27-58.
57. Kaushik, D.; Roychoudhury A. Reactive oxygen species (ROS) and response of antioxidants as ROS-scavengers during environmental stress in plants. *Front. Environ. Sci*. **2014**, *2* (1–13), 53.
58. Kaushik, D.; Roychoudhury, A.Reactive oxygen species (ROS) and response of antioxidants as ROS-scavengers during environmental stress in plants. *Front. Environ. Sci.* **2014**, *2* (1–13), 53.
59. Fang, Y.; Xiong, L. General mechanisms of drought response and their application in drought resistance improvement in plants. *Cell. Mol. Life Sci*. **2015,** *72*, 673-689.
60. Ahmad, P.; Hashem, A.; Abd_Allah, E. .F; Alqarawi, A.A.; John, R.; Egamberdieva, D.; Gucel, S. 2015. Role of *Trichoderma* harzianum in mitigating NaCl stress in Indian mustard (Brassica juncea L.) through antioxidative defense system. *Front. Plant Sci.* **2015**, *6*, 868.

61. Schrimpe-Rutledge, A.C.; Codreanu, S.G.; Sherrod, S.D., McLean, J.A. Untargeted Metabolomics Strategies-Challenges and Emerging Directions. *J Am Soc Mass Spectrom*. **2016**, *27*(12),1897-1905.
62. Mayo-Prieto, S.; Marra, R.; Vinale, F.; Rodríguez-González, Á.; Woo, S.L.; Lorito, M.; Casquero, P.A. Effect of *Trichoderma velutinum* and *Rhizoctonia solani* on the Metabolome of Bean Plants (*Phaseolus vulgaris* L.). *Int. J. Mol. Sci.* **2019**, *20*, 549.
63. Gutierrez-Rosales, F.; Romero, M.P.; Casanovas, M.; Motilva, M.J.; Mínguez-Mosquera, M.I. Metabolites involved in oleuropein accumulation and degradation in fruits of Olea europaea L.: Hojiblanca and Arbequina varieties. J. Agric. Food Chem. **2010**, 58, 12924–12933
64. Damtoft, S.; Franzyk, H.; Jensen, S. R. Biosynthesis of secoiricoid glucosides in Oleaceae. *Phytochemistry,* **1993**, *34,* 1291-1299.
65. Damtoft, S.; Franzyk, H.; Jensen, S. R. Biosynthesis of iridoids in Syringa and Fraxinus: Secoiridoid precursors. *Phytochemistry,* **1995**, *40,* 773-784.
66. Morita, Y.; Hoshino, A. Recent advances in flower color variation and patterning of Japanese morning glory and petunia. *Breed. Sci.* **2018**, *68*, 128–138.
67. Dias, M.C.; Pinto, D.C.G.A.; Freitas, H.; Santos, C.; Silva, A.M.S. The antioxidant system in *Olea europaea* to enhanced UV-B radiation also depends on flavonoids and secoiridoids. *Phytochemistry* **2020**, *170*, 112199.
68. Omar, S.H. Oleuropein in olive and its pharmacological effects. *Sci. Pharm.* **2010**, *78*, 133–154.
69. Montesano, D.; Rocchetti, G.; Cossignani, L.; Senizza, B.; Pollini, L.; Lucini, L.; Blasi, F. Untargeted Metabolomics to Evaluate the Stability of Extra-Virgin Olive Oil with Added *Lycium barbarum* Carotenoids during Storage. *Foods* **2019**, *8*, 179.
70. Xu, H.; Linn, B.S.; Zhang, Y.; Ren, J. A review on the antioxidative and prooxidative properties of luteolin. *React. Oxyg. Species* **2019**, *7*, 136–147.

*Article*

# Supplementary materials: Effect of Selected *Trichoderma* Strains and Metabolites on Olive Drupes

**Irene Dini [1*], Marica Pascale[2], Alessia Staropoli[2,4], Roberta Marra[2], Francesco Vinale [3,4,5*]**

**Table S1.** Analytical parameters used to perform the calibration curves

| Standard | Range [µg/ml] | Equation of the calibration line | $r^2$ |
|---|---|---|---|
| **Oleuropein** | 0.625-25 | y = 3264818.79x + 8921367.34 | 0.99 |
| **Luteolin** | 0.5-25 | y = 2750905.36x + 2774612.53 | 0.99 |
| **Apigenin** | 0.5-50 | y= 1388397.18x + 7259647.69 | 0.96 |
| **Idrossitiro-sol** | 0.62-62.5 | y= 858369x+1000000 | 0.99 |

molecules

MDPI

*Article*

# Bivalent Metal-Chelating Properties of Harzianic Acid Produced by *Trichoderma pleuroticola* Associated to the Gastropod *Melarhaphe neritoides*

**Gaetano De Tommaso [1], Maria Michela Salvatore [1], Rosario Nicoletti [2,3], Marina DellaGreca [1], Francesco Vinale [4,5], Assunta Bottiglieri [3], Alessia Staropoli [3,5], Francesco Salvatore [1], Matteo Lorito [3], Mauro Iuliano [1,*] and Anna Andolfi [1,*]**

[1] Department of Chemical Sciences, University of Naples Federico II, 80126 Naples, Italy; gaetano.detommaso@unina.it (G.D.T.); mariamichela.salvatore@unina.it (M.M.S.); dellagre@unina.it (M.DG.); frsalvat@unina.it (F.S.)
[2] Council for Agricultural Research and Economics, Research Centre for Olive, Fruit and Citrus Crops, 81100 Caserta, Italy; rosario.nicoletti@crea.gov.it
[3] Department of Agricultural Sciences, University of Naples Federico II, 80055 Portici, Italy; assunta_bottiglieri@libero.it (A.B.); alessia.staropoli @unina.it (A.S.); matteo.lorito@unina.it (M.L.)
[4] Department of Veterinary Medicine and Animal Productions, University of Naples Federico II, 80137 Naples, Italy; frvinale@unina.it
[5] Institute for Sustainable Plant Protection, National Research Council, 80055 Portici, Italy
[*] Correspondence: mauro.iuliano@unina.it (M.I.); andolfi@unina.it (A.A.); Tel.: +39-081-2539179 (A.A.)

**Abstract:** Harzianic acid is a secondary metabolite of *Trichoderma*, structurally belonging to the dienyltetramic acid subgroup of the tetramic acids. Biological activities of harzianic acid are of great interest for its antimicrobial and plant growth-promoting activities, which might be related to its chelating properties. In the present work harzianic acid, isolated from cultures of a strain of *Trichoderma pleuroticola* associated to the gastropod *Melarhaphe neritoides*, was studied as a complexant agent of a number of biologically relevant transition metals (i.e., $Zn^{2+}$, $Fe^{2+}$, $Cu^{2+}$, and $Mn^{2+}$), using UV-VIS, potentiometry, MS and NMR techniques. Our findings show the coordination capacity of harzianic acid toward the above cations through the formation of neutral or charged complexes in a variable ratio depending on the metal and pH conditions.

**Keywords:** *Trichoderma* secondary metabolites; bioactive products; chelating metal; tetramic acids; harzianic acid complexes

## 1. Introduction

Species of *Trichoderma* (Sordariomycetes, Hypocreaceae) are widespread in every natural environment on earth, in connection with their extraordinary adaptive capacity to different ecological conditions and lifestyles [1,2]. Particularly, these fungi are able to establish various interactions with plants and other microbes [1–4]. At least in part, this is related to the production of secondary metabolites, belonging to several class of compound such as butenolides, epipolythiodioxopiperazines, thiosilvatins, pyrones, sorbicillinoids, terpenoids [5–11].

Tetramic acids represent a group of *Trichoderma* metabolites, including trichosetin [12] and harzianic acid and its analogs belonging to the subgroup of the dienoyltetramic acid according to a recent classification [13]. Harzianic acid, was first isolated from *Trichoderma harzianum* [14] and characterizes the chemotaxonomic profile of this species [15], along with its analogues isoharzianic acid (C-5″ epimer) [16], demethylharzianic acid, and homoharzianic acid [17]. The production of a

new derivative harziaphilic acid was also detected in co-cultures with a strain of *Talaromyces pinophilus* [18]. However, after the spread of DNA sequencing in fungal taxonomy, recent revisions have shown *T. harzianum* to be a species complex made of many biological species [19,20], suggesting a more accurate assessment of the harzianic acid producers.

The absolute configuration *S*,*S* at the asymmetric carbons C-5′ and C-7 of harzianic acid was assigned by X-ray diffraction studies [21]. Moreover, harzianic acid and its stereoisomers were also prepared in six steps with an overall yield of 22% from the masked 4,4-disubstituted glutamic acid and a polyene fragment [22].

Recent studies reported intriguing bioactivities of harzianic acid, such as antimicrobial activity against phytopathogenic species (*Pythium irregulare*, *Sclerotinia sclerotiorum,* and *Rhizoctonia solani*), promotion of plant growth [21]. Some of these activities might be related to the chelating properties of this metabolite. In fact, it is documented that harzianic acid inhibits the serine/threonine phosphatase type 2A (PP2A) only in presence of zinc in a complex ligand-$Zn^{2+}$ 2:1 [17]. Moreover, its complex with $Fe^{3+}$ has been demonstrated and could be related to the growth promotion activity on tomato seedlings [23]. Hence, the improvement of knowledge on chelating properties of harzianic acid is of great interest to better understand its biological activities also against other microbial targets (.i.e., virus).

Divalent metals (i.e., Mn, Fe, Co, Ni, Cu, and Zn) are essential micronutrients for all life forms, in particular for their catalytic activities, substrate stabilization, and as reaction intermediates. The detection of divalent metals is of special interest because their beneficial effects are affected by concentration. In this respect, many organisms produce metabolites with high metal-binding proprieties [24], and their interactions might be influenced by the capacity to regulate metal levels [25].

The aim of this work is to study the chelating properties of harzianic acid, isolated from a marine strain of *T. pleuroticola*, to evaluate the formation and stability of complexes formed with transition metals with biologically relevant functions (i.e., $Cu^{+2}$, $Fe^{2+}$, $Mn^{2+}$, and $Zn^{2+}$).

## 2. Results and Discussion

### *2.1. Identification of Strain L1 of* Trichoderma pleuroticola *Isolated from* Melarhaphe neritoides

Strain L1 recovered from the gastropod *Melarhaphe neritoides* was identified according to morphological and molecular methods. A blast in GenBank of the TEF sequence obtained (Figure S1) yielded a strain of *T. pleuroticola* (T1295), commonly used as a reference in phylogenetic assessments involving this species [26], as the closest match, with an identity of 98.69% (query cover 100%). *T. pleuroticola* was separated from *T. harzianum* based on mycoparasitic strains from *Pleurotus* [27], but afterwards recovered from various contexts, including marine sediments [28].

### *2.2. Isolation and Identification of Harzianic Acid*

The metabolomic analysis (LC-MS approach) of L1 culture filtrates showed the presence of harzianic acid (Figure 1) as the major compound. LC-ESI mass spectrum, recorded in positive mode, exhibits peaks at *m/z* 366, 388 and 753 corresponding respectively to $[M + H]^+$, $[M + Na]^+$, $[2M + Na]^+$ ions (Figure S2). In order to extract harzianic acid, culture filtrate was treated as previously described [16], with slight modifications. Particularly, a saturated $NaHCO_3$ solution was used in order to separate neutral and basic substances, which are eventually contained in the crude extract. Harzianic acid was subsequently extracted with EtOAc following acidification of the basic aqueous phase (Figure 2). The NMR data, recorded in $CDCl_3$ and $CD_3OD$ (Figures S3–S5), and optical rotation of the purified compound were in agreement with previous reports [22] (Table S1).

Repeated chromatographic and spectral analysis did not demonstrate evidence of the presence of isomeric or degradation products of harzianic acid.

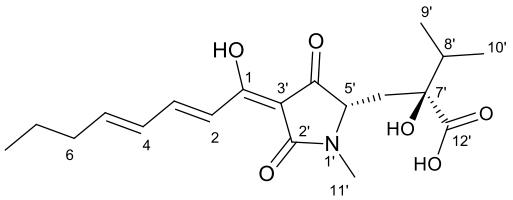


**Figure 1.** Structure of harzianic acid.

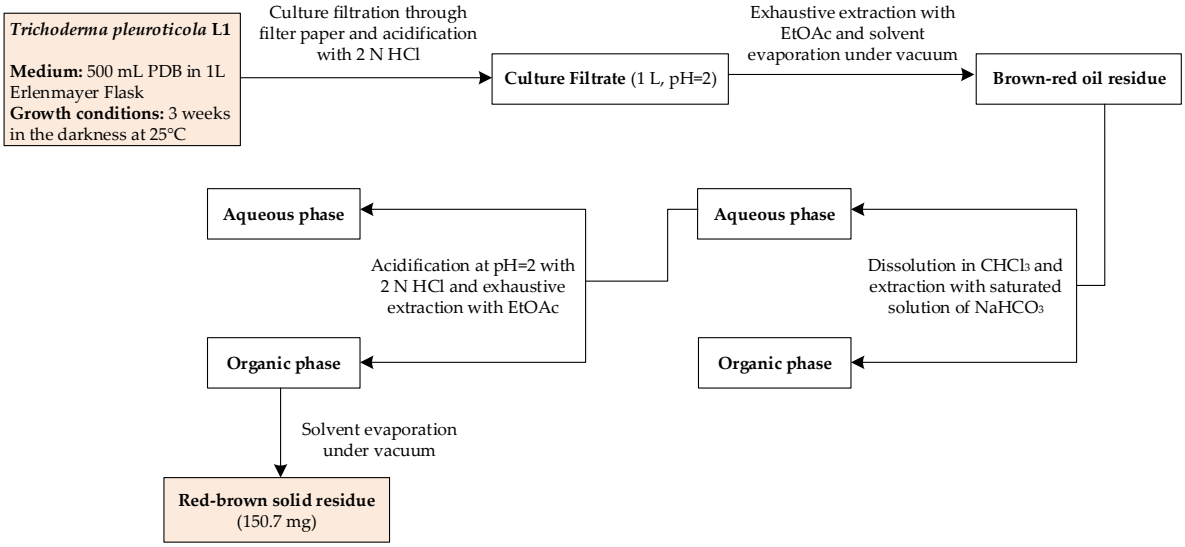


**Figure 2.** Schematic representation of harzianic acid extraction from *Trichoderma pleuroticola* L1 culture filtrate.

## *2.3. Determination of Protonation Constants of Harzianic Acid*

The experimental data were collected by both spectrophotometric titrations in UV-VIS region and potentiometric technique, where the pH measurements were conducted with glass electrode. By reason of low solubility of harzianic acid in aqueous solutions, the measures were performed in $CH_3OH$/0.1 M $NaClO_4$ 50:50 (*w*/*w*) as ionic medium. UV-VIS spectra relating to titration are reported in Figure 3.

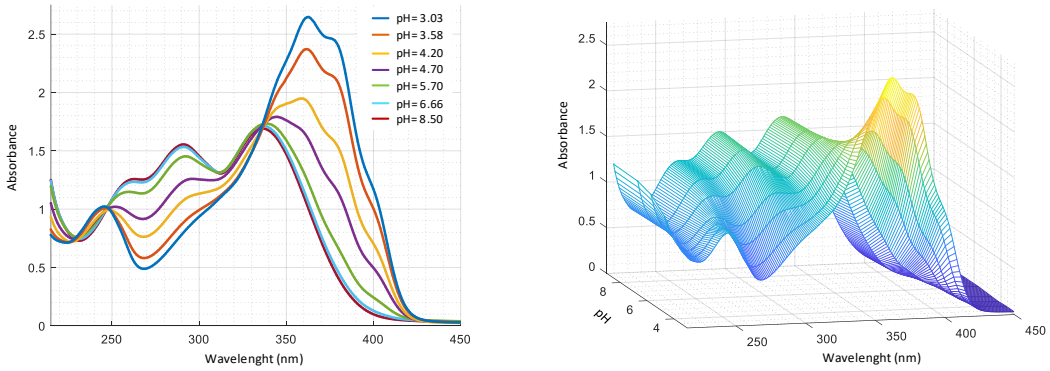


**Figure 3.** UV-VIS spectra as a function of pH for a solution $2.0 \cdot \times 10^{-4}$ M harzianic acid in $CH_3OH$/0.1 M $NaClO_4$ (50:50 *w*/*w*) recorded at pHs: 3.03, 3.58, 4.20, 4.70, 5.70, 6.66, 8.50 (left 2D–right 3D graphics).

By analysis of UV-Vis spectra (Figure 3), in acid solution, it is evident the presence of two bands at 350 nm and 250 nm, that shift in alkaline solution. Two isosbestic points are also observed, at 350 nm and 240 nm respectively, compatible with the presence of two acid–base equilibria as reported in Table 1. To assign the corresponding type of molecular transition to the absorption bands, spectra were recorded in solvents with different polarity, such as methanol and 2–propanol. In particular, at pH = 5.70, band at 250 nm in methanol shows a bathochromic shift ($log\,\varepsilon = 3.89$), compared to 240 nm ($log\,\varepsilon = 4.10$) in 2–propanol (Figure S6). This behavior can be associated with transitions involving the diene system orbitals. Furthermore, band at around 350 nm undergoes a hypsochromic shift -345 nm in methanol ($log\,\varepsilon = 4.12$), compared to 360 nm ($log\,\varepsilon = 4.43$) in 2–propanol, which can be assigned to transitions that involve the non-bonding electrons of oxygen in C4' position [29]. On the basis of the experimental data obtained with potentiometric and spectrophotometric measurements and considering pKa of α-hydroxyacids [30], the protolytic constants of carboxylic and dienoyl groups were assigned as reported in Table 1.

**Table 1.** Summary of acidity constants (cologarithms) of harzianic acid ($H_2L$), obtained by potentiometric and spectrophotometric measurements.

| Equilibria | Dissociation of Acid Group | Spectrophotometry | Potentiometry |
|---|---|---|---|
| $H_2L + H_2O = HL^- + H_3O^+$ | R-$COO^-$ | 4.08 ± 0.02 | 4.00 ± 0.09 |
| $HL^- + H_2O = L^{2-} + H_3O^+$ | 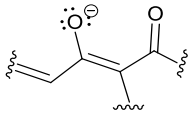 | 5.63 ± 0.08 | 5.9 ± 0.2 |

By the acid constants, it is possible to build up the distribution curves for all the species present in this system, as reported in Figure 4.

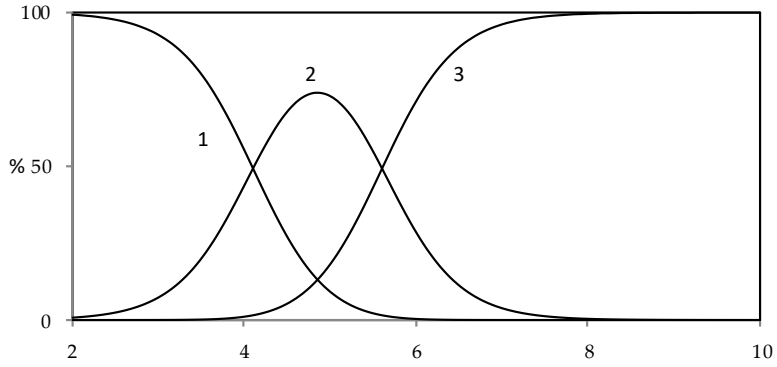


**Figure 4.** Distribution diagram of protolytic species for harzianic acid in $CH_3OH$/0.1 M $NaClO_4$ (50:50 *w/w*) (1: $H_2L$; 2: $HL^-$; 3: $L^{2-}$).

Circular dichroism measurements, conducted in the same conditions as potentiometric and spectrophotometric assessments, show, as the pH of the solution increases, the presence of two peaks (one positive Cotton effect at 285 nm and another negative at 350 nm) as reported in Figure 5. This behavior indicates an increase in the asymmetry of the molecule in alkaline solution, which affects the chirality in position C5′. In effect, by a keto–enolic equilibrium, that involves the carbonyl group in C4′, it is possible to invert the configuration in C5′.

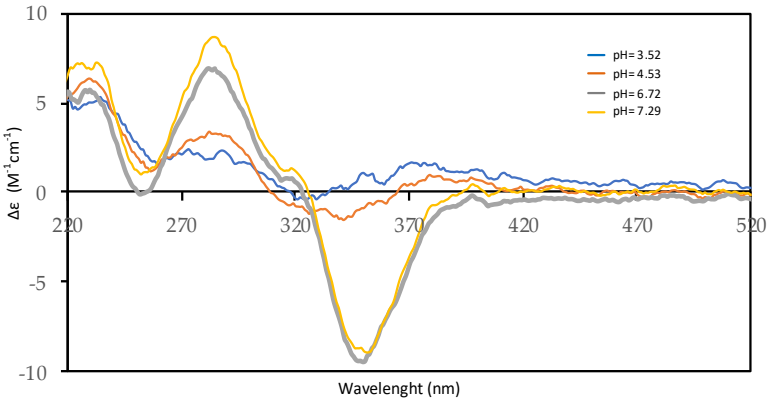


**Figure 5.** Far–UV CD spectra of $2.0 \cdot 10^{-4}$ M harzianic acid in $CH_3OH$/0.1 M $NaClO_4$ (50:50 *w/w*) at different pH values (3.52, 4.53, 6.72, 7.29) (optical path 0.2 cm).

## *2.4. Study of Complexation of Harzianic Acid with Metal Cations*

UV-VIS measurements carried out for $Zn^{2+}$–harzianic acid system at different pH (Figure 6A) show the presence, in alkaline solution, of three bands at 251 nm (log ε = 3.45), 290 nm (log ε = 3.58) and 330 nm (log ε = 3.69). From spectra recorded at different metal/harzianic acid molar ratio (Figure 6B) (at fixed pH), two peaks at 335 nm (log ε = 4.15) and 294 nm (log ε = 3.99) are observed. Measurements show a considerable spectral variation up to a value of 0.5 metal/ligand molar ratio that is compatible with the formation of a 1:2 stoichiometric complex.

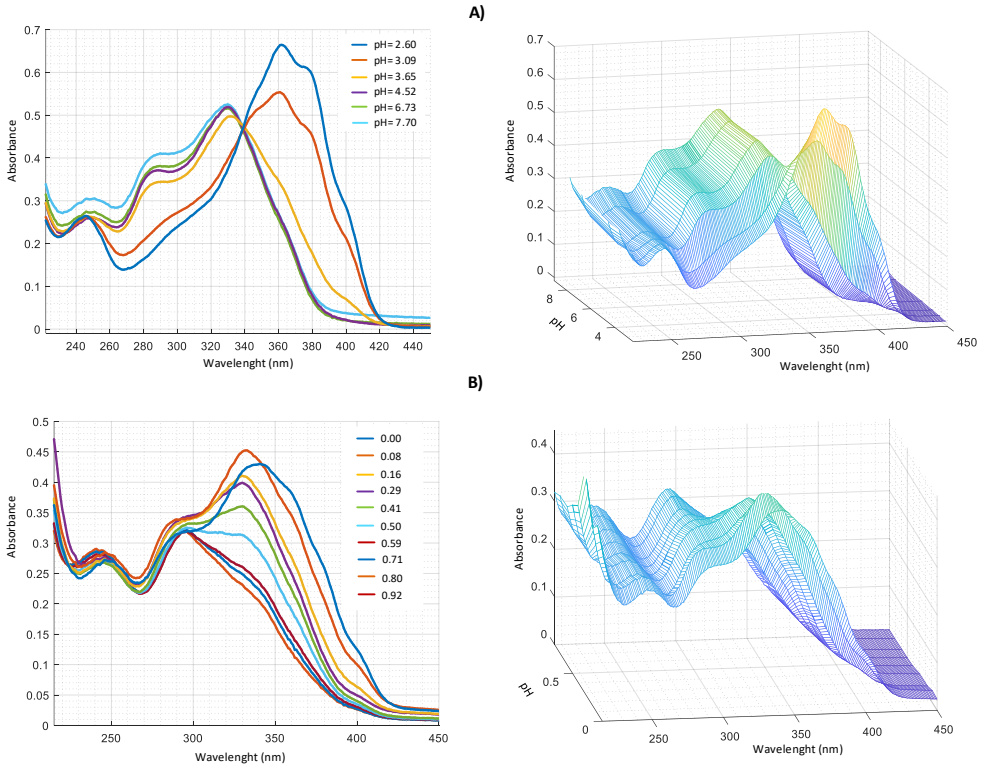


**Figure 6.** UV-VIS spectra in $CH_3OH$/0.1 M $NaClO_4$ (50:50 *w/w* of: (**A**) $2.0 \cdot 10^{-4}$ M harzianic acid and $2.0 \cdot 10^{-4}$ M $Zn(ClO_4)_2$ at different pH (2.60; 3.09; 3.65; 4.52; 6.73; 7.70); (**B**) at different metal/harzianic acid molar ratio (0.08; 0.16; 0.29; 0.41; 0.50; 0.59; 0.71; 0.80; 0.92) at pH = 6.50 (left 2D–right 3D graphics).

Similar measurements were performed in harzianic acid solutions with $Cu^{2+}$, $Fe^{2+}$, and $Mn^{2+}$ (Figures 7–9).

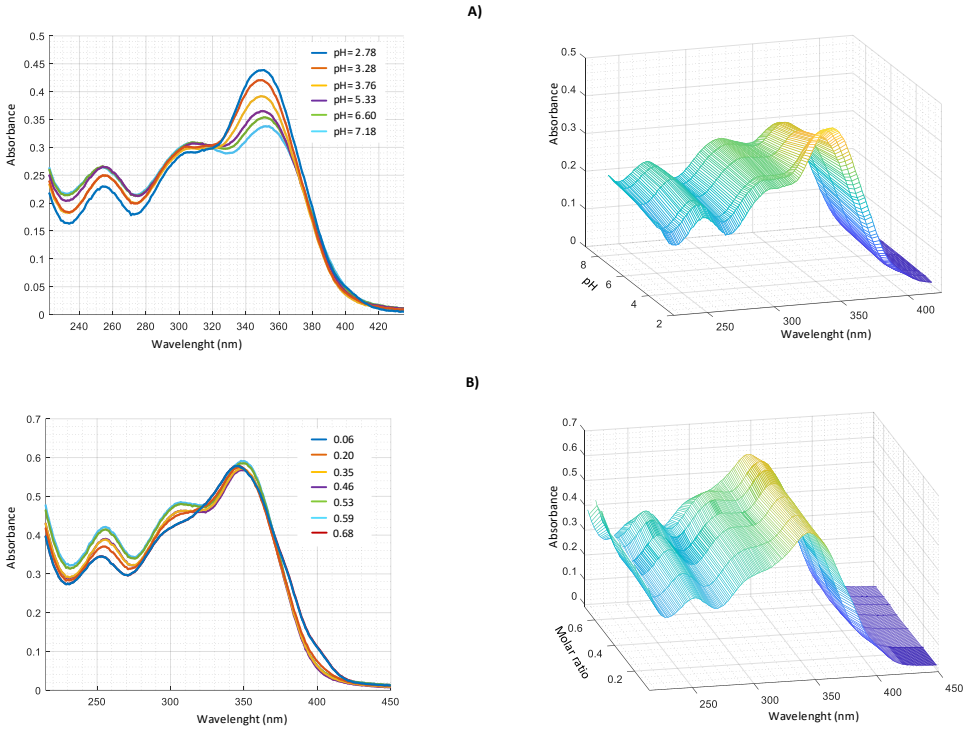


**Figure 7.** UV-VIS spectra in $CH_3OH$/0.1 M $NaClO_4$ (50:50 *w/w*) of: (**A**) $2.0 \cdot 10^{-4}$ M harzianic acid and $2.0 \cdot 10^{-4}$ M $Cu(ClO_4)_2$ at different pH (2.78, 3.28, 3.76, 5.33, 6.60, 7.18); (**B**) at different metal/harzianic acid molar ratio (0.06, 0.20, 0.35, 0.46, 0.53, 0.59, 0.68) at pH = 6.50 (left 2D–right 3D graphics).

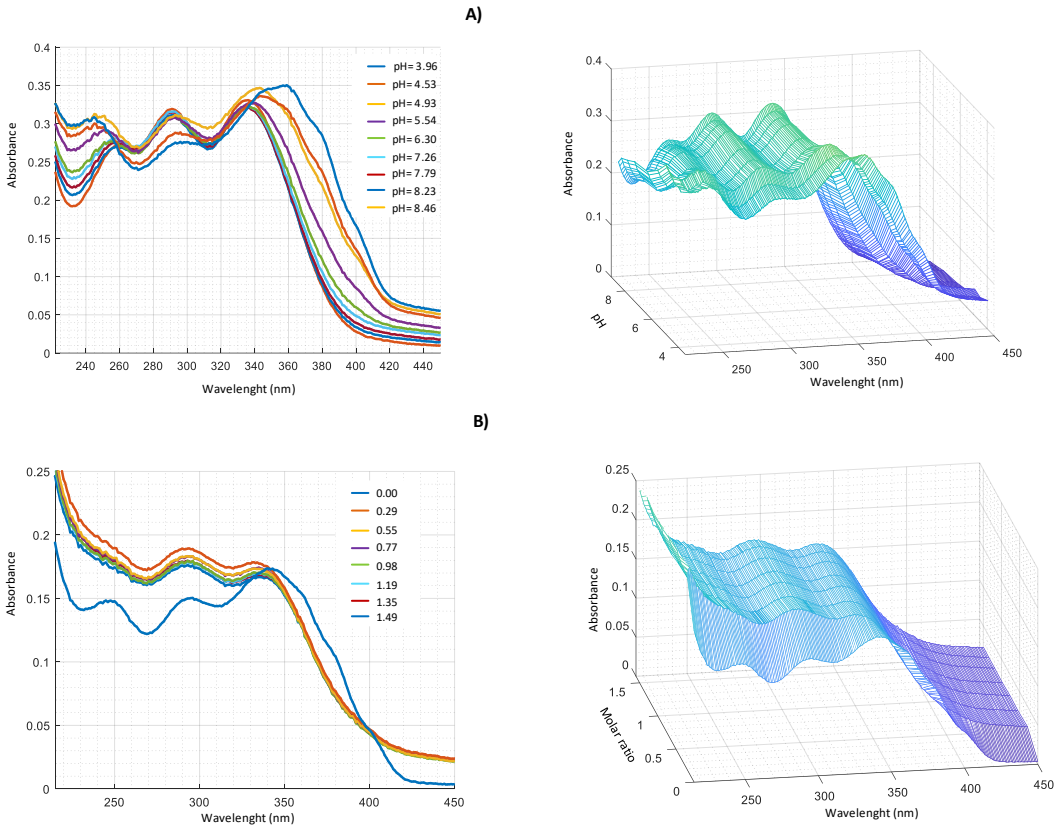

**Figure 8.** UV-VIS spectra in $CH_3OH$/0.1 M $NaClO_4$ (50:50 *w/w*) of: (**A**) $2.0 \cdot 10^{-4}$ M harzianic acid and $2.0 \cdot 10^{-4}$ M $FeSO_4$ at different pH (from 3.96 to 8.46); (**B**) at different metal/harzianic acid molar ratio (from 0.00 to 1.49), at pH = 6.50 (left 2D–right 3D graphics).

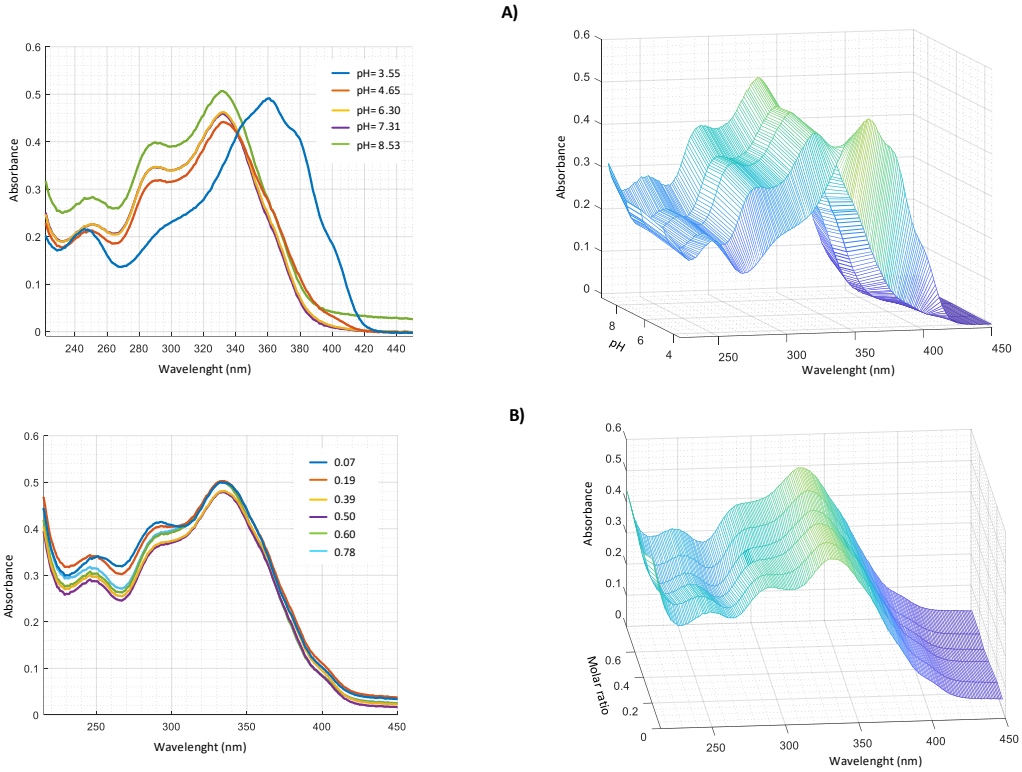


**Figure 9.** UV-VIS spectra in $CH_3OH$/0.1 M $NaClO_4$ (50:50 *w/w*) of: (**A**) $2.0 \cdot 10^{-4}$ M harzianic acid and $2.0 \cdot 10^{-4}$ M $MnCl_2$ at different pH (3.55, 4.65, 6.30, 7.31, 8.53); (**B**) at different metal/harzianic acid molar ratio (0.70, 0.19, 0.39, 0.50, 0.60, 0.78) at pH = 6.50 (left 2D–right 3D graphics).

The collected data were processed numerically by Hyperquand program, obtaining the equilibrium constant reported in Table 2. The stability of stoichiometric complexes 1:2 follows the trend of the Irving–Williams series (Cu > Zn > Mn), while $Fe^{2+}$ exhibits an anomalous behaviour due to the formation of different 1:2 complexes. A similar trend in the stability of the complexes also exists as a function of the first hydrolysis constant, as also observed by Martel and Hancock [31] for metal ions complexes with organic ligands (e.g., malonate and catechol).

**Table 2.** Summary of metal ion/harzianic acid ($H_2L$) stability constants.

| $Me^{2+}$ | Equilibria | log (cost.eq.) ± 3σ * |
|---|---|---|
| $Cu^{2+}$ | $Cu^{2+} + L^{2-} = CuL$ | 9.26 ± 0.08 |
| | $Cu^{2+} + 2\ L^{2-} = CuL_2^{2+}$ | 15.82 ± 0.05 |
| $Zn^{2+}$ | $Zn^{2+} + 2\ L^{2-} = ZnL_2^{2+}$ | 14.42 ± 0.06 |
| $Mn^{2+}$ | $Mn^{2+} + 2\ L^{2-} = MnL_2^{2+}$ | 11.96 ± 0.09 |
| $Fe^{2+}$ | $Fe^{2+} + 2\ HL^{-} = Fe(HL)_2$ | 13.20 ± 0.04 |
| | $Fe^{2+} + 2\ L^{2-} = FeL_2^{2+}$ | 10.22 ± 0.07 |

* denotes standard deviation.

To visualize the amounts of the different species, distribution diagrams were built for Cu(II)–harzianic acid and Fe(II)– harzianic acid systems (Figures 10 and 11).

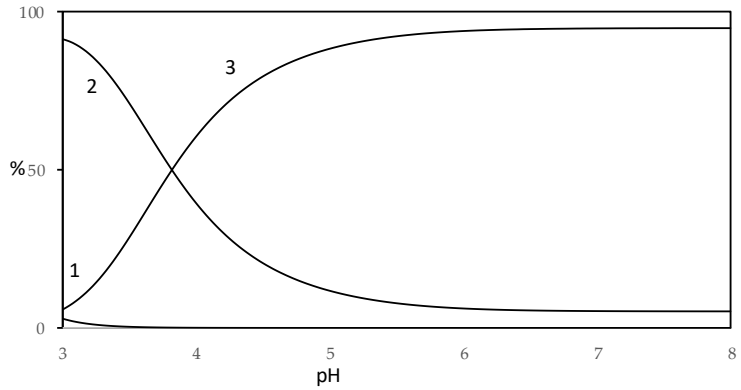


**Figure 10.** Distribution diagram of species for Cu(II)–HA system in $CH_3OH$/0.1 M $NaClO_4$ (50:50 *w/w* with $1.0 \cdot 10^{-4}$ M Cu(II) and $2.0 \cdot 10^{-4}$ M of HA acid ($H_2L$) (1: $Cu^{2+}$; 2: CuL; 3: $CuL_2^{2-}$).

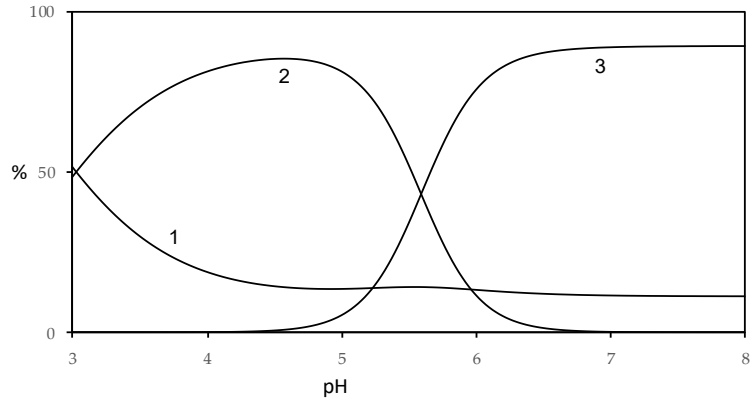


**Figure 11.** Distribution diagram of species for Fe(II)–harzianic acid system in $CH_3OH$/0.1 M $NaClO_4$ (50:50 *w/w* with $1.0 \cdot 10^{-4}$ M Fe(II) and $2.0 \cdot 10^{-4}$ M of harzianic acid ($H_2L$) (1: $Fe^{2+}$; 2: $Fe(HL)_2$; 3: $FeL_2^{2-}$).

From the distribution diagram of Cu(II) –harzianic acid system (metal ion/ligand ratio 1:2), reported in Figure 10, a prevalence of CuL is observed until pH 4, while for pH value higher than 4 there is a prevalence of $CuL_2^{2-}$ complex which reaches a maximum of about 90%. On the other hand, the CuL species is present in a non-significant amount (less than 10%).

By analysis of the distribution diagram of the Fe(II) –harzianic acid system (Figure 11; metal ion/ligand ratio 1:2), the free metal concentration decreases from 50%, at pH = 3, to about 10% for pH range 5–8 in favor of the formation of complex species. In particular, the $Fe(HL)_2$ complex species becomes considerable for pH range 3–5.5 in amount until 85%. While the $FeL_2^{2-}$ complex species predominates in amount until 90% for pH higher than 5.5.

*2.5. LC-MS and NMR Data*

Chelating properties of harzianic acid were confirmed by LC-MS analysis of Metal (II)-HA. The main ions showed in MS spectra (Figures S7–S9) of each solution are reported in Table 3. In addition to ion characteristic of harzianic acid, LC-ESI-HRMS spectra of solutions in the presence of Cu(II), Mn(II) and Zn(II) exhibit dimeric peaks $[2M - H + Metal]^+$ confirming the stoichiometric ratios observed in the previous section. Interestingly, the solution containing copper exhibits a peak at *m/z* 427.1057 corresponding to $[M\text{-}H+Cu]^+$ and characteristic of a complex with stoichiometry 1:1. LC-MS analysis of harzianic acid with Fe(II) did not show any significant peak corresponding to complexes of this metal. Probably, this is due to the production of not charged species.

**Table 3.** Caracterization of Metal$^{2+}$-harzianic acid complex by LC/MS.

| Ion | Experimental Mass | Formula | Exact Mass |
|---|---|---|---|
| **Harzianic acid: $Cu(ClO_4)_2$** | | | |
| $[M+H]^+$ | 366.1921 | $C_{19}H_{28}NO_6$ | 366.1917 |
| $[M+Na]^+$ | 388.1730 | $C_{19}H_{27}NO_6Na$ | 388.1736 |
| $[M-H+Cu]^+$ | 427.1057 | $C_{19}H_{26}NO_6Cu$ | 427.1056 |
| $[M+Cu+ClO_4]^+$ | 527.0619 | $C_{19}H_{27}NO_{10}CuCl$ | 527.0619 |
| $[2M-H+Cu]^+$ | 792.2880 | $C_{38}H_{53}N_2O_{12}Cu$ | 792.2895 |
| **Harzianic Acid: $MnCl_2$** | | | |
| $[M+H]^+$ | 366.1908 | $C_{19}H_{28}NO_6$ | 366.1917 |
| $[M+Na]^+$ | 388.1728 | $C_{19}H_{27}NO_6Na$ | 388.1736 |
| $[2M+Na]^+$ | 753.3549 | $C_{38}H_{54}N_2O_{12}Na$ | 753.3574 |
| $[2M-H+Mn]^+$ | 784.2952 | $C_{38}H_{53}N_2O_{12}Mn$ | 784.2979 |
| **Harzianic Acid: $Zn(ClO_4)_2$** | | | |
| $[M+H]^+$ | 366.1922 | $C_{19}H_{28}NO_6$ | 366.1917 |
| $[M+Na]^+$ | 388.1738 | $C_{19}H_{27}NO_6Na$ | 388.1736 |
| $[M+Zn+ClO_4]^+$ | 528.0612 | $C_{19}H_{27}NO_{10}ZnCl$ | 528.0615 |
| $[2M-H+Zn]^+$ | 793.2886 | $C_{38}H_{53}N_2O_{12}Zn$ | 793.2890 |

Finally, $^1$H NMR spectra of harzianic acid solutions prepared with $Mn^{2+}$ and $Zn^{2+}$ confirmed the capacity of our compound to coordinate these cations. The analyses were recorded in $CD_3OD/D_2O$ 1:1 (*w/w*), hence the proton spectrum of harzianic acid was previously acquired in the same solvent mixture for an accurate data interpretation. Chemical shifts were assigned on the basis of COSY experiment (Figure S10-S11), and data reported in the literature [22]. In fact, $^1$H NMR spectrum of harzianic acid (Figure S10) shows the loss of multiplicity of many signals and the overlap of H-8′ and H-6′B which resonates as multiplet at δ 2.12-1.96. In fact, the COSY spectrum showed a correlation between this signal and H-6′A multiplet at δ 2.41-2.32 and of $H_3$-9′ and doublet $H_3$-10′ resonating at δ 0.99. Moreover, the same spectrum showed a correlation between $H_2$-7 (δ 1.53-1.51) and protons of the methyl group $H_3$-8 (Table S1).

The $^1$H NMR spectrum of harzianic acid recorded in presence of $MnCl_2$ showed some significant shifts for H-3, H-4/5, H-5′ and $H_3$-11′ resonating a δ 7.88 (dd, $J$ =14.9, 11.3 Hz), 6.11-5.93 (m), 4.29 (d, $J$ = 9.7 Hz) and 2.85 (s) respectively. In particular, downfield shift of H-3 and H-5′ of Δ δ 0.35 and 0.46, and upfield shift of H-4/5 and $H_3$-11′ of Δδ 0.42 and 0.10, were respectively observed (Figure S12). A similar result is visible in the harzianic acid spectrum recorded in presence of $Zn(ClO_4)_2$ (Figure S12).

The coordination regioselectivity can be deduced by comparison between of NMR data of harzianic acid and its Cu(II) and Mn(II) complexes. In particular, the shifts of protons H-3 of the residue esadienoyl and H-5′ of the pyrrolidine ring could be related to the metal coordination with external carbonyl and amide groups.

## 3. Materials and Methods

### *3.1. Reagents and Their Analysis*

Solutions of metals were prepared from Merck (Darmstadt, Germany) p.a. products [$Cu(ClO_4)_2$, $Zn(ClO_4)_2$, $MnCl_2$ and $FeSO_4$] dissolved in bidistilled water. The metal concentration was determined by complexometric method with a solution of EDTA at known concentration. Diluted solutions of perchloric acid were prepared from Merck p.a. products and standardized potentiometrically (glass electrode) against tris(hydroxymethyl)amino methane (Sigma-Aldrich, Saint Louis, MO, USA). The results agreed to within 0.1% or better.

Carbonate-free solutions of sodium hydroxide were obtained simply by diluting (after centrifugation) a saturated NaOH solution. To prevent air, contact the tubes were closed with a suba seal rubber. An approximately known quantity of NaOH was injected and immediately transferred under nitrogen atmosphere in a calibrated volumetric flask containing $NaClO_4$ in the desired quantity, freshly boiled bidistilled water, and finally filled to the flask mark. The accurate hydroxide concentration was determined by titration with standard $HClO_4$ using methyl red as a visual indicator. Replicated analyses agreed to within 0.1%.

6 molal solutions of sodium perchlorate ($NaClO_4 \cdot H_2O$, Merck p.a.). contain less than $10^{-5}$ molal concentration of iron, silica, heavy metals chloride, and sulphate ions. Stock solutions were analysed gravimetrically by drying at 130 °C.

### *3.2. General Experimental Procedures*

Optical rotations were measured in $CH_3OH$ using a Jasco P-1010 digital polarimeter (Tokyo, Japan). NMR spectra were recorded at 400 MHz in $CDCl_3$ or $CD_3OD$ or $CD_3OD/D_2O$ 1:1 (*w*/*w*) on a Bruker spectrometer (Ascend$^{TM}$400) (Bremen, Germany). The solvent was used as internal standard. The potentiometric titrations were performed in an air-bath thermostat kept at (25.00 ± 0.05) °C. A programmable computer-controlled data acquisition unit 3421A, supplied by Hewlett and Packard (Palo Alto, CA, USA), was used to perform the potentiometric measurements. The glass electrodes were Metrohm (Herisau, Switzerland) of 60102-100 type and Ag/AgCl electrode was utilized as reference. The EMF values were measured with a precision of ± 0.01 mV using a Keithley 642 type Digital Electrometer (Tektronix Inc., Beaveron, OR, USA).

UV-VIS spectra were recorded by model Cary 5000 Spectrophotometer by Varian C. (Palo Alto, CA, USA), from 200 to 600 nm (optical path 0.2 cm) at 25.0 °C, under a constant flow of nitrogen. The far UV-CD spectra were recorded with a Jasco spectropolarimeter model J-715 (Tokyo, Japan), from 200 to 600 nm (optical path 0.2 cm) at 25.0 ° C, under a constant flow of nitrogen.

### *3.3. Isolation and Identification of Strain L1*

Strain L1 was recovered from a specimen of the mollusc *Melarhaphe neritoides* (Gastropoda, Littorinidae) collected on an outcropping rock in the intertidal zone along the coastline of the isle of Procida, Bay of Naples, Italy. The small specimen was directly placed in a Petri dish containing potato dextrose agar (PDA: Hi Media, Mumbai, India) acidified with lactic acid (10 mL 10% l.a./L) and incubated at 25 °C in darkness. A hyphal tip from an emerging fungal colony was transferred in pure culture on PDA. The subculture developed very rapidly, covering the whole medium in 2 days; the surface promptly turned from white to yellow-green as sporulation progressed, indicative of belonging of L1 to the genus *Trichoderma*.

L1 was inoculated on PDA plates and cultivated for 7 days at 25° C. Five mycelial plugs from actively growing cultures were used to inoculate 50 mL potato dextrose broth (PDB: Hi Media) in a 250 mL Erlenmeyer flask. Stationary culture was kept in the dark at 25 °C for 4 days. The biomass was collected by separating the substrate by filtration with Miracloth (Calbiochem, San Diego, CA, USA) paper, washed repeatedly with sterile distilled water, and dried with absorbent paper. The freeze-dried biomass was ground with a spatula and genomic DNA was isolated by using NucleoSpin® Soil kit (Macherey-Nagel, Düren, Germany), following manufacturer′s instructions. DNA quantity was determined using a Qubit 2.0 fluorometer with the dsDNA BR Assay (Life Technologies, Grand Island, NY, USA). PCR analysis was carried out in 50 µL total reaction volume, with 0.5 µM primer, 0.2 mM dNTP Mix, 1× DreamTaq Green Buffer (Thermo Scientific, Waltham, MA, USA), and 1.25 U of DreamTaq DNA Polymerase (Thermo Scientific). The translation elongation factor -1 alpha (TEF-1α) was amplified by the primer pair TEF-1f (ATGGGTAAGGARGACAAGAC) and TEF-1r (GGARGTACCAG-TSATCATGTT). The products obtained were analyzed by subjecting 5 µL of them to gel

electrophoresis of agarose. The PCR product was purified with the PureLink Quick PCR Purification (Invitrogen, Waltham, MA, USA) kit, following the manufacturer′s instructions. Sequencing reactions were performed by Eurofins Genomics (Ebersberg, Germany) with the same primer sets used for PCR amplification. The nucleotide sequence of the inserts thus obtained was subjected to in silico analysis through the BlastX program which compares the nucleotide sequence with those contained in the GenBank database (Bethesda, MD, USA) of the National Center for Biotechnological information. Sequence has been deposited in GenBank under the reference numbers MT309187.

### *3.4. Production of Culture Filtrates and HA extraction*

Mycelial plugs from actively growing cultures on PDA of strain L1 were used to inoculated in 1 L-Erlenmayer flasks containing 500 mL PDB. Cultures were kept in darkness at 25 °C for 3 weeks, then filtered through filter paper (Whatman, Maidstone, UK). The culture filtrate (1 L) was acidified to pH 2 with 2 N HCl and extracted three time with the same volume of ethyl acetate (EtOAc). The organic extracts were combined, dried with $Na_2SO_4$, and evaporated under reduced pressure to give a brown-red oil residue. The extract was dissolved in $CHCl_3$ and then extracted with a saturated solution of $NaHCO_3$. The aqueous phase was acidified at pH 2 with concentrated HCl and extracted three times with EtOAc. The organic phase obtained was dried with $Na_2SO_4$, and evaporated under reduced pressure affording a red-brown solid residue (150.7 mg) (Figure 2).

### *3.5. LC-MS Analysis*

In order to investigate binding properties of harzianic acid towards bivalent metal, 500µL of each metal water solution (2 mM) were added to 500 µL of a methanolic solution of harzianic acid (1 mg/mL) and directly infused into the LC-MS system. Analyses were done on an Agilent high performance liquid chromatograph (HPLC) 1260 Infinity Series (Agilent Technologies, Santa Clara, CA, USA) coupled to a quadrupole-time of flight (Q-TOF) mass spectrometer model G6540B (Agilent Technologies) with a Dual ESI source (Agilent Technologies). Samples were injected in 7 µL injection volumes and eluted at 100% of 0.1% formic acid in acetonitrile at a flow rate of 0.3 mL/min to the mass spectrometer. MS parameters were set using the Agilent MassHunter Data Acquisition Software, rev. B.05.01 (Agilent Technologies). The system operated in positive ion mode and MS spectra were recorded in *m/z* 50–1000 range as centroid spectra, with a speed of 3.3 spectra/s. The capillary was maintained at 2000 V, fragmentor voltage at 180 V, cone 1 (skimmer 1) at 45 V, Oct RFV at 750 V. Gas flow rate was set at 11 L/min, at 350 °C, and the nebulizer was set at 45 psig. A standard solution was infused by using an Isocratic pump (1260 Infinity Series, Agilent Technologies) in order to perform the real-time lock mass correction. The solution consisted of two reference mass compounds: purine ($C_5H_4N_4$ at *m/z* 121.050873, 10 µmol/L) and hexakis (1H,1H, 3H-tetrafluoropentoxy)-phosphazene ($C_{18}H_{18}O_6N_3P_3F_{24}$ at *m/z* 922.009798, 2 µmol/L). Flow rate was set at 0.06 mL/min, while the detection window and the minimum height were set at 1000 ppm and 10,000 counts, respectively, for reference mass correction.

Analyses of L1 culture filtrates were done on the Agilent system previously reported. Separations were performed on a Zorbax Eclips Plus C18 column, 4.6 x 100 mm, with 3.5 µm particles (Agilent Technologies). Analyses were done at a constant temperature of 37 °C and using a linear gradient system composed of A: 0.1% (*v/v*) formic acid in water, and B: 0.1% (*v/v*) formic acid in acetonitrile. The flow was 0.6 mL $min^{-1}$, 95% A graduating to 100% B in 6 min, 100% B 6–8 min, 95% A 8-10.

### *3.6. Potentiometric and Spectrophotometric Measurements*

The solutions tested ($TS_H$) had the following composition $TS_H$: $C_L$ M $H_2L$, $C_H$ M $HClO_4$, $C_{OH}$ M NaOH, (0.1–$C_H$) M $NaClO_4$/$CH_3OH$ 50:50 (*w*/*w*). The hydrogenionic concentration [$H^+$] was measured using the following cell:

$$RE \,/\, TS_H \,/\, GE$$

where GE represents the glass electrode, while RE is the composition reference cell: Ag $_{(S)}$/AgCl $_{(S)}$/0.1 M $NaClO_4$/$CH_3OH$ (50:50). The e.m.f. of the cell (A) at 25 ° C, results:

$$E_G = E_G^{0\prime} + 0.05916 \cdot log(h \cdot yH)$$

where $[H^+]$ = h, $E_G^{0\prime}$ is a constant in each titration, $y_H$ represents the activity coefficient of $H^+$ which is constant in the ionic medium used. $E_J$ is the liquid junction potential that is generated on contact between the solution 0.1 M $NaClO_4$ / $CH_3OH$ (50:50) and the measuring solution [32]. Putting:

$$E_G = E_G^{0\prime} + 0.05916 \cdot log(yH) + E_J$$

Equation (1) takes the form:

$$E_G = E_G^0 + 0.05916 \cdot log(h)$$

The experimental measurements were carried out in the form of both potentiometric and spectrophotometric titration. Each titration was divided into two parts: in the first, the constant $E_G^0$ was determined in a solution in the absence of harzianic acid and metal ion. In the second part, the harzianic acid and metal ion were added and the acidity of the solution was decreased by addition of a NaOH solution. After each addition, the e.m.f. of cell (A) is measured determining the hydrogenionic concentration h (and therefore the pH) and at the same time, the UV-VIS spectrum of the resulting solution is recorded. Hyperquad program (Protonic Software, Leeds, UK) [33] was used to process the experimental data obtained by potentiometric and spectrophotometric measurements.

## 4. Conclusions

In this paper production of harzianic acid by *T. pleuroticola* is reported for the first time. Considering the recent separation of this specie from *T. harzianum*, it would be interesting to evaluate if the ability to synthesize this tetramic acid occurs in other strains, and whether or not harzianic acid can be regarded as a chemotaxonomic marker of any species within the *T. harzianum* aggregate.

The bioactivities of acetylated tetramic acids are linked to their capacity to form complexes with ions and to their acidic properties. In general, studies conducted on these complexes, such as those concerning tenuazonic acid and cyclopiazonic acid [24] underrate the relevance of the formation conditions and of complex stabilities. Acylated tetramic acids are synthesized by hybrid polyketide synthase-nonribosomal peptide synthetase enzymes (PKS-NRPS; NRPS-PKS) and the properties of this class of compounds may explain their antibiotic activity [24,34]. Metal-chelating metabolites can inhibit virus-induced or microbial-induced enzymes in infected cells by coordinating with metals at their active sites with a significant pharmaceutical impact [24,35]. Moreover, agricultural applications have also been demonstrated in the capability of harzianic acid to cause Fe(III)-promoting plant growth due to the iron solubilization [21,23].

In the present work, physico-chemical properties of harzianic acid were investigated, such as pKa, chelating properties toward metals with relevant biological functions, and stability constants of the derived complexes. Our findings show the coordination capacity of harzianic acid toward Cu(II), Fe(II), Mn(II) and Zn(II) through the formation of neutral or charged complexes in metal(II)/harzianic acid ratio of 1:1 or 1:2 depending on the pH

conditions, as observed for Cu(II) and Fe(II), or in 1:2 ratio as observed for Mn(II) and Zn(II). In particular, the highest affinity constant is obtained for the coordination complex Cu(II)/harzianic acid 1:2 with log β 15.82.

**Supplementary Materials:** The following are available online, Figure S1: ITS sequence of *Trichoderma pleuroticola* L1, Table 1: NMR data of harzianic acid recorded in different solvents, Figure S2: LC-MS mass spectrum of harzianic acid, Figure S3: NMR spectrum of harzianic acid recorded in $CDCl_3$, Figure S4–S5: NMR spectra of harzianic acid recorded in $CD_3OD$, Figure S6: UV-VIS spectra for solutions of harzianic acid, Figure S7–S9: mass spectra ESIMS QTOF of harzianic acid in presence of metals, Figure S10–S11: NMR spectra of harzianic acid record in $CD_3OD/D_2O$, Figure S12: NMR spectra of harzianic acid in presence of metals.

**Author Contributions:** Conceptualization, F.V., M.I. and A.A.; methodology, G.D.T., M.DG., F.V., M.I., A.A..; investigation, G.D.T., MM.S., R.N., A.B., A.S. and A.A.; data curation, G.D.T., MM.S, M.DG., M.L., F.S., M.I. and A.A; writing—Original draft preparation, G.D.T., M.M.S.; writing—Review and editing, R.N., M.DG., F.V., F.S., M.I and A.A.; supervision M.I. and A.A.; project administration, F.V., M.I. and A.A.; funding acquisition, F.V., M.L., and A.A.

**Funding:** This work was supported by "The study was supported by MIURPON grant Marea 03PE_00106, POR FESR CAMPANIA 2014/2020- O.S. 1.1 grant Bioagro 559, MISE CRESO Protection n. F/050421/01-03/ X32, PSR Veneto 2014/2020 Misura 16–Tipologia di intervento 16.1–Azione 2 "Sostegno ai Progetti Operativi di Innovazione (POI)" - Divine n. 3589659, PSR Campania 2014/2020 Misura 16–Tipologia di intervento 16.1–Azione 2 "Sostegno ai Progetti Operativi di Innovazione (POI)"-Progetto "DI.O.N.IS.O.", C.U.P. B98H19005010009 and MIURPON grant Linfa 03PE_00026_1. and by "Financial support was provided by Ministero Italiano dell'Istruzione, dell'Università e della Ricerca (MIUR) through Finanziamento delle Attività Base della Ricerca (FFABR) 2017".

**Conflicts of Interest:** The authors declare no conflict of interest.

## References

1. Harman, G.E.; Howell, C.R.; Viterbo, A.; Chet, I.; Lorito, M. *Trichoderma* species—opportunistic, avirulent plant symbionts. *Nat. Rev. Microbiol*. **2004**, *2*, 43–56.
2. Vinale, F.; Sivasithamparam, K.; Ghisalberti, E.L.; Marra, R.; Woo, S.L.; Lorito, M. *Trichoderma*–plant–pathogen interactions. *Soil Biol. Biochem*. **2008**, *40*, 1–10.
3. Kredics, L.; Hatvani, L.; Naeimi, S.; Körmöczi, P.; Manczinger, L.; Vágvölgyi, C.; Druzhinina, I. Biodiversity of the genus *Hypocrea/Trichoderma* in different habitats. In *Biotechnology and Biology of Trichoderma*; Gupta, V.K., Schmoll, M., Herrera-Estrella, A., Upadhyay, R.S., Druzhinina, I., Tuohy, M.G., Eds.; Elsevier: Oxford, UK, 2014; pp. 3–24. ISBN: 978-0-444-59576-8.
4. Nicoletti, R.; Vinale, F. Bioactive compounds from marine-derived *Aspergillus*, *Penicillium*, *Talaromyces* and *Trichoderma* Species. *Mar. Drugs* **2018**, *16*, 408.
5. Reino, J.L.; Guerrero, R.F.; Hernández-Galán, R.; Collado, I.G. Secondary metabolites from species of the biocontrol agent *Trichoderma*. *Phytochem. Rev.* **2008**, *7*, 89–123.
6. Zeilinger, S.; Gruber, S.; Bansal, R.; Mukherjee, P.K. Secondary metabolism in *Trichoderma*–Chemistry meets genomics. *Fungal Biol. Rev.* **2016**, *30*, 74–90.
7. Marra, R.; Nicoletti, R.; Pagano, E.; DellaGreca, M.; Salvatore, M.M.; Borrelli, F.; Lombardi, N.; Vinale, F. Woo, S.L.; Andolfi, A. Inhibitory effect of trichodermanone C, a sorbicillinoid produced by *Trichoderma citrinoviride* associated to the green

alga *Cladophora* sp., on nitrite production in LPS-stimulated macrophages. *Nat. Prod. Res.* **2018**, *33*, 3389–3397.
8. Song, Y.P.; Miao, F.P.; Fang, S.T.; Yin, X.L.; Ji, N.Y. Halogenated and nonhalogenated metabolites from the marine-alga-endophytic fungus *Trichoderma asperellum* cf44-2. *Mar. Drugs* **2018**, *16*, 266.
9. Meng, J.; Cheng, W.; Heydari, H.; Wang, B.; Zhu, K.; Konuklugil, B.; Lin, W. Sorbicillinoid-based metabolites from a sponge-derived fungus *Trichoderma saturnisporum*. *Mar. Drugs* **2018**, *16*, 226.
10. Yamada, T.; Fujii, A.; Kikuchi, T. New diterpenes with a fused 6-5-6-6 ring system isolated from the marine sponge-derived fungus *Trichoderma harzianum*. *Mar. Drugs* **2019**, *17*, 480.
11. Salvatore, M.M.; Nicoletti, R.; DellaGreca, M.; Andolfi, A. Occurrence and properties of thiosilvatins. *Mar. Drugs* **2019**, *17*, 664.
12. Marfori, E.C.; Kajiyama, S.; Fukusaki, E.; Kobayashi, A. Trichosetin, a novel tetramic acid antibiotic produced in dual culture of *Trichoderma harzianum* and *Catharanthus roseus* callus. *Z. für Naturforschung C J. Biosci.* **2002**, *57*, 465–470.
13. Mo, X.; Li, Q.; Ju, J. Naturally occurring tetramic acid products: Isolation, structure elucidation and biological activity. *RSC Adv.* **2014**, *4*, 50566–50593.
14. Sawa, R.; Mori, Y.; Iinuma, H.; Naganawa, H.; Hamada, M.; Yoshida, S.; Furutani, H.; Kajimura, Y.; Fuwa, T.; Takeuchi, T. Harzianic acid, a new antimicrobial antibiotic from a fungus. *J. Antibiot.* **1994**, *47*, 731–732.
15. Kang, D.; Kim, J.; Choi, J.N.; Liu, K.H.; Lee, C.H. Chemotaxonomy of *Trichoderma* spp. using mass spectrometry-based metabolite profiling. *J. Microbiol. Biotechnol.* **2011**, *21*, 5–13.
16. Vinale, F.; Manganiello, G.; Nigro, M.; Mazzei, P.; Piccolo, A.; Pascale, A.; Ruocco, M.; Marra, R.; Lombardi, N.; Lanzuise, S.; et al. A novel fungal metabolite with beneficial properties for agricultural applications. *Molecules* **2014**, *19*, 9760–9772.
17. Kawada, M.; Yoshimoto, Y.; Kumagai, H.; Someno, T.; Momose, I.; Kawamura, N.; Isshiki, K.; Ikeda, D. PP2A inhibitors, harzianic acid and related compounds produced by fungus strain F-1531. *J. Antibiot.* **2004**, *57*, 235–237.
18. Vinale, F.; Nicoletti, R.; Borrelli, F.; Mangoni, A.; Parisi, O.A.; Marra, R.; Lombardi, N.; Lacatena, F.; Grauso, L.; Finizio, S.; et al. Co-culture of plant beneficial microbes as source of bioactive metabolites. *Sci. Rep.* **2017**, *7*, 14330.
19. Chaverri, P.; Branco-Rocha, F.; Jaklitsch, W.; Gazis, R.; Degenkolb, T.; Samuels, G.J. Systematics of the *Trichoderma harzianum* species complex and the re-identification of commercial biocontrol strains. *Mycologia* **2015**, *107*, 558–590.
20. Kubicek, C.P.; Steindorff, A.S.; Chenthamara, K.; Manganiello, G.; Henrissat, B.; Zhang, J.; Cai, F.; Kopchinkiy, A.G.; Kubicek, E.M.; Kuo, A.; et al. Evolution and comparative genomics of the most common *Trichoderma* species. *BMC Genom.* **2019**, *20*, 485.
21. Vinale, F.; Flematti, G.; Sivasithamparam, K.; Lorito, M.; Marra, R.; Skelton, B.W.; Ghisalberti, E.L. Harzianic acid, an antifungal and plant growth promoting metabolite from *Trichoderma harzianum*. *J. Nat. Prod.* **2009**, *72*, 2032–2035.
22. Healy, A.R.; Vinale, F.; Lorito, M.; Westwood, N.J. Total synthesis and biological evaluation of the tetramic acid based natural product harzianic acid and its stereoisomers. *Org. Lett.* **2015**, *17*, 692–695.
23. Vinale, F.; Nigro, M.; Sivasithamparam, K.; Flematti, G.; Ghisalberti, E.L.; Ruocco, M.; Varlese, R.; Marra, R.; Lanzuise, S.; Eid, A.; et al. Harzianic acid: A novel siderophore from *Trichoderma harzianum*. *FEMS Microbiol. Let.* **2013**, *347*, 123–129.

24. Zaghouani, M.; Nay, B. 3-Acylated tetramic and tetronic acids as natural metal binders: Myth or reality? *Nat. Prod. Rep.* **2016**, *33*, 540–548.
25. Hood, M.I.; Skaar, E.P. Nutritional immunity: Transition metals at the pathogen–host interface. *Nat. Rev. Microbiol.* **2012**, *10*, 525–537.
26. Błaszczyk, L.; Siwulski, M.; Sobieralski, K.; Frużyńska-Jóźwiak, D. Diversity of *Trichoderma* spp. causing *Pleurotus* green mould diseases in Central Europe. *Folia Microbiol.* **2013**, *58*, 325–333.
27. Park, M.S.; Bae, K.S.; Yu, S.H. Two new species of *Trichoderma* associated with green mold of oyster mushroom cultivation in Korea. *Mycobiology* **2006**, *34*, 111–113.
28. Korkmaz, M.N.; Ozdemir, S.C.; Uzel, A. Xylanase production from marine derived *Trichoderma pleuroticola* 08ÇK001 strain isolated from Mediterranean coastal sediments. *J. Basic Microbiol.* **2017**, *57*, 839–851.
29. McConnell, H. Effect of polar solvents on the absorption frequency of n→ π electronic transitions. *J. Chem. Phys.* **1952**, *20*, 700–704.
30. Banerjee, S.; Bhanja, S.K.; Chattopadhyay, P.K. Quantum chemical predictions of aqueous pKa values for OH groups of some α-hydroxycarboxylic acids based on ab initio and DFT calculations. *Comput. Theor. Chem.* **2018**, *1125*, 29–38.
31. Martell, A.E.; Hancock, R.D. *Metal Complexes in Aqueous Solutions, Modern Inorganic Chemistry*; Springer: New York, NY, USA, 1996. ISBN: 978-1-4899-1488-0.
32. Rochester, C.H. The ionic products of water and methanol in methanol–water mixtures. *J. Chem. Soc. Dalton Trans*. **1972**, *1*, 5–8.
33. Gans, P.; Sabatini, A.; Vacca, A. Investigation of equilibria in solution. Determination of equilibrium constants with the HYPERQUAD suite of programs. *Talanta* **1996**, *43*, 1739–1753.
34. Ghisalberti, E.L. Bioactive tetramic acid metabolites. In *Studies in Natural Products Chemistry*; Atta-ur R., Ed.; Elsevier: Oxford, UK; 2003; Volume 28, pp. 109–163.
35. Hutchinson, D.W. Metal chelators as potential antiviral agents. *Antivir. Res.* **1985**, *5*, 193–205.


**Sample Availability:** Samples of harzianic acid is available from the authors.

*Molecules* **2020**, *25*, 2147

*Supplementary material*

# Bivalent Metal-Chelating Properties of Harzianic Acid Produced by a Marine-derived Strain of *Trichoderma pleuroticola*

**Gaetano De Tommaso[1], Maria Michela Salvatore[1], Rosario Nicoletti[2,3], Marina DellaGreca[1], Francesco Vinale[4,5], Assunta Bottiglieri[3], Alessia Staropoli[3,5], Francesco Salvatore[1], Matteo Lorito[3], Mauro Iuliano [1*] and Anna Andolfi[1,*]**

TCTTTTCCCTCGCGTCGGCATCATTCGCCGCTCTGATTCTCCAGACACTTGTGCTAACCG
TCTCCTAGGGGTGCGTATTCCATGAATCCCCTTGAATGTGATCGATCGAACACAACACTG
ACTTGTTACAACAGCCACGTCGACTCCGGCAAGTCGACCACCGTGAGTTGCACCCCCTTC
TCTTGCTCCGGCATCAAGCGAGAGCGTTTGATGCCGGACATGTACTCTTTTGAACCCAGG
GCTGACCATTCATCATGTAGACTGGTCACTTGATCTACCAGTGCGGTGGTATCGATCGTC
GTACCATCGAGAAGTTCGAGAAGGTAAGCTTCAACTGATTTTCGCCTCAATTCTCCCTCC
ACATTCAATTGTGCCCGACGATTCTGCAGAGAATTTTCGTGTCGACAATTTTTCATCACC
CCGCTTTCCGTTACCCCTCCTTTGGCAGCGACGCAAATTTTTTGTGGCAGCCTTTTGGCT
TTGGTGGGGTTTCGTGTGCACCCCACTAGCTCACTGCTTTTTTCTGCTTCACTCTCCCAC
TGCCCAGTCATCATTCAACGTGCTCTGTGTCTCGCCATTCAGCGATGCTAACCACTTTTC
CATCAATAGGAAGCCGCCGAACTCGGCAAGGGTTCCTTCAAGTACGCTTGGGTTCTTGAC
AAGCTCAAGGCCGAGCGTGAGCGTGGTATCACCATCGACATTGCCCTGTGGAAGTTCGAG
ACTCCCAAGTACTATGTCACCGTCATTGGTATGTCTGCTCCATCATCTTGATGCAGGAAT
TGCGAGCTGGTGTTAACAGGTAATTCGCAGATGCTCCCGGCCACCGTGATTTCATCA

**Figure S1**. ITS sequence of *Trichoderma pleuroticola* L1.

**Table S1.** [1]H NMR data of harzianic acid recorded in different solvents.

| Position | $\delta_H$ (*J* in Hz) $CDCl_3$[1] | $\delta_H$ (*J* in Hz) $CD_3OD$[1] | $\delta_H$ (*J* in Hz) $CD_3OD/D_2O$ |
|---|---|---|---|
| 2 | 7.02 d 15.2 | 7.12 d 15.2 | 7.14-6.99 brs |
| 3 | 7.60-7.55 m | 7.58-7.52 brs | 7.68-7.46 brs |
| 4 | 6.41-6.38 m[2] | 6.44-6.38 m[2] | 6.58-6.32 brs[2] |
| 5 | 6.38-6.36 m[2] | 6.44-6.38 m[2] | 6.58-6.32 brs[2] |
| 6 | 2.29-2.21 m | 2.30-2.20 m | 2.30-2.17 brs |
| 7 | 1.51 sest 7.4 | 1.52 sept 7.4 | 1.53-1.51 m |
| 8 | 0.97 t 7.3 | 1.01-0.95 m[2] | 0.99 m[a] |
| 5’ | 3.65 brd 10.2 | 3.83 dd 8.6, 2.0 | 3.91-3.82 brs |
| 6’A | 2.50 brd 14.3 | 2.36 dd 14.6, 2.0 | 2.41-2.32 brs |
| 6’B | 1.93 dd 14.3, 10.2 | 2.00 m[2] | 2.12-1.96 br[2] |
| 8’ | 2.03 hept 6.8 | 2.05 m[2] | 2.12-1.96 brs[2] |
| 9’ | 1.00 d 6.8 | 1.01-0.95 m[2] | 0.99 m[2] |
| 10’ | 1.00 d 6.8 | 1.01-0.95 m[2] | 0.99 m[2] |
| 11’ | 3.00 s | 2.96 s | 2.96 s |

[1]Spectroscopic data are in accordance with those previously reported (Healy et al., 2015)

[2] Overlapping signals

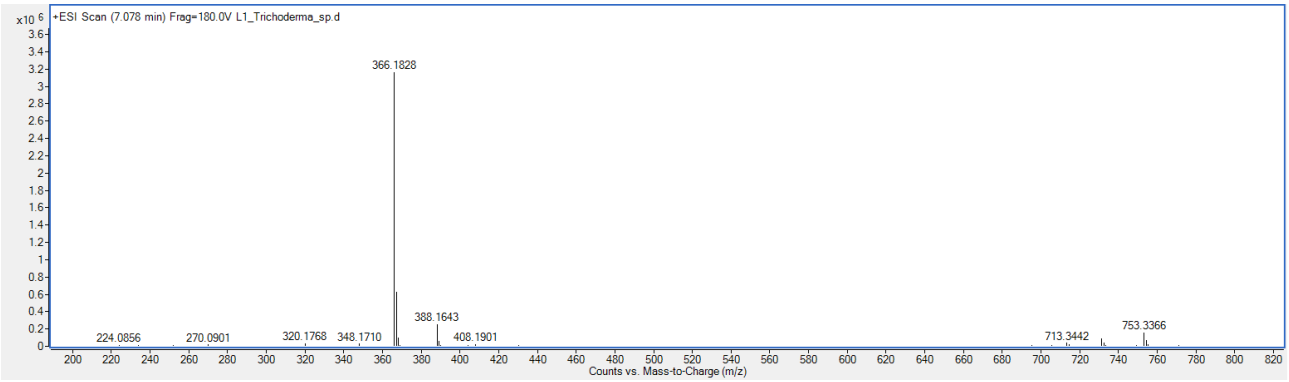


**Figure S2.** Harzianic acid mass spectrum obtained by LC-MS analysis in ESI positive mode.

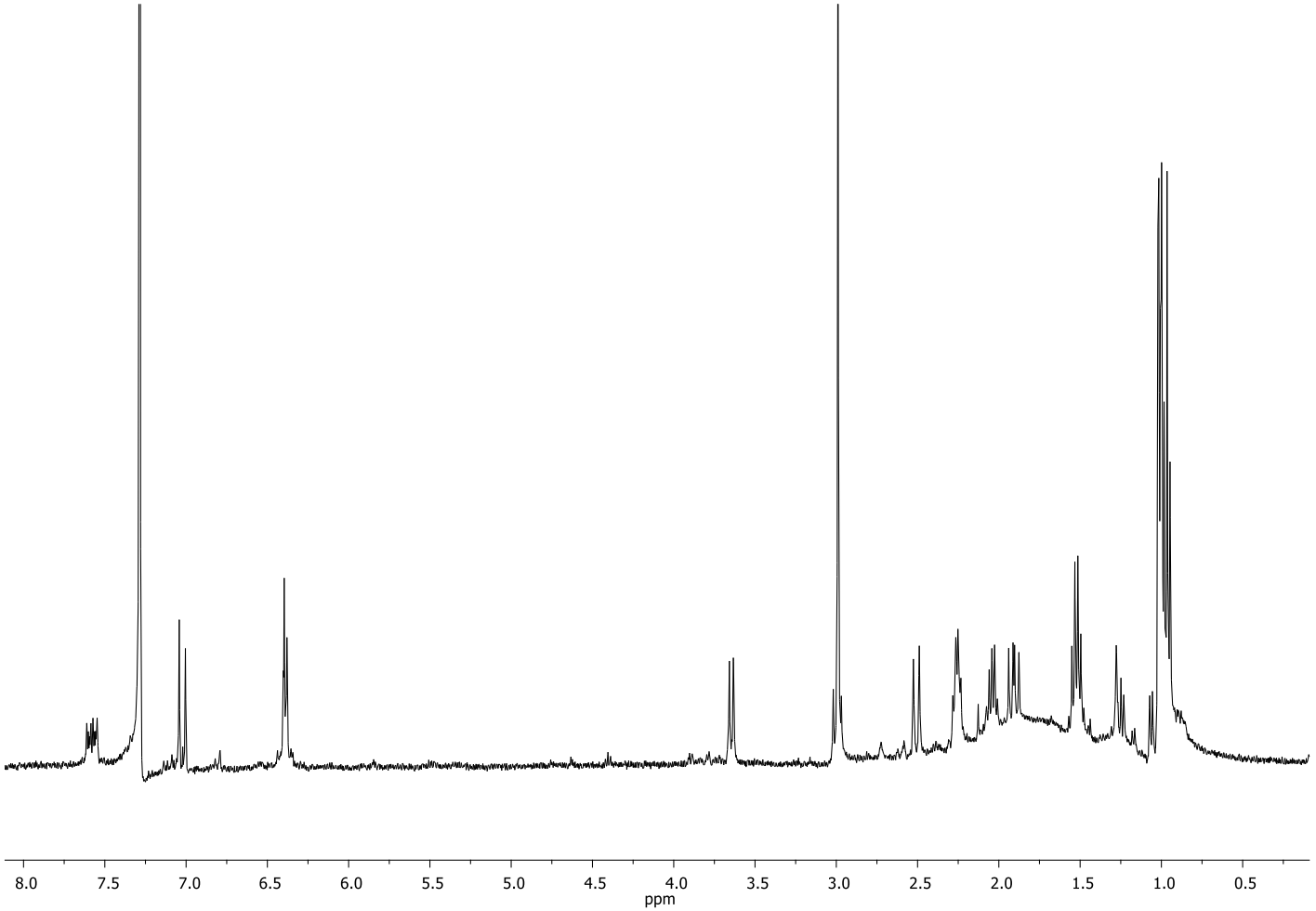


**Figure S3**. $^{1}$H NMR spectrum of harzianic acid recorded in $CDCl_3$ at 400 MHz

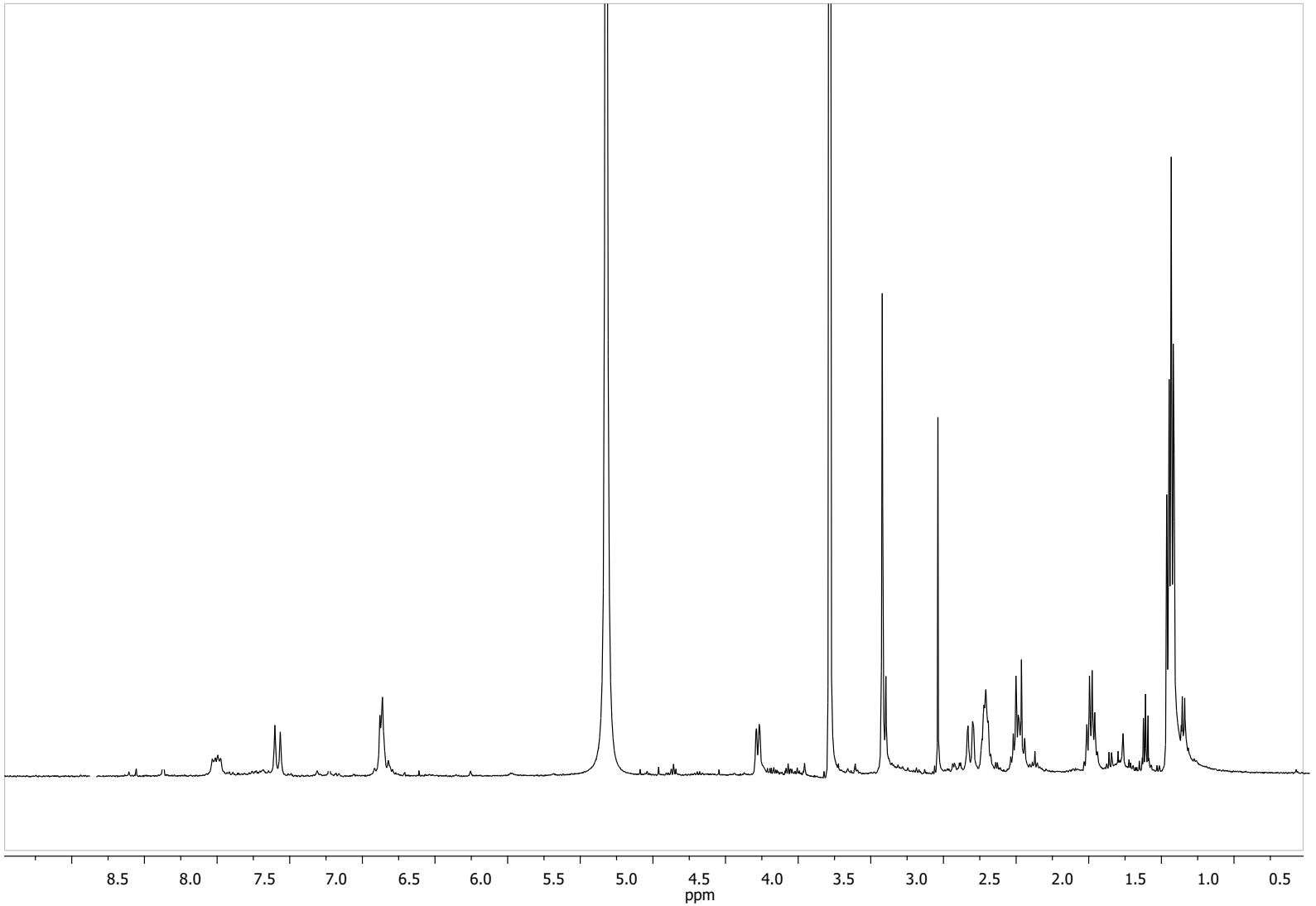


**Figure S4**. $^{1}$H NMR spectrum of harzianic acid recorded in $CD_3OD$ at 400 MHz

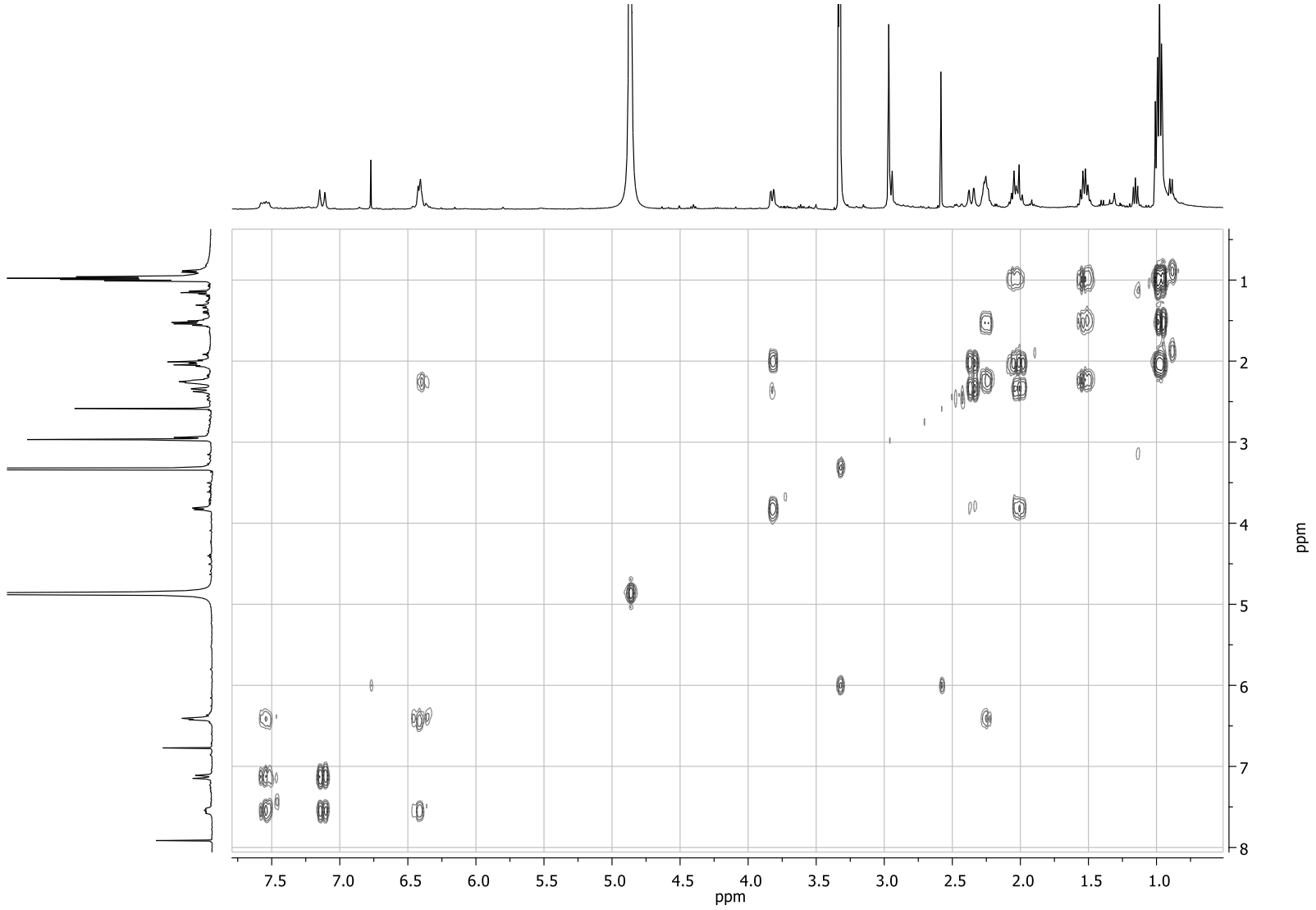


**Figure S5.** COSY spectrum of harzianic acid recorded in $CD_3OD$ at 400 MHz

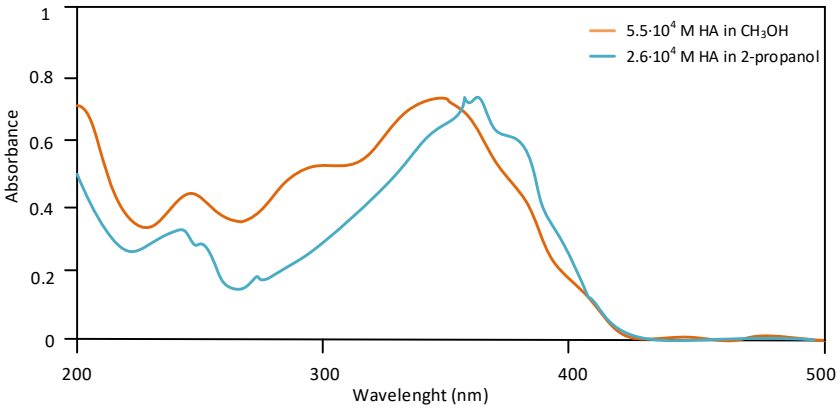


**Figure S6.** UV–Vis spectra for solutions: $5.5 \cdot 10^{-4}$ M harzianic acid in $CH_3OH$; $2.6 \cdot 10^{-4}$ M harzianic acid in 2–propanol (optical path 0.1 cm).

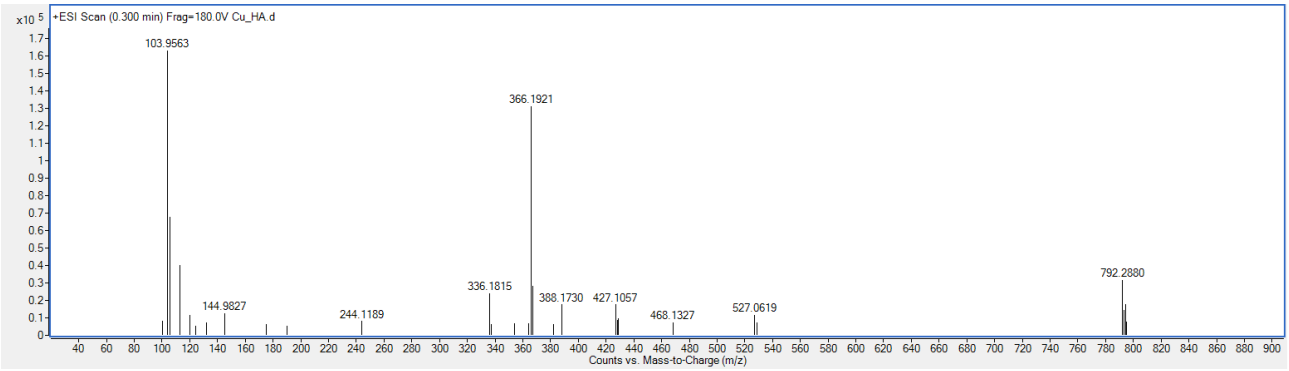


**Figure S7.** Mass spectrum ESIMS QTOF obtained by LC-MS analysis in ESI positive mode of a solution $1.0 \cdot 10^{-3}$ M of harzianic acid and $1.0 \cdot 10^{-3}$ M of $Cu(ClO_4)_2$ in MeOH/$H_2O$ 50:50 (*w/w*).

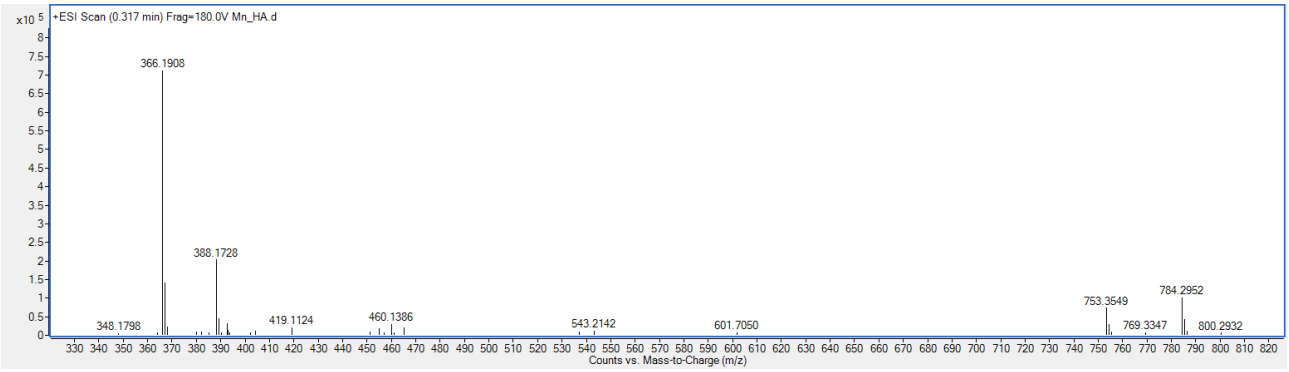


**Figure S8.** Mass spectrum ESIMS QTOF obtained by LC-MS analysis in ESI positive mode of a solution $1.0 \cdot 10^{-3}$ M of harzianic acid and $1.0 \cdot 10^{-3}$ M of $MnCl_2$ in MeOH/$H_2O$ 50:50 (*w/w*).

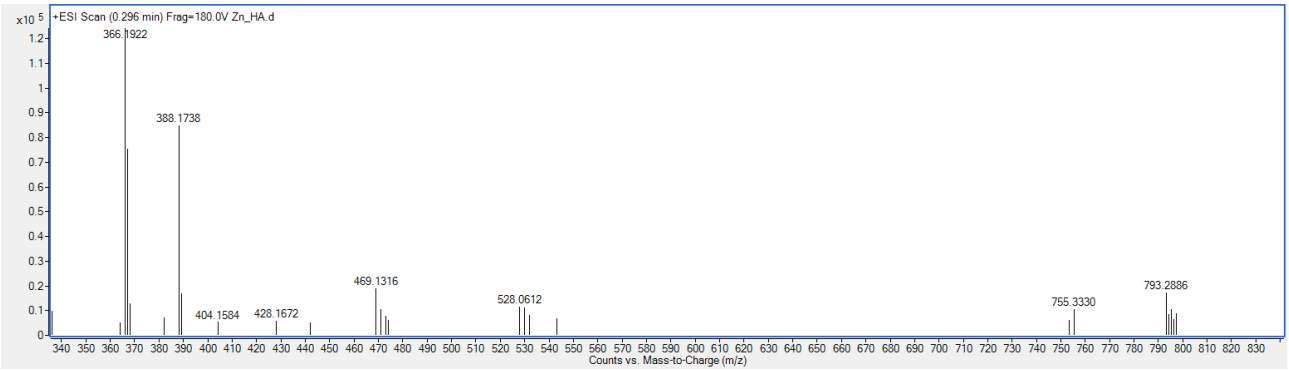


**Figure S9.** Mass spectrum ESIMS QTOF obtained by LC-MS analysis in ESI positive mode of a solution $1.0 \cdot 10^{-3}$ M of harzianic acid and $1.0 \cdot 10^{-3}$ M of $Zn(ClO_4)_2$ in MeOH/$H_2O$ 50:50 (*w/w*).

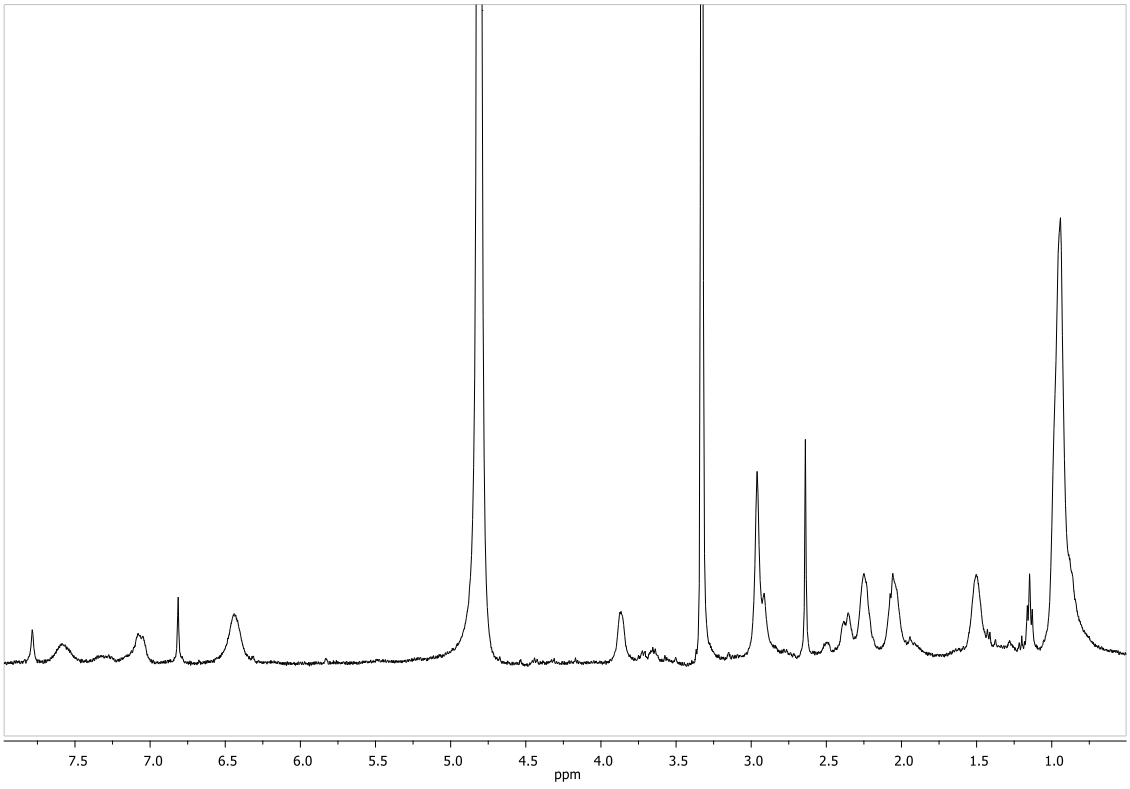


**Figure S10.** $^{1}$H NMR spectrum of harzianic acid recorded in $CD_3OD/D_2O$ (50:50 *w/w*) at 400 MHz

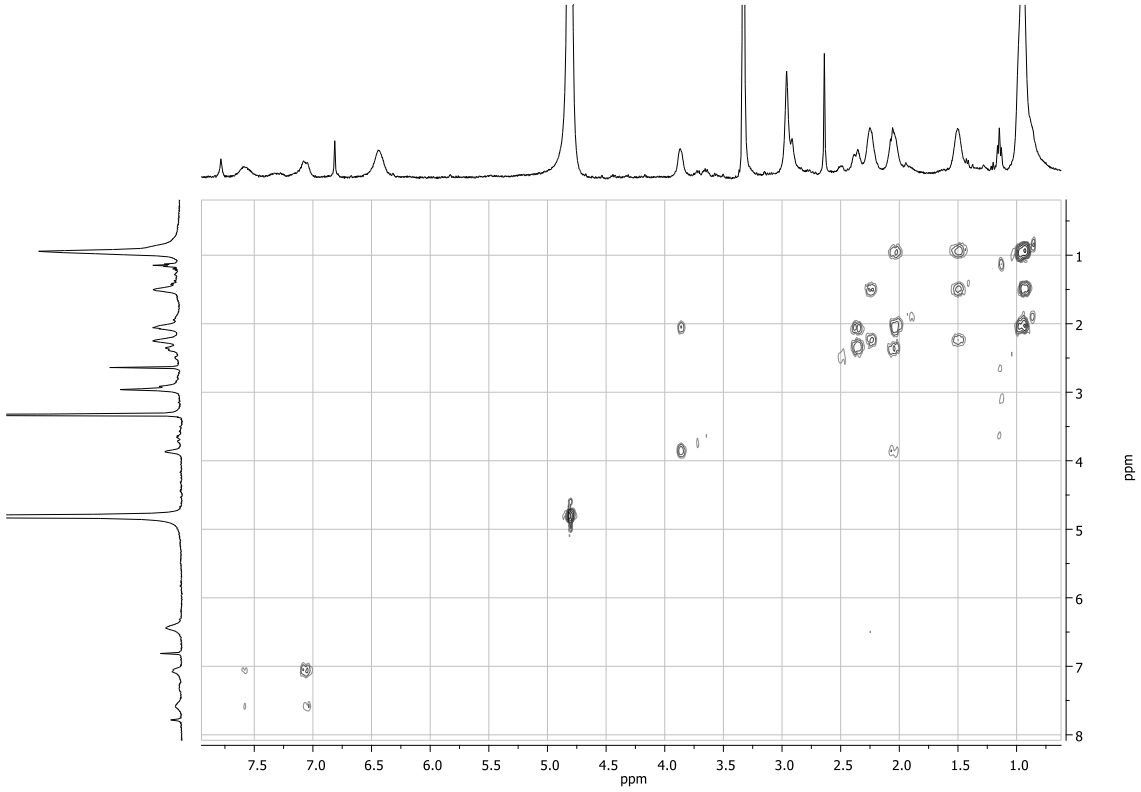


**Figure S11**. COSY spectrum of harzianic acid recorded in $CD_3OD/D_2O$ (50:50 *w/w*) at 400 MHz

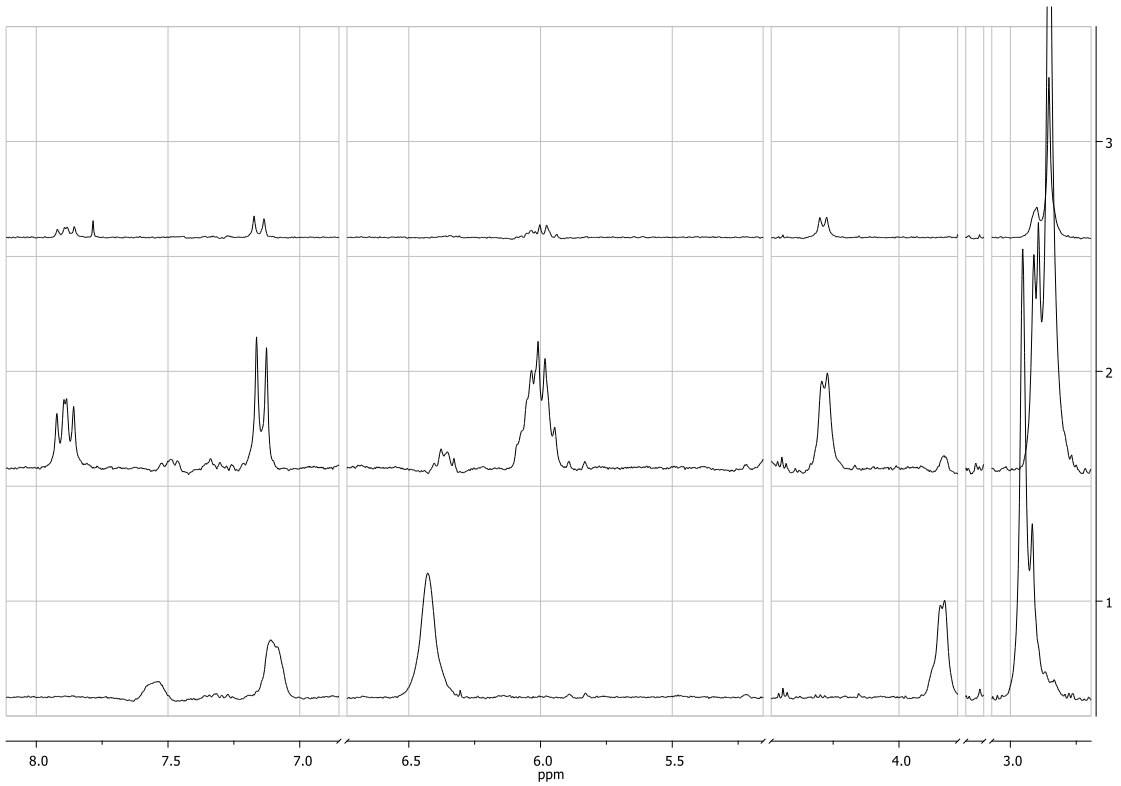


**Figure S12**. Detail of $^{1}$H NMR spectra of harzianic acid (down), $Zn^{2+}$-HA (middle) and $Mn^{2+}$-HA (up) recorded in $CD_3OD/D_2O$ (50:50 *w/w*) at 400 MHz. Solvent peak is removed.

toxics

MDPI

*Article*

# Coordination Properties of the Fungal Metabolite Harzianic Acid toward Toxic Heavy Metals

**Gaetano De Tommaso [1], Maria Michela Salvatore [1], Rosario Nicoletti [2,3], Marina DellaGreca [1], Francesco Vinale [4,5,6], Alessia Staropoli [3], Francesco Salvatore [1], Matteo Lorito [3], Mauro Iuliano [1,*] and Anna Andolfi [1,6,*]**

[1] Department of Chemical Sciences, University of Naples Federico II, 80126 Naples, Italy; gaetano.detommaso@unina.it (G.D.T.); mariamichela.salvatore@unina.it (M.M.S.); dellagre@unina.it (M.D.); frsalvat@unina.it (F.S.)
[2] Council for Agricultural Research and Economics, Research Centre for Olive, Fruit and Citrus Crops, 81100 Caserta, Italy; rosario.nicoletti@crea.gov.it
[3] Department of Agricultural Sciences, University of Naples Federico II, Portici 80055, Italy; alessia.staropoli@unina.it (A.S.); matteo.lorito@unina.it (M.L.)
[4] Department of Veterinary Medicine and Animal Productions, University of Naples Federico II, 80137, Italy; frvinale@unina.it
[5] Institute for Sustainable Plant Protection, National Research Council, 80055 Portici, Italy
[6] BAT Center—Interuniversity Center for Studies on Bioinspired Agro-Environmental Technology, University of Naples Federico II, 80055 Portici, Italy
* Correspondence: mauro.iuliano@unina.it (M.I.); andolfi@unina.it (A.A.); Tel.: +39-081-2539179 (A.A.)

**Abstract:** Some *Trichoderma* strains are known for their capacity to produce harzianic acid, a metabolite belonging to the tetramic acid derivatives. Harzianic acid has interesting biological properties, such as antimicrobial activities against phytopathogenic fungi and promotion of plant growth. It also possesses remarkable chemical properties, including the chelating properties toward essential transition metals, which might be related to the biological activities. Increasing knowledge on chelating properties might be relevant for understanding the various beneficial effects of harzianic acid in the interaction between the producer fungi and plants. In this work, the coordination capacity of harzianic acid was studied to evaluate the formation and stability of complexes formed with toxic heavy metals (i.e., $Cd^{2+}$, $Co^{2+}$, $Ni^{2+}$, and $Pb^{2+}$), which might have a crucial role in the tolerance of plants growing in metal-contaminated soils and in abiotic stress.

**Keywords:** *Trichoderma*; secondary metabolites; abiotic stress; metal-chelating properties

## 1. Introduction

Heavy metals are present in different concentrations in many rocks and soils, but the major sources of these elements are anthropogenic activities, including industrial emissions and agricultural treatments [3]. Some heavy metals are essential elements for physiological functions, e.g., iron (Fe), copper (Cu), zinc (Zn), and manganese (Mn), while many of them are commonly considered as toxic elements to plants and humans, e.g., lead (Pb), cobalt (Co), cadmium (Cd), nickel (Ni), chromium (Cr), mercury (Hg) [4]. There is ample literature on the acute and/or chronic toxic effects of these heavy metals for plants and animals [5–7]. For instance, in humans, nickel can have an impact on the immune, respiratory, nervous, and reproductive systems [8]; cobalt is mainly responsible for neurological, cardiovascular, and endocrine deficits [9]. Cadmium intoxication can lead to kidney, bone, and pulmonary damages [10]. Finally, lead exposure can

cause an increase of oxidative stress, producing various deleterious effects on the hematopoietic, renal, reproductive, and central nervous systems [11].

Rapid industrialization and urbanization have caused environmental contamination and pollution by toxic heavy metals, and their concentrations above threshold levels (which are defined by national guidelines) can have negative effects on the ecological health and fertility of soils due to their bioaccumulation [12]. Bioavailability of heavy metals is mainly affected by their total content in soil and by the presence of microbial and plant species [13]. In this respect, fungi can contribute to increase the tolerance of plants growing in metal-contaminated soils, and the production of metal-chelating compounds has been demonstrated in some fungi, such as *Pleurotus ostreatus* [14], *Beauveria caledonica* [15], and *Aspergillus niger* [16]. In fact, organic acids may affect potentially toxic metals desorption, solubility, and mobility through the formation of complexes [17,18]. The most frequent fungal organic acids involved in the complexation of heavy metals in soils are oxalic, succinic, tartaric, and citric acids, which have the valuable capacity to remove heavy metals without destroying the soil matrix [19,20]. Moreover, several fungal genera (e.g., *Saccharomyces*, *Aspergillus,* and *Penicillium* [21]) produce a wide range of siderophores, which have strong affinity for ferric ion, but despite their preference for iron, they can chelate numerous metals (e.g., aluminum, cadmium, cobalt, silver, copper) with diverse affinity, having an impact on the transport and tolerance of these metal ions [22,23]. Hence, the heavy metals chelation by organic acids may represent an important detoxification mechanism, both by the fungi and plants [24], but it is dependent upon metals, ligands, and environmental conditions [25].

Beneficial microbes belonging to the genus *Trichoderma* are model organisms to study plant-microbe interactions, and some selected strains are present as active ingredients in bioformulations for agriculture [26,27]. Methods for remediating polluted soils or water, and for removing toxic substances using *Trichoderma* spp. in plant-microbes systems have been proposed [28]. These microbes are known to control plant pathogens and improve plant growth, also due to the production of a remarkable range of secondary metabolites showing different biological activities [27–35].

One of these effector metabolites is harzianic acid, a natural compound with notable biological activities and interesting chemical properties, including affinity to ferric iron, antimicrobial activity (e.g., *Staphylococcus pseudintermedius*, *Pythium irregulare*, *Sclerotinia sclerotiorum,* and *Rhizoctonia solani*) and promotion of plant growth (e.g., tomato) [36–39]. It has been recently obtained by total synthesis [40], and classified in the subgroup of the dienoyl tetramic acids [41].

In this work, the capacity of harzianic acid, obtained from cultures of a marine-derived strain of *Trichoderma pleuroticola* [42], to complex some dipositive toxic heavy metals (i.e., $Cd^{2+}$, $Co^{2+}$, $Ni^{2+}$ and $Pb^{2+}$), was studied. Several techniques have been used (i.e., mass spectrometry (MS), circular dichroism (CD) spectrometry, nuclear magnetic resonance (NMR), Fourier transform-infrared spectroscopy (FT-IR)) either to demonstrate qualitatively the capacity of harzianic acid to complex the targeted cations or to obtain clues on the coordination mode, although the stoichiometry and formation constants of complex species, in a $CH_3OH$/0.1 M $NaClO_4$ (50:50 *w/w*) mixed solvent at 25 °C, were ultimately obtained from UV-VIS spectrophotometric data collected in a wide pH and spectral range.

## 2. Materials and Methods

### *2.1. Reagents and Their Analysis*

Analytical grade products $Pb(ClO_4)_2$, $Cd(ClO_4)_2$, $CoCl_2$, and $NiCl_2$ Merck (Darmstadt, Germany) were used to prepare stock aqueous solutions of metals whose concentrations were determined by complexometric titration with a standard solution of EDTA. Solutions of perchloric acid were prepared from analytical grade products and standardized potentiometrically (glass electrode) against tris(hydroxymethyl)amino methane

(Sigma-Aldrich, Saint Louis, MO, USA). The results agreed to within 0.1% or better. Carbonate-free NaOH and $NaClO_4$ solutions were prepared as previously described [42].

Harzianic acid was isolated as product of *Trichoderma pleuroticola* L1 recovered from a specimen of the mollusk *Melarhaphe neritoides* (Gastropoda, Littorinidae) collected along the coastline of the isle of Procida, Bay of Naples, Italy. The isolation and identification of this compound were previously explained in details [42]. Briefly, culture filtrate of *T. pleuroticola* was exhaustively extracted in acid conditions with ethyl acetate. The residue obtained was dissolved in chloroform and extracted with a saturated solution of $NaHCO_3$. The aqueous phase was acidified and extracted with ethyl acetate to obtain a residue identified as harzianic acid, comparing the NMR data with previous reports [40].

### *2.2. Preparation of Test Solutions, Potentiometric, UV-VIS, CD, NMR, and IR Measurements*

Test Solutions (TS), for CD and UV-VIS spectrometry, were prepared in an air-bath thermostat kept at (25.00 ± 0.05) °C by the procedure described in section 3.

Potential of cell $-\mathrm{RE/TS/GE}+$, which serves to evaluate the pH (= $-\log[H^+]$) of Test Solutions for UV-VIS and CD spectrometric measurements, was measured at 25.0 °C with a precision of ± 0.01 mV using a Keithley 642 type Digital Electrometer (Tektronix Inc., Beaverton, OR, USA). The pH indicator glass electrodes (GE) were Metrohm (Herisau, Switzerland) of 60102-100 type and an Ag/AgCl(s)/0.1 M NaCl/(0.1 M $NaClO_4/CH_3OH$, 50/50 *w/w*) electrode was utilized as reference (RE).

UV-VIS spectra were recorded by Cary model 5000 Spectrophotometer by Varian C. (Palo Alto, CA, USA), from 200 to 600 nm (optical path 0.2 cm) at 25.0 °C, under a constant flow of nitrogen.

The far UV-CD spectra were recorded with a JASCO CD spectrometer model J-715 (Tokyo, Japan), from 200 to 600 nm (optical path 0.2 cm) at 25.0 ° C, under a constant flow of nitrogen.

NMR spectra were recorded at 400 MHz in $CD_3OD/D_2O$ 1:1 (*w/w*) on a Bruker spectrometer (Ascend$^{TM}$400) (Bremen, Germany). The solvent was used as internal standard.

FT-IR spectra were recorded in modality attenuated total reflectance (ATR) with model Nicolet 5700 by Thermo Electric Corporation (Waltham, MA, USA). The measuring cell consisted of a mono crystal of zinc selenide. The blank was recorded using air as reference. The solid compounds, metal-harzianic acid, were prepared by mixing and evaporating equimolar solutions of the individual components.

### *2.3. HPLC-MS Analyses*

HPLC-MS analyses were done with the methods described by [42] on an Agilent high performance liquid chromatograph (HPLC) 1260 Infinity Series (Agilent Technologies, Santa Clara, CA, USA) coupled to a quadrupole-time of flight (Q-TOF) mass spectrometer model G6540B (Agilent Technologies) with a Dual ESI source (Agilent Technologies). Briefly, 500 µL of a 2 mM solution (in water) of each metal ($Cd(ClO_4)_2$, $CoCl_2$, $NiCl_2$ and $Pb(ClO_4)_2$) were mixed with 500 µL of harzianic acid (solubilized in methanol, 1 $mg \cdot mL^{-1}$) and directly infused into the LC-MS system (7 µL injection volumes, eluted with 0.1% formic acid in acetonitrile at a flow rate of 0.3 $mL \cdot min^{-1}$ to the mass spectrometer). The system was operated in positive ion mode and a standard solution of purine and hexakis(1H,1H,3H-tetrafluoropentoxy)-phosphazene was infused to obtain the real-time lock mass correction. All parameters and acquisitions were set using the Agilent MassHunter Data Acquisition Software, rev. B.05.01 (Agilent Technologies).

## 3. Results and Discussion

Since harzianic acid is a diprotic acid, in the following text we use the abbreviation $H_2L$, which represents the fully protonated species. Dissociation of protons by $H_2L$

produces in sequence $HL^-$ and $L^{2-}$, according to the dissociation constants exposed in Figure 1 [42]. In addition, when appropriate, the symbol $M^{2+}$ will be used to generically represent the dipositive metal cations investigated in this study, i.e., $Cd^{2+}$, $Co^{2+}$, $Ni^{2+}$, and $Pb^{2+}$.

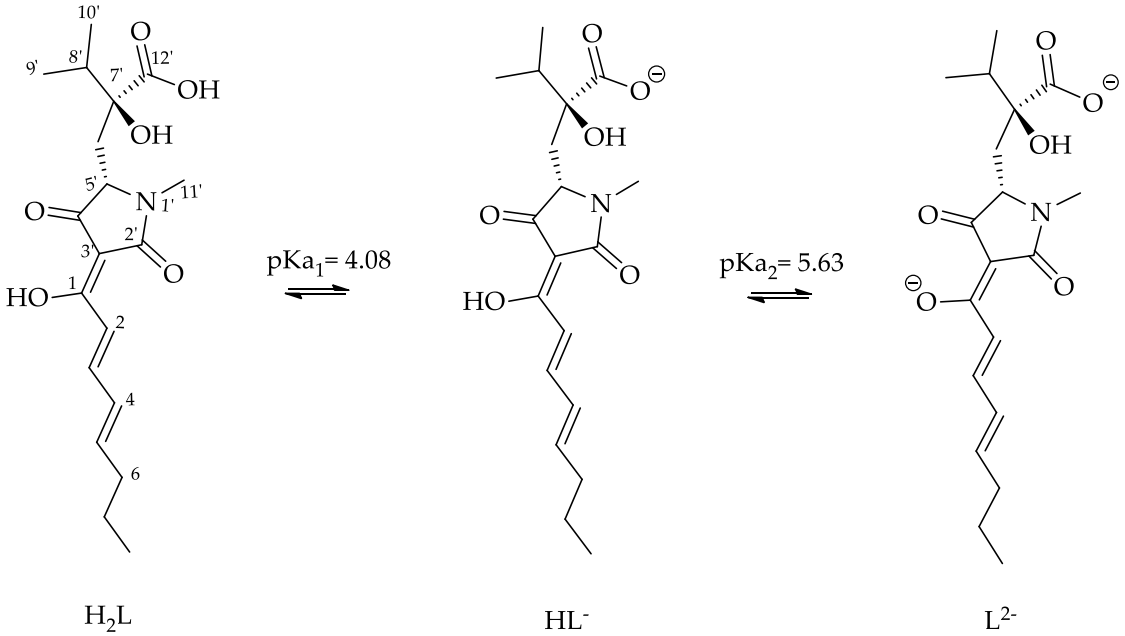


**Figure 1.** Structures of harzianic acid ($H_2L$) and its acid dissociation products ($HL^-$ and $L^{2-}$). Reported dissociation constants of harzianic acid have been separately determined at 25 °C in the mixed solvent $CH_3OH$/0.1 M $NaClO_4$ (50:50 *w/w*), which is the solvent employed in this study.

A rather unconventional approach has been used in this study to investigate the capacity of harzianic acid to complex bivalent heavy metal cations, $M^{2+}$. In fact, in order to obtain clues on the formation and stoichiometry of complexes eventually present in solutions of the metal cations and harzianic acid, we first collected LC-ESI-HRMS of solutions of harzianic acid in the presence, respectively, of $Cd^{2+}$, $Co^{2+}$, $Ni^{2+}$, and $Pb^{2+}$.

To this aim, solutions of each $M^{2+}$ cation and harzianic acid were prepared by mixing 500 µL of 2 mM solution of each metal cation in water (prepared by dissolving $Cd(ClO_4)_2$, $CoCl_2$, $NiCl_2$, and $Pb(ClO_4)_2$, respectively) with 500 µL of 1 $mg \cdot ml^{-1}$ harzianic acid in methanol. Finally, 7 µL of each solution were directly infused into the LC-MS system operated in the positive ion mode.

The most abundant ions in MS of each solution (Figures S1–S4) are reported in Table 1. From Table 1, it can be seen that, in the collected MS, a well-developed MS peak can be detected whose accurate mass corresponds to the composition $[H_3L_2 + Metal]^+$. Furthermore, in the case of $Pb^{2+}$, a complex ion of composition $[HL + Pb]^+$ was also detected.

**Table 1.** Characterization of $M^{2+}$- harzianic acid complexes by LC-MS. $H_2L$ represents the full protonated harzianic acid molecule, $C_{19}H_{27}NO_6$.

| Ion | Experimental Mass | Formula | Exact Mass |
|---|---|---|---|
| | Harzianic Acid + $Cd(ClO_4)_2$ | | |
| $[H_2L + H]^+$ | 366.1915 | $C_{19}H_{28}NO_6$ | 366.1917 |
| $[H_2L + Cd + ClO_4]^+$ | 578.0335 | $C_{19}H_{27}NO_{10}CdCl$ | 578.0331 |
| $[2H_2L - H + Cd]^+$ | 843.2624 | $C_{38}H_{53}N_2O_{12}Cd$ | 843.2632 |
| | Harzianic Acid + $CoCl_2$ | | |
| $[H_2L + H]^+$ | 366.1913 | $C_{19}H_{28}NO_6$ | 366.1917 |

| | | | |
|---|---|---|---|
| $[H_2L + Na]^+$ | 388.1721 | $C_{19}H_{27}NO_6Na$ | 388.1736 |
| $[2H_2L - H + Co]^+$ | 788.2910 | $C_{38}H_{53}N_2O_{12}Co$ | 788.2931 |
| Harzianic Acid + $NiCl_2$ | | | |
| $[H_2L + H]^+$ | 366.1910 | $C_{19}H_{28}NO_6$ | 366.1917 |
| $[H_2L + Na]^+$ | 388.1762 | $C_{19}H_{27}NO_6Na$ | 388.1736 |
| $[2H_2L - H + Ni]^+$ | 787.2938 | $C_{38}H_{53}N_2O_{12}Ni$ | 787.2952 |
| Harzianic acid + $Pb(ClO_4)_2$ | | | |
| $[H_2L + H]^+$ | 366.1912 | $C_{19}H_{28}NO_6$ | 366.1917 |
| $[H_2L - H + Pb]^+$ | 572.1507 | $C_{19}H_{26}NO_6Pb$ | 572.1526 |
| $[2H_2L - H + Pb]^+$ | 937.3326 | $C_{38}H_{53}N_2O_{12}Pb$ | 937.3365 |

Based on our experience, MS data in Table 1 represent a conspicuous indication that complex species of the same or different stoichiometry may exist in solution.

In order to provide evidence for complex formation taking place in solution between targeted $M^{2+}$ cations and harzianic acid, and to eventually ascertain their stoichiometry and evaluate their formation constants, circular dichroism (CD) and UV-VIS spectra of solutions of the $M^{2+}$ cations and harzianic acid were acquired in a wide pH and spectral range.

Because of the low solubility of harzianic acid in water, $CH_3OH$/0.1 M $NaClO_4$ (50:50 *w/w*) was employed as solvent. The constant concentration of $NaClO_4$ in the solvent is high enough, with respect to the reagent concentrations employed in this study, to provide a constant ionic strength in all of the investigated solutions. So much so that activity coefficients of reagents and products of complex formation reactions can be considered constant, and equilibrium constants can be expressed using concentrations in place of activities. In this context, the standard symbol pH merely indicates the molar concentration of solvated protons into the tested solutions (i.e., briefly, $pH = -\log[H^+]$).

Preparation of test solutions (TS), of accurately known pH and analytical composition, of each metal cation and harzianic acid, was performed at 25.0 °C, in a potentiometric multi-neck titration cell equipped with an Ag/AgCl(s)/0.1 M NaCl/(0.1 M $NaClO_4$-$CH_3OH$, 50/50 *w/w*) double junction reference electrode (RE) and a pH indicator glass electrode (GE) (Scheme 1).

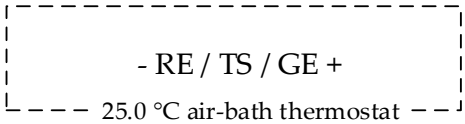


(G)

**Scheme 1.** Sketch of the potentiometric apparatus employed to prepare test solutions, TS, of accurately known pH and analytical composition. RE represents the double junction Ag/AgCl(s)/0.1 M NaCl/(0.1 M $NaClO_4$-$CH_3OH$, 50/50 *w/w*) reference electrode and GE a pH indicator glass electrode

Because of the large concentration of $NaClO_4$ in the salt bridge of the double junction reference electrode and in the test solution, TS, the potential of cell (G) can be expressed, at 25 °C, by the simple equation (1), in which $E_G^0$(volt) is a constant that was determined before each experiment by ad hoc potentiometric measurements.

$$E_G = E_G^0 + 0.05916 \cdot \log[H^+] \quad (1)$$

In fact, in order to assess the value of $E_G^0$, each experiment started with a measured volume of pure solvent (i.e., $CH_3OH$/0.1 M $NaClO_4$ (50:50 *w/w*)) in the titration vessel. The potential, $E_G$ (volt) of cell (G) was measured after stepwise addition of measured volumes of a standard solution of $HClO_4$ in the same solvent, and the collected data were employed to evaluate $E_G^0$. After this initial glass electrode calibration procedure, pH (=

$-\log[H^+]$) of any test solution in the potentiometric vessel can be evaluated from the measured potential, $E_G$ (volt) of cell (G), at 25.0 °C, using the simple equation (2):

$$\mathrm{p\,H} = -\log[H^+] = \frac{E_G^0 - E_G}{0.05916} \quad (2)$$

Subsequently, to the acidic solution in the titration vessel of cell (G), measured volumes of stock solutions of the metal cation and of harzianic acid were added so that the solution in the potentiometric vessel assumed the general composition specified by the analytical array (3).

$$\{C_{H_2L}^0\ \mathrm{M}\ H_2L + C_M^0\ \mathrm{M}\ M(ClO_4)_2 + C_H^0\ \mathrm{M}\ HClO_4\} \quad (3)$$

Then, the resulting solution (whose pH was accurately known), was sampled by withdrawing an accurately measured volume, which was transferred to the spectrometer cuvette (0.2 cm optical path) and processed at 25 °C.

After this, the pH of the solution in the titration vessel of cell (G) was systematically modified by successive additions of small volumes of a standard solution of NaOH, in the solvent $CH_3OH$/0.1 M $NaClO_4$, so that it assumed the general analytical composition specified by the analytical array (4), which could be accurately calculated from the preparation data.

$$\{C_{H_2L}\ \mathrm{M}\ H_2L + C_M\ \mathrm{M}\ M(ClO_4)_2 + C_H\ \mathrm{M}\ HClO_4 + C_{NaOH}\ \mathrm{M}\ NaOH\} \quad (4)$$

After each addition of NaOH, samples of the solution, whose pH could be obtained from equation (2), were withdrawn from the titration vessel, transferred to the spectrometer cuvette and processed at 25 °C.

Obviously, all of the successive solutions prepared by this procedure share the same ligand to metal ratio, which keeps equal to the initial ratio $C_{H_2L}^0/C_M^0$, while the metal cation and harzianic acid concentrations, $C_{H_2L}$ and $C_M$, respectively, in the withdrawn samples, decrease as their pH increases.

The acquired CD spectra are exposed in Figure 2.

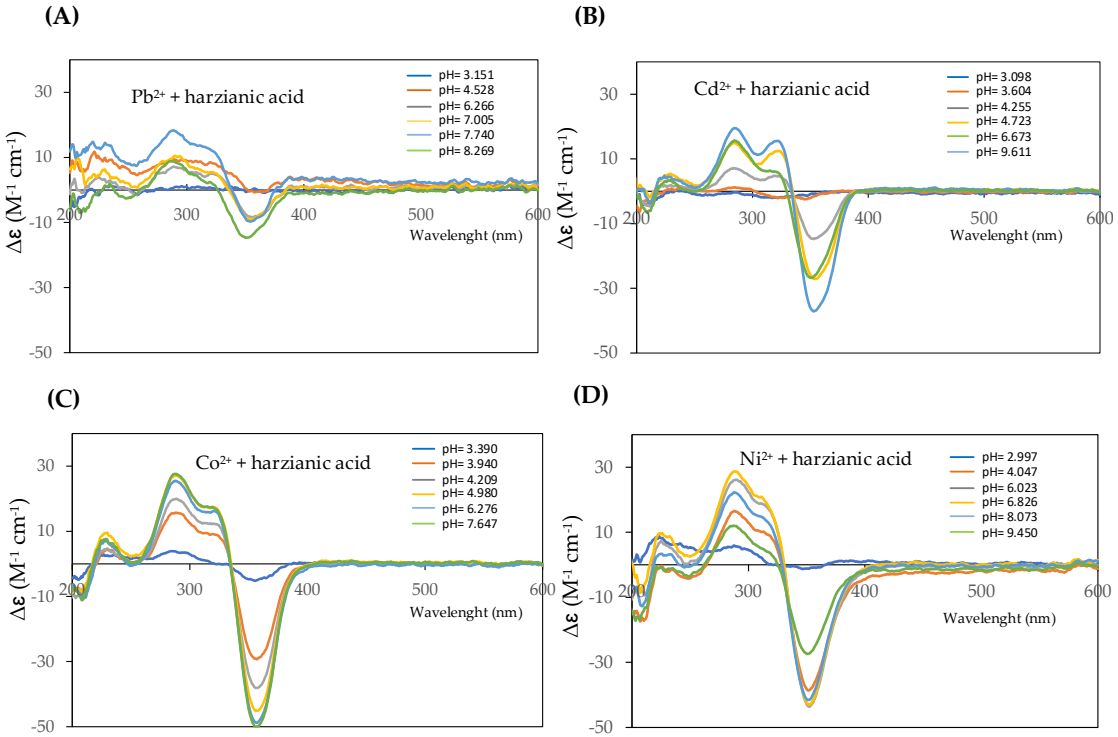

**Figure 2.** Far–UV circular dichroism (CD) spectra (optical path 0.2 cm) in $CH_3OH$/0.1 M $NaClO_4$ (50:50 *w/w*) at different pH values: (**A**) $C^0_{Pb}$ = 5.4 × $10^{-5}$ M $Pb(ClO_4)_2$ and $C^0_{H_2L}$ = 1.1 × $10^{-4}$ M; (**B**) $C^0_{Cd}$ = 1.4·$10^{-4}$ M $Cd(ClO_4)_2$ and $C^0_{H_2L}$ = 2.6 × $10^{-4}$ M; (**C**) $C^0_{Co}$ = 6.9 × $10^{-5}$ M $CoCl_2$ and $C^0_{H_2L}$= 1.4 × $10^{-4}$ M; (**D**) $C^0_{Ni}$ = 1.1·$10^{-4}$ M $NiCl_2$ and $C^0_{H_2L}$ = 2.1 × $10^{-4}$ M. $H_2L$ = harzianic acid.

Inspection of CD spectra shows the presence of two peaks whose intensity increases by increasing pH. One positive peak at 285 nm (Cotton effect) is attributed to transitions involving the diene system orbitals, and the second negative peak at 350 nm is associated to transitions that involve the non-bonding electrons of oxygen in C4' position of harzianic acid [42].

Qualitatively, similar effects are also observed in solutions of only harzianic acid, but the dependence of CD spectra on the specific metal cation undoubtedly points toward specific interactions between $M^{2+}$ cations and the ligand.

Next, UV-VIS spectrophotometric data, used for the evaluation of the stoichiometry of complexes and of their formation constants, were collected.

For each metal, two spectrophotometric datasets were acquired, by fine-tuning the initial addition of the harzianic acid and metal cation stock solutions, to the acidified solvent in cell (G), so that $C^0_{H_2L}$ = 2.0 × $10^{-4}$ M and $C^0_M$ = 2.0 × $10^{-4}$ M (i.e., 1:1 ligand to metal ratio) or $C^0_{H_2L}$ = 2.0 × $10^{-4}$ M and $C^0_M$ = 4.0 × $10^{-4}$ (i.e., 1:2 ligand to metal ratio).

The full set of spectrophotometric data collected is shown in Figure 3 ($M^{2+}$ = $Cd^{2+}$), Figure 4 ($M^{2+}$ = $Co^{2+}$), Figure 5 ($M^{2+}$ = $Ni^{2+}$) and Figure 6 ($M^{2+}$ = $Pb^{2+}$), and represents the basis of successive evaluations.

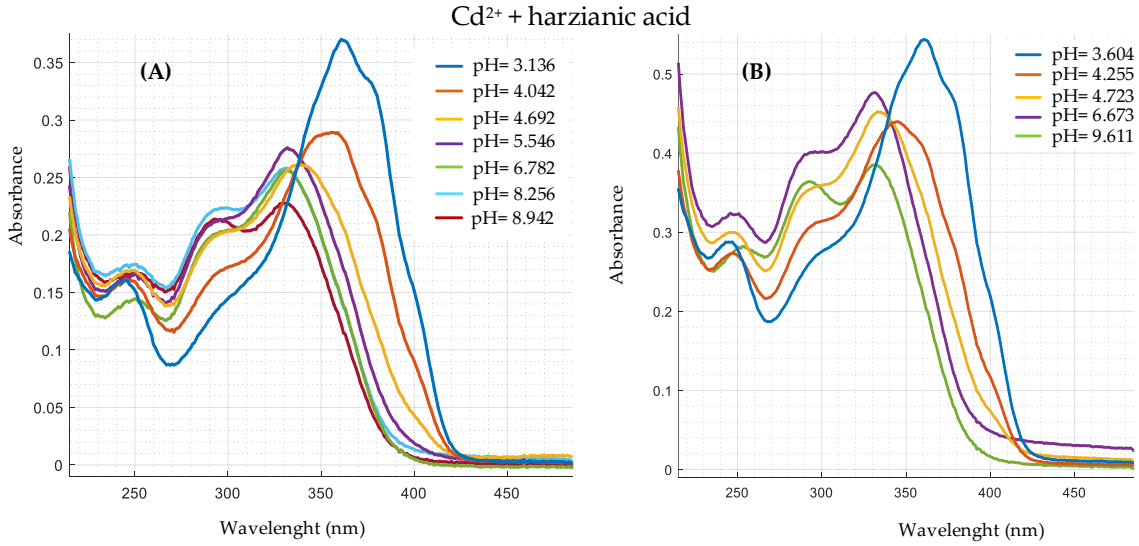


**Figure 3.** UV-VIS spectra in $CH_3OH$/0.1 M $NaClO_4$ (50:50 *w/w*) at different pH of: (**A**) $C^0_{H_2L}$ = 2.0 × $10^{-4}$ M and $C^0_{Cd}$ = 2.0 × $10^{-4}$ $Cd(ClO_4)_2$ (ligand to metal ratio 1:1); (**B**) $C^0_{H_2L}$ = 2.0 × $10^{-4}$ M and $C^0_{Cd}$ = 4.0 × $10^{-4}$ $Cd(ClO_4)_2$ (ligand to metal ratio 1:2).

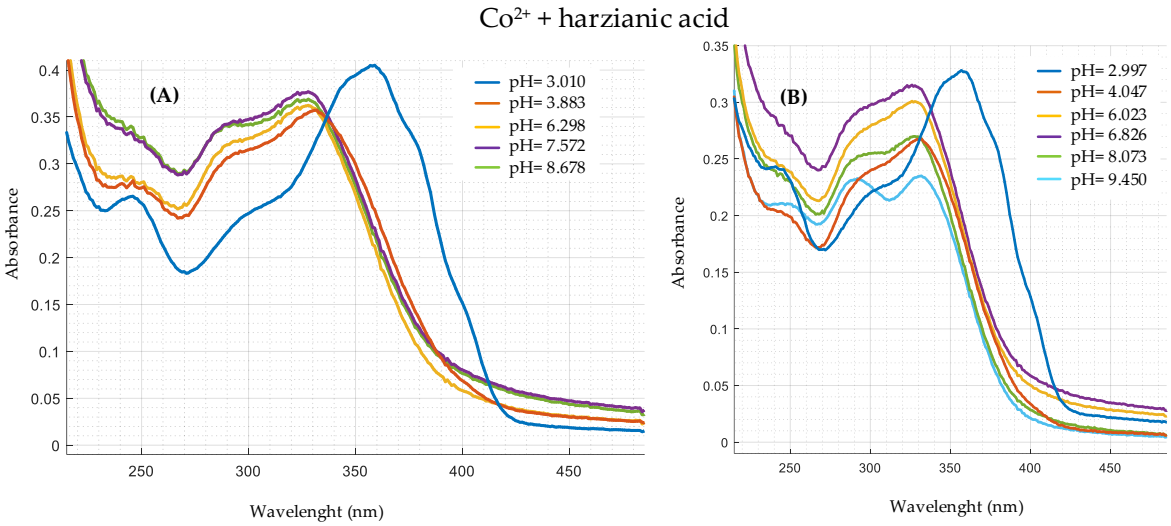


**Figure 4.** UV-VIS spectra in $CH_3OH$/0.1 M $NaClO_4$ (50:50 *w/w*) at different pH of: (**A**) $C^0_{H_2L} = 2.0 \times 10^{-4}$ M and $C^0_{Co} = 2.0 \times 10^{-4}$ $CoCl_2$ (ligand to metal ratio 1:1); (**B**) $C^0_{H_2L} = 2.0 \times 10^{-4}$ M and $C^0_{Co} = 4.0 \times 10^{-4}$ $CoCl_2$ (ligand to metal ratio 1:2).

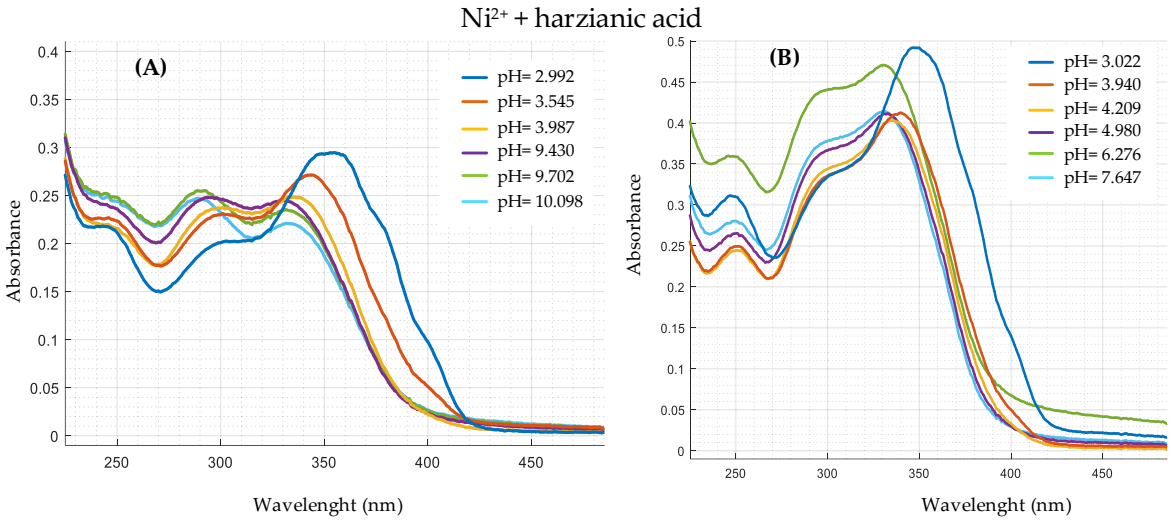


**Figure 5.** UV-VIS spectra in $CH_3OH$/0.1 M $NaClO_4$ (50:50 *w/w*) at different pH of: (**A**) $C^0_{H_2L} = 2.0 \times 10^{-4}$ M and $C^0_{Ni} = 2.0 \times 10^{-4}$ $NiCl_2$ (ligand to metal ratio 1:1); (B) $C^0_{H_2L} = 2.0 \times 10^{-4}$ M and $C^0_{Ni} = 4.0 \times 10^{-4}$ $NiCl_2$ (ligand to metal ratio 1:2).

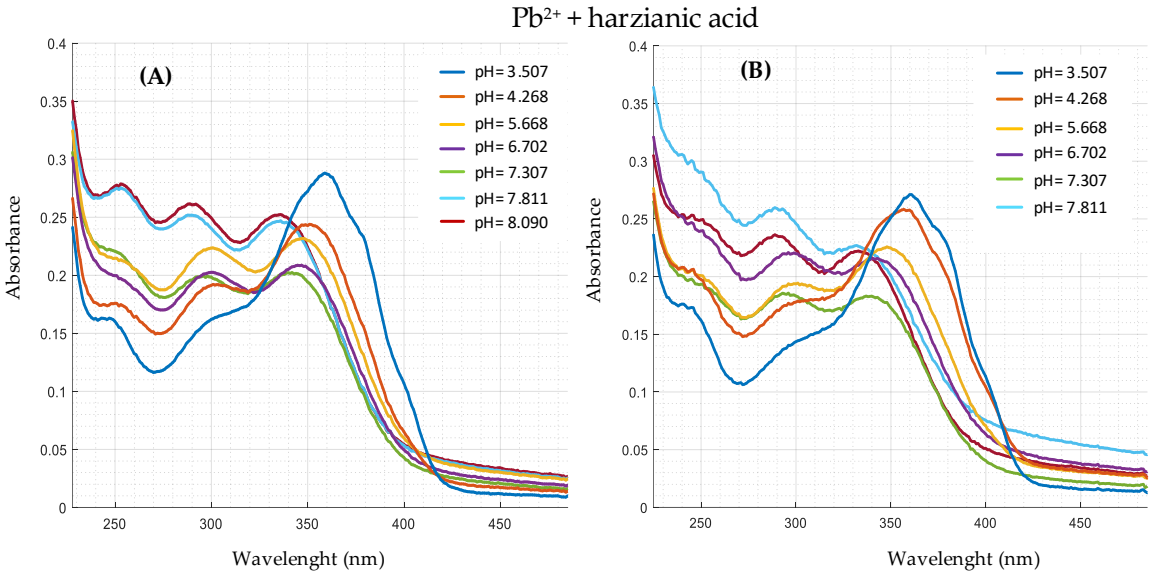


**Figure 6.** UV-VIS spectra in $CH_3OH$/0.1 M $NaClO_4$ (50:50 *w/w*) at different pH of: (**A**) $C^0_{H_2L}$ = 2.0 × $10^{-4}$ M and $C^0_{Pb}$ = 2.0 × $10^{-4}$ $Pb(ClO_4)_2$ (ligand to metal ratio 1:1); (**B**) $C^0_{H_2L}$ = 2.0 × $10^{-4}$ M and $C^0_{Pb}$ = 4.0 × $10^{-4}$$Pb(ClO_4)_2$ (ligand to metal ratio 1:2).

By inspecting the UV-VIS spectra reported above, it is clear that complex species are formed in the $M^{2+}$/harzianic acid solutions. This can be deduced from the fact that UV-VIS spectra not only are substantially different at different pH, but they considerably depend on the ligand to metal ratio and, even more, from the nature of the $M^{2+}$ cation present in the solution [43].

Finally, in order to evaluate the stoichiometry and formation constants of complex species responsible for the observed trend of UV-VIS spectra as a function of pH, and of the ligand to metal ratio, the collected spectrophotometric data, for each metal cation, were processed by the Hyperquad program [44].

This well-known program for the interpretation of equilibrium data fits the experimental data by systematically modifying the equilibrium constants of an assumed set of species to minimize the sum of squared weighted residuals ($U$).

In equation (5), $A_{ik}$is the absorbance measured at the $k–th$ wavelength for the $i–th$ solution,$(A_{ik})_c$ represents the absorbance calculated for a fixed set of equilibrium constants, and $w_k$ are the weights assigned to each measurement. In the present work, we have assumed $w_k = 1$.

$$U = \Sigma_i \Sigma_k w_k (A_{ik} - (A_{ik})_c)^2 \quad (5)$$

The acid dissociation constants of harzianic acid, which were determined separately and are reported in Figure 1, and the value $K_w = 10^{-14.5}$, for the ionic product of water [45], were separately introduced in the model and kept constant throughout.

Obviously, in whatever solution containing a metal cation and water, side reactions of hydroxo complexes formation may take place and their effect on the experimental data must be considered.

Providentially, the hydrolysis of the $M^{2+}$ cations investigated in this study, in water and in a number of mixed solvents, is well known [46–48]. All four hydrated $M^{2+}$ ions of interest here are weak acids, which dissociate producing a number of mononuclear hydroxo complexes, $M(OH)_n^{2-n}$ ($n$ from 1 to 3 for $Pb^{2+}$; $n$ from 1 to 4 for $Cd^{2+}$, $Co^{2+}$, $Ni^{2+}$) and a few polynuclear species, $M_m(OH)_n^{2m-n}$ whose stoichiometry may depend on the nature of the $M^{2+}$ cation. This state of affair, when observed on a wide pH range, gives rise to a rather complex equilibrium scenario.

For instance, Figure 7 represents what would happen when an aqueous solution, containing $10^{-4}$ M $Pb^{2+}$, is submitted to a virtual pH scan.

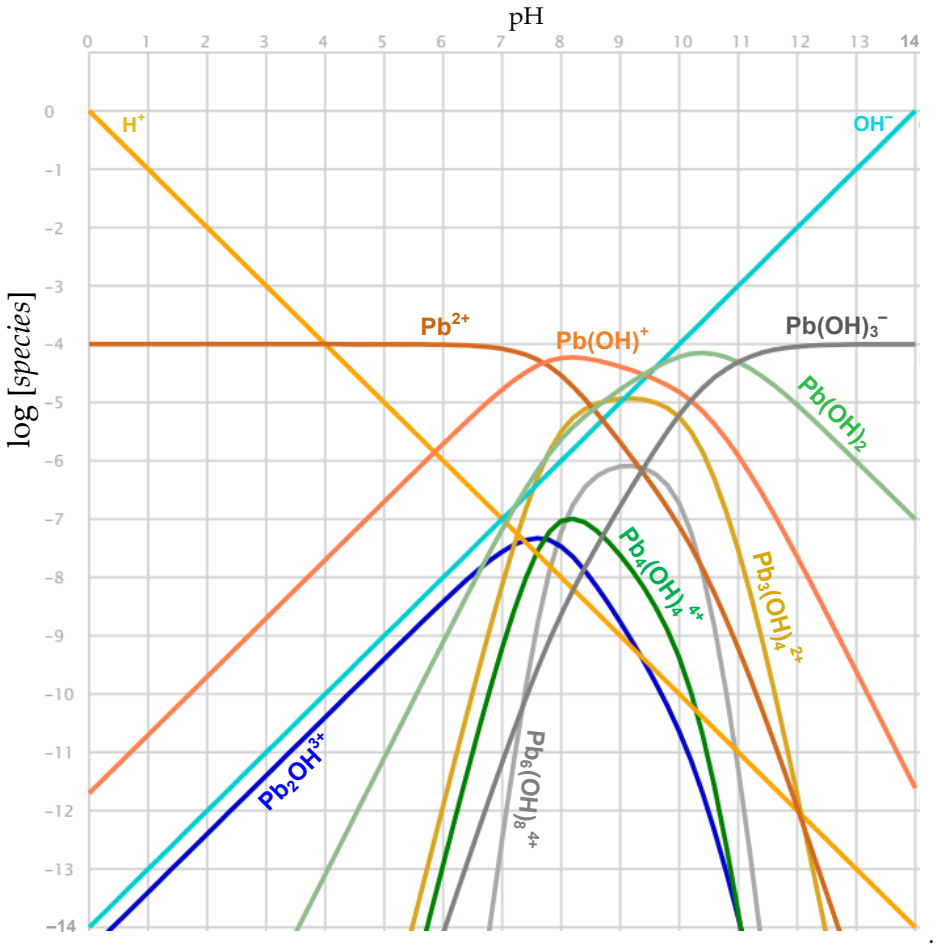


**Figure 7.** pH scan of a $10^{-4}$ M aqueous solution of $Pb^{2+}$ based on stoichiometry and formation constants of $Pb_m(OH)_n^{2m-n}$ hydroxo complexes gathered from literature [45,46].

Even a superficial inspection of Figure 7 shows that, at the concentration of metal considered, polynuclear species account only for a small fraction of lead in the solution, so that most of the effect of the side reactions of the hydroxo complexes formation could be accounted for by introducing, in the model, only the conventional $Pb(OH)_n^{2-n}$ species. However, above pH~8 significant concentrations of $Pb_3(OH)_4^{2+}$ are produced. Finally, we hypothesize that, in the mixed (0.1 M $NaClO_4/CH_3OH$, 50/50 *w/w*) solvent used in this study, the situation is not much different from that described in Figure 7. On this basis, we introduced in the model used to fit the spectrophotometric data for lead the hydrolysis species $PbOH^+$, $Pb(OH)_2$, $Pb(OH)_3^-$, and $Pb_3(OH)_4^{2+}$, whose formation constants were refined by Hyperquad during the process of minimization of the sum of squared residuals (5) (starting from their values at zero ionic strength taken from reference [48]).

From the point of view of the formation of hydroxo complexes, $Pb^{2+}$ represents the most severe case, since $Cd^{2+}$, $Co^{2+}$, $Ni^{2+}$ are weaker acids, and only the mononuclear $M(OH)_n^{2-n}$ complexes have been considered (since no species $M_3(OH)_4^{2+}$ is described and the $M_2OH^+$ and $M_4(OH)_4^{4+}$ polynuclear complexes are clearly irrelevant at the metal concentrations investigated in this study).

Results of Hyperquad processing of spectrophotometric data in Figures 3–6 are summarized in Table 2.

**Table 2.** Summary of $M^{2+}$/harzianic acid ($H_2L$) stability constants. **σ** denotes the estimated standard deviation.

| $M^{2+}$ | Reaction | Log (Formation Constant) ± 3σ |
|---|---|---|
| $Cd^{2+}$ | $Cd^{2+} + L^{2-} \rightleftharpoons CdL$ | 3.82 ± 0.19 |
| | $Cd^{2+} + HL^{-} + L^{2-} \rightleftharpoons Cd(HL)L^{-}$ | 9.13 ± 0.23 |
| $Co^{2+}$ | $Co^{2+} + L^{2-} \rightleftharpoons CoL$ | 4.70 ± 0.12 |
| | $Co^{2+} + HL^{-} + L^{2-} \rightleftharpoons Co(HL)L^{-}$ | 11.93 ± 0.06 |
| $Ni^{2+}$ | $Ni^{2+} + HL^{-} + L^{2-} \rightleftharpoons Ni(HL)L^{-}$ | 11.85 ± 0.12 |
| $Pb^{2+}$ | $Pb^{2+} + L^{2-} \rightleftharpoons PbL$ | 4.25 ± 0.5 |
| | $Pb^{2+} + HL^{-} + L^{2-} \rightleftharpoons Pb(HL)L^{-}$ | 10.77 ± 0.3 |

Obviously, in order to calculate $(A_{ik})_c$ in equation (5), besides refining values of the formation constant for each assumed species, in the process of minimizing the sum of squared residuals, $U$, Hyperquad also assigns and refines, for each species, a value of the molar extinction coefficient, $\varepsilon_\lambda(M^{-1}cm^{-1})$ at each measured wavelength. By consequence, as a result of data processing by Hyperquad, the $\varepsilon_\lambda$ finally assigned to the complex species are obtained.

For instance, the molar extinction coefficients calculated by Hyperquad for all absorbing species in solutions of $Co^{2+}$/harzianic acid and $Ni^{2+}$/harzianic acid are presented in Figure 8.

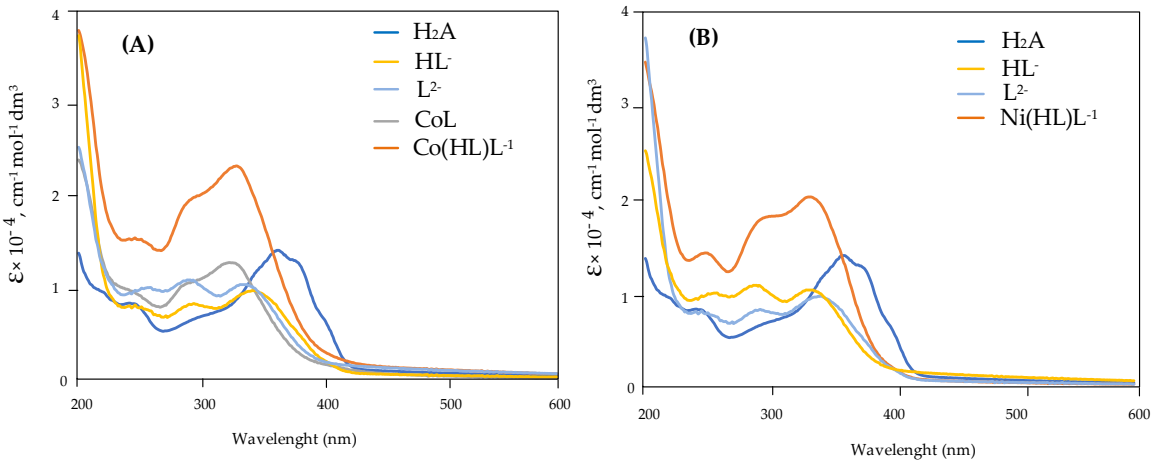


**Figure 8.** Molar extinction coefficients, $\varepsilon_\lambda(M^{-1}cm^{-1})$, of the absorbing species calculated by Hyperquad for the systems: (**A**) $Co^{2+}$-harzianic acid; (**B**) $Ni^{2+}$-harzianic acid.

From Figure 8, it can be seen that the bis-complex $M(HL)L^-$ is a very efficient UV absorber, which presumably is responsible for most of the spectral variations in the recorded spectra in Figures 3–6.

From data in Table 2, distribution diagrams, showing the fraction of the total metal concentration present in the form of each species, as a function of pH, can easily be drawn for whatever assumed concentration of the metal cation and harzianic acid.

For instance, distribution diagrams for $M^{2+} = Cd^{2+}$ and $M^{2+} = Co^{2+}$ are presented in Figures 9 and 10, respectively, from which it can be seen that the bis-complex $M(HL)L^-$ is, under the conditions assumed to draw the diagrams, the prevailing species at pH around 6 which is close to the pH of natural ecosystems. However, at the highest pH investigated, $M(HL)L^-$ is converted to the 1:1 ML complex, which is the prevailing species at the highest pH investigated. $Ni^{2+}$ represents an exception to this general pattern, since the NiL complex is not formed in the pH range investigated.

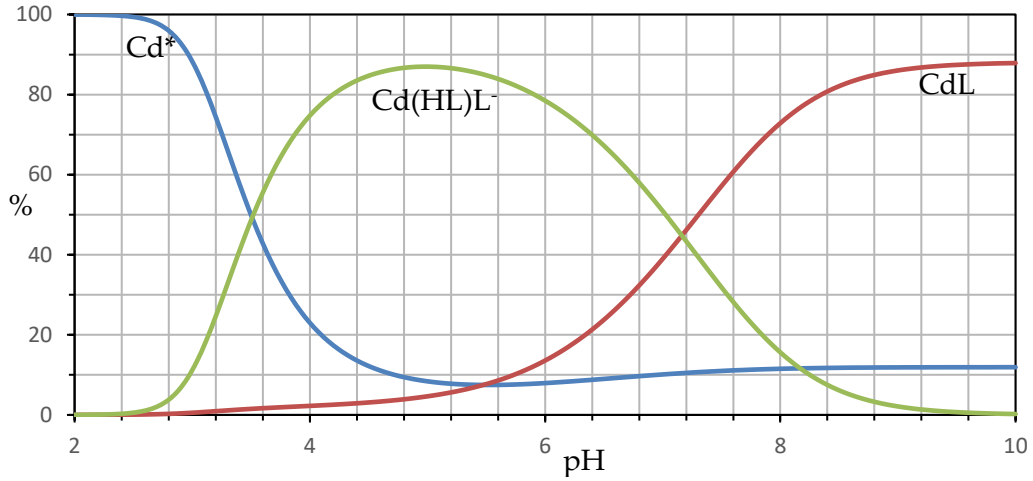


**Figure 9.** Distribution diagram of species in $Cd^{2+}$-harzianic acid system in $CH_3OH$/0.1 M $NaClO_4$ (50:50 *w/w*) calculated from formation constants in Table 2 assuming a $C_{Cd}$ = 1.0 × $10^{-3}$ M and $C_{H_2L}$ = 2.0 × $10^{-3}$ M ($H_2L$ = harzianic acid). The symbol Cd* is used to represent all species in the solution that contain the metal cation, but do not contain harzianic acid.

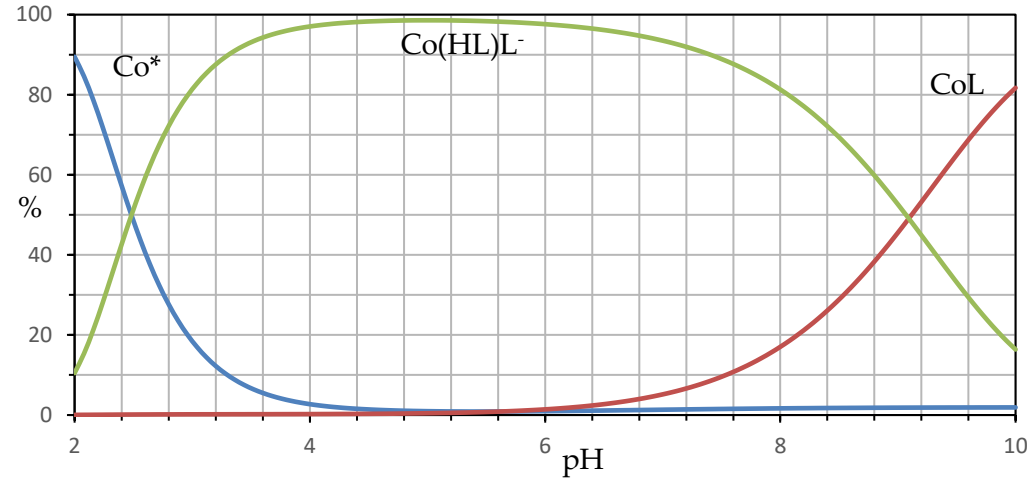


**Figure 10.** Distribution diagram of species in $Co^{2+}$-harzianic acid system in $CH_3OH$/0.1 M $NaClO_4$ (50:50 *w/w*) calculated from formation constants in Table 2 assuming $C_{Co}$ = 1.0 × $10^{-3}$ M and $C_{H_2L}$= 2.0 × $10^{-3}$ M ($H_2L$ = harzianic acid). The symbol Co* is used to represent all species in the solution that contain the metal cation, but do not contain harzianic acid.

Because of differences in stoichiometry of complexes (and, hence, in dimensions of formation constants) and in solvents employed, a direct comparison between the formation constants of $M^{2+}$ complexes with harzianic exposed above and reported apparent affinity constants for other natural chelators is not generally possible or, at best, very uncertain. However, to characterize the efficiency of a ligand, it has been suggested the use of a parameter termed "pM" [49]. Here, we intend pM to represent the minus logarithm (anti-logarithm) of the concentration of the free (solvated) metal cation (i.e., briefly, pM = −log [$M^{2+}$]) in a reference solution of pH = 7.4 containing 1 mM of the ligand and 1 µM total metal concentration. By consequence, a larger pM value corresponds to a lower concentration of the free metal ion in solution at equilibrium and, in principle, to a higher affinity of the relevant ligand for the $M^{2+}$ cation.

For instance, from the above reported formation constants we calculate: pPb = 8.5, pCd = 7.2, pCo = 9.7, pNi = 9.6 when the ligand is harzianic acid. For comparison, pPb = 18.1 is obtained, when the ligand is EDTA in water at zero ionic strength.

Obviously, although in the reference solution, less than 1% of the total metal in solution is found non-bonded to harzianic acid (except for cadmium, for which the metal fraction non-bonded to harzianic acid is about 7%), harzianic acid is a much less efficient chelator than EDTA toward the investigated dipositive metal cations.

This is not unexpected, since based on its structure and previous reports, harzianic acid may, at best, be a bidentate chelator toward $M^{2+}$ cations, as are many synthetic products and naturally occurring molecules exposing the 3-acetyl-pyrrolidine-2,4-dione heterocycle. Generally, it is assumed that chelation takes place by the formation of a six membered ring, which includes the metal cation, the amide carbonyl and hydroxyl group on C1. In the case of harzianic acid, this would correspond to the sketch in Scheme 2:

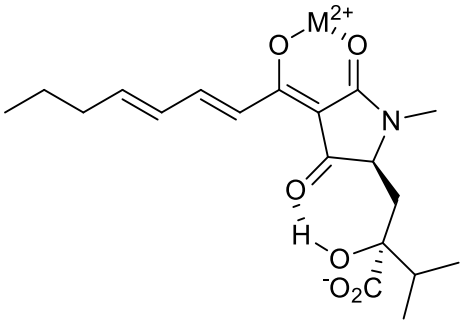


**Scheme 2.** Chelation of bivalent metal cations, $M^{2+}$, by harzianic acid.

In order to further explore the mode harzianic acid coordinates to $M^{2+}$ cations, $^1$H NMR spectra of harzianic acid in presence of $Cd^{2+}$ and $Pb^{2+}$ were acquired (Figure S5).

In $^1$H NMR spectra particularly interesting are the changes in proton chemical shifts of the hexadienoyl residue and of the pyrrolidine ring in presence and absence of the metal cations.

$^1$H NMR spectrum of harzianic acid recorded in presence of $CdCl_2$ in $CD_3OD/D_2O$ (1:1 *w/w*) showed up-field shifts for H3 (Δδ 0.06) resonating as multiplet at δ 7.52, H4/5 (Δδ 0.05) resonating at δ 7.40 as multiplet, and H5′(Δδ 0.06) resonating as doublet at δ 3.78 (d, $J$ = 9.8 Hz). In the same spectrum, a downfield shift was observed for H2 (Δδ 0.15) resonating as doublet at δ 7.22 (d, $J$ = 16.8 Hz). A similar behavior can be seen in the $^1$H NMR spectrum of harzianic acid recorded in presence of $Pb^{2+}$ ion (Figure S5).

The observed differences on the chemical shifts, obtained by comparison between NMR data of harzianic acid and its metal complexes, confirm the involvement in the coordination complexes of the C = O group of the amide and the external carbonyl groups of the ligand. The 2-carboxy-2-hydroxy-3-methylbutyl group in C5′ seems not to be involved in the coordination because there are no significant differences in the chemical shifts of its protons, and may also be due to the formation of hydrogen bond between the hydroxyl group in C7′ and the carbonyl group in C4′ [50] (Scheme 2). This is in accordance with what was previously reported for tetramic acids, such as tenuazonic acid and analogues [51]. This hypothesis could be also confirmed by the solid-state FT-IR data concerning the complexation between the toxic metals and harzianic acid. In fact, by analysis of the spectra (Figures S6–10), it is evident a shift of the frequency of the stretching band of the CO and of the C = C towards lower wavenumbers compared to the free ligand, as reported in similar compounds [52].

Our findings show that harzianic acid forms stable chelating complexes with a range of metal ions. Natural ligands containing hydroxyl, carboxylic, and carbonyl groups are structurally suitable to form coordination complexes. In fact, studies conducted on kojic acid [53] and dehydroacetic acid [54] show the formation of complex species with high stability in mixed solvents.

Despite the considerable interest in relation to numerous potential use and applications of chelating compounds, including decontamination of soils, few studies evaluate chelating properties of fungal compounds to find promising candidates for practical applications in biotechnologies. In fact, the contamination of soils with heavy metals represents a challenge because many synthetic chelating agents destroy the soil matrix and remove nutrients. On the contrary, natural compounds might have the capacity to remove heavy metals without deteriorating the soil properties [19]. Furthermore, the possible interest of natural chelating compounds is not exclusively related to the agriculture field, but also in many sections of medicine and biology [23,55].

## 4. Conclusions

In this study, the investigations conducted on the chelating properties of harzianic acid toward some toxic heavy metals show the capacity of this fungal metabolite to form stable neutral or negatively charged coordination complexes in metal/harzianic acid ratio 1:1 or 1:2 depending on the pH conditions. In fact, as can be seen from the distribution diagrams (e.g., Figures 9 and 10), although both species are present, the neutral or charged coordination complexes predominate at different pH ranges.

It seems likely that the biological activities of harzianic acid are related to its complexing ability. In particular, the capacity to form complexes with toxic heavy metals might be important for the decontamination of soils with high heavy metal contents.

**Supplementary Materials:** the following are available online at https://www.mdpi.com/2305-6304/9/2/19/s1, Figure S1: Mass spectrum ESIMS QTOF obtained by LC-MS analysis in ESI positive mode of a solution 1.0 x $10^{-3}$ M of harzianic acid and 1.0 x $10^{-3}$ M of $Cd(ClO_4)_2$ in MeOH/$H_2O$ 50:50 (*w/w*), Figure S2: Mass spectrum ESIMS QTOF obtained by LC-MS analysis in ESI positive mode of a solution 1.0 x $10^{-3}$ M of harzianic acid and 1.0 x $10^{-3}$ M of $CoCl_2$ in MeOH/$H_2O$ 50:50 (*w/w*), Figure S3: Mass spectrum ESIMS QTOF obtained by LC-MS analysis in ESI positive mode of a solution 1.0 x $10^{-3}$ M of harzianic acid and 1.0 x $10^{-3}$ M of $NiCl_2$ in MeOH/$H_2O$ 50:50 (*w/w*), Figure S4. Mass spectrum ESIMS QTOF obtained by LC-MS analysis in ESI positive mode of a solution 1.0 x $10^{-3}$ M of harzianic acid and 1.0 x $10^{-3}$ M of $Pb(ClO_4)_2$ in MeOH/$H_2O$ 50:50 (*w/w*), Figure S5. $^1H$ NMR spectra of harzianic acid (HA) (down), $Cd(ClO_4)_2$ : HA (middle) and $Pb(ClO_4)_2$ : HA (up) recorded in $CD_3OD/D_2O$ (50:50 *w/w*) at 400 MHz. Solvent peaks are removed, Figure S6. Solid-state FT-IR spectrum of harzianic acid, Figure S7. Solid-state FT-IR spectrum of Cd (II)/harzianic acid complex, Figure S8. Solid-state FT-IR spectrum of Co (II)/harzianic acid complex, Figure S9. Solid-state FT-IR spectrum of Ni (II)/harzianic acid complex, Figure S10. Solid-state FT-IR spectrum of Pb (II)/harzianic acid complex.

**Author Contributions:** conceptualization, F.V., M.I., and A.A.; methodology, G.D.T., M.D., F.V., M.I., A.A.; investigation, G.D.T., M.M.S., A.S., R.N. and A.A.; data curation, G.D.T., M.M.S., M.D., M.L., F.S., M.I., and A.A.; writing—original draft preparation, G.D.T., M.M.S.; writing—review and editing, R.N., M.D., F.V., F.S., M.I., and A.A.; supervision M.I. and A.A.; project administration, F.V., M.I., and A.A.; funding acquisition, F.V., M.L., and A.A.

**Funding:** F.V., M.L., and A.S.: MIURPON (Grant number Linfa 03PE_00026_1; grant number Marea 03PE_00106); POR FESR CAMPANIA 2014/2020-O.S. 1.1 (grant number Bioagro 559); MISE CRESO (Grant number Protection n. F/050421/01-03/X32); PSR Veneto 16.1.1 (grant number Divine n. 3589659); PSR Campania 2014/2020 Misura 16—Tipologia di intervento 16.1—Azione 2 'Sostegno ai Progetti Operativi di Innovazione (POI)'—Progetto 'DI.O.N.I.S.O.', C.U.P. B98H19005010009.

**Data Availability Statement:** All the data are reported in the manuscript in the Supporting Materials.

**Conflicts of Interest:** The authors declare no conflict of interest.

## References


(1) Margesin, R.; Zimmerbauer, A.; Schinner, F. Monitoring of Bioremediation by Soil Biological Activities. *Chemosphere* **2000**, *40* (4), 339–346. https://doi.org/10.1016/S0045-6535(99)00218-0.

(2) Srivastava, J.; Naraian, R.; Kalra, S. J. S.; Chandra, H. Advances in Microbial Bioremediation and the Factors Influencing the Process. *Int. J. Environ. Sci. Technol.* **2014**, *11* (6), 1787–1800. https://doi.org/10.1007/s13762-013-0412-z.

(3) Ali, H.; Khan, E.; Ilahi, I. Environmental Chemistry and Ecotoxicology of Hazardous Heavy Metals: Environmental Persistence, Toxicity, and Bioaccumulation. *Journal of Chemistry* **2019**. https://doi.org/10.1155/2019/6730305.

(4) Singh, J.; Kalamdhad, A. S. Effects of Heavy Metals on Soil, Plants, Human Health and Aquatic Life Making Bricks Using Variety of Solid Waste View Project Anaerobic Digestion. *International journal of Research in Chemistry and Environment* **2011**, *1*, 15–21.

(5) Jaishankar, M.; Tseten, T.; Anbalagan, N.; Mathew, B. B.; Beeregowda, K. N. Toxicity, Mechanism and Health Effects of Some Heavy Metals. *Interdisciplinary Toxicology* **2014**, *7*, 60–72.

(6) Nagajyoti, P. C.; Lee, K. D.; Sreekanth, T. V. M. Heavy Metals, Occurrence and Toxicity for Plants: A Review. *Environmental Chemistry Letters* **2010**, *8*, 199–216.

(7) Pandey, G.; Madhuri, S. Heavy Metals Causing Toxicity in Humans, Animals and Environment. *Research Journal of Animal, Veterinary and Fishery Sciences* **2014**, *2*, 17–23.

(8) Das, K. K.; Reddy, R. C.; Bagoji, I. B.; Das, S.; Bagali, S.; Mullur, L.; Khodnapur, J. P.; Biradar, M. S. Primary Concept of Nickel Toxicity - An Overview. *Journal of Basic and Clinical Physiology and Pharmacology* **2019**, *30*, 141–152.

(9) Leyssens, L.; Vinck, B.; Van Der Straeten, C.; Wuyts, F.; Maes, L. Cobalt Toxicity in Humans—A Review of the Potential Sources and Systemic Health Effects. *Toxicology* **2017**, *387*, 43–56.

(10) Godt, J.; Scheidig, F.; Grosse-Siestrup, C.; Esche, V.; Brandenburg, P.; Reich, A.; Groneberg, D. A. The Toxicity of Cadmium and Resulting Hazards for Human Health. *Journal of Occupational Medicine and Toxicology* **2006**, *1*, 1–6.

(11) Flora, G.; Gupta, D.; Tiwari, A. Toxicity of Lead: A Review with Recent Updates. *Interdisciplinary Toxicology* **2012**, *5*, 47–58.

(12) Tóth, G.; Hermann, T.; Da Silva, M. R.; Montanarella, L. Heavy Metals in Agricultural Soils of the European Union with Implications for Food Safety. *Environment International* **2016**, *88*, 299–309.

(13) Cheng, W. da; Zhang, G. ping; Yao, H. gen; Wu, W.; Xu, M. Genotypic and Environmental Variation in Cadmium, Chromium, Arsenic, Nickel, and Lead Concentrations in Rice Grains. *Journal of Zhejiang University. Science. B.* **2006**, *7*, 565–571.

(14) Wang, Y.; Yi, B.; Sun, X.; Yu, L.; Wu, L.; Liu, W.; Wang, D.; Li, Y.; Jia, R.; Yu, H.; Li, X. Removal and Tolerance Mechanism of Pb by a Filamentous Fungus: A Case Study. *Chemosphere* **2019**, *225*, 200–208.

(15) Fomina, M.; Hillier, S.; Charnock, J. M.; Melville, K.; Alexander, I. J.; Gadd, G. M. Role of Oxalic Acid Overexcretion in Transformations of Toxic Metal Minerals by Beauveria Caledonica. *Applied and Environmental Microbiology* **2005**, *71*, 371–381.

(16) Arwidsson, Z.; Johansson, E.; Von Kronhelm, T.; Allard, B.; Van Hees, P. Remediation of Metal Contaminated Soil by Organic Metabolites from Fungi I-Production of Organic Acids. *Water, Air, and Soil Pollution* **2010**, *205*, 215–226.

(17) Machuca, A.; Pereira, G.; Aguiar, A.; Milagres, A. M. F. Metal-Chelating Compounds Produced by Ectomycorrhizal Fungi Collected from Pine Plantations. *Letters in Applied Microbiology* **2007**, *44*, 7–12.

(18) Renella, G.; Landi, L.; Nannipieri, P. Degradation of Low Molecular Weight Organic Acids Complexed with Heavy Metals in Soil. *Geoderma* **2004**, *122*, 311–315.
(19) Ousmanova, D.; Parker, W. Fungal Generation of Organic Acids for Removal of Lead from Contaminated Soil. *Water, Air, and Soil Pollution* **2007**, *179*, 365–380. https://doi.org/10.1007/s11270-006-9241-8.
(20) Salvatore, M. M.; Nicoletti, R.; Salvatore, F.; Naviglio, D.; Andolfi, A. GC–MS Approaches for the Screening of Metabolites Produced by Marine-Derived Aspergillus. *Marine Chemistry* **2018**, *206* (May), 19–33.
(21) Das, A.; Prasad, R.; Srivastava, A.; Giang, P. H.; Bhatnagar, K.; Varma, A. Fungal Siderophores: Structure, Functions and Regolation. In *Microbial siderophores*; Springer: Berlin, Heidelberg, 2007; pp 1–42.
(22) Schalk, I. J.; Hannauer, M.; Braud, A. New Roles for Bacterial Siderophores in Metal Transport and Tolerance. *Environmental Microbiology* **2011**, *13*, 2844–2854.
(23) Ahmed, E.; Holmström, S. J. M. Siderophores in Environmental Research: Roles and Applications. *Microbial Biotechnology* **2014**, *7*, 196–208.
(24) Khan, A. G.; Kuek, C.; Chaudhry, T. M.; Khoo, C. S.; Hayes, W. J. Role of Plants, Mycorrhizae and Phytochelators in Heavy Metal Contaminated Land Remediation. *Chemosphere* **2000**, *41*, 197–207.
(25) Schwab, A. P.; Zhu, D. S.; Banks, M. K. Influence of Organic Acids on the Transport of Heavy Metals in Soil. *Chemosphere* **2008**, *72*, 986–994.
(26) Woo, S. L.; Pepe, O. Microbial Consortia: Promising Probiotics as Plant Biostimulants for Sustainable Agriculture. *Frontiers in Plant Science* **2018**, *9*, 7–12.
(27) Vinale, F.; Sivasithamparam, K.; Ghisalberti, E. L.; Marra, R.; Woo, S. L.; Lorito, M. Trichoderma-Plant-Pathogen Interactions. *Soil Biology and Biochemistry* **2008**, *40*, 1–10.
(28) Harman, G. E.; Howell, C. R.; Viterbo, A.; Chet, I.; Lorito, M. Trichoderma Species - Opportunistic, Avirulent Plant Symbionts. *Nature Reviews Microbiology* **2004**, *2*, 43–56.
(29) Kredics, L. ; Hatvani, L. ; Naeimi, S. ; Körmöczi, P. ; Manczinger, L. ; Vágvölgyi, C. ;; Druzhinina, I. Biodiversity of the Genus Hypocrea/Trichoderma in Different Habitats. In *Biodiversity of the genus Hypocrea/Trichoderma in different habitats*; Gupta, V. K., Schmoll, M., Herrera-Estrella, A., Upadhyay, R. S., Druzhinina, I., Tuohy, M. G., Eds.; Elsevier: Oxford, UK, 2014; pp 3–24.
(30) Nicoletti, R.; Vinale, F. Bioactive Compounds from Marine-Derived Aspergillus, Penicillium, Talaromyces and Trichoderma Species. *Marine Drugs* **2018**, *16*, 408.
(31) Marra, R.; Nicoletti, R.; Pagano, E.; DellaGreca, M.; Salvatore, M. M. M. M.; Borrelli, F.; Lombardi, N.; Vinale, F.; Woo, S. L. S. L.; Andolfi, A. Inhibitory Effect of Trichodermanone C, a Sorbicillinoid Produced by Trichoderma Citrinoviride Associated to the Green Alga Cladophora Sp., on Nitrite Production in LPS-Stimulated Macrophages. *Natural Product Research* **2019**, *33* (23), 3389–3397. https://doi.org/10.1080/14786419.2018.1479702.
(32) Salvatore, M. M.; Nicoletti, R.; DellaGreca, M.; Andolfi, A. Occurrence and Properties of Thiosilvatins. *Marine Drugs* **2019**, *17* (12), 1–14.
(33) Vinale, F.; Sivasithamparam, K.; Ghisalberti, E. L.; Ruocco, M.; Woo, S.; Lorito, M. Trichoderma Secondary Metabolites That Affect Plant Metabolism. *Natural Product Communications* **2012**, *7*, 1545–1550.
(34) Vinale, F.; Sivasithamparam, K. Beneficial Effects of Trichoderma Secondary Metabolites on Crops. *Phytotherapy Research* **2020**, 2835–2842.
(35) Vinale, F.; Nicoletti, R.; Borrelli, F.; Mangoni, A.; Parisi, O. A.; Marra, R.; Lombardi, N.; Lacatena, F.; Grauso, L.; Finizio, S.; Lorito, M.; Woo, S. L. Co-Culture of Plant Beneficial Microbes as Source of Bioactive Metabolites. *Scientific Reports* **2017**, *7*, 1–12.
(36) Vinale, F.; Nigro, M.; Sivasithamparam, K.; Flematti, G.; Ghisalberti, E. L.; Ruocco, M.; Varlese, R.; Marra, R.; Lanzuise, S.; Eid, A.; Woo, S. L.; Lorito, M. Harzianic Acid: A Novel Siderophore from Trichoderma Harzianum. *FEMS Microbiology Letters* **2013**, *347*, 123–129.

(37) Vinale, F.; Flematti, G.; Sivasithamparam, K.; Lorito, M.; Marra, R.; Skelton, B. W.; Ghisalberti, E. L. Harzianic Acid, an Antifungal and Plant Growth Promoting Metabolite from Trichoderma Harzianum. *Journal of Natural Products* **2009**, *72*, 2032–2035.

(38) Manganiello, G.; Sacco, A.; Ercolano, M. R.; Vinale, F.; Lanzuise, S.; Pascale, A.; Napolitano, M.; Lombardi, N.; Lorito, M.; Woo, S. L. Modulation of Tomato Response to Rhizoctonia Solani by Trichoderma Harzianum and Its Secondary Metabolite Harzianic Acid. *Frontiers in Microbiology* **2018**, *9*, 1966.

(39) De Filippis, A.; Nocera, F. P.; Tafuri, S.; Ciani, F.; Staropoli, A.; Comite, E.; Bottiglieri, A.; Gioia, L.; Lorito, M.; Woo, S. L.; Vinale, F.; De Martino, L. Antimicrobial Activity of Harzianic Acid against Staphylococcus Pseudintermedius. *Natural Product Research* **2020**, 1–6.

(40) Healy, A. R.; Vinale, F.; Lorito, M.; Westwood, N. J. Total Synthesis and Biological Evaluation of the Tetramic Acid Based Natural Product Harzianic Acid and Its Stereoisomers. *Organic Letters* **2015**, *17*, 692–695.

(41) Mo, X.; Li, Q.; Ju, J. Naturally Occurring Tetramic Acid Products: Isolation, Structure Elucidation and Biological Activity. *RSC Adv.* **2014**, *4*, 50566–50593.

(42) De Tommaso, G.; Salvatore, M. M.; Nicoletti, R.; DellaGreca, M.; Vinale, F.; Bottiglieri, A.; Staropoli, A.; Salvatore, F.; Lorito, M.; Iuliano, M.; Andolfi, A. Bivalent Metal-Chelating Properties of Harzianic Acid Produced by Trichoderma Pleuroticola Associated to the Gastropod Melarhaphe Neritoides. *Molecules* **2020**, *25* (9), 2147.

(43) Meloun, M.; Havel, J.; Högfeldt, E. *Computation of Solution Equilibria a Guide to Methods in Potentiometry, Extraction and Spectrophotometry*; John Wiley & Sons: New York, NY, USA, 1988.

(44) Gans, P.; Sabatini, A.; Vacca, A. Investigation of Equilibria in Solution. Determination of Equilibrium Constants with the HYPERQUAD Suite of Programs. *Talanta* **1996**, *43*, 1739–1753.

(45) Ohtaki, H.; Tanaka, N. Ionic Equilibria in Mixed Solvents. VI. Dissociation Constants of Aliphatic Diamines in Water-Methanol Solutions. *The Journal of Physical Chemistry* **1971**, *75*, 90–92.

(46) Matsui, H.; Ohtaki, H. Ionic Equilibria in Mixed Solvents. XII. Hydrolysis of Cadmium (II) Ion in Dioxane–Water and Methanol–Water Mixtures. *Bulletin of the Chemical Society of Japan* **1977**, *50*.

(47) Baes, C. F.; Mesmer, R. S. The Hydrolysis of Cations. In *Berichte der Bunsengesellschaft für physikalische Chemie*; John Wiley & Sons: New York, NY, USA, 1977; pp 245–246. https://doi.org/10.1002/bbpc.19770810252.

(48) Martell, A. E.; Smith, R. M. *Critical Stability Constants*; Springer US: New York, NY, USA, 1989.

(49) Kaufmann, G. F.; Sartorio, R.; Lee, S. H.; Rogers, C. J.; Meijler, M. M.; Moss, J. A.; Clapham, B.; Brogan, A. P.; Dickerson, T. J.; Janda, K. D. Revisiting Quorum Sensing: Discovery of Additional Chemical and Biological Functions for 3-Oxo-N-Acylhomoserine Lactones. In *National Academy of Sciences of the United States of America*; 2005; Vol. 102, pp 309–314. https://doi.org/10.1073/pnas.0408639102.

(50) Zaghouani, M.; Nay, B. 3-Acylated Tetramic and Tetronic Acids as Natural Metal Binders: Myth or Reality? *Natural Product Reports* **2016**, *33*, 540–548.

(51) Markopoulou, O.; Markopoulos, J.; Nicholls, D. Synthesis of 3-Butanoyl- and 3-Benzoyl-4-Hydroxy-3-Pyrrolin-2-Ones and Their Complexes with Metal Ions. *Journal of Inorganic Biochemistry* **1990**, *39*, 307–316.

(52) Heaton, B. T.; Jacob, C.; Sampanthar, J. T. Rhodium Carbonyl Complexes Containing Pyridine; Crystal Structure of an Unusual Octahedral Rhodium(I) Complex [Rh2(μ-CO)3Cl2(Py)4]. *Journal of the Chemical Society - Dalton Transactions* **1998**, *2*, 1403–1410.

(53) Burgess, J.; Rangel, M. Hydroxypyranones, Hydroxypyridinones, and Their Complexes. In *Advances in Inorganic chemistry*; Accademic Press: London, UK, 2008; pp 167–243.

(54) Al Alousi, A. S.; Shehata, M. R.; Shoukry, M. M.; Hassan, S. A.; Mahmoud, N. Coordination Properties of Dehydroacetic Acid - Binary and Ternary Complexes. *Journal of Coordination Chemistry* **2008**, *61*, 1906–1916.

(55) Pinto, I. S. S.; Neto, I. F. F.; Soares, H. M. V. M. Biodegradable Chelating Agents for Industrial, Domestic, and Agricultural Applications—a Review. *Environmental Science and Pollution Research* **2014**, *21*, 11893–11906.

*Toxics* ***2021***, *9, 19*

*Supplementary Materials*

# Coordination Properties of the Fungal Metabolite Harzianic Acid toward Toxic Heavy Metals

**Gaetano De Tommaso [1], Maria Michela Salvatore [1], Rosario Nicoletti [2,3], Marina DellaGreca [1], Francesco Vinale [4,5,6], Alessia Staropoli [3], Francesco Salvatore [1], Matteo Lorito [3], Mauro Iuliano [1,*] and Anna Andolfi [1,6,*]**

**Figure S1.** Mass spectrum ESIMS QTOF obtained by LC-MS analysis in ESI positive mode of a solution 1.0 x 10−3 M of harzianic acid and 1.0 x 10−3 M of Cd(ClO4)2 in MeOH/H2O 50:50 (*w/w*).

**Figure S2.** Mass spectrum ESIMS QTOF obtained by LC-MS analysis in ESI positive mode of a solution 1.0 x 10−3 M of harzianic acid and 1.0 x 10−3 M of CoCl2 in MeOH/H2O 50:50 (*w/w*).

**Figure S3.** Mass spectrum ESIMS QTOF obtained by LC-MS analysis in ESI positive mode of a solution 1.0 x 10−3 M of harzianic acid and 1.0 x 10−3 M of NiCl2 in MeOH/H2O 50:50 (*w/w*).

**Figure S4.** Mass spectrum ESIMS QTOF obtained by LC-MS analysis in ESI positive mode of a solution 1.0 x 10−3 M of harzianic acid and 1.0 x 10−3 M of Pb(ClO4)2 in MeOH/H2O 50:50 (*w/w*).

**Figure S5**. 1H NMR spectra of harzianic acid (HA) (down), Cd(ClO4)2 : HA (middle) and Pb(ClO4)2 : HA (up) recorded in CD3OD/D2O (50:50 *w/w*) at 400 MHz. Solvent peaks are removed.

**Figure S6**. Solid-state FT-IR spectrum of harzianic acid.

**Figure S7**. Solid-state FT-IR spectrum of Cd (II)/harzianic acid complex.

**Figure S8**. Solid-state FT-IR spectrum of Co (II)/harzianic acid complex.

**Figure S9**. Solid-state FT-IR spectrum of Ni (II)/harzianic acid complex.

**Figure S10**. Solid-state FT-IR spectrum of Pb (II)/harzianic acid complex.

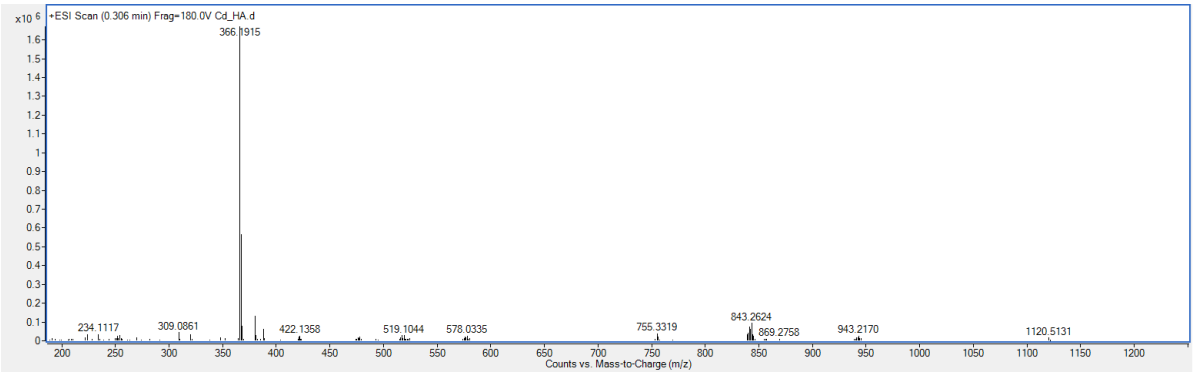


**Figure S1.** Mass spectrum ESIMS QTOF obtained by LC-MS analysis in ESI positive mode of a solution $1.0 \cdot 10^{-3}$ M of harzianic acid and $1.0 \cdot 10^{-3}$ M of $Cd(ClO_4)_2$ in MeOH/$H_2O$ 50:50 (*w/w*).

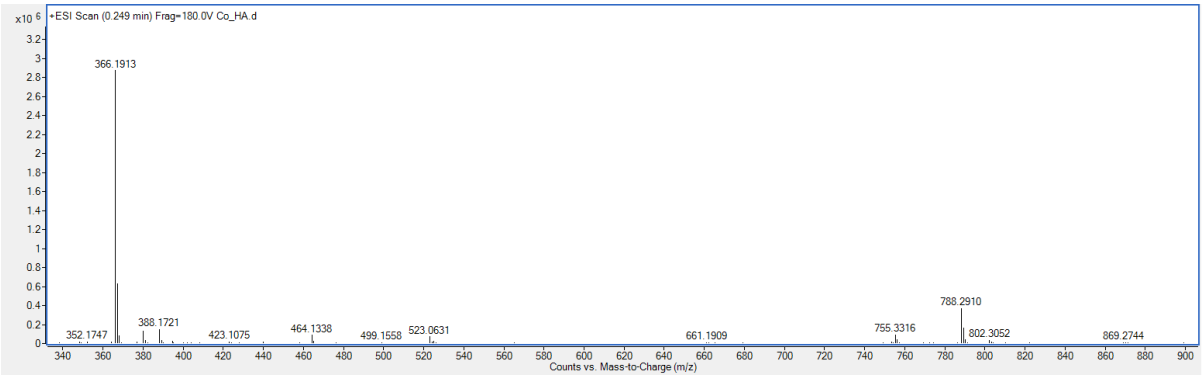


**Figure S2.** Mass spectrum ESIMS QTOF obtained by LC-MS analysis in ESI positive mode of a solution $1.0 \cdot 10^{-3}$ M of harzianic acid and $1.0 \cdot 10^{-3}$ M of $CoCl_2$ in MeOH/$H_2O$ 50:50 (*w/w*).

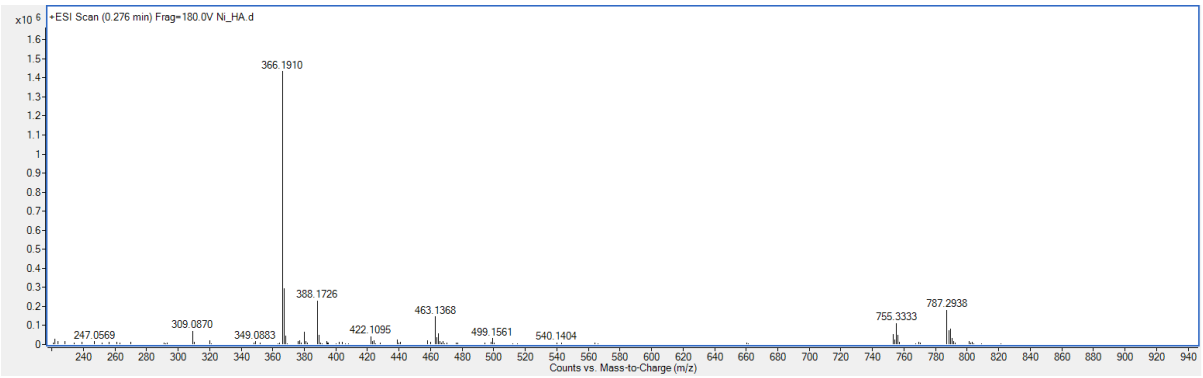


**Figure S3.** Mass spectrum ESIMS QTOF obtained by LC-MS analysis in ESI positive mode of a solution $1.0 \cdot 10^{-3}$ M of harzianic acid and $1.0 \cdot 10^{-3}$ M of $NiCl_2$ in MeOH/$H_2O$ 50:50 (*w/w*).

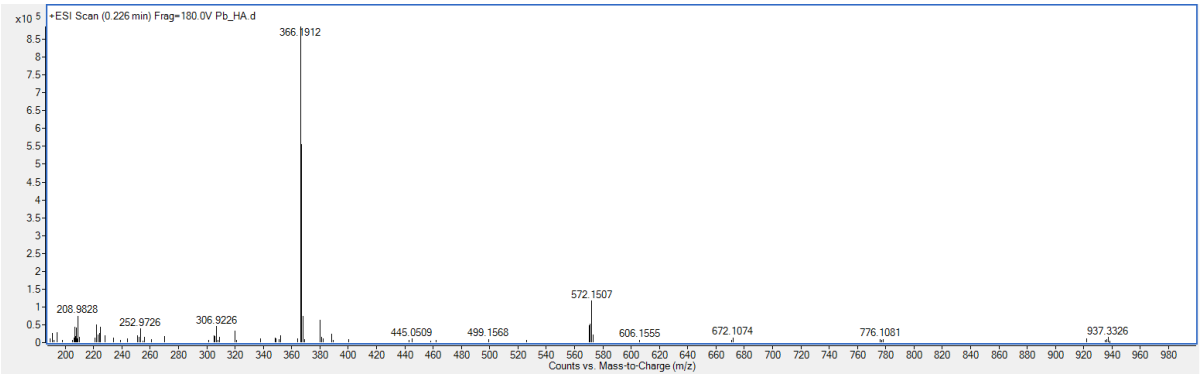


**Figure S4.** Mass spectrum ESIMS QTOF obtained by LC-MS analysis in ESI positive mode of a solution $1.0 \cdot 10^{-3}$ M of harzianic acid and $1.0 \cdot 10^{-3}$ M of $Pb(ClO_4)_2$ in $MeOH/H_2O$ 50:50 (*w/w*).

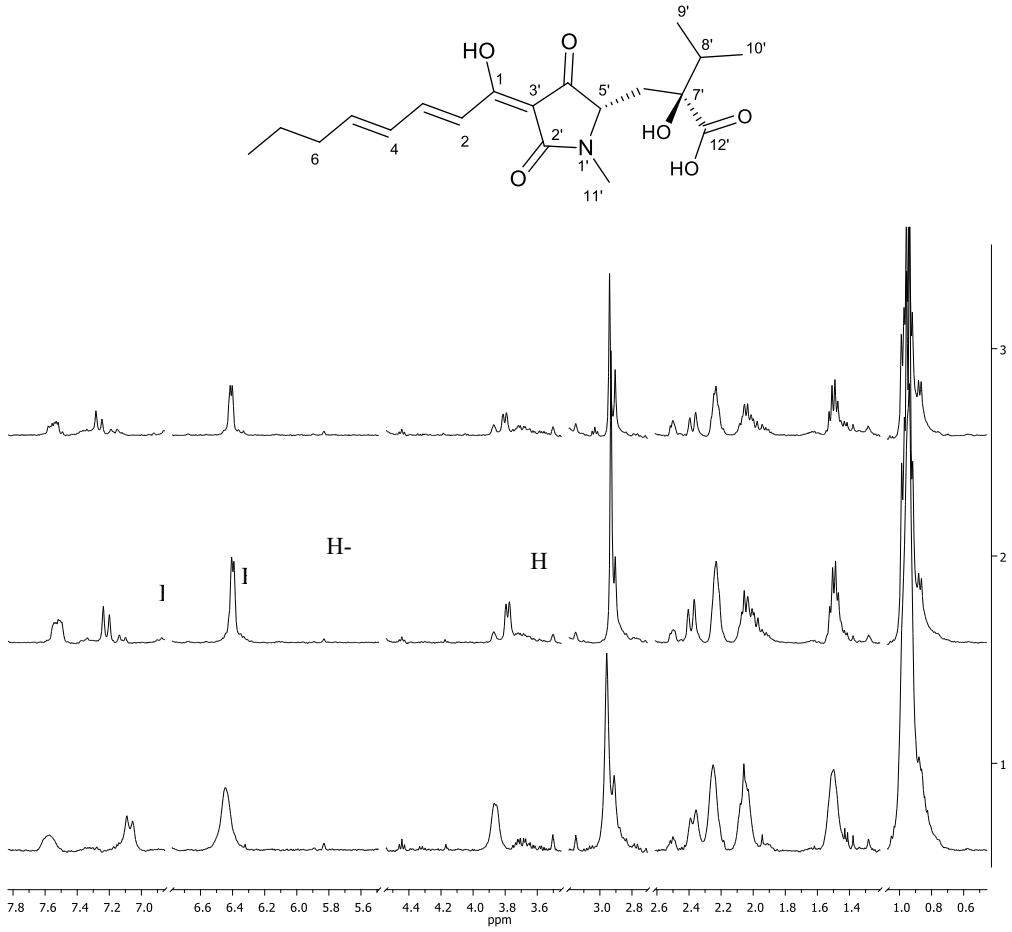


**Figure S5**. $^1H$ NMR spectra of harzianic acid (HA) (down), $Cd(ClO_4)_2$ : HA (middle) and $Pb(ClO_4)_2$ : HA (up) recorded in $CD_3OD/D_2O$ (50:50 *w/w*) at 400 MHz. Solvent peaks are removed.

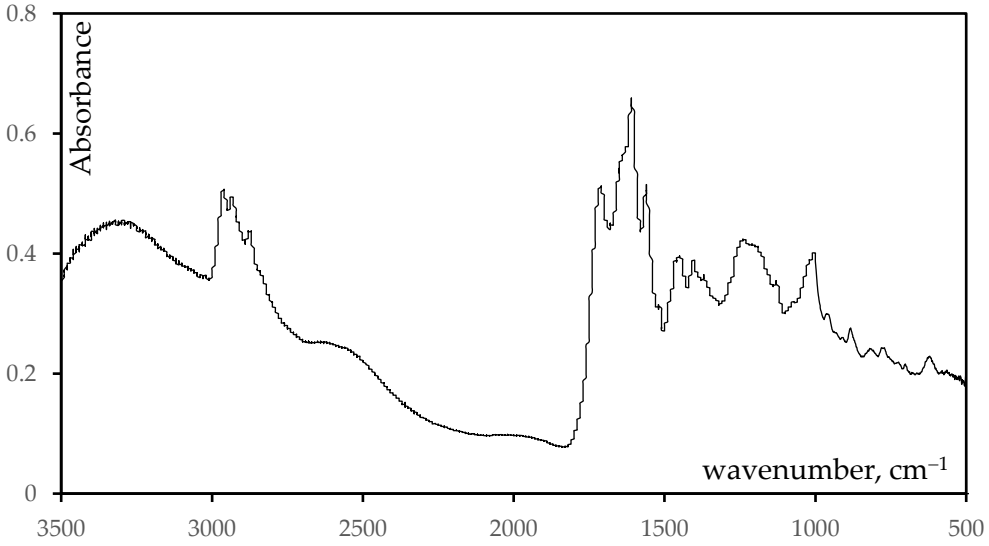


**Figure S6**. FT-IR spectrum of harzianic acid.

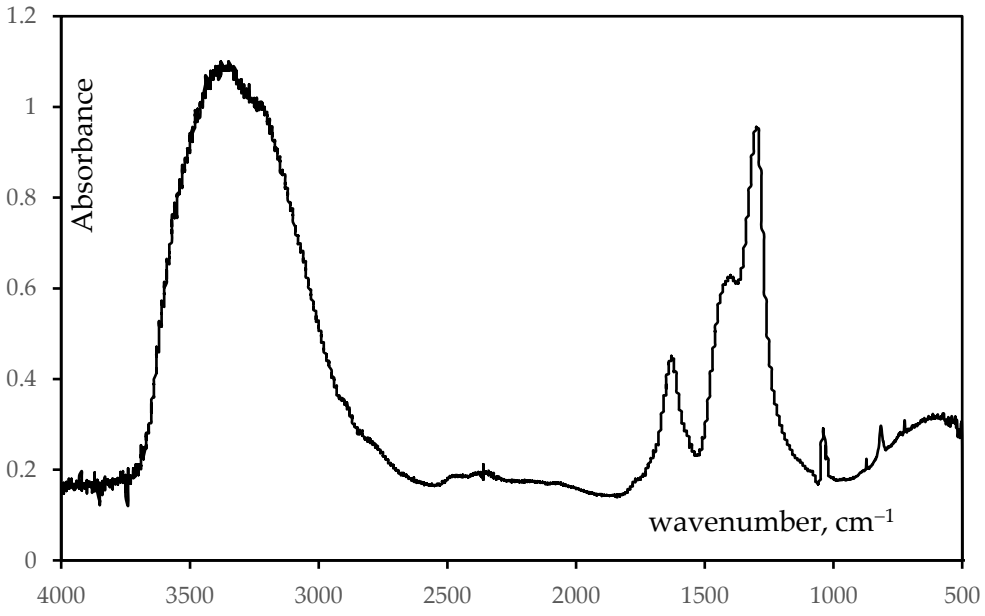


**Figure S7**. FT-IR spectrum of Cd (II)/harzianic acid complex

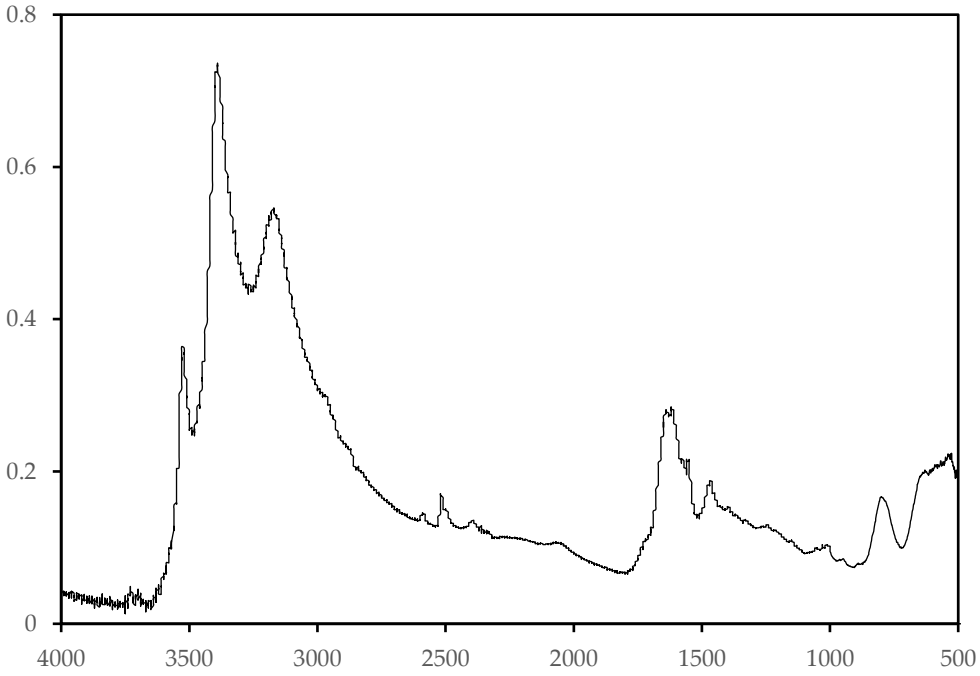


**Figure S8**. FT-IR spectrum of Co (II)/harzianic acid complex

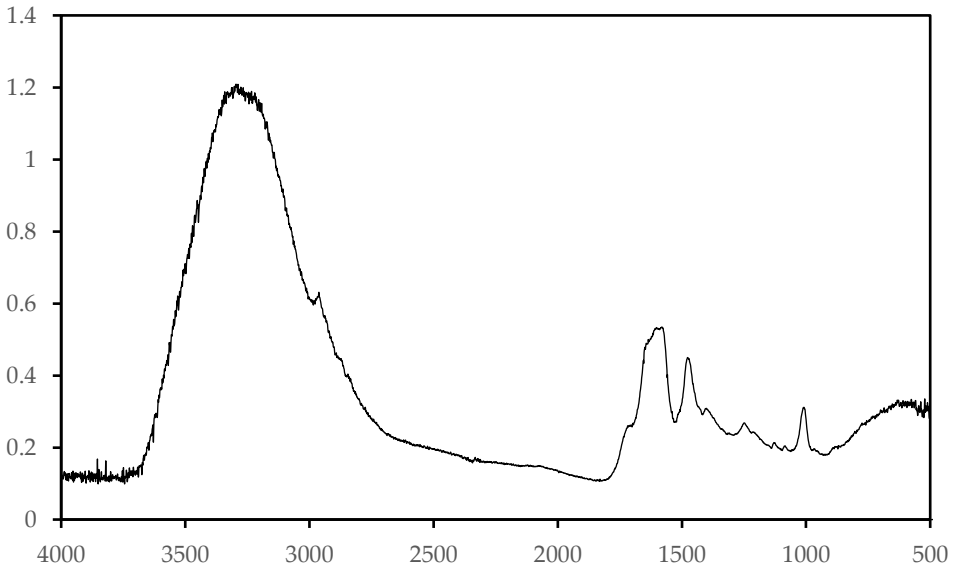


**Figure S9**. FT-IR spectrum of Ni (II)/harzianic acid complex

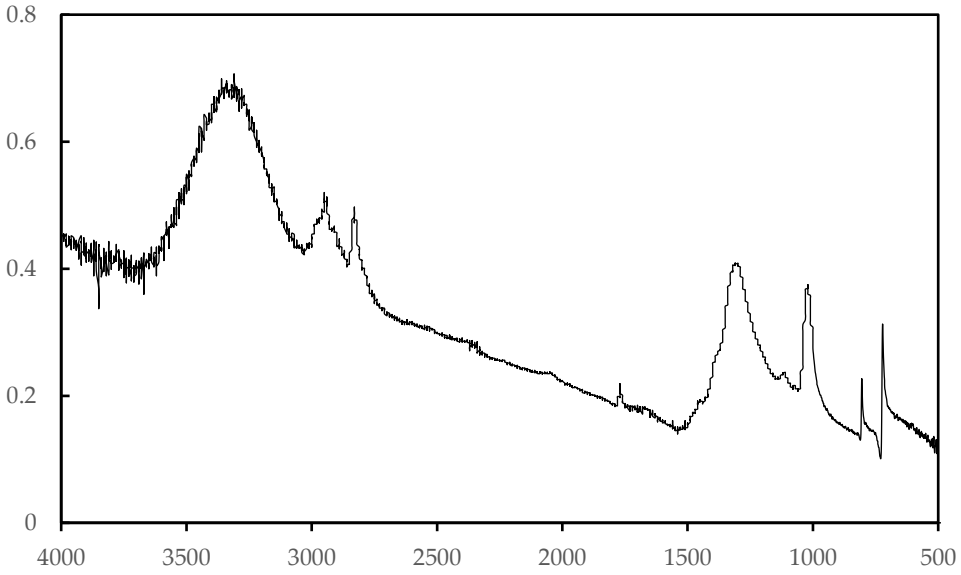


**Figure S10**. FT-IR spectrum of Pb (II)/harzianic acid complex

## Conclusions

In this research, metabolomics has been used (by extensive application of mass spectrometry technologies), together with other approaches, to investigate the interaction between different microorganisms, and the effects of microbial-based treatments on plants.

The application of *Streptomyces fulvissimus* strain AtB-42 and *Trichoderma harzianum* strain M10, singly or in combination could improve the commercial value of parsley. Isorhamnetin 3,7-di-*O*-beta-glucopyranoside, piperochromanoic acid and capsanthone are new compounds detected for the first time in parsley, and significantly induced after microbial applications. Further research is needed to gain deeper understanding of the biosynthetic pathway that results in the production of these plant molecules and their role on plant resistance and development.

The bioformulations developed to treat Genovese basil, composed of bioactive substances, selected beneficial microbes and a biopolymer (polysaccharides based), positively affected plant growth, yield and photosynthesis. Furthermore, these applications significantly altered plant metabolome and differently increased the production of three bioactive phenols: *p*-coumaric acid, caffeic acid and rosmarinic acid. These tested bioformulates can help achieving the goal of eco-sustainable agriculture and can lead to a final product with improved yield and nutraceutical value.

Formulates based on living *Trichoderma* strains and/or selected bioactive metabolites used on olive trees influenced drupes weight and phenols composition. In particular, all the treatments affected the whole metabolome and the production of flavonoids more than secoiridoids. This ability could depend on selective interaction with the enzymes involved in flavonoid and secoiridoid production. The tested *Trichoderma* strains and metabolites could be an interesting alternative to chemicals because they also positively influence desirable characteristics such as the size and antioxidant activity of olive drupes.

The complexing ability of harzianic acid, a known *Trichoderma* siderophore, has been evaluated using different bivalent metals (comprising heavy metals). Metabolomics has been used to measure the chelating capability of this metabolites in several pH conditions demonstrating that neutral or charged complexes with biologically relevant metals were formed. In the case of Cu(II), the ratio depends on the pH and is 1:1 or 1:2, while is 1:2 for Mn(II) and Zn(II). Harzianic acid was also proven to be able to form neutral or negatively charged complexes with toxic heavy metals in a metal/harzianic acid ratio 1:1 or 1:2 depending on pH (both species are present, but only one is predominant at different pH ranges). This activities are important for a potential application of harzianic acid for soil decontamination and for plant uptake of minerals.

Use of different techniques, including metabolomics, allows to discover the beneficial interactions of plant and microbes and recognize the underlying mechanisms for improvement of agricultural production. The characterization of consortia, based on selected strains (one or more) and bioactive metabolites and their influence on plants is

fundamental to develop novel bioformulates. These can be used for agricultural applications and as sustainable alternative in agro-ecosystem to improve crop production and soil quality. It is also possible to explore the potential of microbes and microbial metabolites for new applications in biodegradation and bioremediation.

In a market that constantly needs environmental-friendly and highly performing products, microbial consortia, co-inoculants and microbes-metabolites combinations represent a valid option to overcome the use of chemicals (pesticides/fertilizers) and traditional single strain-based formulations, and achieve the desired effects on crops.

## References


1 Deguine, J.-P.; Aubertot, J.-N.; Flor, R. J.; Lescourret, F.; Wyckhuys, K. A. G.; Ratnadass, A. Integrated Pest Management: Good Intentions, Hard Realities. A Review. *Agron. Sustain. Dev.* **2021**, *41* (3), 38. doi.org/10.1007/s13593-021-00689-w.

2 Leake, A. The Development of Integrated Crop Management in Agricultural Crops: Comparisons with Conventional Methods. *Pest Manag Sci* **2000**, 4. doi.org/10.1002/1526-4998(200011)56:11<950::AID-PS234>3.0.CO;2-5.

3 Chandler, D.; Davidson, G.; Grant, W. P.; Greaves, J.; Tatchell, G. M. Microbial Biopesticides for Integrated Crop Management: An Assessment of Environmental and Regulatory Sustainability. *Trends Food Sci. Technol.* **2008**, *19* (5), 275–283. doi.org/10.1016/j.tifs.2007.12.009.

4 Pimentel, D.; Zuniga, R.; Morrison, D. Update on the Environmental and Economic Costs Associated with Alien-Invasive Species in the United States. *Ecol. Econ.* **2005**, *52* (3), 273–288. doi.org/10.1016/j.ecolecon.2004.10.002.

5 Ortiz, A.; Sansinenea, E. Recent Advancements for Microorganisms and Their Natural Compounds Useful in Agriculture. *Appl. Microbiol. Biotechnol.* **2021**, *105* (3), 891–897. doi.org/10.1007/s00253-020-11030-y.

6 Burdon, F. J.; Munz, N. A.; Reyes, M.; Focks, A.; Joss, A.; Räsänen, K.; Altermatt, F.; Eggen, R. I. L.; Stamm, C. Agriculture versus Wastewater Pollution as Drivers of Macroinvertebrate Community Structure in Streams. *Sci. Total Environ.* **2019**, *659*, 1256–1265. doi.org/10.1016/j.scitotenv.2018.12.372.

7 Hedlund, J.; Longo, S. B.; York, R. Agriculture, Pesticide Use, and Economic Development: A Global Examination (1990–2014). *Rural Sociol.* **2020**, *85* (2), 519–544. doi.org/10.1111/ruso.12303.

8 Coll, M.; Wajnberg, E. *Environmental Pest Management: Challenges for Agronomists, Ecologists, Economists and Policymakers*; John Wiley & Sons, 2017.

9 Wyckhuys, K. A. G.; Aebi, A.; Bijleveld van Lexmond, M. F. I. J.; Bojaca, C. R.; Bonmatin, J.-M.; Furlan, L.; Guerrero, J. A.; Mai, T. V.; Pham, H. V.; Sanchez-Bayo, F.; Ikenaka, Y. Resolving the Twin Human and Environmental Health Hazards of a Plant-Based Diet. *Environ. Int.* **2020**, *144*, 106081. doi.org/10.1016/j.envint.2020.106081.

10 Alori, E. T.; Babalola, O. O. Microbial Inoculants for Improving Crop Quality and Human Health in Africa. *Front. Microbiol.* **2018**, *9*, 2213. doi.org/10.3389/fmicb.2018.02213.

11 Herrero, M.; Thornton, P. K.; Power, B.; Bogard, J. R.; Remans, R.; Fritz, S.; Gerber, J. S.; Nelson, G.; See, L.; Waha, K.; Watson, R. A.; West, P. C.; Samberg, L. H.; Steeg, J. van de; Stephenson, E.; Wijk, M. van; Havlík, P. Farming and the Geography of Nutrient Production for Human Use: A Transdisciplinary Analysis. *Lancet Planet. Health* **2017**, *1* (1), 33–42. doi.org/10.1016/S2542-5196(17)30007-4.

12 UN. Report of the World Commission on Environment and Development. *Rep. World Comm. Environ. Dev.* **1987**.

13 REPORT OF THE COUNCIL OF FAO https://www.fao.org/3/t0087e/t0087e00.htm

14 *Building a Common Vision for Sustainable Food and Agriculture: Principles and Approaches*; FAO, Ed.; FAO: Rome, 2014.

15 Integrated Crop Management Systems in the EU. 157.

16 *Save and Grow: A Policymaker's Guide to Sustainable Intensification of Smallholder Crop Production*; Rai, M., Reeves, T. G., Pandey, S., Collette, L., Food and Agriculture Organization of the United Nations, Eds.; Food and Agriculture Organization of the United Nations: Rome, 2011.

17 *Potato Health Management. Second Edition;* Powelson, M. L., Johnson, D. A., Eds.; Amer Phytopathological Society, St. Paul, MN, USA, 2007.

18 Mosa, W. F. A. E.-G.; Paszt, L. S.; Frąc, M.; Trzciński, P.; Treder, W.; Klamkowski, K. The Role of Biofertilizers in Improving Vegetative Growth, Yield and Fruit Quality of Apple. *Hortic. Sci.* **2018**, *45 (2018)* (No. 4), 173–180 doi.org/10.17221/101/2017-HORTSCI.

19 Costanzo, A.; Bàrberi, P. Functional Agrobiodiversity and Agroecosystem Services in Sustainable Wheat Production. A Review. *Agron. Sustain. Dev.* **2014**, *34* (2), 327–348. doi.org/10.1007/s13593-013-0178-1.

20 Cobb, A. B.; Wilson, G. W. T.; Goad, C. L.; Grusak, M. A. Influence of Alternative Soil Amendments on Mycorrhizal Fungi and Cowpea Production. *Heliyon* **2018**, *4* (7). doi.org/10.1016/j.heliyon.2018.e00704.

21 Koskey, G.; Avio, L.; Lazzaro, M.; Pellegrini, F.; Sbrana, C.; Turrini, A.; Bàrberi, P. *Smart Use of Microbial-Rich Vermicomposting to Enhance Tripartite Plant-Microbe-Soil Interactions*; EGU2020-3345; Copernicus Meetings, 2020. doi.org/10.5194/egusphere-egu2020-3345.

22 Carson, R.; Darling, L.; Darling, L.; Houghton Mifflin Company; Riverside Press (Cambridge, Mass. ). *Silent Spring*; 1962.

23 van den Bosch, R.; Stern, V. M. The Integration of Chemical and Biological Control of Arthropod Pests. *Annu. Rev. Entomol.* **1962**, *7* (1), 367–386. doi.org/10.1146/annurev.en.07.010162.002055.

24 International Code of Conduct on the Distribution and Use of Pesticides https://www.fao.org/3/y4544e/y4544e00.htm#Contents.

25 Higley, L. G.; Pedigo, L. P. *Economic Thresholds for Integrated Pest Management*; U of Nebraska Press, 1996.

26 Pedigo, L. P.; Hutchins, S. H.; Higley, L. G. Economic Injury Levels in Theory and Practice. *Annu. Rev. Entomol.* **1986**, *31* (1), 341–368. doi.org/10.1146/annurev.en.31.010186.002013.

27 EU. Directive 2009/128/EC of the European Parliament and of the Council of 21 October 2009 Establishing a Framework for Community Action to Achieve the Sustainable Use of Pesticides. *Off. J. Eur. Union* **2009**, *L*, 309.

28 Kvakkestad, V.; Steiro, Å. L.; Vatn, A. Pesticide Policies and Farm Behavior: The Introduction of Regulations for Integrated Pest Management. *Agriculture* **2021**, *11* (9), 828. doi.org/10.3390/agriculture11090828.

29 EU. Regulation (EC) No 1107/2009 of the European Parliament and of the Council of 21 October 2009 Concerning the Placing of Plant Protection Products on the Market and Repealing Council Directives 79/117/EEC and 91/414/EEC. *Off J Eur Union.* **2009**, *L*, 309.

30 Kowalska, J.; Tyburski, J.; Matysiak, K.; Tylkowski, B.; Malusá, E. Field Exploitation of Multiple Functions of Beneficial Microorganisms for Plant Nutrition and Protection: Real

Possibility or Just a Hope? *Front. Microbiol.* **2020**, *11*, 1904. doi.org/10.3389/fmicb.2020.01904.

31 Saxena, R.; Kumar, M.; Tomar, R. S. Plant–Rhizobacteria Interactions to Induce Biotic and Abiotic Stress Tolerance in Plants. In *Plant, Soil and Microbes in Tropical Ecosystems*; Dubey, S. K., Verma, S. K., Eds.; Rhizosphere Biology; Springer Singapore: Singapore, 2021; pp 1–18. doi.org/10.1007/978-981-16-3364-5_1.

32 Ahkami, A. H.; Allen White, R.; Handakumbura, P. P.; Jansson, C. Rhizosphere Engineering: Enhancing Sustainable Plant Ecosystem Productivity. *Rhizosphere* **2017**, *3*, 233–243. doi.org/10.1016/j.rhisph.2017.04.012.

33 Hakim, S.; Naqqash, T.; Nawaz, M. S.; Laraib, I.; Siddique, M. J.; Zia, R.; Mirza, M. S.; Imran, A. Rhizosphere Engineering With Plant Growth-Promoting Microorganisms for Agriculture and Ecological Sustainability. *Front. Sustain. Food Syst.* **2021**, *5*, 16. doi.org/10.3389/fsufs.2021.617157.

34 *Secondary Metabolites of Plant Growth Promoting Rhizomicroorganisms: Discovery and Applications*; Singh, H. B., Keswani, C., Reddy, M. S., Royano, E. S., García-Estrada, C., Eds.; Springer Singapore, 2019. doi.org/10.1007/978-981-13-5862-3.

35 Stenberg, J. A.; Sundh, I.; Becher, P. G.; Björkman, C.; Dubey, M.; Egan, P. A.; Friberg, H.; Gil, J. F.; Jensen, D. F.; Jonsson, M.; Karlsson, M.; Khalil, S.; Ninkovic, V.; Rehermann, G.; Vetukuri, R. R.; Viketoft, M. When Is It Biological Control? A Framework of Definitions, Mechanisms, and Classifications. *J. Pest Sci.* **2021**, *94* (3), 665–676. doi.org/10.1007/s10340-021-01354-7.

36 Köhl, J.; Kolnaar, R.; Ravensberg, W. J. Mode of Action of Microbial Biological Control Agents Against Plant Diseases: Relevance Beyond Efficacy. *Front. Plant Sci.* **2019**, *10*, 845. doi.org/10.3389/fpls.2019.00845.

37 Thomashow, L. S.; Bonsall, R. F.; Weller, D. M. Detection of Antibiotics Produced by Soil and Rhizosphere Microbes In Situ. In *Secondary Metabolites in Soil Ecology*; Karlovsky, P., Ed.; Soil Biology; Springer: Berlin, Heidelberg, 2008; pp 23–36. doi.org/10.1007/978-3-540-74543-3_2.

38 Bérdy, J. Bioactive Microbial Metabolites. *J. Antibiot. (Tokyo)* **2005**, *58* (1), 1–26. doi.org/10.1038/ja.2005.1.

39 Saxena, A. K.; Pal, K. K.; Tilak, K. V. B. R. Bacterial Biocontrol Agents and Their Role in Plant Disease Management. In *Biocontrol Potential and its Exploitation in Sustainable Agriculture: Crop Diseases, Weeds, and Nematodes*; Upadhyay, R. K., Mukerji, K. G., Chamola, B. P., Eds.; Springer US: Boston, MA, 2000; pp 25–3.7 doi.org/10.1007/978-1-4615-4209-4_3.

40 Raaijmakers, J. M.; Vlami, M.; de Souza, J. T. Antibiotic Production by Bacterial Biocontrol Agents. *Antonie Van Leeuwenhoek* **2002**, *81* (1), 537. doi.org/10.1023/A:1020501420831.

41 Ali, S.; Hameed, S.; Shahid, M.; Iqbal, M.; Lazarovits, G.; Imran, A. Functional Characterization of Potential PGPR Exhibiting Broad-Spectrum Antifungal Activity. *Microbiol. Res.* **2020**, *232*, 126389. doi.org/10.1016/j.micres.2019.126389.

42 Ongena, M.; Jacques, P. *Bacillus* Lipopeptides: Versatile Weapons for Plant Disease Biocontrol. *Trends Microbiol.* **2008**, *16* (3), 115–125. doi.org/10.1016/j.tim.2007.12.009.

43 Melo, A. L. de A.; Soccol, V. T.; Soccol, C. R. *Bacillus Thuringiensis*: Mechanism of Action, Resistance, and New Applications: A Review. *Crit. Rev. Biotechnol.* **2016**, *36* (2), 317–326. doi.org/10.3109/07388551.2014.960793.

44 Liu, X.; Cao, A.; Yan, D.; Ouyang, C.; Wang, Q.; Li, Y. Overview of Mechanisms and Uses of Biopesticides. *Int. J. Pest Manag.* **2021**, *67* (1), 65–72. doi.org/10.1080/09670874.2019.1664789.

45 Raaijmakers, J. M.; Mazzola, M. Diversity and Natural Functions of Antibiotics Produced by Beneficial and Plant Pathogenic Bacteria. *Annu. Rev. Phytopathol.* **2012**, *50* (1), 403–424. doi.org/10.1146/annurev-phyto-081211-172908.

46 Bhattacharyya, P. N.; Jha, D. K. Plant Growth-Promoting Rhizobacteria (PGPR): Emergence in Agriculture. *World J. Microbiol. Biotechnol.* **2012**, *28* (4), 1327–1350. doi.org/10.1007/s11274-011-0979-9.

47 McGuire, A. V.; Northfield, T. D. Tropical Occurrence and Agricultural Importance of *Beauveria Bassiana* and *Metarhizium Anisopliae*. *Front. Sustain. Food Syst.* **2020**, *4*, 6. doi.org/10.3389/fsufs.2020.00006.

48 Zimmermann, G. Review on Safety of the Entomopathogenic Fungus *Metarhizium Anisopliae*. *Biocontrol Sci. Technol.* **2007**, *17* (9), 879–920 doi.org/10.1080/09583150701593963.

49 Vinale, F.; Flematti, G.; Sivasithamparam, K.; Lorito, M.; Marra, R.; Skelton, B. W.; Ghisalberti, E. L. Harzianic Acid, an Antifungal and Plant Growth Promoting Metabolite from *Trichoderma Harzianum*. *J. Nat. Prod.* **2009**, *72* (11), 2032–2035. doi.org/10.1021/np900548p.

50 Vinale, F.; Sivasithamparam, K. Beneficial Effects of *Trichoderma* Secondary Metabolites on Crops. *Phytother. Res.* **2020**, *34* (11), 2835–2842. doi.org/10.1002/ptr.6728.

51 Jeffries, P. Biology and Ecology of Mycoparasitism. *Can. J. Bot.* **1995**, *73* (S1), 1284–1290. doi.org/10.1139/b95-389.

52 Budi, S. W.; van Tuinen, D.; Arnould, C.; Dumas-Gaudot, E.; Gianinazzi-Pearson, V.; Gianinazzi, S. Hydrolytic Enzyme Activity of *Paenibacillus* Sp. Strain B2 and Effects of the Antagonistic Bacterium on Cell Integrity of Two Soil-Borne Pathogenic Fungi. *Appl. Soil Ecol.* **2000**, *15* (2), 191–199. doi.org/10.1016/S0929-1393(00)00095-0.

53 Someya, N.; Kataoka, N.; Komagata, T.; Hirayae, K.; Hibi, T.; Akutsu, K. Biological Control of Cyclamen Soilborne Diseases by *Serratia Marcescens* Strain B2. *Plant Dis.* **2000**, *84* (3), 334–340. doi.org/10.1094/PDIS.2000.84.3.334.

54 Mun, B.-G.; Lee, W.-H.; Kang, S.-M.; Lee, S.-U.; Lee, S.-M.; Lee, D. Y.; Shahid, M.; Yun, B.-W.; Lee, I.-J. *Streptomyces* Sp. LH 4 Promotes Plant Growth and Resistance against *Sclerotinia Sclerotiorum* in Cucumber via Modulation of Enzymatic and Defense Pathways. *Plant Soil* **2020**, *448* (1), 87–103 doi.org/10.1007/s11104-019-04411-4.

55 Karthika, S.; Midhun, S. J.; Jisha, M. S. A Potential Antifungal and Growth-Promoting Bacterium *Bacillus* Sp. KTMA4 from Tomato Rhizosphere. *Microb. Pathog.* **2020**, *142*, 104049. doi.org/10.1016/j.micpath.2020.104049.

56 Azizoglu, U. *Bacillus Thuringiensis* as a Biofertilizer and Biostimulator: A Mini-Review of the Little-Known Plant Growth-Promoting Properties of Bt. *Curr. Microbiol.* **2019**, *76* (11), 1379–1385. doi.org/10.1007/s00284-019-01705-9.

57 McNeely, D.; Chanyi, R. M.; Dooley, J. S.; Moore, J. E.; Koval, S. F. Biocontrol of *Burkholderia Cepacia* Complex Bacteria and Bacterial Phytopathogens by *Bdellovibrio Bacteriovorus*. *Can. J. Microbiol.* **2017**, *63* (4), 350–358. doi.org/10.1139/cjm-2016-0612.

58 Harman, G. E.; Kubicek, C. P. *Trichoderma And Gliocladium, Volume 2: Enzymes, Biological Control and Commercial Applications*; CRC Press, 1998.

59 Harman, G. E.; Howell, C. R.; Viterbo, A.; Chet, I.; Lorito, M. *Trichoderma* Species — Opportunistic, Avirulent Plant Symbionts. *Nat. Rev. Microbiol.* **2004**, *2* (1), 43–56. doi.org/10.1038/nrmicro797.

60 Harman, G. E. Myths and Dogmas of Biocontrol Changes in Perceptions Derived from Research on *Trichoderma Harzinum* T-22. *Plant Dis.* **2000**, *84* (4), 377–393. doi.org/10.1094/PDIS.2000.84.4.377.

61 Vinale, F.; Sivasithamparam, K.; Ghisalberti, E. L.; Marra, R.; Woo, S. L.; Lorito, M. *Trichoderma*–Plant–Pathogen Interactions. *Soil Biol. Biochem.* **2008**, *40* (1), 1–10. doi.org/10.1016/j.soilbio.2007.07.002.

62 Mukherjee, M.; Mukherjee, P. K.; Horwitz, B. A.; Zachow, C.; Berg, G.; Zeilinger, S. *Trichoderma*–Plant–Pathogen Interactions: Advances in Genetics of Biological Control. *Indian J. Microbiol.* **2012**, *52* (4), 522–529. doi.org/10.1007/s12088-012-0308-5.

63 Lorito, M.; Harman, G. E.; Hayes, C. K.; Broadway, R. M.; Tronsmo, A.; Woo, S. L.; Di Pietro, A. Chitinolytic Enzymes Produced by *Trichoderma Harzianum*: Antifungal Activity of Purified Endochitinase and Chitobiosidase. *Phytopathol. USA* **1993**.

64 Schirmböck, M.; Lorito, M.; Wang, Y. L.; Hayes, C. K.; Arisan-Atac, I.; Scala, F.; Harman, G. E.; Kubicek, C. P. Parallel Formation and Synergism of Hydrolytic Enzymes and Peptaibol Antibiotics, Molecular Mechanisms Involved in the Antagonistic Action of *Trichoderma Harzianum* against Phytopathogenic Fungi. *Appl. Environ. Microbiol.* **1994**, *60* (12), 4364–4370. doi.org/10.1128/aem.60.12.4364-4370.1994.

65 Lorito, M.; Peterbauer, C.; Hayes, C. K.; Harman, G. E. Y. 1994. Synergistic Interaction between Fungal Cell Wall Degrading Enzymes and Different Antifungal Compounds Enhances Inhibition of Spore Germination. *Microbiology 140* (3), 623–629. doi.org/10.1099/00221287-140-3-623.

66 Köhl, J.; Fokkema, N. J. *Biological Control of Necrotrophic Foliar Fungal Pathogens*; 1998.

67 Tewari, S.; Shrivas, V. L.; Hariprasad, P.; Sharma, S. Harnessing Endophytes as Biocontrol Agents. *Plant Health Biot. Stress* **2019**, 189–218. doi.org/10.1007/978-981-13-6040-4_10.

68 Spadaro, D.; Droby, S. Development of Biocontrol Products for Postharvest Diseases of Fruit: The Importance of Elucidating the Mechanisms of Action of Yeast Antagonists. *Trends Food Sci. Technol.* **2016**, *47*, 39–49. doi.org/10.1016/j.tifs.2015.11.003.

69 Whipps, J. M. Microbial Interactions and Biocontrol in the Rhizosphere. *J. Exp. Bot.* **2001**, *52* (suppl_1), 487–511. doi.org/10.1093/jxb/52.suppl_1.487.

70 van Loon, L. C. Helping Plants To Defend Themselves: Biocontrol By Disease-Suppressing Rhizobacteria. In *Developments in Plant Genetics and Breeding*; de Vries, G. E., Metzlaff, K., Eds.; Highlights in European Plant Biotechnology Research and Technology Transfer; Elsevier, 2000; Vol. 6, pp 203–213 doi.org/10.1016/S0168-7972(00)80123-1.

71 Renshaw, J. C.; Robson, G. D.; Trinci, A. P. J.; Wiebe, M. G.; Livens, F. R.; Collison, D.; Taylor, R. J. Fungal Siderophores: Structures, Functions and Applications. *Mycol. Res.* **2002**, *106* (10), 1123–1142. doi.org/10.1017/S0953756202006548.

72 Hider, R. C.; Kong, X. Chemistry and Biology of Siderophores. *Nat. Prod. Rep.* **2010**, *27* (5), 637–657. doi.org/10.1039/B906679A.

73 Riquelme, M. Fungal Siderophores in Plant-Microbe Interactions. *Microbiol. Madr. Spain* **1996**, *12* (4), 537–546.

74 *Microbial Siderophores*; Varma, A., Chincholkar, S. B., Eds.; Soil biology; Springer: Berlin ; New York, 2007.

75 Mustafa, S.; Kabir, S.; Shabbir, U.; Batool, R. Plant Growth Promoting Rhizobacteria in Sustainable Agriculture: From Theoretical to Pragmatic Approach. *Symbiosis* **2019**, *78* (2), 115–123. doi.org/10.1007/s13199-019-00602-w.

76 Conrath, U.; Beckers, G. J. M.; Langenbach, C. J. G.; Jaskiewicz, M. R. Priming for Enhanced Defense. *Annu. Rev. Phytopathol.* **2015**, *53* (1), 97–119. doi.org/10.1146/annurev-phyto-080614-120132.

77 Bukhat, S.; Imran, A.; Javaid, S.; Shahid, M.; Majeed, A.; Naqqash, T. Communication of Plants with Microbial World: Exploring the Regulatory Networks for PGPR Mediated Defense Signaling. *Microbiol. Res.* **2020**, *238*, 126486 doi.org/10.1016/j.micres.2020.126486.

78 Nowak, J.; Shulaev, V. Priming for Transplant Stress Resistance in In Vitro Propagation. *Vitro Cell. Dev. Biol. - Plant* **2003**, *39* (2), 107–124. doi.org/10.1079/IVP2002403.

79 Choudhary, D. K.; Prakash, A.; Johri, B. N. Induced Systemic Resistance (ISR) in Plants: Mechanism of Action. *Indian J. Microbiol.* **2007**, *47* (4), 289–297 doi.org/10.1007/s12088-007-0054-2.

80 Choudhary, D. K.; Johri, B. N. Interactions of *Bacillus* Spp. and Plants – With Special Reference to Induced Systemic Resistance (ISR). *Microbiol. Res.* **2009**, *164* (5), 493–513. doi.org/10.1016/j.micres.2008.08.007.

81 Mazzei, P.; Vinale, F.; Woo, S. L.; Pascale, A.; Lorito, M.; Piccolo, A. Metabolomics by Proton High-Resolution Magic-Angle-Spinning Nuclear Magnetic Resonance of Tomato Plants Treated with Two Secondary Metabolites Isolated from *Trichoderma*. *J. Agric. Food Chem.* **2016**, *64* (18), 3538–3545. doi.org/10.1021/acs.jafc.6b00801.

82 Velazquez-Robledo, R.; Contreras-Cornejo, H. A.; Macias-Rodriguez, L.; Hernandez-Morales, A.; Aguirre, J.; Casas-Flores, S.; Lopez-Bucio, J.; Herrera-Estrella, A. Role of the 4-Phosphopantetheinyl Transferase of *Trichoderma Virens* in Secondary Metabolism and Induction of Plant Defense Responses. *Mol. Plant-Microbe Interact. MPMI* **2011**, *24* (12), 1459–1471. doi.org/10.1094/MPMI-02-11-0045.

83 Malmierca, M. G.; Barua, J.; McCormick, S. P.; Izquierdo-Bueno, I.; Cardoza, R. E.; Alexander, N. J.; Hermosa, R.; Collado, I. G.; Monte, E.; Gutiérrez, S. Novel Aspinolide Production by *Trichoderma Arundinaceum* with a Potential Role in *Botrytis Cinerea* Antagonistic Activity and Plant Defence Priming. *Environ. Microbiol.* **2015**, *17* (4), 1103–1118. doi.org/10.1111/1462-2920.12514.

84 Lorito, M.; Woo, S. L.; Harman, G. E.; Monte, E. Translational Research on *Trichoderma* : From 'Omics to the Field. *Annu. Rev. Phytopathol.* **2010**, *48* (1), 395–417. doi.org/10.1146/annurev-phyto-073009-114314.

85 Pandey, A.; Tripathi, A.; Srivastava, P.; Choudhary, K. K.; Dikshit, A. 1 - Plant GrowthPromoting Microorganisms in Sustainable Agriculture. In *Role of Plant Growth Promoting Microorganisms in Sustainable Agriculture and Nanotechnology*; Kumar, A., Singh, A. K., Choudhary, K. K., Eds.; Woodhead Publishing, 2019; pp 1–19. doi.org/10.1016/B978-0-12-817004-5.00001-4.

86 Abhilash, P. C.; Dubey, R. K.; Tripathi, V.; Gupta, V. K.; Singh, H. B. Plant Growth-Promoting Microorganisms for Environmental Sustainability. *Trends Biotechnol.* **2016**, *34* (11), 847–850. doi.org/10.1016/j.tibtech.2016.05.005.

87 Sharma, S. B.; Sayyed, R. Z.; Trivedi, M. H.; Gobi, T. A. Phosphate Solubilizing Microbes: Sustainable Approach for Managing Phosphorus Deficiency in Agricultural Soils. *Springer Plus* **2013**, *2* (1), 587. doi.org/10.1186/2193-1801-2-587.

88 Sharma, S.; Kumar, V.; Tripathi, R. B. Isolation of Phosphate Solubilizing Microorganism (PSMs) From Soil. *J. Microbiol. Biotechnol. Res.* **2011**, *1*, 90–95.

89 Illmer, P.; Schinner, F. Solubilization of Inorganic Calcium Phosphates—Solubilization Mechanisms. *Soil Biol. Biochem.* **1995**, *27* (3), 257–263. doi.org/10.1016/0038-0717(94)00190-C.

90 Rengel, Z.; Marschner, P. Nutrient Availability and Management in the Rhizosphere: Exploiting Genotypic Differences. *New Phytol.* **2005**, *168* (2), 305–312. doi.org/10.1111/j.1469-8137.2005.01558.x.

91 Khan, Md. S.; Zaidi, A.; Ahmad, E. Mechanism of Phosphate Solubilization and Physiological Functions of Phosphate-Solubilizing Microorganisms. In *Phosphate Solubilizing Microorganisms*; Khan, M. S., Zaidi, A., Musarrat, J., Eds.; Springer International Publishing: Cham, 2014; pp 31–62. doi.org/10.1007/978-3-319-08216-5_2.

92 Antoun, H. Beneficial Microorganisms for the Sustainable Use of Phosphates in Agriculture. *Procedia Eng.* **2012**, *46*, 62–67. doi.org/10.1016/j.proeng.2012.09.446.

93 Patel, D.; Goswami, D. Phosphorus Solubilization and Mobilization: Mechanisms, Current Developments, and Future Challenge. In *Advances in Plant Microbiome and Sustainable Agriculture*; Yadav, A. N., Rastegari, A. A., Yadav, N., Kour, D., Eds.; Microorganisms for Sustainability; Springer Singapore: Singapore, 2020; Vol. 20, pp 1–20. doi.org/10.1007/978-981-15-3204-7_1.

94 Kalayu, G. Phosphate Solubilizing Microorganisms: Promising Approach as Biofertilizers. *Int. J. Agron.* **2019**, *2019*, e4917256. doi.org/10.1155/2019/4917256.

95 Park, K.-H.; Lee, C.-Y.; Son, H.-J. Mechanism of Insoluble Phosphate Solubilization by *Pseudomonas Fluorescens* RAF15 Isolated from Ginseng Rhizosphere and Its Plant Growth-Promoting Activities. *Lett. Appl. Microbiol.* **2009**, *49* (2), 222–228. doi.org/10.1111/j.1472-765X.2009.02642.x.

96 Hanif, M. K.; Malik, K. A.; Hameed, S.; Saddique, M. J.; Ayesha; Fatima, K.; Naqqash, T.; Majeed, A.; Iqbal, M. J.; Imran, A. Growth Stimulatory Effect of AHL Producing *Serratia* Spp. from Potato on Homologous and Non-Homologous Host Plants. *Microbiol. Res.* **2020**, *238*, 126506. doi.org/10.1016/j.micres.2020.126506.

97 Din, M.; Nelofer, R.; Salman, M.; Abdullah; Khan, F. H.; Khan, A.; Ahmad, M.; Jalil, F.; Din, J. U.; Khan, M. Production of Nitrogen Fixing *Azotobacter* (SR-4) and Phosphorus Solubilizing *Aspergillus Niger* and Their Evaluation on *Lagenaria Siceraria* and *Abelmoschus Esculentus*. *Biotechnol. Rep.* **2019**, *22*, e00323. doi.org/10.1016/j.btre.2019.e00323.

98 Altomare, C.; Norvell, W. A.; Björkman, T.; Harman, G. E. Solubilization of Phosphates and Micronutrients by the Plant-Growth-Promoting and Biocontrol Fungus *Trichoderma Harzianum* Rifai 1295-22. *Appl. Environ. Microbiol.* **1999**, *65* (7), 2926–2933. doi.org/10.1128/AEM.65.7.2926-2933.1999.

99 Azeem, M.; Riaz, A.; Chaudhary, A. N.; Hayat, R.; Hussain, Q.; Tahir, M. I.; Imran, M. Microbial Phytase Activity and Their Role in Organic P Mineralization. *Arch. Agron. Soil Sci.* **2015**, *61* (6), 751–766. doi.org/10.1080/03650340.2014.963796.

100 Aseri, G.; Jain, N.; Tarafdar, J. Hydrolysis of Organic Phosphate Forms by Phosphatases and Phytase Producing Fungi of Arid and Semi-Arid Soils of India. *Eurasian J Agric Environ Sci* **2009**, *5*, 564–570.

101 Chouyia, F. E.; Romano, I.; Fechtali, T.; Fagnano, M.; Fiorentino, N.; Visconti, D.; Idbella, M.; Ventorino, V.; Pepe, O. P-Solubilizing *Streptomyces Roseocinereus* MS1B15 With Multiple Plant Growth-Promoting Traits Enhance Barley Development and Regulate Rhizosphere Microbial Population. *Front. Plant Sci.* **2020**, *11*, 1137. doi.org/10.3389/fpls.2020.01137.

102 Zhang, X.; Zhang, D.; Sun, W.; Wang, T. The Adaptive Mechanism of Plants to Iron Deficiency via Iron Uptake, Transport, and Homeostasis. *Int. J. Mol. Sci.* **2019**, *20* (10), 2424. doi.org/10.3390/ijms20102424.

103 Takagi, S. Naturally Occurring Iron-Chelating Compounds in Oat- and Rice-Root Washings. *Soil Sci. Plant Nutr.* **1976**, *22* (4), 423–433. doi.org/10.1080/00380768.1976.10433004.

104 Mori, S. Iron Acquisition by Plants. *Curr. Opin. Plant Biol.* **1999**, *2* (3), 250–253. doi.org/10.1016/S1369-5266(99)80043-0.

105 Ghosh, S. K.; Bera, T.; Chakrabarty, A. M. Microbial Siderophore – A Boon to Agricultural Sciences. *Biol. Control* **2020**, *144*, 104214. doi.org/10.1016/j.biocontrol.2020.104214.

106 Curie, C.; Panaviene, Z.; Loulergue, C.; Dellaporta, S. L.; Briat, J.-F.; Walker, E. L. Maize Yellow Stripe1 Encodes a Membrane Protein Directly Involved in Fe(III) Uptake. *Nature* **2001**, *409* (6818), 346–349. doi.org/10.1038/35053080.

107 Oh, Y. J.; Kim, H.; Seo, S. H.; Hwang, B. G.; Chang, Y. S.; Lee, J.; Lee, D. W.; Sohn, E. J.; Lee, S. J.; Lee, Y.; Hwang, I. Cytochrome B5 Reductase 1 Triggers Serial Reactions That Lead to Iron Uptake in Plants. *Mol. Plant* **2016**, *9* (4), 501–513. doi.org/10.1016/j.molp.2015.12.010.

108 Gupta, G.; Panwar, J.; Akhtar, M. S.; Jha, P. N. Endophytic Nitrogen-Fixing Bacteria as Biofertilizer. In *Sustainable Agriculture Reviews: Volume 11*; Lichtfouse, E., Ed.; Sustainable Agriculture Reviews; Springer Netherlands: Dordrecht, 2012; pp 183–221. doi.org/10.1007/978-94-007-5449-2_8.

109 Beeckman, F.; Motte, H.; Beeckman, T. Nitrification in Agricultural Soils: Impact, Actors and Mitigation. *Curr. Opin. Biotechnol.* **2018**, *50*, 166–173. doi.org/10.1016/j.copbio.2018.01.014.

110 Andrews, M.; Andrews, M. E. Specificity in Legume-Rhizobia Symbioses. *Int. J. Mol. Sci.* **2017**, *18* (4), 705. doi.org/10.3390/ijms18040705.

111 Gupta, G.; Parihar, S. S.; Ahirwar, N. K.; Snehi, S. K.; Singh, V. Plant Growth Promoting Rhizobacteria (PGPR): Current and Future Prospects for Development of Sustainable Agriculture. *J. Microb. Biochem. Technol.* **2015**, *07* (02), 96–102. doi.org/10.4172/1948-5948.1000188.

112 Burris, R. H.; Roberts, G. P. Biological Nitrogen Fixation. *Annu. Rev. Nutr.* **1993**, *13* (1), 317–335. doi.org/10.1146/annurev.nu.13.070193.001533.

113 Dance, I. Elucidating the Coordination Chemistry and Mechanism of Biological Nitrogen Fixation. *Chem. – Asian J.* **2007**, *2* (8), 936–946. doi.org/10.1002/asia.200700131.

114 Peleg, Z.; Blumwald, E. Hormone Balance and Abiotic Stress Tolerance in Crop Plants. *Curr. Opin. Plant Biol.* **2011**, *14* (3), 290–295. doi.org/10.1016/j.pbi.2011.02.001.

115 Oleńska, E.; Małek, W.; Wójcik, M.; Swiecicka, I.; Thijs, S.; Vangronsveld, J. Beneficial Features of Plant Growth-Promoting Rhizobacteria for Improving Plant Growth and Health in Challenging Conditions: A Methodical Review. *Sci. Total Environ.* **2020**, *743*, 140682. doi.org/10.1016/j.scitotenv.2020.140682.

116 Illescas, M.; Pedrero-Méndez, A.; Pitorini-Bovolini, M.; Hermosa, R.; Monte, E. Phytohormone Production Profiles in *Trichoderma* Species and Their Relationship to Wheat Plant Responses to Water Stress. *Pathogens* **2021**, *10* (8), 991. doi.org/10.3390/pathogens10080991.

117 Amara, U.; Khalid, R.; Hayat, R. Soil Bacteria and Phytohormones for Sustainable Crop Production. In *Bacterial Metabolites in Sustainable Agroecosystem*; Maheshwari, D. K., Ed.; Sustainable Development and Biodiversity; Springer International Publishing: Cham, 2015; Vol. 12, pp 87–103. doi.org/10.1007/978-3-319-24654-3_5.

118 Spaepen, S.; Vanderleyden, J.; Remans, R. Indole-3-Acetic Acid in Microbial and Microorganism-Plant Signaling. *FEMS Microbiol. Rev.* **2007**, *31* (4), 425–448. doi.org/10.1111/j.1574-6976.2007.00072.x.

119 Fu, S.-F.; Wei, J.-Y.; Chen, H.-W.; Liu, Y.-Y.; Lu, H.-Y.; Chou, J.-Y. Indole-3-Acetic Acid: A Widespread Physiological Code in Interactions of Fungi with Other Organisms. *Plant Signal. Behav.* **2015**, *10* (8), e1048052. doi.org/10.1080/15592324.2015.1048052.

120 Numponsak, T.; Kumla, J.; Suwannarach, N.; Matsui, K.; Lumyong, S. Biosynthetic Pathway and Optimal Conditions for the Production of Indole-3-Acetic Acid by an Endophytic Fungus, *Colletotrichum Fructicola* CMU-A109. *PLOS ONE* **2018**, *13* (10), e0205070. doi.org/10.1371/journal.pone.0205070.

121 Myo, E. M.; Ge, B.; Ma, J.; Cui, H.; Liu, B.; Shi, L.; Jiang, M.; Zhang, K. Indole-3-Acetic Acid Production by *Streptomyces Fradiae* NKZ-259 and Its Formulation to Enhance Plant Growth. *BMC Microbiol.* **2019**, *19* (1), 155. doi.org/10.1186/s12866-019-1528-1.

122 Contreras-Cornejo, H. A.; Macías-Rodríguez, L.; Cortés-Penagos, C.; López-Bucio, J. *Trichoderma Virens* , a Plant Beneficial Fungus, Enhances Biomass Production and Promotes Lateral Root Growth through an Auxin-Dependent Mechanism in *Arabidopsis*. *Plant Physiol.* **2009**, *149* (3), 1579–1592. doi.org/10.1104/pp.108.130369.

123 Osugi, A.; Sakakibara, H. Q&A: How Do Plants Respond to Cytokinins and What Is Their Importance? *BMC Biol.* **2015**, *13* (1), 102 doi.org/10.1186/s12915-015-0214-5.

124 Chanclud, E.; Morel, J. Plant Hormones: A Fungal Point of View. *Mol. Plant Pathol.* **2016**, *17* (8), 1289–1297. doi.org/10.1111/mpp.12393.

125 Greene, E. M. Cytokinin Production by Microorganisms. *Bot. Rev.* **1980**, *46* (1), 25–74. doi.org/10.1007/BF02860866.

126 Crafts, C. B.; Miller, C. O. Detection and Identification of Cytokinins Produced by Mycorrhizal Fungi. *Plant Physiol.* **1974**, *54* (4), 586–588. doi.org/10.1104/pp.54.4.586.

127 Binenbaum, J.; Weinstain, R.; Shani, E. Gibberellin Localization and Transport in Plants. *Trends Plant Sci.* **2018**, *23* (5), 410–421. doi.org/10.1016/j.tplants.2018.02.005.

128 Tudzynski, B.; Studt, L.; Rojas, M. C. Gibberellins in Fungi, Bacteria and Lower Plants: Biosynthesis, Function and Evolution. In *Annual Plant Reviews, Volume 49*; John Wiley & Sons, Ltd, 2016; pp 121–152. doi.org/10.1002/9781119210436.ch5.

129 Atzorn, R.; Crozier, A.; Wheeler, C. T.; Sandberg, G. Production of Gibberellins and Indole-3-Acetic Acid by *Rhizobium Phaseoli* in Relation to Nodulation of *Phaseolus Vulgaris* Roots. *Planta* **1988**, *175* (4), 532–538. doi.org/10.1007/BF00393076.

130 Borrow, A.; Brian, P. W.; Chester, V. E.; Curtis, P. J.; Hemming, H. G.; Henehan, C.; Jeffreys, E. G.; Lloyd, P. B.; Nixon, I. S.; Norris, G. L. F.; Radley, M. Gibberellic Acid, a Metabolic Product of the Fungus *Gibberella Fujikuroi*: Some Observations on Its Production and Isolation. *J. Sci. Food Agric.* **1955**, *6* (6), 340–348. doi.org/10.1002/jsfa.2740060609.

131 Kim, M.-J.; Radhakrishnan, R.; Kang, S.-M.; You, Y.-H.; Jeong, E.-J.; Kim, J.-G.; Lee, I.-J. Plant Growth Promoting Effect of *Bacillus Amyloliquefaciens* H-2-5 on Crop Plants and Influence on Physiological Changes in Soybean under Soil Salinity. *Physiol. Mol. Biol. Plants* **2017**, *23* (3), 571–580. doi.org/10.1007/s12298-017-0449-4.

132 Kang, S.-M.; Radhakrishnan, R.; Khan, A. L.; Kim, M.-J.; Park, J.-M.; Kim, B.-R.; Shin, D.-H.; Lee, I.-J. Gibberellin Secreting Rhizobacterium, *Pseudomonas Putida* H-2-3 Modulates the Hormonal and Stress Physiology of Soybean to Improve the Plant Growth under Saline and Drought Conditions. *Plant Physiol. Biochem.* **2014**, *84*, 115–124. doi.org/10.1016/j.plaphy.2014.09.001.

133 Kamalov, L. S.; Turgunov, K. K.; Aripova, S. F.; Abdilalimov, O. Gibberillin A-3 from the Microscopic Fungus *Trichoderma Harzianum*. *Chem. Nat. Compd.* **2018**, *54* (2), 421–422. doi.org/10.1007/s10600-018-2368-1.

134 Coleman-Derr, D.; Tringe, S. G. Building the Crops of Tomorrow: Advantages of Symbiont-Based Approaches to Improving Abiotic Stress Tolerance. *Front. Microbiol.* **2014**, *5* doi.org/10.3389/fmicb.2014.00283.

135 Jiang, Q.-Y.; Zhuo, F.; Long, S.-H.; Zhao, H.-D.; Yang, D.-J.; Ye, Z.-H.; Li, S.-S.; Jing, Y.-X. Can Arbuscular Mycorrhizal Fungi Reduce Cd Uptake and Alleviate Cd Toxicity of *Lonicera Japonica* Grown in Cd-Added Soils? *Sci. Rep.* **2016**, *6* (1), 21805. doi.org/10.1038/srep21805.

136 Singh, A.; Roychoudhury, A. Augmenting the Abiotic Stress Tolerance in Plants Through Microbial Association. In *Microbial Metatranscriptomics Belowground*; Nath, M., Bhatt, D., Bhargava, P., Choudhary, D. K., Eds.; Springer Singapore: Singapore, 2021; pp 179–198. doi.org/10.1007/978-981-15-9758-9_9.

137 Asghari, B.; Khademian, R.; Sedaghati, B. Plant Growth Promoting Rhizobacteria (PGPR) Confer Drought Resistance and Stimulate Biosynthesis of Secondary Metabolites in Pennyroyal (*Mentha Pulegium* L.) under Water Shortage Condition. *Sci. Hortic.* **2020**, *263*, 109132. doi.org/10.1016/j.scienta.2019.109132.

138 Dana, M. de las M.; Pintor-Toro, J. A.; Cubero, B. Transgenic Tobacco Plants Overexpressing Chitinases of Fungal Origin Show Enhanced Resistance to Biotic and Abiotic Stress Agents. *Plant Physiol.* **2006**, *142* (2), 722–730. doi.org/10.1104/pp.106.086140.

139 Khan, M. A.; Asaf, S.; Khan, A. L.; Jan, R.; Kang, S.-M.; Kim, K.-M.; Lee, I.-J. Extending Thermotolerance to Tomato Seedlings by Inoculation with SA1 Isolate of *Bacillus Cereus* and Comparison with Exogenous Humic Acid Application. *PLOS ONE* **2020**, *15* (4), e0232228. doi.org/10.1371/journal.pone.0232228.

140 Khan, A. L.; Hamayun, M.; Kang, S.-M.; Kim, Y.-H.; Jung, H.-Y.; Lee, J.-H.; Lee, I.-J. Endophytic Fungal Association via Gibberellins and Indole Acetic Acid Can Improve Plant Growth under Abiotic Stress: An Example of *Paecilomyces Formosus* LHL10. *BMC Microbiol.* **2012**, *12* (1), 3. doi.org/10.1186/1471-2180-12-3.

141 Ripa, F. A.; Cao, W.; Tong, S.; Sun, J. Assessment of Plant Growth Promoting and Abiotic Stress Tolerance Properties of Wheat Endophytic Fungi. *BioMed Res. Int.* **2019**, *2019*, 1–12. doi.org/10.1155/2019/6105865.

142 Kaushal, M.; Wani, S. P. Rhizobacterial-Plant Interactions: Strategies Ensuring Plant Growth Promotion under Drought and Salinity Stress. *Agric. Ecosyst. Environ.* **2016**, *231*, 68–78. doi.org/10.1016/j.agee.2016.06.031.

143 Ngumbi, E.; Kloepper, J. Bacterial-Mediated Drought Tolerance: Current and Future Prospects. *Appl. Soil Ecol.* **2016**, *105*, 109–125. doi.org/10.1016/j.apsoil.2016.04.009.

144 Van Oosten, M. J.; Pepe, O.; De Pascale, S.; Silletti, S.; Maggio, A. The Role of Biostimulants and Bioeffectors as Alleviators of Abiotic Stress in Crop Plants. *Chem. Biol. Technol. Agric.* **2017**, *4* (1), 5. doi.org/10.1186/s40538-017-0089-5.

145 Gupta, S.; Schillaci, M.; Walker, R.; Smith, P. M. C.; Watt, M.; Roessner, U. Alleviation of Salinity Stress in Plants by Endophytic Plant-Fungal Symbiosis: Current Knowledge, Perspectives and Future Directions. *Plant Soil* **2021**, *461* (1–2), 219–244. doi.org/10.1007/s11104-020-04618-w.

146 Meena, K. K.; Sorty, A. M.; Bitla, U. M.; Choudhary, K.; Gupta, P.; Pareek, A.; Singh, D. P.; Prabha, R.; Sahu, P. K.; Gupta, V. K.; Singh, H. B.; Krishanani, K. K.; Minhas, P. S. Abiotic Stress Responses and Microbe-Mediated Mitigation in Plants: The Omics Strategies. *Front. Plant Sci.* **2017**, *8.* doi.org/10.3389/fpls.2017.00172.

147 Ali, Sk. Z.; Sandhya, V.; Grover, M.; Kishore, N.; Rao, L. V.; Venkateswarlu, B. *Pseudomonas* Sp. Strain AKM-P6 Enhances Tolerance of Sorghum Seedlings to Elevated Temperatures. *Biol. Fertil. Soils* **2009**, *46* (1), 45–55. doi.org/10.1007/s00374-009-0404-9.

148 Tank, N.; Saraf, M. Salinity-Resistant Plant Growth Promoting Rhizobacteria Ameliorates Sodium Chloride Stress on Tomato Plants. *J. Plant Interact.* **2010**, *5* (1), 51–58. doi.org/10.1080/17429140903125848.

149 Sorty, A. M.; Meena, K. K.; Choudhary, K.; Bitla, U. M.; Minhas, P. S.; Krishnani, K. K. Effect of Plant Growth Promoting Bacteria Associated with Halophytic Weed (*Psoralea Corylifolia* L) on Germination and Seedling Growth of Wheat Under Saline Conditions. *Appl. Biochem. Biotechnol.* **2016**, *180* (5), 872–882. doi.org/10.1007/s12010-016-2139-z.

150 Van Oosten, M. J.; Di Stasio, E.; Cirillo, V.; Silletti, S.; Ventorino, V.; Pepe, O.; Raimondi, G.; Maggio, A. Root Inoculation with *Azotobacter Chroococcum* 76A Enhances Tomato Plants Adaptation to Salt Stress under Low N Conditions. *BMC Plant Biol.* **2018**, *18* (1), 205. doi.org/10.1186/s12870-018-1411-5.

151 Shahzad, R.; Khan, A. L.; Bilal, S.; Waqas, M.; Kang, S.-M.; Lee, I.-J. Inoculation of Abscisic Acid-Producing Endophytic Bacteria Enhances Salinity Stress Tolerance in *Oryza Sativa*. *Environ. Exp. Bot.* **2017**, *136*, 68–77. doi.org/10.1016/j.envexpbot.2017.01.010.

152 Waqas, M.; Khan, A. L.; Kamran, M.; Hamayun, M.; Kang, S.-M.; Kim, Y.-H.; Lee, I.-J. Endophytic Fungi Produce Gibberellins and Indoleacetic Acid and Promotes Host-Plant Growth during Stress. *Molecules* **2012**, *17* (9), 10754–10773. doi.org/10.3390/molecules170910754.

153 Waller, F.; Achatz, B.; Baltruschat, H.; Fodor, J.; Becker, K.; Fischer, M.; Heier, T.; Huckelhoven, R.; Neumann, C.; von Wettstein, D.; Franken, P.; Kogel, K.-H. The Endophytic Fungus *Piriformospora Indica* Reprograms Barley to Salt-Stress Tolerance, Disease Resistance, and Higher Yield. *Proc. Natl. Acad. Sci.* **2005**, *102* (38), 13386–13391. doi.org/10.1073/pnas.0504423102.

154 Radhakrishnan, R.; Khan, A. L.; Kang, S. M.; Lee, I.-J. A Comparative Study of Phosphate Solubilization and the Host Plant Growth Promotion Ability of *Fusarium Verticillioides* RK01 and *Humicola* Sp. KNU01 under Salt Stress. *Ann. Microbiol.* **2015**, *65* (1), 585–593. doi.org/10.1007/s13213-014-0894-z.

155 Khan, A. L. Salinity Stress Resistance Offered by Endophytic Fungal Interaction Between *Penicillium Minioluteum* LHL09 and *Glycine Max*. L. *J. Microbiol. Biotechnol.* **2011**, *21* (9), 893–902. doi.org/10.4014/jmb.1103.03012.

156 Contreras-Cornejo, H. A.; Macías-Rodríguez, L.; Alfaro-Cuevas, R.; López-Bucio, J. *Trichoderma* Spp. Improve Growth of *Arabidopsis* Seedlings Under Salt Stress Through Enhanced Root Development, Osmolite Production, and Na $^{+}$ Elimination Through Root Exudates. *Mol. Plant-Microbe Interactions*® **2014**, *27* (6), 503–514. doi.org/10.1094/MPMI-09-13-0265-R.

157 Ikram, M.; Ali, N.; Jan, G.; Iqbal, A.; Hamayun, M.; Jan, F. G.; Hussain, A.; Lee, I.-J. *Trichoderma Reesei* Improved the Nutrition Status of Wheat Crop under Salt Stress. *J. Plant Interact.* **2019**, *14* (1), 590–602 doi.org/10.1080/17429145.2019.1684582.

158 Xu, Z. Z.; Zhou, G. S. Combined Effects of Water Stress and High Temperature on Photosynthesis, Nitrogen Metabolism and Lipid Peroxidation of a Perennial Grass *Leymus Chinensis*. *Planta* **2006**, *224* (5), 1080–1090. doi.org/10.1007/s00425-006-0281-5.

159 Osakabe, Y.; Osakabe, K.; Shinozaki, K.; Tran, L.-S. P. Response of Plants to Water Stress. *Front. Plant Sci.* **2014**, *5.* doi.org/10.3389/fpls.2014.00086.

160 Xu, Z.; Shimizu, H.; Ito, S.; Yagasaki, Y.; Zou, C.; Zhou, G.; Zheng, Y. Effects of Elevated $CO_2$, Warming and Precipitation Change on Plant Growth, Photosynthesis and Peroxidation in Dominant Species from North China Grassland. *Planta* **2014**, *239* (2), 421–435. doi.org/10.1007/s00425-013-1987-9.

161 Osakabe, Y.; Arinaga, N.; Umezawa, T.; Katsura, S.; Nagamachi, K.; Tanaka, H.; Ohiraki, H.; Yamada, K.; Seo, S.-U.; Abo, M.; Yoshimura, E.; Shinozaki, K.; Yamaguchi-Shinozaki, K. Osmotic Stress Responses and Plant Growth Controlled by Potassium Transporters in *Arabidopsis*. *Plant Cell* **2013**, *25* (2), 609–624. doi.org/10.1105/tpc.112.105700.

162 Naseem, H.; Bano, A. Role of Plant Growth-Promoting Rhizobacteria and Their Exopolysaccharide in Drought Tolerance of Maize. *J. Plant Interact.* **2014**, *9* (1), 689–701. doi.org/10.1080/17429145.2014.902125.

163 Cohen, A. C.; Bottini, R.; Pontin, M.; Berli, F. J.; Moreno, D.; Boccanlandro, H.; Travaglia, C. N.; Piccoli, P. N. *Azospirillum Brasilense* Ameliorates the Response of *Arabidopsis Thaliana* to Drought Mainly via Enhancement of ABA Levels. *Physiol. Plant.* **2015**, *153* (1), 79–90. doi.org/10.1111/ppl.12221.

164 Silletti, S.; Di Stasio, E.; Van Oosten, M. J.; Ventorino, V.; Pepe, O.; Napolitano, M.; Marra, R.; Woo, S. L.; Cirillo, V.; Maggio, A. Biostimulant Activity of *Azotobacter Chroococcum* and *Trichoderma Harzianum* in Durum Wheat under Water and Nitrogen Deficiency. *Agronomy* **2021**, *11* (2), 380. doi.org/10.3390/agronomy11020380.

165 Iba, K. Acclimative Response to Temperature Stress in Higher Plants : Approaches of Gene Engineering for Temperature Tolerance. *Annu. Rev. Plant Biol.* **2002**, *53* (1), 225–245. doi.org/10.1146/annurev.arplant.53.100201.160729.

166 Sarkar, J.; Chakraborty, B.; Chakraborty, U. Plant Growth Promoting Rhizobacteria Protect Wheat Plants Against Temperature Stress Through Antioxidant Signaling and Reducing

Chloroplast and Membrane Injury. *J. Plant Growth Regul.* **2018**, *37* (4), 1396–1412. doi.org/10.1007/s00344-018-9789-8.

167 Kumar Meena, R.; Kumar Singh, R.; Pal Singh, N.; Kumari Meena, S.; Singh Meena, V. Isolation of Low Temperature Surviving Plant Growth – Promoting Rhizobacteria (PGPR) from Pea (*Pisum Sativum* L.) and Documentation of Their Plant Growth Promoting Traits. *Biocatal. Agric. Biotechnol.* **2015**, *4* (4), 806–811. doi.org/10.1016/j.bcab.2015.08.006.

168 Bunn, R.; Lekberg, Y.; Zabinski, C. Arbuscular Mycorrhizal Fungi Ameliorate Temperature Stress in Thermophilic Plants. *Ecology* **2009**, *90* (5), 1378–1388. doi.org/10.1890/07-2080.1.

169 Chen, S.; Jin, W.; Liu, A.; Zhang, S.; Liu, D.; Wang, F.; Lin, X.; He, C. Arbuscular Mycorrhizal Fungi (AMF) Increase Growth and Secondary Metabolism in Cucumber Subjected to Low Temperature Stress. *Sci. Hortic.* **2013**, *160*, 222–229. doi.org/10.1016/j.scienta.2013.05.039.

170 Li, C.; Zhou, K.; Qin, W.; Tian, C.; Qi, M.; Yan, X.; Han, W. A Review on Heavy Metals Contamination in Soil: Effects, Sources, and Remediation Techniques. *Soil Sediment Contam. Int. J.* **2019**, *28* (4), 380–394. doi.org/10.1080/15320383.2019.1592108.

171 Delangiz, N.; Varjovi, M. B.; Lajayer, B. A.; Ghorbanpour, M. Chapter 33 - Beneficial Microorganisms in the Remediation of Heavy Metals. In *Molecular Aspects of Plant Beneficial Microbes in Agriculture*; Sharma, V., Salwan, R., Al-Ani, L. K. T., Eds.; Academic Press, 2020; pp 417–423. doi.org/10.1016/B978-0-12-818469-1.00034-1.

172 Verma, S.; Kuila, A. Bioremediation of Heavy Metals by Microbial Process. *Environ. Technol. Innov.* **2019**, *14*, 100369. doi.org/10.1016/j.eti.2019.100369.

173 Abdu, N.; Abdullahi, A. A.; Abdulkadir, A. Heavy Metals and Soil Microbes. *Environ. Chem. Lett.* **2017**, *15* (1), 65–84. doi.org/10.1007/s10311-016-0587-x.

174 Das, S.; Dash, H. R. Microbial Bioremediation. In *Microbial Biodegradation and Bioremediation*; Elsevier, 2014; pp 1–21. doi.org/10.1016/B978-0-12-800021-2.00001-7.

175 Margesin, R.; Zimmerbauer, A.; Schinner, F. Monitoring of Bioremediation by Soil Biological Activities. *Chemosphere* **2000**, *40* (4), 339–346. doi.org/10.1016/S0045-6535(99)00218-0.

176 Srivastava, J.; Naraian, R.; Kalra, S. J. S.; Chandra, H. Advances in Microbial Bioremediation and the Factors Influencing the Process. *Int. J. Environ. Sci. Technol.* **2014**, *11* (6), 1787–1800. doi.org/10.1007/s13762-013-0412-z.

177 Keller, N. P.; Turner, G.; Bennett, J. W. Fungal Secondary Metabolism — from Biochemistry to Genomics. *Nat. Rev. Microbiol.* **2005**, *3* (12), 937–947. doi.org/10.1038/nrmicro1286.

178 Demain, A. L.; Fang, A. The Natural Functions of Secondary Metabolites. In *History of Modern Biotechnology I*; Fiechter, A., Ed.; Scheper, T., Babel, W., Blanch, H. W., Cooney, C. L., Endo, I., Enfors, S.-O., Eriksson, K.-E. L., Fiechter, A., Hoare, M., Mattiasson, B., Rehm, H. J., Rogers, P. L., Sahm, H., Schügerl, K., Stephanopoulos, G., Tsao, G. T., Venkat, K., Villadsen, J., von Stockar, U., Wandrey, C., Series Eds.; Advances in Biochemical Engineering/Biotechnology; Springer Berlin Heidelberg: Berlin, Heidelberg, 2000; Vol. 69, pp 1–39. doi.org/10.1007/3-540-44964-7_1.

179 Vinale, F.; Sivasithamparam, K. Beneficial Effects of *Trichoderma* Secondary Metabolites on Crops. *Phytother. Res.* **2020**, *34* (11), 2835–2842. doi.org/10.1002/ptr.6728.

180 Keswani, C.; Singh, H. B.; Hermosa, R.; García-Estrada, C.; Caradus, J.; He, Y.-W.; Mezaache-Aichour, S.; Glare, T. R.; Borriss, R.; Vinale, F.; Sansinenea, E. Antimicrobial

Secondary Metabolites from Agriculturally Important Fungi as next Biocontrol Agents. *Appl. Microbiol. Biotechnol.* **2019**, *103* (23–24), 9287–9303. doi.org/10.1007/s00253-019-10209-2.

181 Tyc, O.; Song, C.; Dickschat, J. S.; Vos, M.; Garbeva, P. The Ecological Role of Volatile and Soluble Secondary Metabolites Produced by Soil Bacteria. *Trends Microbiol.* **2017**, *25* (4), 280–292 doi.org/10.1016/j.tim.2016.12.002.

182 Hermosa, R.; Cardoza, R. E.; Rubio, M. B.; Gutiérrez, S.; Monte, E. Secondary Metabolism and Antimicrobial Metabolites of *Trichoderma*. In *Biotechnology and Biology of Trichoderma*; Elsevier, 2014; pp 125–137. doi.org/10.1016/B978-0-444-59576-8.00010-2.

183 Hai, Y.; Jenner, M.; Tang, Y. Fungal Siderophore Biosynthesis Catalysed by an Iterative Nonribosomal Peptide Synthetase. *Chem. Sci.* **2020**, *11* (42), 11525–11530. doi.org/10.1039/D0SC03627G.

184 Johnstone, T. C.; Nolan, E. M. Beyond Iron: Non-Classical Biological Functions of Bacterial Siderophores. *Dalton Trans.* **2015**, *44* (14), 6320–6339. doi.org/10.1039/C4DT03559C.

185 Schuemann, J.; Hertweck, C. Biosynthesis of Fungal Polyketides. In *Physiology and Genetics. The Mycota (A Comprehensive Treatise on Fungi as Experimental Systems for Basic and Applied Research)*; Springer: Berlin, Heidelberg, 2009; Vol. 15, pp 331–351.

186 Daley, D. K.; Brown, K. J.; Badal, S. Fungal Metabolites. In *Pharmacognosy*; Elsevier, 2017; pp 413–421. doi.org/10.1016/B978-0-12-802104-0.00020-2.

187 Du, L.; Sánchez, C.; Shen, B. Hybrid Peptide–Polyketide Natural Products: Biosynthesis and Prospects toward Engineering Novel Molecules. *Metab. Eng.* **2001**, *3* (1), 78–95. doi.org/10.1006/mben.2000.0171.

188 Partida-Martinez, L. P.; Hertweck, C. A Gene Cluster Encoding Rhizoxin Biosynthesis in "*Burkholderia Rhizoxina*", the Bacterial Endosymbiont of the Fungus *Rhizopus Microsporus*. *Chem. Bio. Chem.* **2007**, *8* (1), 41–45- doi.org/10.1002/cbic.200600393.

189 Brendel, N.; Partida-Martinez, L. P.; Scherlach, K.; Hertweck, C. A Cryptic PKS–NRPS Gene Locus in the Plant Commensal *Pseudomonas Fluorescens* Pf-5 Codes for the Biosynthesis of an Antimitotic Rhizoxin Complex. *Org. Biomol. Chem.* **2007**, *5* (14), 2211–2213. doi.org/10.1039/B707762A.

190 Loper, J. E.; Henkels, M. D.; Shaffer, B. T.; Valeriote, F. A.; Gross, H. Isolation and Identification of Rhizoxin Analogs from *Pseudomonas Fluorescens* Pf-5 by Using a Genomic Mining Strategy. *Appl. Environ. Microbiol.* **2008**, *74* (10), 3085–3093. doi.org/10.1128/AEM.02848-07.

191 Miller, D. A.; Luo, L.; Hillson, N.; Keating, T. A.; Walsh, C. T. Yersiniabactin Synthetase: A Four-Protein Assembly Line Producing the Nonribosomal Peptide/ Polyketide Hybrid Siderophore of *Yersinia Pestis*. *Chem. Biol.* **2002**, *9*, 333–344. doi.org/10.1016/S1074-5521(02)00115-1.

192 Vinale, F.; Nigro, M.; Sivasithamparam, K.; Flematti, G.; Ghisalberti, E. L.; Ruocco, M.; Varlese, R.; Marra, R.; Lanzuise, S.; Eid, A.; Woo, S. L.; Lorito, M. Harzianic Acid: A Novel Siderophore from *Trichoderma Harzianum*. *FEMS Microbiol. Lett.* **2013**, *347* (2), 123–129. doi.org/10.1111/1574-6968.12231.

193 Vinale, F.; Manganiello, G.; Nigro, M.; Mazzei, P.; Piccolo, A.; Pascale, A.; Ruocco, M.; Marra, R.; Lombardi, N.; Lanzuise, S.; Varlese, R.; Cavallo, P.; Lorito, M.; Woo, S. A Novel Fungal Metabolite with Beneficial Properties for Agricultural Applications. *Molecules* **2014**, *19* (7), 9760–9772. doi.org/10.3390/molecules19079760.

194 Bohlmann, J.; Keeling, C. I. Terpenoid Biomaterials. *Plant J.* **2008**, *54* (4), 656–669. doi.org/10.1111/j.1365-313X.2008.03449.x.

195 Sharma, A.; Gautam, S.; Saxena, S. *Streptomyces*. In *Encyclopedia of Food Microbiology*; Elsevier, 2014; pp 560–566. doi.org/10.1016/B978-0-12-384730-0.00326-8.

196 Pandey, K. D.; Patel, A. K.; Singh, M.; Vandana; Kumari, A.; Jalaluddin. Secondary Metabolites from Bacteria and Viruses. In *Natural Bioactive Compounds*; Elsevier, 2021; pp 19–40. doi.org/10.1016/B978-0-12-820655-3.00002-1.

197 Chapter 5. Terpenoid Fungal Metabolites. In *The Chemistry of Fungi*; Royal Society of Chemistry: Cambridge, 2008; pp 73–119 doi.org/10.1039/9781847558329-00073.

198 Woo, S. L.; Pepe, O. Microbial Consortia: Promising Probiotics as Plant Biostimulants for Sustainable Agriculture. *Front. Plant Sci.* **2018**, *9*, 1801. doi.org/10.3389/fpls.2018.01801.

199 *Principles of Plant-Microbe Interactions*; Lugtenberg, B., Ed.; Springer International Publishing: Cham, 2015. doi.org/10.1007/978-3-319-08575-3.

200 Tabacchioni, S.; Passato, S.; Ambrosino, P.; Huang, L.; Caldara, M.; Cantale, C.; Hett, J.; Del Fiore, A.; Fiore, A.; Schlüter, A.; Sczyrba, A.; Maestri, E.; Marmiroli, N.; Neuhoff, D.; Nesme, J.; Sørensen, S. J.; Aprea, G.; Nobili, C.; Presenti, O.; Giovannetti, G.; Giovannetti, C.; Pihlanto, A.; Brunori, A.; Bevivino, A. Identification of Beneficial Microbial Consortia and Bioactive Compounds with Potential as Plant Biostimulants for a Sustainable Agriculture. *Microorganisms* **2021**, *9* (2), 426. doi.org/10.3390/microorganisms9020426.

201 Bradáčová, K.; Florea, A.; Bar-Tal, A.; Minz, D.; Yermiyahu, U.; Shawahna, R.; Kraut-Cohen, J.; Zolti, A.; Erel, R.; Dietel, K.; Weinmann, M.; Zimmermann, B.; Berger, N.; Ludewig, U.; Neumann, G.; Poşta, G. Microbial Consortia versus Single-Strain Inoculants: An Advantage in PGPM-Assisted Tomato Production? *Agronomy* **2019**, *9* (2), 105. doi.org/10.3390/agronomy9020105.

202 Vishwakarma, K.; Kumar, N.; Shandilya, C.; Mohapatra, S.; Bhayana, S.; Varma, A. Revisiting Plant–Microbe Interactions and Microbial Consortia Application for Enhancing Sustainable Agriculture: A Review. *Front. Microbiol.* **2020**, *11*, 560406. doi.org/10.3389/fmicb.2020.560406.

203 Ahmad, I.; Khan, M. S. A.; Aqil, F.; Singh, M. Microbial Applications in Agriculture and the Environment: A Broad Perspective. In *Microbes and Microbial Technology*; Ahmad, I., Ahmad, F., Pichtel, J., Eds.; Springer New York: New York, NY, 2011; pp 1–27. doi.org/10.1007/978-1-4419-7931-5_1.

204 Berg, G.; Grube, M.; Schloter, M.; Smalla, K. Unraveling the Plant Microbiome: Looking Back and Future Perspectives. *Front. Microbiol.* **2014**, *5*. doi.org/10.3389/fmicb.2014.00148.

205 du Jardin, P. Plant Biostimulants: Definition, Concept, Main Categories and Regulation. *Sci. Hortic.* **2015**, *196*, 3–14. doi.org/10.1016/j.scienta.2015.09.021.

206 Wargo, M. J.; Hogan, D. A. Fungal—Bacterial Interactions: A Mixed Bag of Mingling Microbes. *Curr. Opin. Microbiol.* **2006**, *9* (4), 359–364. doi.org/10.1016/j.mib.2006.06.001.

207 Gunatilaka, A. A. L. Natural Products from Plant-Associated Microorganisms: Distribution, Structural Diversity, Bioactivity, and Implications of Their Occurrence. *J. Nat. Prod.* **2006**, *69* (3), 509–526. doi.org/10.1021/np058128n.

208 Deng, Z.-L.; Du, C.-X.; Li, X.; Hu, B.; Kuang, Z.-K.; Wang, R.; Feng, S.-Y.; Zhang, H.-Y.; Kong, D.-X. Exploring the Biologically Relevant Chemical Space for Drug Discovery. *J. Chem. Inf. Model.* **2013**, *53* (11), 2820–2828 .doi.org/10.1021/ci400432a.

209 Scherlach, K.; Hertweck, C. Triggering Cryptic Natural Product Biosynthesis in Microorganisms. *Org. Biomol. Chem.* **2009**, *7* (9), 1753. doi.org/10.1039/b821578b.

210 Omura, S.; Ikeda, H.; Ishikawa, J.; Hanamoto, A.; Takahashi, C.; Shinose, M.; Takahashi, Y.; Horikawa, H.; Nakazawa, H.; Osonoe, T.; Kikuchi, H.; Shiba, T.; Sakaki, Y.; Hattori, M. Genome Sequence of an Industrial Microorganism *Streptomyces Avermitilis*: Deducing the Ability of Producing Secondary Metabolites. *Proc. Natl. Acad. Sci.* **2001**, *98* (21), 12215–12220. doi.org/10.1073/pnas.211433198.

211 Bentley, S. D.; Chater, K. F.; Harper, D.; Bateman, A.; Brown, S.; Chandra, G.; Chen, C. W.; Collins, M.; Cronin, A.; Fraser, A.; Goble, A.; Hidalgo, J.; Hornsby, T.; Howarth, S.; Rutter, S.; Seeger, K.; Saunders, D.; Sharp, S.; Squares, R.; Squares, S.; Taylor, K.; Warren, T.; Wietzorrek, A.; Woodward, J.; Barrell, B. G.; Parkhill, J.; Hopwood, D. A. Complete Genome Sequence of the Model Actinomycete *Streptomyces Coelicolor* A3(2). *Nature* **2002**, *417*, 7. doi.org/10.1038/417141°.

212 Galagan, J. E.; Calvo, S. E.; Cuomo, C.; Ma, L.-J.; Wortman, J. R.; Batzoglou, S.; Lee, S.-I.; Baştürkmen, M.; Spevak, C. C.; Clutterbuck, J.; Kapitonov, V.; Jurka, J.; Scazzocchio, C.; Farman, M.; Butler, J.; Purcell, S.; Harris, S.; Braus, G. H.; Draht, O.; Busch, S.; D'Enfert, C.; Bouchier, C.; Goldman, G. H.; Bell-Pedersen, D.; Griffiths-Jones, S.; Doonan, J. H.; Yu, J.; Vienken, K.; Pain, A.; Freitag, M.; Selker, E. U.; Archer, D. B.; Peñalva, M. Á.; Oakley, B. R.; Momany, M.; Tanaka, T.; Kumagai, T.; Asai, K.; Machida, M.; Nierman, W. C.; Denning, D. W.; Caddick, M.; Hynes, M.; Paoletti, M.; Fischer, R.; Miller, B.; Dyer, P.; Sachs, M. S.; Osmani, S. A.; Birren, B. W. Sequencing of *Aspergillus Nidulans* and Comparative Analysis with *A*. *Fumigatus* and *A*. *Oryzae*. *Nature* **2005**, *438* (7071), 1105–1115. doi.org/10.1038/nature04341.

213 Wilkinson, B.; Micklefield, J. Mining and Engineering Natural-Product Biosynthetic Pathways. *Nat. Chem. Biol.* **2007**, *3* (7), 379–386. doi.org/10.1038/nchembio.2007.7.

214 Wasil, Z.; Pahirulzaman, K. A. K.; Butts, C.; Simpson, T. J.; Lazarus, C. M.; Cox, R. J. One Pathway, Many Compounds: Heterologous Expression of a Fungal Biosynthetic Pathway Reveals Its Intrinsic Potential for Diversity. *Chem. Sci.* **2013**, *4* (10), 3845. doi.org/10.1039/c3sc51785c.

215 Gross, H. Strategies to Unravel the Function of Orphan Biosynthesis Pathways: Recent Examples and Future Prospects. *Appl. Microbiol. Biotechnol.* **2007**, *75* (2), 267–277. doi.org/10.1007/s00253-007-0900-5.

216 Bode, H. B.; Bethe, B.; Höfs, R.; Zeeck, A. Big Effects from Small Changes: Possible Ways to Explore Nature's Chemical Diversity. *Chem. Bio. Chem.* **2002**, *3* (7), 619. doi.org/10.1002/1439-7633(20020703)3:7<619::AID-CBIC619>3.0.CO;2-9.

217 Singh, V.; Haque, S.; Niwas, R.; Srivastava, A.; Pasupuleti, M.; Tripathi, C. K. M. Strategies for Fermentation Medium Optimization: An In-Depth Review. *Front. Microbiol.* **2017**, *7*. doi.org/10.3389/fmicb.2016.02087.

218 Gibson, A. M.; Bratchell, N.; Roberts, T. A. Predicting Microbial Growth: Growth Responses of Salmonellae in a Laboratory Medium as Affected by pH, Sodium Chloride and Storage Temperature. *Int. J. Food Microbiol.* **1988**, *6* (2), 155–178. doi.org/10.1016/0168-1605(88)90051-7.

219 Tan, Y.; Wang, Z.-X.; Marshall, K. C. Modeling pH Effects on Microbial Growth: A Statistical Thermodynamic Approach. *Biotechnol. Bioeng.* **1998**, *59* (6), 724–731. doi.org/10.1002/(SICI)1097-0290(19980920)59:6<724::AID-BIT9>3.0.CO;2-H.

220 Fuchser, J.; Thiericke, R.; Zeeck, A. Biosynthesis of Aspinonene, a Branched Pentaketide Produced by *Aspergillus Ochraceus*, Related to Aspyrone. *J. Chem. Soc. Perkin 1* **1995**, No. 13, 1663. doi.org/10.1039/p19950001663.

221 Marmann, A.; Aly, A.; Lin, W.; Wang, B.; Proksch, P. Co-Cultivation—A Powerful Emerging Tool for Enhancing the Chemical Diversity of Microorganisms. *Mar. Drugs* **2014**, *12* (2), 1043–1065. doi.org/10.3390/md12021043.

222 Marfori, E. C.; Kajiyama, S.; Fukusaki, E.; Kobayashi, A. Trichosetin, a Novel Tetramic Acid Antibiotic Produced in Dual Culture of *Trichoderma Harzianum* and *Catharanthus Roseus Callus*. *Z. Für Naturforschung C* **2002**, *57* (5–6), 465–470. doi.org/10.1515/znc-2002-5-611.

223 Vinale, F.; Nicoletti, R.; Borrelli, F.; Mangoni, A.; Parisi, O. A.; Marra, R.; Lombardi, N.; Lacatena, F.; Grauso, L.; Finizio, S.; Lorito, M.; Woo, S. L. Co-Culture of Plant Beneficial Microbes as Source of Bioactive Metabolites. *Sci. Rep.* **2017**, *7* (1), 14330. doi.org/10.1038/s41598-017-14569-5.